

UC Irvine

UC Irvine Electronic Theses and Dissertations

Title

New bioorthogonal chemistries for multi-component detection

Permalink

<https://escholarship.org/uc/item/1vh6s9fz>

Author

Patterson, David Michael

Publication Date

2015

Peer reviewed|Thesis/dissertation

UNIVERSITY OF CALIFORNIA,
IRVINE

New bioorthogonal chemistries for multi-component detection

DISSERTATION

submitted in partial satisfaction of the requirements
for the degree of

DOCTOR OF PHILOSOPHY

in Chemistry

by

David Michael Patterson

Dissertation Committee:
Assistant Professor Jennifer A. Prescher, Chair
Professor Gregory Weiss
Professor Zhibin Guan

2015

Chapter 2 © 2012 American Chemical Society
Chapter 1 © 2014 American Chemical Society
Chapter 3 © 2014 The Royal Society of Chemistry
All other materials © 2015 David Michael Patterson

DEDICATION

To

my parents, Emmett and Karyn Patterson,
in recognition of their love and support

TABLE OF CONTENTS

	Page
LIST OF FIGURES	vii
LIST OF TABLES	x
LIST OF SCHEMES	xi
ACKNOWLEDGMENTS	xii
CURRICULUM VITAE	xiv
ABSTRACT OF THE DISSERTATION	xvi
CHAPTER 1: Finding the right (bioorthogonal) chemistry	
1.1 Introduction	1
1.2 Meet the candidates	3
1.3 Making a match	10
1.4 Moving forward	20
1.5 Conclusions	24
1.6 Objectives	24
References	24
CHAPTER 2: Functionalized cyclopropenes as bioorthogonal chemical reporters	
2.1 Introduction	45
2.2 Results and discussion	48
2.2a Design and synthesis of biocompatible cyclopropenes	48
2.2b Analysis of cyclopropene-tetrazine reactivity	55
2.2c Protein modification via cyclopropene-tetrazine ligation	64

2.2d	Metabolic incorporation of cyclopropenes onto live cell surfaces	78
2.3	Conclusions	84
2.4	Materials and methods	84
2.4a	Cyclopropene stability	84
2.4b	Rate studies	85
2.4c	Reaction analyses by HPLC	86
2.4d	Protein labeling	86
2.4e	Cross-reactivity analysis	88
2.4f	Metabolic labeling studies	88
2.4g	General synthetic procedures	89
2.4h	Synthetic procedures	90
	References	101
 CHAPTER 3: Improved cyclopropene reporters for probing protein glycosylation		
3.1	Introduction	107
3.2	Results and Discussion	109
3.3	Conclusions	127
3.4	Materials and Methods	127
3.4a	Metabolic labeling studies with cultured cells	127
3.4b	Western blot analyses	128
3.4c	Microscopy	129
3.4d	General synthetic procedures	131
3.4e	Synthetic procedures	132
	References	136

CHAPTER 4: Orthogonal bioorthogonal chemistries

4.1	Introduction	140
4.2	Mutually orthogonal bioorthogonal reactions	142
4.2a	Unique reaction mechanisms	142
4.2b	Tuning reactions for orthogonality	145
4.3	Orthogonal reactivity via controlled reagent activation	148
4.3a	Metal-catalyzed reactions	148
4.3b	Light-activated reactions	149
4.3c	Chemical activation	151
4.4	Identifying new mutually orthogonal reactions	152
4.5	Conclusions	157
4.6	Materials and methods	158
4.6a	Rate studies	158
4.6b	HPLC analysis	159
4.6c	Synthetic procedures	159
	References	161

CHAPTER 5: Progress towards an “off-the-shelf” luciferase for imaging implanted cells

5.1	Introduction	169
5.2	Results and Discussion	171
5.2a	Aldehyde-tagged Gaussia luciferase	171
5.2b	Sortagging of Gaussia luciferase	174
5.3	Conclusions and future directions	177
5.4	Materials and Methods	178

5.4a	Plasmids	178
5.4b	Expression of Gaussia luciferase	179
5.4c	Cell culture	179
5.4d	Sortase-mediated Gaussia luciferase modification	180
5.4e	Cell surface attachment of Gaussia luciferase	180
5.4f	General synthetic procedures	181
5.4g	Synthetic procedures	182
References		185
APPENDIX: NMR Spectra		189

LIST OF FIGURES

	Page	
Figure 1-1	A bioorthogonal chemical reaction	2
Figure 1-2	Selecting an appropriate bioorthogonal chemistry	11
Figure 1-3	Installing bioorthogonal functionality into target biomolecules	13
Figure 1-4	“On-demand” bioorthogonal reactivity	21
Figure 1-5	Identifying mutually orthogonal transformations	23
Figure 2-1	Chemical reporters and bioorthogonal chemistries	47
Figure 2-2	Cyclopropenes are stable upon storage	51-52
Figure 2-3	Cyclopropenes are stable in the presence of biological nucleophiles	53-54
Figure 2-4	Cyclopropenes react with tetrazines to form covalent adducts	56
Figure 2-5	HPLC analyses of cyclopropene-tetrazine reaction	57-59
Figure 2-6	Plots used to calculate second-order rate constants by UV-Vis	61-62
Figure 2-7	Plot used to calculate the rate constant between 2.2b and 2.12	62
Figure 2-8	NOESY spectrum of cycloadduct 2.15	65
Figure 2-9	HMBC spectrum of cycloadduct 2.15	65
Figure 2-10	Mechanism of cycloadduct 2.22 formation	66
Figure 2-11	Mechanism of cycloadduct 2.21 formation	66
Figure 2-12	NOESY spectrum of cycloadduct 2.21	67
Figure 2-13	Mechanism of cycloadduct 2.18 formation	67
Figure 2-14	NOESY spectrum of cycloadduct 2.18	68
Figure 2-15	Methylcyclopropenes can be selectively modified on protein surfaces	69
Figure 2-16	Mass spectrum analysis of protein conjugates	71-72

Figure 2-17	Cyclopropene carbonate 2.10 can be modified on protein surfaces	73
Figure 2-18	DBCO-Rho and Tz-Rho cross-reactivity analysis by HPLC	76
Figure 2-19	DBCO-Rho and Tz-Rho cross-reactivity analysis by protein labeling	77
Figure 2-20	Cyclopropenes can be metabolically incorporated onto live cell surfaces	79
Figure 2-21	Flow cytometry analysis of 9-Az-NeuAc metabolism in Jurkat cells	80
Figure 2-22	Cyclopropenes and azides can be utilized in tandem for cellular metabolic labeling	82
Figure 2-23	Control data for cellular metabolic labeling	83
Figure 3-1	Cyclopropene ManNAc derivatives can be metabolically incorporated onto Jurkat cell surfaces	110
Figure 3-2	Ac₄ManCCp is metabolically incorporated into 4T1 and HEK293 cell surface glycans	113
Figure 3-3	Western blot images of Jurkat glycoproteins	114
Figure 3-4	Ponceau S staining control of Jurkat glycoproteins	114
Figure 3-5	Ac₄GalCCp and Ac₄GlcCCp are metabolically incorporated onto cell surface glycans	116
Figure 3-6	Western blot images of HEK293 and 4T1 glycoproteins	118
Figure 3-7	Fluorescence microscopy of Ac₄ManCCp labeled 4T1 cells	119
Figure 3-8	Fluorescence microscopy of Ac₄GalCCp labeled 4T1 cells	120
Figure 3-9	Fluorescence microscopy of Ac₄GlcCCp labeled 4T1 cells	121
Figure 3-10	Fluorescence microscopy of Ac₄ManNCyc labeled 4T1 cells	122
Figure 3-11	Distinct metabolic targets can be simultaneously imaged using cyclopropene and azide reporters	124
Figure 3-12	Control images for Figure 3-11	125
Figure 4-1	Targeting multiple components requires ‘orthogonal bioorthogonal’ reactions	141

Figure 4-2	Orthogonal bioorthogonal ligations with distinct reaction mechanisms	144
Figure 4-3	Tetrazines and cyclooctynes can be tuned to generate mutually orthogonal reaction pairs	147
Figure 4-4	Isomeric cyclopropenes exhibit unique bioorthogonal reactivities	151
Figure 4-5	Difluorinated cyclooctyne and norbornene react preferentially with nitrones and disubstituted tetrazines, respectively	154
Figure 4-6	Plots used to calculate second-order rate constants for DIFO reactions	155
Figure 5-1	Design for “off-the-shelf” bioluminescent cell tracking	171
Figure 5-2	Gluc attachment strategy utilizing the oxime ligation	173
Figure 5-3	Gluc cell surface attachment method via sortagging	176

LIST OF TABLES

		Page
Table 1-1	Bioorthogonal chemistries	4-5
Table 2-1	Cycloaddition rates observed between cyclopropene and tetrazine scaffolds	60

LIST OF SCHEMES

	Page	
Scheme 2-1	Synthesis of functionalized cyclopropenes	48
Scheme 2-2	Synthesis of 2.24 and 9-Cp-NeuAc	70
Scheme 2-3	Synthesis of tetrazine conjugates	70
Scheme 3-1	Synthesis of Ac₄ManCCp , Ac₄GalCCp , and Ac₄GlcCCp	111
Scheme 3-2	Synthesis of DBCO-FLAG	126
Scheme 4-1	DIFO reaction schemes and HRMS	156
Scheme 5-1	Synthesis of reagents for sortase-mediated cell surface attachment	177

ACKNOWLEDGMENTS

First and foremost, my sincerest appreciation goes to my advisor and committee chair, Professor Jennifer Prescher for her mentorship. I have learned so much about what it takes to be a good scientist and you provided me with every opportunity to succeed. You showed endless patience through my growing pains and enthusiasm for my successes. Regardless of my concerns, personal or professional, you spent the time to lend an ear and offer advice. Thank you!

I also thank my committee members, Professors Gregory Weiss and Zhibin Guan. You both have been supportive and encouraging throughout my career. Greg, I still recall advice you offered on poise during those joint Prescher-Weiss group meetings. Zhibin, you played a large role in recruiting me to UCI and I have always enjoyed our conversations.

I also thank the entire UCI chemistry faculty, staff, and students. From top to bottom, the department has provided a very supportive, friendly environment. Thank you to Professors Chris Vanderwal and Liz Jarvo for participating in my qualifying exam as well as guiding our student-hosted seminar program (even if it didn't quite work out!). Thank you to James Nowick for several hours of assistance with NMR analysis. Thank you Professors Andy Borovik and Andrej Luptak for providing the comic relief and for giving Jenn a hard time! Thank you to Dr. Beniam Berhane and Dr. John Greaves for helpful conversations, entertainment, and maintaining our mass spec facilities. Also, thanks to Dr. Phil Dennison for his stellar work maintaining our NMR facilities and guiding me through new NMR experiments.

Thank you to my fellow Prescher lab members. Every single person has helped me at some point and I have enjoyed your company these last 5 years. The first five members of the Prescher group, Dr. Miranda Paley, Rachel Steinhardt, Lidia Nazarova, and Dave McCutcheon, are a smart, fun, and hardworking crew. Lidia Nazarova, in particular, was a stellar colleague. We published several papers together and it was always a pleasure, which is not common and I cannot say I was always as pleasant. Thank you also to David Kamber, who I have worked extensively with and is an incredibly passionate and hardworking chemist. Thank you to Krysten Jones who is hands-down the most productive graduate student I know and provided me with an incredible amount of experimental assistance, along with a fair amount of sass! Thank you to Bryan Xie for your hard work and friendship. You were a joy to train and I have no doubt that you will have a stellar graduate career of your own. Thank you Dr. Hui-Wen Shih for sharing your experience and knowledge with me in the lab. I am a much better scientist thanks to your influence. Thank you to Will Porterfield for being the best bay mate around and coolest guy I know. Thank you to Joanna Laird, Colin Rathbun, and Brendan Zheng for being excellent friends and labmates.

Thank you to the many graduate students who made me feel welcome in southern California and taught me so much: Dr. Iva Yonova, Dr. Hanna Wisniewski, Dr. Buck Taylor, Dr. Peg Green, Dr. Florence Williams, Dr. Mike Shaghafi, Dr. Elizabeth Swift, Dr. Jess Arter, Dr. Greg Williams, Dr. Tivoli Olsen, Dr. Maureen Reilly, Dr. Avinash Khanna, Dr. Jonathan Lam, Dr. Jonathan Paretsky, Dr. Janice Wong, Dr. David Schaeffer, and probably many more. Of course, thank you to the many other graduate students at UCI including Dang Nguyen, Moritz

Limpinsel, Dr. Josette Marerro, Jason Schroeder, Olivia Cromwell, Domarin Khago, Kritika Mohan, Luz Marina Meneghini, and many more!

Thank you to my undergraduate advisor Professor Edward Fenlon. You gave me my first taste of research and helped send me down the path to my PhD. Thank you also to Professor Ryan Mehl. I always value your friendship and mentorship. Thank you to my friends/mentors at DuPont. John Marcone, Steve Bair, and the late Joe Foster. All three of you helped me survive and DuPont. I not only learned research and professionalism, but how to maintain a sense of humor through the daily stress.

Thank you to my great “Hucking Amish” friends for continually inspiring me through the years: Matt and Karen Thurston, Julia and Drew Korn, Brandon Ito, Dr. Eric Socrates, Miles Gibson, Robert Bell, Dr. Monica Arienzo, and Fred Martino. Your success, ambition, and most of all, friendship, motivate me to continually work to be a better person.

Thank you to the “Naughty Love” ultimate community for helping keep me sane throughout graduate school by providing me great friends and teammates: Andrew Boyle, Jessie Fix, Pat Senatore, Claire Dobson, Kristi Lin, John Wong, Sean McDougall, Micah Seabrook, Heather Engstrom, Heidi Wroblicky, Tyler Monroe, Eric Bechtle, and Davida Marion.

Thank you to my roommate, teammate, and friend, Paul Stroik. Even though you are probably the worst person I know, you have been an excellent friend. Thank you for dealing with my exhausted, short-tempered, critical moods at the end of a long day.

Thank you to my parents for being so supportive and loving in spite of the fact that I moved across the country. I am proud to be your son and I will never stop trying to make you both proud! Thank you to John, Chris, Sean, and Emily. It was so much fun growing up with you and I love having a big family to see when I come home. Thank you to my aunts Danielle Sunderland and Kathleen Lambe for encouraging my quiet introversion and nerdiness. Thank you to my uncle Joe for guiding me through my first real job at McDonald’s. Thank you to my big sister, Maria. It has been great getting to know you all over again after not seeing each other for so long. Thank you to my grandma, Sara, for your love and encouragement. Thank you to all of my extended family that make leaving home so difficult: Teah and Aviana Patterson, Amelia Patterson, Dan and Taylor Ellenberger, Sam, Stephanie Miller, and Jack Lambe.

Finally, thank you, my love, Aneeka Hancock! You are brilliant and beautiful and bring out the best in me. Thank you for showing me so much love and support. I am so lucky that you put up with me and I look forward to continuing our journey together!

Financial support for this work was provided by Allergan, the NSF, and the University of California, Irvine.

CURRICULUM VITAE

David M. Patterson
University of California, Irvine
Irvine, CA 92697

Telephone: (717) 818-4636
Email: dmpatter@uci.edu

EDUCATION

University of California, Irvine, Irvine, CA <i>Ph.D. Chemistry</i> GPA: 3.99	2010–2015
Franklin & Marshall College, Lancaster, PA <i>B.A. Chemistry (Biochemistry emphasis)</i> GPA: 3.49	2004–2008

RESEARCH EXPERIENCE

University of California, Irvine, Irvine, CA Graduate Student, Department of Chemistry Advisor: Prof. Jennifer Prescher <i>Developed a bioorthogonal reaction based on cyclopropene.</i> <i>Established cyclopropene as a chemical reporter for studying glycans in live cells.</i> <i>Identified compatible bioorthogonal reactions for targeting multiple biomolecules simultaneously.</i>	2010–present
DuPont Central Research and Development, Wilmington, DE Associate Investigator, Chemical Science and Engineering Supervisor: Dr. Simona Percec <i>Developed new ionomer formulations for anti-corrosive paint applications.</i>	2008–2010
Franklin & Marshall College, Lancaster, PA Undergraduate Researcher Advisor: Prof. Edward Fenlon <i>Synthesized molecular hydrocarbon trefoil knots.</i>	2007–2008

PUBLICATIONS

- Patterson, D. M.**; Nazarova, L. A.; Xie, B.; Kamber, D. N.; Prescher, J. A. Functionalized Cyclopropenes as bioorthogonal chemical reporters. *J. Am. Chem. Soc.* **2012**, *134* (45), 18638–18643.
- Kamber, D. N.; Nazarova, L. N.; Liang, Y.; Lopez, S. A.; **Patterson, D. M.**; Shih, H. W.; Houk, K. N.; Prescher, J. A. Isomeric cyclopropenes exhibit unique bioorthogonal reactivities. *J. Am. Chem. Soc.* **2013**, *135* (37), 13680–13683.
- Patterson, D. M.**; Nazarova, L. A.; Prescher, J. A. Finding the right (bioorthogonal) chemistry. *ACS Chem. Biol.*, **2014**, *9* (3), 592–605.
- Patterson, D. M.**; Jones, K. A.; Prescher, J. A. Improved cyclopropene reporters for probing protein glycosylation. *Mol. BioSyst.*, **2014**, *10*, 1693–1697.
- Liang, Y.; Lopez, S. A.; **Patterson, D. M.**; Shih, H. W.; Kamber, D. N.; Prescher, J. A.; Houk, K. N., *Manuscript in preparation.*
- Patterson, D. M.**; Prescher, J. A. Expanding the protein imaging toolbox. *Curr. Opin. Chem. Biol.* Invited submission.

RESEARCH PRESENTATIONS

5. Building new bioorthogonal reactions with functionalized cyclopropenes. Gordon Research Conference (Bioorganic), poster presentation, Proctor Academy; June 2014.
4. Cyclopropenes as novel bioorthogonal chemical reporters. Graduate Student and Post-Doc Symposium, oral presentation, University of California, Irvine; November 2012.
3. Development of cyclopropenes as bioorthogonal chemical reporters. 10th Annual UC Irvine Immunology Fair, poster presentation, University of California, Irvine; November 2012.
2. Progress towards a polyethylene trefoil knot. 72nd Intercollegiate Student Chemists' Convention, oral presentation, Elizabethtown College; April 2008.
Awarded "Best Presentation" in the Organic Division
1. Progress towards a polyethylene trefoil knot. 235th American Chemical Society National Meeting, poster presentation, New Orleans, LA; April 2008.

TEACHING AND SERVICE

Student-Hosted Seminar Committee , University of California, Irvine	2013-2014
Graduate Student Instructor , University of California, Irvine Chemical Biology Graduate Class	Winter 2013
Chemical Biology, Organic and General Chemistry Undergraduate Labs	2010-2012
CLEAN Education , University of California, Irvine Assistant and Lead Presenter	2011
Science Teaching Intern , Franklin & Marshall College Fulton Elementary 5 th Grade	Spring 2006

HONORS AND AWARDS

Allergan Graduate Fellowship	2013
ISCC – Best Presentation, Organic Division	2008
Hackman Scholarship (Franklin & Marshall)	2007
2007 Leser Grant Award (Franklin & Marshall)	2007
Honor's list (Franklin & Marshall)	2005-2006
Dean's list (Franklin & Marshall)	2005-2008
Presidential Scholarship (Franklin & Marshall)	2004-2008

REFERENCES

Professor Jennifer Prescher
Department of Chemistry
University of California, Irvine
(949) 824-1706
jpresche@uci.edu

Professor Zhibin Guan
Department of Chemistry
University of California, Irvine
(949) 824-5172
zguan@uci.edu

Professor Gregory Weiss
Department of Chemistry
University of California, Irvine
(949) 824-5566
gweiss@uci.edu

Professor Aaron-Esser Kahn
Department of Chemistry
University of California, Irvine
(949) 824-4936
aesserka@uci.edu

ABSTRACT OF THE DISSERTATION

New bioorthogonal chemistries for multi-component detection

By

David Michael Patterson

Doctor of Philosophy in Chemistry

University of California, Irvine, 2015

Assistant Professor Jennifer A. Prescher, Chair

Bioorthogonal chemistries enable the selective visualization and identification of biomolecules in complex cellular environments. Significant advances in the speed and selectivity of these reactions have been reported over the past few years. Despite these successes, challenges remain in applying bioorthogonal chemistries to studies of complex biological functions. Many bioorthogonal reagents cross-react with one another, limiting their utility for visualizing multi-component processes. Additionally, many bioorthogonal reagents are not small or stable enough to label native biomolecules in living systems. To address these issues, I have developed new classes of functionalized cyclopropenes for bioorthogonal labeling experiments. These small motifs are stable in cells and other environments, yet robustly reactive with tetrazines and various 1,3-dipoles. Cyclopropenes can also be readily tuned to elicit desired covalent reactivity, facilitating the development of “mutually orthogonal” bioorthogonal transformations. I utilized these bioorthogonal cyclopropene chemistries to target glycans and proteins, as well as to tag cells with imaging agents for in vivo cell tracking.

CHAPTER 1: Finding the right (bioorthogonal) chemistry

1.1 Introduction

Interactions among proteins, glycans, and numerous other biopolymers and metabolites drive cellular processes. Thus, a complete understanding of living systems requires methods to probe biomolecules in real time. GFP and other genetically encoded reporters are available for tracking protein products in live cells and organisms. While powerful, such genetic tagging tools are not amenable to monitoring glycans, lipids, and other critical cellular components [1]. To address this need, the chemical biology community has developed a general platform to target cellular molecules with visual tags and other probes. This strategy relies on the installation of unique functional groups into target biomolecules and their selective reaction with covalent probes (Figure 1-1A). The chemistries employed in this approach must be selective and non-perturbing to biological systems. For these reasons, they have been collectively termed bioorthogonal [2].

The earliest work in bioorthogonal reaction development—nearly two decades ago—focused on methods to covalently target unique amino acid sequences with small molecule probes [3, 4]. Since then, dozens more unique transformations have been added to the bioorthogonal toolkit. The majority of these chemistries are applicable not only to protein tagging, but also studies with glycans, lipids, and numerous other biomolecules. The reactions differ widely, though, in terms of their selectivities, rates, and other attributes, and choosing among them can be difficult.

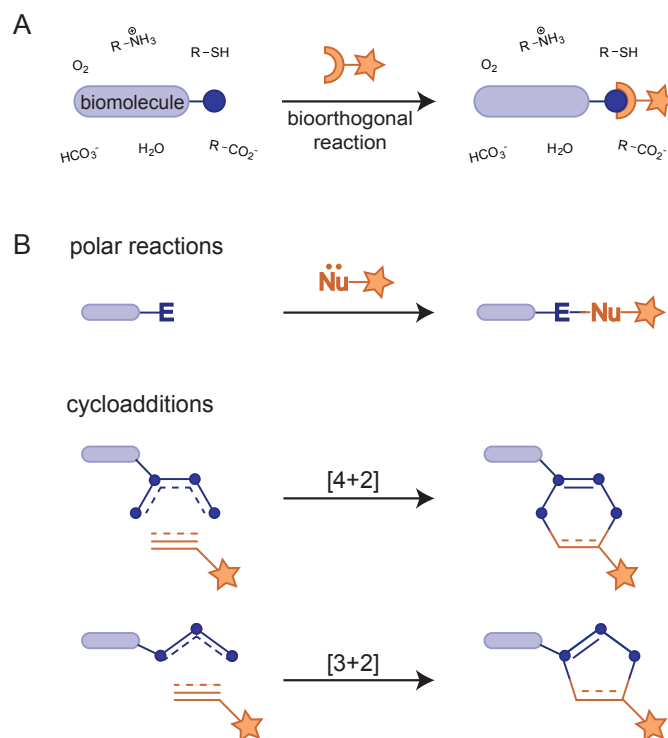


Figure 1-1. A bioorthogonal chemical reaction. (A) A unique functional group (blue circle) appended to a target biomolecule is covalently ligated with a complementary probe (orange arc). The two reagents must react selectively with one another and be inert to the biological surroundings (i.e., bioorthogonal). Depending on the choice of probe (star), this method enables the selective visualization or identification of biomolecules in complex environments. (B) Two types of transformations are predominant in the bioorthogonal toolkit: polar reactions between nucleophiles and electrophiles and cycloaddition chemistries.

This chapter deconstructs the major classes of bioorthogonal chemistries and draws relevant comparisons and contrasts between them. Our focus is on those reactions that are applicable to tagging diverse types of molecules in complex environments. We first introduce the common bioorthogonal transformations and highlight their utility in various experiments. We then provide a general set of considerations for selecting a suitable reaction for a given application. Last, we highlight existing challenges to the development and implementation of

bioorthogonal reactions. The continued use of these tools is painting a more complete picture of organismal biology.

1.2 Meet the candidates

The selective, covalent tagging of biomolecules—especially in live cells and tissues—is no easy task. For one, the biological milieu is replete with functional groups that can interfere with the desired labeling reaction. The bioorthogonal probes must also be stable in aqueous environments, yet readily reactive with one another. Furthermore, the chemistries must be nontoxic. The challenges involved in designing such reactions have captured the imagination of several chemists, and over the past decade, transformations have emerged that meet most or all of the criteria for bioorthogonality. The majority can be classified as either polar reactions or cycloadditions, although notable exceptions exist (Figure 1-1B). The chemistries differ in terms of the functional groups employed, reaction rates, and overall selectivities, but all are suitable for use in aqueous environments and, in some cases, live cells and animals (Table 1-1).

Table 1-1. Bioorthogonal chemistries

Reaction type	Reactant 1	Reactant 2	Approximate rate (M ⁻¹ s ⁻¹)	Comments	References	
Aldehyde/ketone condensation			0.001 (H ₂ O)	adducts prone to hydrolysis; aniline catalyst can be used	Jencks 1959	
			0.26 (100 mM sodium phosphate)	reaction provides more stable C-C linkages	Agarwal 2013	
Staudinger ligation	R-N ₃		0.003 (PBS)	phosphines susceptible to oxidation	Saxon 2000	
Cyanobenzothiazole condensation			9.19 (PBS)	side reactivity with free thiols	Rao 2009	
CuAAC	R-N ₃		k _{obs} 10-100 (10-100 μM Cu)	copper catalyst required	Tornøe 2002	
Strain-promoted azide-alkyne cycloadditions (SPAAC)			OCT, DIFO, BCN	0.0012-0.14 (ACN)	no metal catalyst; some octynes susceptible to thiol attack	Agard 2004
			BARAC, DIBO, DIBAC	0.17-0.96 (ACN)		Baskin 2006
Alternative 1,3-dipolar cycloadditions			0.013-3.9 (ACN/H ₂ O)	some nitrones susceptible to hydrolysis	McKay 2010	
			30 (H ₂ O)	nitrile oxide generated <i>in situ</i> (photolysis)	Gutsmiedl 2009	
			0.15-58 (1:1 ACN:PBS)	nitrile imine generated <i>in situ</i> (photolysis)	Yu 2012	
			13.5 (ACN/H ₂ O)	diazo generated <i>via</i> Staudinger reduction	McGrath 2012	
			70,000-106,000 (H ₂ O)	oxanorbornadiene susceptible to reactivity with basic amino acids	van Berkel 2007	

Inverse Electron-Demand Diels-Alder (IED-DA)			210-2,800,000 (PBS, 37°C)	TCO isomerizes over time	Blackman 2008
			0.12-9.46 (95:5 H ₂ O:MeOH)	norbornene and functionalized cyclopropenes are shelf stable	Devaraj 2008
			0.03-13 (12-15% DMSO in PBS)		Yang 2012
Hetero-Diels-Alder			0.0015 (5:1 H ₂ O:MeOH)	quinone methide generated <i>in situ</i>	Li 2013
Miscellaneous ligations			0.03-0.3 (PBS/tBuOH)	ruthenium catalyst required	Lin 2013
			0.25 (PBS/EtOH)	requires nickel-stabilization of pi-electrons	Sletten 2011
			0.12-0.57 (THF/H ₂ O)	products hydrolyze in water	Stockmann 2011
	Ar-X	R-B(OH) ₂ , [Pd]	N/A	palladium catalyst required; boronic acids are moderately cytotoxic	Chalker 2009
	Ar-X			palladium catalyst required	Kodama 2007

1.2a Polar reactions

Reactions between nucleophiles and electrophiles (i.e., polar reactions) are omnipresent in organic synthesis, but only a handful are suitable for use in biological settings. Among the most well established for biomolecule labeling are aldehyde and ketone condensations [5, 6]. Aldehydes and ketones—as electrophiles—are rare commodities on proteins and other biopolymers, and they can be selectively ligated with alpha-effect nucleophiles (e.g., hydrazides and aminoxy compounds) to form relatively stable Schiff bases [7-12]. Ketones and aldehydes have been appended to a variety of biomolecules, including proteins [13, 14] and glycans, [15, 16] and ultimately targeted with functionalized hydrazides or aminoxy compounds for visualization or retrieval.

While versatile, these chemistries have some liabilities with regard to biomolecule labeling. For example, the reaction products—hydrazones, in particular—are susceptible to hydrolysis in cellular environments [17]. To generate more stable adducts, Bertozzi and colleagues recently developed an aldehyde condensation that exploits aminoxy-tryptamines [18, 19]. This transformation is a variant of the classic Pictet-Spengler reaction: the aldehyde and tryptamine initially react to form an oxyiminium ion; this intermediate is subject to further indole attack and ultimately C-C bond formation. Ketone and aldehyde condensations are also not 'bioorthogonal' in the truest sense of the word. Aldehydes are present in glucose and other abundant intracellular metabolites; ketones are found in mammalian hormones and microbial natural products. These endogenous molecules can be inadvertently labeled when cells are exposed to aminoxy or hydrazide probes.

To avoid cross-reactivity altogether, reactions that employ non-natural functional groups are highly prized. The quintessential example of this sort is the Staudinger ligation of organic

azides and triaryl phosphines [20]. Organic azides are mild electrophiles and have yet to be found in eukaryotes. Similarly, triaryl phosphines—as soft nucleophiles—are virtually absent in living systems [21, 22]. While tolerant of biological functionality, azides and phosphines react readily with one another [23, 24]. In the case of the Staudinger ligation, the reaction forges stable amide linkages between the two reactants. This transformation is slower than most bioorthogonal chemistries, but remains a popular choice for *in vivo* work, owing to its remarkable selectivity and compatibility with cells, tissues, and even live animals [25-29].

1.2b Cycloadditions

Nearly all recent additions to the bioorthogonal toolkit comprise cycloadditions. Two classes, in particular—dipolar cycloadditions and Diels-Alder chemistries—have emerged as excellent options for derivatizing biomolecules with visual tags and other probes.

Dipolar cycloadditions. The most popular bioorthogonal cycloadditions also capitalize on the unique features of azides [30]. In addition to being mild electrophiles, organic azides are 1,3-dipoles capable of reacting with terminal alkynes [31-33]. To proceed at a reasonable rate, though, this reaction requires a Cu(I) catalyst. The copper-catalyzed azide-alkyne cycloaddition (CuAAC)—or “click” chemistry—occurs readily in aqueous environments and provides chemically robust triazoles [34-36]. The speed and relative simplicity of this transformation has been widely exploited for biomolecule visualization (mostly in fixed cells) [37-39] and biomolecule retrieval in various “-omics” studies [40-43]. Azides and alkynes also rank among the smallest bioorthogonal motifs and are non-perturbing to most biomolecules. For this reason, CuAAC has been the “go-to” choice for monitoring the activities and targets of numerous small molecules, including enzyme inhibitors and therapeutic drugs [44-47].

While routinely applied *in vitro*, CuAAC has been slower to transition *in vivo*. This is due, in part, to the tri-component nature of the reaction and its requirement for a cytotoxic metal catalyst. To obviate the need for Cu(I), Bertozzi and colleagues exploited an alternative mechanism to drive azide-alkyne cycloaddition: ring strain [48, 49]. They initially designed a cyclooctyne scaffold (OCT) comprising C≡C-C bonds that were “bent” from the preferred linear geometry by 17 degrees [50]. The free energy from such bond deformation was sufficient to promote azide-alkyne reaction under ambient conditions and without metal catalyst. This strain-promoted azide-alkyne cycloaddition (SPAAC) has been widely used to tag azido proteins and other biomolecules on live cells [51, 52] and in living organisms [53-55].

Iterative modifications to OCT have been reported over the past five years, and there are now over 10 different cyclooctynes suitable for bioorthogonal labeling [56]. Notable examples include DIBO [52] and BARAC [57] (Table 1-1). These reagents comprise cyclooctyne cores fused to benzene rings. The pendant rings provide increased strain energy and ultimately accelerate the cycloaddition reaction with azides [58]. While DIBO and BARAC provide among the fastest SPAAC rates, their increased hydrophobicity can result in non-specific “sticking” to other biomolecules and insertion into cell membranes [59].

Cyclooctynes are also reactive partners for 1,3-dipoles other than azides. Nitrones [60, 61], nitrile oxides [62, 63], and diazo groups [64, 65] have all been appended to various proteins and selectively ligated with strained alkynes. Most of these cycloadditions are quite fast, with second order rate constants ranging from 1-50 M⁻¹ s⁻¹ [60, 66]. However, the rapid reactivity afforded by these strong dipoles often comes at the expense of their poor stability in aqueous media. Nitrile oxides are particularly prone to hydrolysis and must be generated *in situ*—near the site of intended reactivity—for efficient ligation.

In addition to alkynes, strained *alkenes* are good candidates for bioorthogonal dipolar cycloadditions. Lin and coworkers recently reported that cyclopropene—a highly strained alkene—reacts readily with nitrile imines to form pyrazoline adducts [67]. Nitrile imines, like other strong dipoles, are prone to rapid hydrolysis and must be generated *in situ*. Fortunately, these motifs can be generated from relatively stable precursors, including tetrazoles and chlorooximes, using fairly mild conditions (short pulses of UV light and mild base, respectively) [67-69]. These conditions are compatible with a variety of biomolecules and, in some cases, live cells.

Diels–Alder cycloadditions. Strained molecules also play lead roles in the second major class of bioorthogonal cycloadditions: Diels–Alder ligations. In 2008, Fox and coworkers demonstrated that the strained molecule *trans*-cyclooctene (TCO) reacts efficiently with electron-deficient tetrazines in aqueous solution and in the presence of model proteins [70]. These inverse electron-demand Diels–Alder (IED-DA) reactions are the fastest bioorthogonal transformations on record, with rate constants ranging from 10^3 - 10^6 M⁻¹ s⁻¹ in some cases [71, 72]. Due to their rapid reactivity, TCO-tetrazine ligations have found immediate application in a variety of biological pursuits, most notably live animal imaging [73-76]. Covalent tagging reactions in rodents and other organisms demand ultra-fast reactions as only small amounts of reagent can typically be used. Unreacted/unbound probe (which cannot be simply rinsed away) is thus kept to a minimum, resulting in high signal-to-noise ratios [77]. A variety of sterically and electronically modified tetrazines have also been developed that exhibit different IED-DA rates, enabling relatively facile “tuning” of the reaction [71, 78, 79].

Tetrazine reactivity with other strained alkenes has also been exploited for bioorthogonal ligation [76, 80, 81]. Coinciding with the initial report on TCO, Hilderbrand and coworkers

demonstrated IED-DA reactivity with norbornene (NB) and electron-deficient tetrazines. NB reacts more sluggishly than TCO, but is far more stable in solution and upon storage. The embedded *trans*-double bond in TCO can isomerize to the *cis* configuration over time, resulting in the accumulation of a non-reactive scaffold [73]. We and others have also shown that another strained alkene—cyclopropene—is amenable to reactions with various tetrazines. Cyclopropenes possess a distinct advantage over TCO owing to their smaller size and broad compatibility with cellular enzymes [67, 81, 82]. However, the IED-DA reactions between these small microcycles and tetrazine are considerably slower than those with TCO. Further modifications to the cyclopropene core may improve these rates.

1.3 Making a match

With over 20 bioorthogonal transformations now reported in the literature, and new ones being discovered at a rapid pace, selecting the “best fit” for a given application is non-trivial. The chemistries vary widely in terms of their selectivities and biocompatibilities, and many of their perceived strengths and weaknesses remain anecdotal. Below, we outline some general considerations for the end user of bioorthogonal chemistries and offer some guidelines for selecting among the options (Figure 1-2). In general, experiments with live cells or tissues demand the most selective reactions, with little tolerance for off-target labeling. Experiments with fixed cells or isolated biomolecules, by contrast, are typically less demanding in terms of reagent selectivity. Thus, they can interface with a larger number of chemistries.

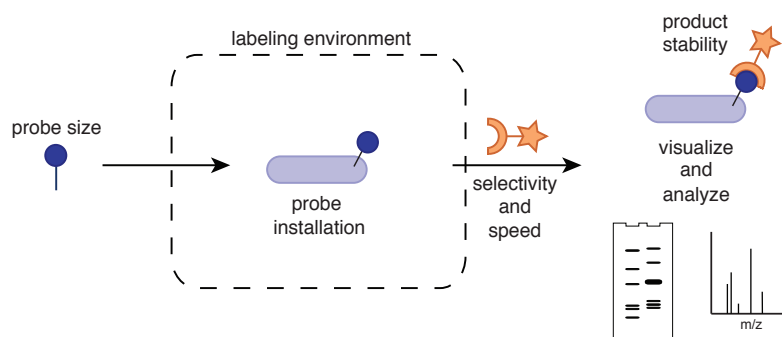


Figure 1-2. Selecting an appropriate bioorthogonal chemistry. Considerations include the target biomolecule and mode of functional group installation, the size of the labeling agents, and the stability of the covalent adduct. Bioorthogonal reaction selectivity and speed are also important parameters.

Seeing the big picture. The selective tagging of any biomolecule requires that one of the chemical motifs (e.g., aldehyde, azide, alkyne) is directly attached to the target of interest. Several options exist for installing bioorthogonal functionality onto protein targets (Figure 1-3A). These biopolymers can be readily derivatized at their N- or C-termini using mild chemistries [83-85]. A variety of bioconjugation reactions can also be employed to affix bioorthogonal motifs to Lys and Cys residues [86], as well as to aromatic amino acids [87-90]. For example, Van Hest and colleagues reported a facile method to install azido groups onto Lys side chains via diazo transfer [91]. While efficient, these approaches are inherently non-specific and typically result in more than one modification to the protein backbone.

For *site-specific* installation of bioorthogonal motifs, enzymatic tagging platforms are available. Most of these strategies exploit ligases that have been engineered to append modified substrates (bearing ketones, cyclooctynes and other reactive motifs) to defined acceptor peptides [92-98]. In a recent example, Ting and coworkers generated a lipoic acid ligase variant (LplA) capable of appending small molecule azides to lysine residues within a 13-residue consensus sequence [99-102]. Once installed, the azido motifs were subsequently ligated with a variety of

functionalized cyclooctynes and visualized over time. This two-step, enzyme-mediated tagging strategy can be used to tag protein targets *in vitro* and in a variety of cellular compartments. Additionally, the LplA acceptor peptide, similar to those for other engineered enzymes, is highly modular, and can be grafted into multiple proteins.

Bioorthogonal motifs can also be introduced site-specifically into proteins using unnatural amino acid mutagenesis [103, 104]. This strategy exploits unique amino-acyl tRNA synthetase (AARS)/tRNA pairs to deliver non-natural amino acids into growing polypeptide chains in response to unique codons. Keto, azido, and alkynyl versions of Phe have all been introduced into protein targets (at defined positions) via this approach [105, 106]. Amino acids outfitted with larger motifs—including TCO and various cyclooctynes—have been similarly incorporated into protein targets using newly engineered AARS/tRNA pairs [67, 107-113]. Continued advancements in this field will enable multiple bioorthogonal units to be selectively installed in protein targets both *in vitro* and *in vivo* [114, 115]. It is also possible to incorporate bioorthogonal amino acids into target proteins relying on the cell's own endogenous machinery, without the need for unique AARS/tRNA pairs [116, 117]. These *residue*-specific replacement strategies are inherently non-selective, but are nonetheless attractive for generating functionalized proteins owing to their high yields and relative simplicity. Since these methods rely on native biosynthetic pathways—and enzymes with stringent substrate specificities—they are only compatible with non-natural amino acids bearing small chemical appendages (e.g. ketones, azides, alkynes).

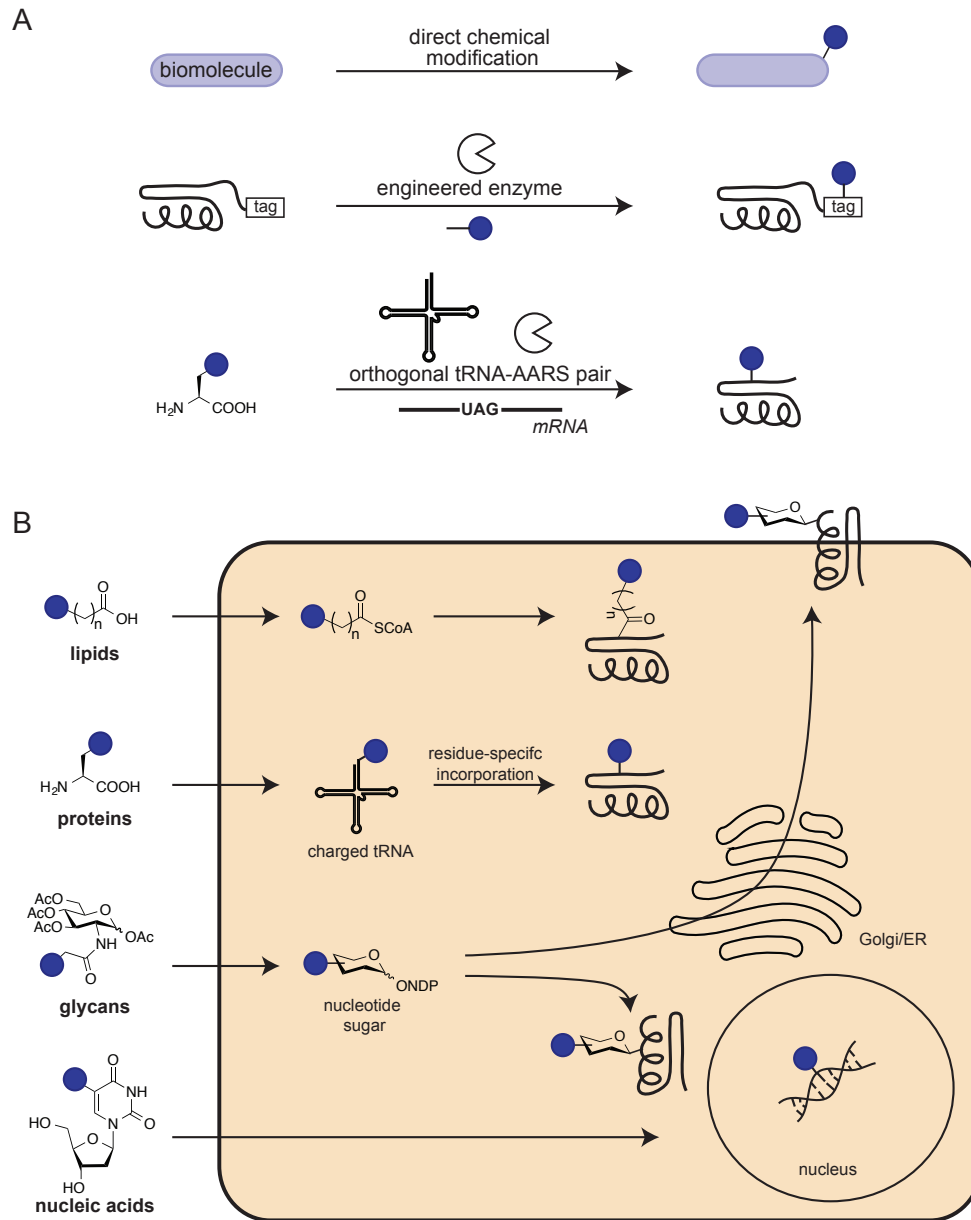


Figure 1-3. Installing bioorthogonal functionality into target biomolecules. (A) Several strategies exist to introduce bioorthogonal motifs (blue circles) into protein targets. These include direct chemical functionalization (top), enzymatic ligation of the requisite motifs onto defined acceptor peptides (tags, middle), and unnatural amino acid mutagenesis with functionalized amino acids and orthogonal tRNA/AARS pairs (bottom). (B) Unique chemical handles can be metabolically introduced into proteins and non-proteinaceous biomolecules alike via cellular biosynthesis. In this approach, metabolic precursors (left) outfitted with bioorthogonal functional groups (blue circles) are supplied to cells and ultimately incorporated into target biomolecules via the cell's own enzymatic machinery.

For non-proteinaceous biomolecules, fewer methods exist for installing bioorthogonal functional groups. Direct chemical modification is possible, although impractical for most applications [9, 118]. Mutant enzymes are also available to append reactive motifs to glycans, but most are not generalizable and confined to *in vitro* work [119]. For experiments in cells and tissues, the majority of non-proteinaceous biomolecules can be outfitted with bioorthogonal probes via cellular biosynthesis (Figure 1-3B). This approach relies on metabolic precursors that are supplied to cells and ultimately installed into target biomolecules using the cell's own enzymatic machinery [2]. Similar to the residue-specific tagging of proteins mentioned above, only small bioorthogonal motifs are broadly compatible with native cellular enzymes and thus good candidates for this approach. Upon installation, the bioorthogonal motifs can be covalently ligated with probes for visualization or enrichment.

Setting the limits. A primary consideration in choosing chemistries for biological use is the biocompatibility of the reagents. Comprehensive toxicity profiles have not been generated for most of the common bioorthogonal transformations. However, most can be safely used (with milli- to micromolar concentrations of reagents) without detriment to biological systems. One exception is the copper-catalyzed azide-alkyne cycloaddition (CuAAC). Copper ions are readily chelated by native amino acids and can induce the formation of reactive oxygen species, resulting in damage to cells and tissues. Concerns about copper cytotoxicity have largely relegated CuAAC to experiments with isolated biomolecules and fixed cells/tissues over the past decade. In recent years, though, Finn, Wu and others have identified ligands that sequester copper from unintended targets and offer improved cell compatibility [120-124]. Ting and coworkers also devised a strategy to reduce the overall amount of copper required for efficient

CuAAC [125]. Their approach features picolyl azide, a chelating scaffold that pre-organizes the copper and azido reactants. This arrangement promotes cycloaddition at exceedingly low—and biocompatible—concentrations of metal [126, 127]. The picolyl azide unit can also be appended to numerous proteins of interest using the engineered LplA ligase [100]. Collectively, these advancements will facilitate the wider adoption of CuAAC in live cell labeling applications.

A second consideration relevant to biocompatibility involves the selectivity of the reactants. For the majority of the transformations in Table 1-1, some degree of non-specific labeling has been observed. Cyclooctynes, for example, are prone to attack by cysteine and other biological nucleophiles [58, 128, 129]. This side reactivity has stymied their use in some intracellular labeling applications, but can largely be avoided in environments devoid of free thiols (e.g., extracellular spaces or where thiols have been capped with acylating agents). Non-specific reactivity has also been observed in CuAAC reactions when excess alkyne is used [130, 131]. These conditions promote the formation of reactive copper acetylides. Fortunately, such side reactivity can be mitigated by simply “reversing” the reactants—using low concentrations of alkyne and excess azide to drive the reaction. Cravatt and Speers were among the first to note improved signal-to-noise ratios with these conditions in protein profiling experiments [131].

A final point to consider with regard to reagent biocompatibility is the overall solution stability of the reactants and their covalent adducts. Azides, alkynes, and their triazole products are remarkably stable in aqueous buffers and a variety of cellular environments. Many of the most reactive bioorthogonal reagents, though, are prone to hydrolysis. For example, the most electron-deficient tetrazines used for rapid IED-DA reactions generally hydrolyze readily in water and only tolerate incubation times on the minutes-to-hours time scale (ligation reactions on

the seconds-to-minutes time scale). Similarly, nitrile imines and other 1,3-dipoles (other than azides) react readily with water and must be generated *in situ* for covalent tagging experiments.

Based on toxicity and selectivity considerations, the Staudinger ligation of azides and triaryl phosphines ranks among the best reactions for biological labeling applications. Minimal-to-no background labeling has been observed with these reagents under a variety of conditions. Indeed, this reaction has been employed in proteomics studies where the analytes of interest are in low abundance and sensitive detection is required [132, 133]. It should be noted, though, that phosphine reagents are prone to non-specific oxidation over time [20]. While these reactivities do not contribute to background labeling *per se*, they do reduce the effective concentration of the probe available for labeling.

Sizing up the competition. Small bioorthogonal motifs are generally desired in any application to avoid perturbing the biological system under study. For experiments requiring the metabolic installation of chemical probes, reagent size can be the deciding factor as native cellular enzymes do not often tolerate large chemical appendages. Based on size considerations alone, azides and terminal alkynes have emerged as preferred scaffolds in bioorthogonal labeling [134]. Both of these moieties are remarkably compact, comprising a mere three atoms, and are innocuous to most (but not all) biosynthetic pathways [135]. Azido metabolites have been used to target proteins [117, 136], glycans [137-139], and lipids [140, 141], among other biomolecules [142]. In all cases, the azido species were readily detected upon covalent reaction with a complementary alkyne, cyclooctyne, or phosphine reagent. Alkynyl metabolites have been similarly employed in biological experiments [38, 143-148]. A suite of alkyne-selective reactions does not yet exist; therefore, these probes are typically detected using CuAAC. Ketones and

aldehydes rival azides and alkynes in terms of size. However, their somewhat sluggish reactivities at neutral pH have limited their broad utilization *in cellulo*.

Identifying alternatives to the azide and alkyne—that rival these motifs in terms of size and selective reactivity—is an ongoing challenge. Alkenes are options, although these small motifs are not robustly reactive with complementary probes [149]. Nitrile imines and other 1,3-dipoles are also candidates, though most are not amenable to long-term storage and must be generated *in situ* [62, 69, 150-154]. Cyclopropene, a recently reported bioorthogonal reagent, appears to strike a balance between robust reactivity and shelf stability. We and others have shown that these microcycles can be appended to discrete monosaccharides and metabolically incorporated into cellular glycans and proteins [80-82, 149]. More work must be done, though, to assess the long-range biological compatibility and versatility of these motifs.

Assessing the need for speed. Reaction rate is another important parameter to assess when selecting suitable bioorthogonal chemistries. For slow reactions, a large amount of one reagent must typically be used to drive the labeling event. Large amounts of any of reagent can be prohibitively expensive or potentially toxic. Fast reactions largely avoid these issues, as only minimal quantities are required. When the need for speed is paramount, the IED-DA reaction between tetrazine and TCO is unrivaled. The rates of these reactions range from 10^3 - 10^6 $M^{-1}s^{-1}$, making them appropriate for biological processes that occur on the minutes-to-seconds time scale or that involve biomolecule targets in low abundance (e.g., *in vivo* imaging) [71, 155]. In a recent example, Weissleder and coworkers utilized the TCO-tetrazine reaction to image tumor cells in whole animals. TCO was appended to a tumor-targeting antibody (α -A33) that localized to colon cancer grafts upon injection [74]. Following clearance of unbound antibody, the cancer

cells could be readily visualized using as little as 2 mM of a tetrazine-¹⁸F conjugate to tag the tumor-bound TCOs. Similar imaging experiments with Staudinger ligation and SPAAC chemistries failed to provide adequate signal-to-noise ratios, owing to the slower kinetics of these transformations and the need for a large amount of reagent [156-158].

Activatable probes can be considered when using large amounts of labeling reagent is unavoidable. These reagents produce detectable signal only upon covalent reaction. Thus, the probe can be added in excess to drive the reaction without the need for extensive rinsing. Fluorogenic cyclooctynes have been developed for this purpose; these scaffolds “turn on” fluorescence only upon reaction with azides [159-161]. In a recent example, Boons and coworkers reported an activatable version of DIBO that exhibits a 1000-fold increase in fluorescence upon azide ligation [160]. Activatable tetrazines [159, 162] and azides [163, 164] are also available.

Fine-tuning the selection. Like most experiments, the application of any bioorthogonal chemistry often requires some degree of optimization. Thus, it is helpful to have access to a variety of scaffolds that operate via a similar mechanism, but differ in such parameters as rate, solubility, and lipophilicity. As mentioned above, a panel of cyclooctynes that differ in their electronic and solubility properties is now available; these reagents can be “matched” to a given application involving azide ligation. Similarly, a wide variety of tetrazine probes for IED-DA cycloadditions have been reported [78, 165]. Mehl and colleagues recently capitalized on tetrazine “tunability” to install these non-natural motifs into recombinant proteins [108]. Tetrazines exploited for rapid IED-DA reactivity comprise electron-withdrawing groups, making them susceptible to hydrolysis and reactivity with endogenous thiols. This instability is not

detrimental in most applications where short labeling times are employed. In the case of recombinant protein production, though, long incubation times are necessary to biosynthetically introduce amino acids into growing polypeptide chains. The authors identified a tetrazine with electron-*donating* groups that harbored the requisite stability and compatibility for long-term *in vivo* use and incorporation into recombinant proteins [53, 166].

The Staudinger ligation is also quite “tunable,” although most methods to boost reactivity also accelerate phosphine oxidation [167, 168]. Phosphine probes can be manipulated to produce “turn-on” fluorescence in response to azide ligation, similar to their octyne counterparts [169]. Raines and others have also developed phosphine scaffolds that can be cleaved from the product post-ligation, leaving behind native amide bonds [170, 171]. These latter reagents participate in “traceless” Staudinger ligations and have been particularly useful in protein semi-synthesis [172], installing photo-crosslinking groups on cellular metabolites [173], and templating biomaterials *in vivo* [174].

Knowing the market. The accessibility of required reactants can also be a deciding factor when selecting a bioorthogonal chemistry. Based on reagent availability and ease of use, CuAAC ranks among the most accessible reactions to date. A variety of alkyne- and azide-modified substrates can be purchased from commercial sources, and many can be used directly in metabolic labeling experiments. Several additional azide and alkyne precursors are available that can be readily appended to biomolecules using straightforward chemistries. The availability of reagents, coupled with the relatively user-friendly features of the reaction, have enabled the rapid adoption of CuAAC in diverse disciplines. This chemistry has been used to monitor

oligonucleotide production [38, 136], construct organotypic hydrogels [175, 176], and even visualize temporal changes in glycosylation relevant to development [138, 177].

Other bioorthogonal transformations have been slower to transition to the wider biological community, mostly owing to their more challenging syntheses and lack of commercial suppliers. However, a number of reagent precursors (based on BCN, TCO, tetrazine, and phosphine scaffolds) have been recently made available. We anticipate that these probes will bolster new discoveries in a wide variety of fields.

1.4 Moving forward

Identifying chemistries for efficient biomolecule tagging in increasingly complex environments—cells, animal models, and even humans—is an ongoing challenge [155]. The search for ever faster and more selective reactions will be aided by explorations into new realms of chemical space. Already, Rao, Chin and others have discovered that cyanobenzothiazole condensations exhibit both rapid and specific reactivity with aminothiols [178, 179]. Similar advances are being made in the realm of bioorthogonal organometallic transformations. In seminal work, the Davis group reported ruthenium-catalyzed cross-metathesis reactions for efficient protein tagging [180-183], along with palladium-catalyzed cross-couplings amenable to targeting proteins, glycans, and nucleotides [184-189].

A corollary challenge to identifying new transformations is elucidating methods to *control* bioorthogonality (i.e., turning functional groups “on” and “off”). Such “on-demand” reactivity is especially critical for reagents that are only semi-stable in biological environments. Photochemical activation is a particularly attractive mechanism for generating reactivity “on demand” [68, 69, 190-195]. Pulsed light can be controlled both spatially and temporally, and

thus offers a method to release bioorthogonal reagents and localize reactivity [196, 197] (Figure 1-4). Popik and coworkers exploited the photo-triggered release of cyclooctyne reagents to control azide-alkyne reactivity [195, 198]. In related work, Lin and colleagues utilized “photo-click” chemistry to tag alkene-modified proteins [68]. The derivatized proteins were incubated with tetrazole probes. Upon UV illumination, tetrazoles photolyze to generate nitrile imines that can ligate terminal alkenes. The spatial resolution of these and other photo-click reactions is dependent on the lifetime of the liberated reagent. For nitrile imine, the lifetime is relatively short, as the 1,3-dipole is subject to rapid water quenching [67]. This “react” or “self-destruct” scenario enables more focal labeling and thus excellent spatial resolution. Continued development of mild methods to release bioorthogonal reagents “on-demand,” including two-photon absorption and selective chemical reactions, are important pursuits [192, 193, 199-201].

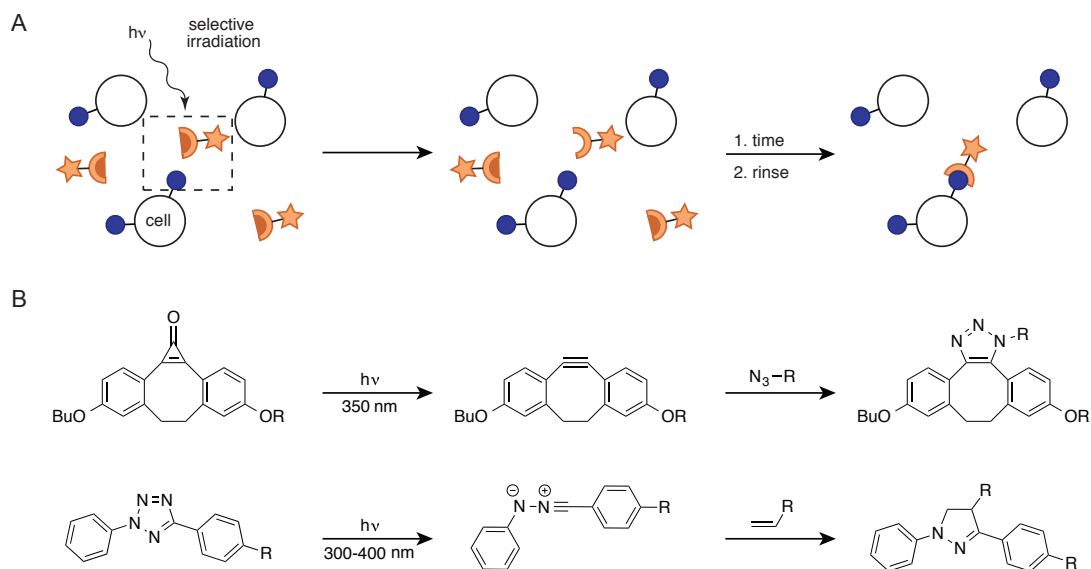


Figure 1-4. “On-demand” bioorthogonal reactivity. (A) Bioorthogonal functionality can be revealed *in situ* in live cells using pulsed light. Selective irradiation liberates the desired functionality only in the region of interest, conferring both spatial and temporal resolution on the labeling reaction. (B) Two examples of “photo-click” reactions. Irradiation of the cyclopropanone scaffold releases a functional cyclooctyne capable of reacting with azides (top). Similarly, irradiation of the tetrazole scaffold generates a nitrile imine (bottom). This 1,3-dipole can covalently label nearby alkenes.

As new bioorthogonal reagents continue to be explored and validated, another major challenge looms: identifying transformations that not only work well *in vivo*, but also work well with *existing* bioorthogonal chemistries. Many of the most common bioorthogonal reactions are incompatible with one another in live cells. For example, certain cycloalkynes have been shown to be highly reactive with tetrazine and therefore do not lend themselves to multi-component studies (Figure 1-5) [202, 203]. However, careful selection of bioorthogonal reagents can enable simultaneous and selective labeling [110, 202]. Recently, we and others demonstrated the mutual orthogonality of the alkene-tetrazine ligation with variants of SPAAC [81, 109, 149, 204, 205] In one example, Hilderbrand and coworkers utilized Herceptin-TCO and cetuximab-DBCO antibody conjugates to target A431 and SKBR3 cells, respectively [204]. Upon co-administration of the complementary azido- and tetrazine-fluorophores, both cell populations were selectively labeled and visualized.

The identification of mutually orthogonal transformations is being aided by computational studies. Houk and colleagues developed a distortion-interaction model that has proven effective at predicting reactivity of strained molecules with 1,3-dipoles and dienes [58, 206, 207]. Steric clashes between many of the large, strained molecules can be exploited to disfavor certain cycloadditions, while promoting others [203]. In recent work, we utilized this model to identify two sets of cyclopropenes—differing by the presence of a single methyl group—that exhibit unique cycloaddition preferences [208]. These unique reactivities were employed to append unique fluorophores to model proteins. We anticipate that computational algorithms will continue to have a major impact in identifying combinations of mutually orthogonal transformations or those that can be used sequentially [203, 209]. Assays to rapidly identify candidate classes of probes will also be helpful in this regard [210].

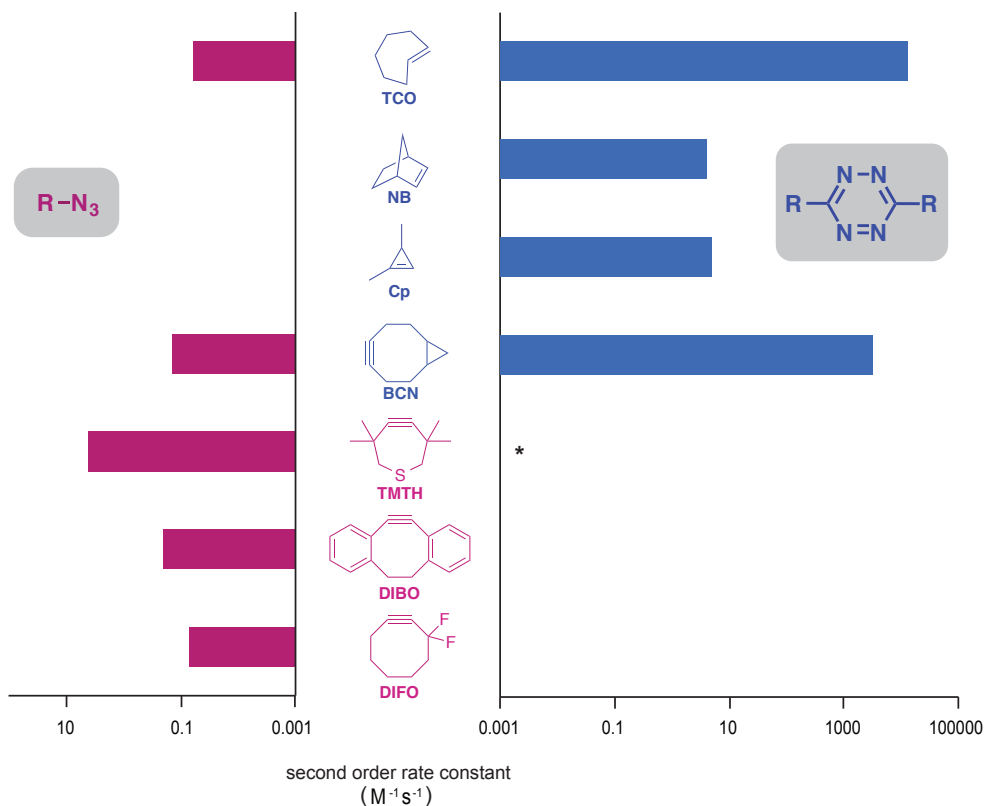


Figure 1-5. Identifying mutually orthogonal transformations. Strained alkenes and alkynes possess dramatically different reactivities with azido (left) and tetrazine (right) probes. The alkenes in blue react rapidly with tetrazine via IED-DA chemistries, while the alkynes in red demonstrate rapid reactivity with azides. Bicyclononyne (BCN, black) does not significantly favor tetrazines or azides in terms of reaction rate. With judicious selection, some of these reagents can be used concurrently in bioorthogonal labeling applications. *Determined computationally to be unreactive with disubstituted tetrazines [203].

1.5 Conclusions

The past decade has seen a marked expansion of the bioorthogonal toolkit, with a variety of polar reactions and cycloaddition chemistries demonstrating utility for biomolecule labeling in complex environments. As the number of bioorthogonal reactions continues to grow, selecting an appropriate chemistry for a given application is increasingly challenging. The reactions differ in a number of key attributes, including selectivities and rates, and understanding the “personalities” of each transformation is key to their successful implementation.

1.6 Objectives

Bioorthogonal chemistry had been largely focused on the azide. I sought to develop new ligations to both improve upon the azide ligations weaknesses, but also to be used in conjunction with the azide for multi-target detection. Objectives included the following:

1. Identify small, stable cyclopropene scaffolds compatible with biological functional.
2. Characterize selective reactions of cyclopropenes with tetrazines and 1,3-dipoles.
3. Establish cyclopropene as a broadly useful chemical reporter.
4. Develop cyclopropene ligations to use in tandem with bioorthogonal azide ligations for probing multiple biomolecules in tandem.
5. Identify new mutually orthogonal reactions with new cyclopropene scaffolds and other existing bioorthogonal reagents.

References

1. Chang, P. V., and Bertozzi, C. R. (2012) Imaging beyond the proteome, *Chem Commun (Camb)* 48, 8864-8879.
2. Prescher, J. A., and Bertozzi, C. R. (2005) Chemistry in living systems, *Nat Chem Biol* 1, 13-21.

3. Giepmans, B. N., Adams, S. R., Ellisman, M. H., and Tsien, R. Y. (2006) The fluorescent toolbox for assessing protein location and function, *Science* 312, 217-224.
4. Scheck, R. A., and Schepartz, A. (2011) Surveying protein structure and function using bis-arsenical small molecules, *Acc Chem Res* 44, 654-665.
5. Cornish, V. W., Hahn, K. M., and Schultz, P. G. (1996) Site-specific protein modification using a ketone handle, *J Am Chem Soc* 118, 8150-8151.
6. Sletten, E. M., and Bertozzi, C. R. (2009) Bioorthogonal chemistry: fishing for selectivity in a sea of functionality, *Angew Chem Int Edit* 48, 6974-6998.
7. Rideout, D. (1986) Self-assembling cytotoxins, *Science* 233, 561-563.
8. Shao, J., and Tam, J. P. (1995) Unprotected peptides as building-blocks for the synthesis of peptide dendrimers with oxime, hydrazone, and thiazolidine linkages, *J Am Chem Soc* 117, 3893-3899.
9. Zeng, Y., Ramya, T. N., Dirksen, A., Dawson, P. E., and Paulson, J. C. (2009) High-efficiency labeling of sialylated glycoproteins on living cells, *Nat Methods* 6, 207-209.
10. Crisalli, P., and Kool, E. T. (2013) Water-soluble organocatalysts for hydrazone and oxime formation, *J Org Chem* 78, 1184-1189.
11. Dirksen, A., and Dawson, P. E. (2008) Rapid oxime and hydrazone ligations with aromatic aldehydes for biomolecular labeling, *Bioconjug Chem* 19, 2543-2548.
12. Dutta, D., Pulsipher, A., Luo, W., and Yousaf, M. N. (2011) Synthetic chemoselective rewiring of cell surfaces: generation of three-dimensional tissue structures, *J Am Chem Soc* 133, 8704-8713.
13. Wang, L., Zhang, Z., Brock, A., and Schultz, P. G. (2003) Addition of the keto functional group to the genetic code of Escherichia coli, *Proc Natl Acad Sci U S A* 100, 56-61.
14. Wang, L., Xie, J., and Schultz, P. G. (2006) Expanding the genetic code, *Annu Rev Biophys Biomol Struct* 35, 225-249.

15. Mahal, L. K., Yarema, K. J., and Bertozzi, C. R. (1997) Engineering chemical reactivity on cell surfaces through oligosaccharide biosynthesis, *Science* 276, 1125-1128.
16. Chang, P. V., Prescher, J. A., Hangauer, M. J., and Bertozzi, C. R. (2007) Imaging cell surface glycans with bioorthogonal chemical reporters, *J Am Chem Soc* 129, 8400-8401.
17. Kalia, J., and Raines, R. T. (2008) Hydrolytic stability of hydrazones and oximes, *Angew Chem Int Ed* 47, 7523-7526.
18. Agarwal, P., van der Weijden, J., Sletten, E. M., Rabuka, D., and Bertozzi, C. R. (2013) A Pictet-Spengler ligation for protein chemical modification, *Proc Natl Acad Sci U S A* 110, 46-51.
19. Agarwal, P., Kudirka, R., Albers, A. E., Barfield, R. M., de Hart, G. W., Drake, P. M., Jones, L. C., and Rabuka, D. (2013) Hydrazino-pictet-spengler ligation as a biocompatible method for the generation of stable protein conjugates, *Bioconjug Chem* 24, 846-851.
20. Schilling, C. I., Jung, N., Biskup, M., Schepers, U., and Brase, S. (2011) Bioconjugation via azide-Staudinger ligation: an overview, *Chem Soc Rev* 40, 4840-4871.
21. Griffin, R. J. (1994) The medicinal chemistry of the azido group, *Prog Med Chem* 31, 121-232.
22. Brase, S., Gil, C., Knepper, K., and Zimmermann, V. (2005) Organic azides: an exploding diversity of a unique class of compounds, *Angew Chem Int Ed Engl* 44, 5188-5240.
23. Saxon, E., and Bertozzi, C. R. (2000) Cell surface engineering by a modified Staudinger reaction, *Science* 287, 2007-2010.
24. van Berkel, S. S., van Eldijk, M. B., and van Hest, J. C. (2011) Staudinger ligation as a method for bioconjugation, *Angew Chem Int Ed Engl* 50, 8806-8827.
25. Prescher, J. A., Dube, D. H., and Bertozzi, C. R. (2004) Chemical remodelling of cell surfaces in living animals, *Nature* 430, 873-877.

26. Neves, A. A., Stockmann, H., Harmston, R. R., Pryor, H. J., Alam, I. S., Ireland-Zecchini, H., Lewis, D. Y., Lyons, S. K., Leeper, F. J., and Brindle, K. M. (2011) Imaging sialylated tumor cell glycans in vivo, *FASEB Journal* 25, 2528-2537.
27. Hang, H. C., Geutjes, E. J., Grotenbreg, G., Pollington, A. M., Bijlmakers, M. J., and Ploegh, H. L. (2007) Chemical probes for the rapid detection of fatty-acylated proteins in mammalian cells, *J Am Chem Soc* 129, 2744-2745.
28. Kho, Y., Kim, S. C., Jiang, C., Barma, D., Kwon, S. W., Cheng, J., Jaunbergs, J., Weinbaum, C., Tamanoi, F., Falck, J., and Zhao, Y. (2004) A tagging-via-substrate technology for detection and proteomics of farnesylated proteins, *Proc Natl Acad Sci U S A* 101, 12479-12484.
29. Kaewsapsak, P., Esonu, O., and Dube, D. H. (2013) Recruiting the host's immune system to target *Helicobacter pylori*'s surface glycans, *ChemBioChem* 14, 721-726.
30. Debets, M. F., van der Doelen, C. W., Rutjes, F. P., and van Delft, F. L. (2010) Azide: a unique dipole for metal-free bioorthogonal ligations, *ChemBioChem* 11, 1168-1184.
31. Kolb, H. C., Finn, M. G., and Sharpless, K. B. (2001) Click chemistry: diverse chemical function from a few good reactions, *Angew Chem Int Ed* 40, 2004-2021.
32. Hein, J. E., and Fokin, V. V. (2010) Copper-catalyzed azide-alkyne cycloaddition (CuAAC) and beyond: new reactivity of copper(I) acetylides, *Chem Soc Rev* 39, 1302-1315.
33. Huisgen, R. (1963) 1,3-Dipolar cycloadditions. past and future, *Angew Chem Int Ed* 2, 565-598.
34. Rostovtsev, V. V., Green, L. G., Fokin, V. V., and Sharpless, K. B. (2002) A stepwise huisgen cycloaddition process: copper(I)-catalyzed regioselective "ligation" of azides and terminal alkynes, *Angew Chem Int Ed* 41, 2596-2599.
35. Tornøe, C. W., Christensen, C., and Meldal, M. (2002) Peptidotriazoles on solid phase: [1,2,3]-triazoles by regiospecific copper(i)-catalyzed 1,3-dipolar cycloadditions of terminal alkynes to azides, *J Org Chem* 67, 3057-3064.

36. Worrell, B. T., Malik, J. A., and Fokin, V. V. (2013) Direct evidence of a dinuclear copper intermediate in Cu(I)-catalyzed azide-alkyne cycloadditions, *Science* 340, 457-460.
37. Gramlich, P. M., Wirges, C. T., Manetto, A., and Carell, T. (2008) Postsynthetic DNA modification through the copper-catalyzed azide-alkyne cycloaddition reaction, *Angew Chem Int Ed Engl* 47, 8350-8358.
38. Salic, A., and Mitchison, T. J. (2008) A chemical method for fast and sensitive detection of DNA synthesis in vivo, *Proc Natl Acad Sci U S A* 105, 2415-2420.
39. Dieterich, D. C., Lee, J. J., Link, A. J., Graumann, J., Tirrell, D. A., and Schuman, E. M. (2007) Labeling, detection and identification of newly synthesized proteomes with bioorthogonal non-canonical amino-acid tagging, *Nat Protoc* 2, 532-540.
40. Salisbury, C. M., and Cravatt, B. F. (2007) Click chemistry-led advances in high content functional proteomics, *QSAR Comb Sci* 26, 1229-1238.
41. Nessen, M. A., Kramer, G., Back, J., Baskin, J. M., Smeenk, L. E., de Koning, L. J., van Maarseveen, J. H., de Jong, L., Bertozzi, C. R., Hiemstra, H., and de Koster, C. G. (2009) Selective enrichment of azide-containing peptides from complex mixtures, *J Proteome Res* 8, 3702-3711.
42. Zaro, B. W., Hang, H. C., and Pratt, M. R. (2013) Incorporation of unnatural sugars for the identification of glycoproteins, *Methods Mol Biol* 951, 57-67.
43. Leonard, S. E., and Carroll, K. S. (2011) Chemical 'omics' approaches for understanding protein cysteine oxidation in biology, *Curr Opin Chem Biol* 15, 88-102.
44. Speers, A. E., Adam, G. C., and Cravatt, B. F. (2003) Activity-based protein profiling in vivo using a copper(i)-catalyzed azide-alkyne [3 + 2] cycloaddition, *J Am Chem Soc* 125, 4686-4687.
45. Willems, L. I., van der Linden, W. A., Li, N., Li, K. Y., Liu, N., Hoogendoorn, S., van der Marel, G. A., Florea, B. I., and Overkleeft, H. S. (2011) Bioorthogonal chemistry: applications in activity-based protein profiling, *Acc Chem Res* 44, 718-729.
46. Cravatt, B. F., Wright, A. T., and Kozarich, J. W. (2008) Activity-based protein profiling: from enzyme chemistry to proteomic chemistry, *Annu Rev Biochem* 77, 383-414.

47. Bateman, L. A., Zaro, B. W., Miller, S. M., and Pratt, M. R. (2013) An alkyne-aspirin chemical reporter for the detection of aspirin-dependent protein modification in living cells, *J Am Chem Soc* 135, 14568-14573.
48. Sletten, E. M., and Bertozzi, C. R. (2011) From mechanism to mouse: a tale of two bioorthogonal reactions, *Acc Chem Res* 44, 666-676.
49. Jewett, J. C., and Bertozzi, C. R. (2010) Cu-free click cycloaddition reactions in chemical biology, *Chem Soc Rev* 39, 1272-1279.
50. Agard, N. J., Prescher, J. A., and Bertozzi, C. R. (2004) A strain-promoted [3 + 2] azide-alkyne cycloaddition for covalent modification of biomolecules in living systems, *J Am Chem Soc* 126, 15046-15047.
51. Baskin, J. M., Prescher, J. A., Laughlin, S. T., Agard, N. J., Chang, P. V., Miller, I. A., Lo, A., Codelli, J. A., and Bertozzi, C. R. (2007) Copper-free click chemistry for dynamic in vivo imaging, *Proc Natl Acad Sci U S A* 104, 16793-16797.
52. Ning, X., Guo, J., Wolfert, M. A., and Boons, G. J. (2008) Visualizing metabolically labeled glycoconjugates of living cells by copper-free and fast Huisgen cycloadditions, *Angew Chem Int Ed* 47, 2253-2255.
53. Chang, P. V., Prescher, J. A., Sletten, E. M., Baskin, J. M., Miller, I. A., Agard, N. J., Lo, A., and Bertozzi, C. R. (2010) Copper-free click chemistry in living animals, *Proc Natl Acad Sci U S A* 107, 1821-1826.
54. van den Bosch, S. M., Rossin, R., Renart Verkerk, P., Ten Hoeve, W., Janssen, H. M., Lub, J., and Robillard, M. S. (2013) Evaluation of strained alkynes for Cu-free click reaction in live mice, *Nucl Med Biol* 40, 415-423.
55. Baskin, J. M., Dehnert, K. W., Laughlin, S. T., Amacher, S. L., and Bertozzi, C. R. (2010) Visualizing enveloping layer glycans during zebrafish early embryogenesis, *Proc Natl Acad Sci U S A* 107, 10360-10365.
56. Ramil, C. P., and Lin, Q. (2013) Bioorthogonal chemistry: strategies and recent developments, *Chem Commun (Camb)*.
57. Jewett, J. C., Sletten, E. M., and Bertozzi, C. R. (2010) Rapid Cu-free click chemistry with readily synthesized biarylazacyclooctynones, *J Am Chem Soc* 132, 3688-3690.

58. Gordon, C. G., Mackey, J. L., Jewett, J. C., Sletten, E. M., Houk, K. N., and Bertozzi, C. R. (2012) Reactivity of biarylazacyclooctynones in copper-free click chemistry, *J Am Chem Soc* *134*, 9199-9208.
59. Debets, M. F., van Berkel, S. S., Dommerholt, J., Dirks, A. T., Rutjes, F. P., and van Delft, F. L. (2011) Bioconjugation with strained alkenes and alkynes, *Acc Chem Res* *44*, 805-815.
60. Ning, X., Temming, R. P., Dommerholt, J., Guo, J., Ania, D. B., Debets, M. F., Wolfert, M. A., Boons, G. J., and van Delft, F. L. (2010) Protein modification by strain-promoted alkyne-nitrone cycloaddition, *Angew Chem Int Ed Engl* *49*, 3065-3068.
61. McKay, C. S., Blake, J. A., Cheng, J., Danielson, D. C., and Pezacki, J. P. (2011) Strain-promoted cycloadditions of cyclic nitrones with cyclooctynes for labeling human cancer cells, *Chem Commun (Camb)* *47*, 10040-10042.
62. Sanders, B. C., Friscourt, F., Ledin, P. A., Mbua, N. E., Arumugam, S., Guo, J., Boltje, T. J., Popik, V. V., and Boons, G. J. (2011) Metal-free sequential [3 + 2]-dipolar cycloadditions using cyclooctynes and 1,3-dipoles of different reactivity, *J Am Chem Soc* *133*, 949-957.
63. Wendeln, C., Singh, I., Rinnen, S., Schulz, C., Arlinghaus, H. F., Burley, G. A., and Ravoo, B. J. (2012) Orthogonal, metal-free surface modification by strain-promoted azide-alkyne and nitrile oxide-alkene/alkyne cycloadditions, *Chem Sci* *3*, 2479-2484.
64. McGrath, N. A., and Raines, R. T. (2012) Diazo compounds as highly tunable reactants in 1,3-dipolar cycloaddition reactions with cycloalkynes, *Chem Sci* *3*, 3237-3240.
65. Chou, H. H., and Raines, R. T. (2013) Conversion of azides into diazo compounds in water, *J Am Chem Soc* *135*, 14936-14939.
66. McKay, C. S., Chigrinova, M., Blake, J. A., and Pezacki, J. P. (2012) Kinetics studies of rapid strain-promoted [3 + 2]-cycloadditions of nitrones with biaryl-aza-cyclooctynone, *Org Biomol Chem* *10*, 3066-3070.
67. Yu, Z., Pan, Y., Wang, Z., Wang, J., and Lin, Q. (2012) Genetically encoded cyclopropene directs rapid, photoclick-chemistry-mediated protein labeling in mammalian cells, *Angew Chem Int Ed* *51*, 10600-10604.

68. Song, W., Wang, Y., Yu, Z., Vera, C. I., Qu, J., and Lin, Q. (2010) A metabolic alkene reporter for spatiotemporally controlled imaging of newly synthesized proteins in mammalian cells, *ACS Chem Biol* 5, 875-885.
69. Song, W., Wang, Y., Qu, J., Madden, M. M., and Lin, Q. (2008) A photoinducible 1,3-dipolar cycloaddition reaction for rapid, selective modification of tetrazole-containing proteins, *Angew Chem Int Ed* 47, 2832-2835.
70. Blackman, M. L., Royzen, M., and Fox, J. M. (2008) Tetrazine ligation: fast bioconjugation based on inverse-electron-demand Diels-Alder reactivity, *J Am Chem Soc* 130, 13518-13519.
71. Selvaraj, R., and Fox, J. M. (2013) *trans*-Cyclooctene-a stable, voracious dienophile for bioorthogonal labeling, *Curr Opin Chem Biol* 17, 753-760.
72. Bach, R. D. (2009) Ring strain energy in the cyclooctyl system. The effect of strain energy on [3 + 2] cycloaddition reactions with azides, *J Am Chem Soc* 131, 5233-5243.
73. Rossin, R., van den Bosch, S. M., Ten Hoeve, W., Carvelli, M., Versteegen, R. M., Lub, J., and Robillard, M. S. (2013) Highly reactive *trans*-cyclooctene tags with improved stability for Diels-Alder chemistry in living systems, *Bioconjug Chem* 24, 1210-1217.
74. Devaraj, N. K., Thurber, G. M., Keliher, E. J., Marinelli, B., and Weissleder, R. (2012) Reactive polymer enables efficient in vivo bioorthogonal chemistry, *Proc Natl Acad Sci USA* 109, 4762-4767.
75. Rossin, R., Verkerk, P. R., van den Bosch, S. M., Vulderson, R. C., Verel, I., Lub, J., and Robillard, M. S. (2010) In vivo chemistry for pretargeted tumor imaging in live mice, *Angew Chem Int Ed Engl* 49, 3375-3378.
76. Devaraj, N. K., Weissleder, R., and Hilderbrand, S. A. (2008) Tetrazine-based cycloadditions: application to pretargeted live cell imaging, *Bioconjug Chem* 19, 2297-2299.
77. Budin, G., Chung, H. J., Lee, H., and Weissleder, R. (2012) A magnetic gram stain for bacterial detection, *Angew Chem Int Edit* 51, 7752-7755.

78. Karver, M. R., Weissleder, R., and Hilderbrand, S. A. (2011) Synthesis and evaluation of a series of 1,2,4,5-tetrazines for bioorthogonal conjugation, *Bioconjug Chem* 22, 2263-2270.
79. Seckute, J., and Devaraj, N. K. (2013) Expanding room for tetrazine ligations in the in vivo chemistry toolbox, *Curr Opin Chem Biol* 17, 761-767.
80. Yang, J., Seckute, J., Cole, C. M., and Devaraj, N. K. (2012) Live-cell imaging of cyclopropene tags with fluorogenic tetrazine cycloadditions, *Angew Chem Int Ed* 51, 7476-7479.
81. Patterson, D. M., Nazarova, L. A., Xie, B., Kamber, D. N., and Prescher, J. A. (2012) Functionalized cyclopropenes as bioorthogonal chemical reporters, *J Am Chem Soc* 134, 18638-18643.
82. Cole, C. M., Yang, J., Seckute, J., and Devaraj, N. K. (2013) Fluorescent live-cell imaging of metabolically incorporated unnatural cyclopropene-mannosamine derivatives, *ChemBioChem* 14, 205-208.
83. Yi, L., Sun, H., Wu, Y. W., Triola, G., Waldmann, H., and Goody, R. S. (2010) A highly efficient strategy for modification of proteins at the C terminus, *Angew Chem Int Ed* 49, 9417-9421.
84. Gilmore, J. M., Scheck, R. A., Esser-Kahn, A. P., Joshi, N. S., and Francis, M. B. (2006) N-terminal protein modification through a biomimetic transamination reaction, *Angew Chem Int Ed* 45, 5307-5311.
85. Scheck, R. A., and Francis, M. B. (2007) Regioselective labeling of antibodies through N-terminal transamination, *ACS Chem Biol* 2, 247-251.
86. Hermanson, G. T. (1996) *Bioconjugate techniques*, Academic Press, San Diego.
87. Stephanopoulos, N., and Francis, M. B. (2011) Choosing an effective protein bioconjugation strategy, *Nat Chem Biol* 7, 876-884.
88. Antos, J. M., and Francis, M. B. (2006) Transition metal catalyzed methods for site-selective protein modification, *Curr Opin Chem Biol* 10, 253-262.

89. Popp, B. V., and Ball, Z. T. (2010) Structure-selective modification of aromatic side chains with dirhodium metallopeptide catalysts, *J Am Chem Soc* 132, 6660-6662.
90. Antos, J. M., McFarland, J. M., Iavarone, A. T., and Francis, M. B. (2009) Chemoselective tryptophan labeling with rhodium carbenoids at mild pH, *J Am Chem Soc* 131, 6301-6308.
91. van Dongen, S. F. M., Teeuwen, R. L. M., Nallani, M., van Berkel, S. S., Cornelissen, J. J. L. M., Nolte, R. J. M., and van Hest, J. C. M. (2009) Single-step azide introduction in proteins via an aqueous diazo transfer, *Bioconjug Chem* 20, 20-23.
92. Chen, I., Howarth, M., Lin, W., and Ting, A. Y. (2005) Site-specific labeling of cell surface proteins with biophysical probes using biotin ligase, *Nat Methods* 2, 99-104.
93. Fernandez-Suarez, M., Baruah, H., Martinez-Hernandez, L., Xie, K. T., Baskin, J. M., Bertozzi, C. R., and Ting, A. Y. (2007) Redirecting lipoic acid ligase for cell surface protein labeling with small-molecule probes, *Nat Biotechnol* 25, 1483-1487.
94. Carrico, I. S., Carlson, B. L., and Bertozzi, C. R. (2007) Introducing genetically encoded aldehydes into proteins, *Nat Chem Biol* 3, 321-322.
95. Popp, M. W., and Ploegh, H. L. (2011) Making and breaking peptide bonds: protein engineering using sortase, *Angew Chem Int Ed* 50, 5024-5032.
96. Los, G. V., Encell, L. P., McDougall, M. G., Hartzell, D. D., Karassina, N., Zimprich, C., Wood, M. G., Learish, R., Ohana, R. F., Urh, M., Simpson, D., Mendez, J., Zimmerman, K., Otto, P., Vidugiris, G., Zhu, J., Darzins, A., Klaubert, D. H., Bulleit, R. F., and Wood, K. V. (2008) HaloTag: a novel protein labeling technology for cell imaging and protein analysis, *ACS Chem Biol* 3, 373-382.
97. Wu, P., Shui, W., Carlson, B. L., Hu, N., Rabuka, D., Lee, J., and Bertozzi, C. R. (2009) Site-specific chemical modification of recombinant proteins produced in mammalian cells by using the genetically encoded aldehyde tag, *Proc Natl Acad Sci U S A* 106, 3000-3005.
98. Rashidian, M., Kumarapperuma, S. C., Gabrielse, K., Fegan, A., Wagner, C. R., and Distefano, M. D. (2013) Simultaneous dual protein labeling using a triorthogonal reagent, *J Am Chem Soc* 135, 16388-16396.

99. Puthenveetil, S., Liu, D. S., White, K. A., Thompson, S., and Ting, A. Y. (2009) Yeast display evolution of a kinetically efficient 13-amino acid substrate for lipoic acid ligase, *J Am Chem Soc* *131*, 16430-16438.
100. Uttamapinant, C., Sanchez, M. I., Liu, D. S., Yao, J. Z., and Ting, A. Y. (2013) Site-specific protein labeling using PRIME and chelation-assisted click chemistry, *Nat Protoc* *8*, 1620-1634.
101. Liu, D. S., Tangpeerachaikul, A., Selvaraj, R., Taylor, M. T., Fox, J. M., and Ting, A. Y. (2012) Diels-Alder cycloaddition for fluorophore targeting to specific proteins inside living cells, *J Am Chem Soc* *134*, 792-795.
102. Cohen, J. D., Zou, P., and Ting, A. Y. (2012) Site-specific protein modification using lipoic acid ligase and bis-aryl hydrazone formation, *ChemBioChem* *13*, 888-894.
103. Davis, L., and Chin, J. W. (2012) Designer proteins: applications of genetic code expansion in cell biology, *Nat Rev Mol Cell Biol* *13*, 168-182.
104. Liu, C. C., and Schultz, P. G. (2010) Adding new chemistries to the genetic code, *Annu Rev Biochem* *79*, 413-444.
105. Zhang, Z., Smith, B. A., Wang, L., Brock, A., Cho, C., and Schultz, P. G. (2003) A new strategy for the site-specific modification of proteins in vivo, *Biochemistry* *42*, 6735-6746.
106. Deiters, A., Cropp, T. A., Mukherji, M., Chin, J. W., Anderson, J. C., and Schultz, P. G. (2003) Adding amino acids with novel reactivity to the genetic code of *Saccharomyces cerevisiae*, *J Am Chem Soc* *125*, 11782-11783.
107. Lee, Y. J., Wu, B., Raymond, J. E., Zeng, Y., Fang, X., Wooley, K. L., and Liu, W. R. (2013) A genetically encoded acrylamide functionality, *ACS Chem Biol* *8*, 1664-1670.
108. Seitchik, J. L., Peeler, J. C., Taylor, M. T., Blackman, M. L., Rhoads, T. W., Cooley, R. B., Refakis, C., Fox, J. M., and Mehl, R. A. (2012) Genetically encoded tetrazine amino acid directs rapid site-specific in vivo bioorthogonal ligation with *trans*-cyclooctenes, *J Am Chem Soc* *134*, 2898-2901.

109. Plass, T., Milles, S., Koehler, C., Szymanski, J., Mueller, R., Wiessler, M., Schultz, C., and Lemke, E. A. (2012) Amino acids for Diels-Alder reactions in living cells, *Angew Chem Int Edit* 51, 4166-4170.
110. Lang, K., Davis, L., Wallace, S., Mahesh, M., Cox, D. J., Blackman, M. L., Fox, J. M., and Chin, J. W. (2012) Genetic encoding of bicyclononynes and trans-cyclooctenes for site-specific protein labeling in vitro and in live mammalian cells via rapid fluorogenic Diels-Alder reactions, *J Am Chem Soc* 134, 10317-10320.
111. Lang, K., Davis, L., Torres-Kolbus, J., Chou, C., Deiters, A., and Chin, J. W. (2012) Genetically encoded norbornene directs site-specific cellular protein labelling via a rapid bioorthogonal reaction, *Nat Chem* 4, 298-304.
112. Li, F., Zhang, H., Sun, Y., Pan, Y., Zhou, J., and Wang, J. (2013) Expanding the Genetic Code for Photoclick Chemistry in *E. coli*, Mammalian Cells, and *A. thaliana*, *Angew Chem Int Ed* 52, 9700-9704.
113. Bianco, A., Townsley, F. M., Greiss, S., Lang, K., and Chin, J. W. (2012) Expanding the genetic code of *Drosophila melanogaster*, *Nat Chem Biol* 8, 748-750.
114. Neumann, H., Wang, K., Davis, L., Garcia-Alai, M., and Chin, J. W. (2010) Encoding multiple unnatural amino acids via evolution of a quadruplet-decoding ribosome, *Nature* 464, 441-444.
115. Wan, W., Huang, Y., Wang, Z., Russell, W. K., Pai, P. J., Russell, D. H., and Liu, W. R. (2010) A facile system for genetic incorporation of two different noncanonical amino acids into one protein in *Escherichia coli*, *Angew Chem Int Ed* 49, 3211-3214.
116. Dieterich, D. C., Link, A. J., Graumann, J., Tirrell, D. A., and Schuman, E. M. (2006) Selective identification of newly synthesized proteins in mammalian cells using bioorthogonal noncanonical amino acid tagging (BONCAT), *Proc Natl Acad Sci U S A* 103, 9482-9487.
117. Ngo, J. T., and Tirrell, D. A. (2011) Noncanonical amino acids in the interrogation of cellular protein synthesis, *Acc Chem Res* 44, 677-685.
118. Geoghegan, K. F., and Stroh, J. G. (1992) Site-directed conjugation of nonpeptide groups to peptides and proteins via periodate oxidation of a 2-amino alcohol. Application to modification at N-terminal serine, *Bioconjug Chem* 3, 138-146.

119. Clark, P. M., Dweck, J. F., Mason, D. E., Hart, C. R., Buck, S. B., Peters, E. C., Agnew, B. J., and Hsieh-Wilson, L. C. (2008) Direct in-gel fluorescence detection and cellular imaging of O-GlcNAc-modified proteins, *J Am Chem Soc* *130*, 11576-11577.
120. Soriano Del Amo, D., Wang, W., Jiang, H., Besanceney, C., Yan, A. C., Levy, M., Liu, Y., Marlow, F. L., and Wu, P. (2010) Biocompatible copper(I) catalysts for in vivo imaging of glycans, *J Am Chem Soc* *132*, 16893-16899.
121. Besanceney-Webler, C., Jiang, H., Zheng, T., Feng, L., Soriano del Amo, D., Wang, W., Klivansky, L. M., Marlow, F. L., Liu, Y., and Wu, P. (2011) Increasing the efficacy of bioorthogonal click reactions for bioconjugation: a comparative study, *Angew Chem Int Ed* *50*, 8051-8056.
122. Hong, V., Presolski, S. I., Ma, C., and Finn, M. G. (2009) Analysis and optimization of copper-catalyzed azide-alkyne cycloaddition for bioconjugation, *Angew Chem Int Ed Engl* *48*, 9879-9883.
123. Hong, V., Steinmetz, N. F., Manchester, M., and Finn, M. G. (2010) Labeling live cells by copper-catalyzed alkyne-azide click chemistry, *Bioconjug Chem* *21*, 1912-1916.
124. Kennedy, D. C., McKay, C. S., Legault, M. C., Danielson, D. C., Blake, J. A., Pegoraro, A. F., Stolow, A., Mester, Z., and Pezacki, J. P. (2011) Cellular consequences of copper complexes used to catalyze bioorthogonal click reactions, *J Am Chem Soc* *133*, 17993-18001.
125. Uttamapinant, C., Tangpeerachaikul, A., Grecian, S., Clarke, S., Singh, U., Slade, P., Gee, K. R., and Ting, A. Y. (2012) Fast, cell-compatible click chemistry with copper-chelating azides for biomolecular labeling, *Angew Chem Int Ed* *51*, 5852-5856.
126. Brotherton, W. S., Michaels, H. A., Simmons, J. T., Clark, R. J., Dalal, N. S., and Zhu, L. (2009) Apparent copper(II)-accelerated azide-alkyne cycloaddition, *Org Lett* *11*, 4954-4957.
127. Kuang, G. C., Guha, P. M., Brotherton, W. S., Simmons, J. T., Stankee, L. A., Nguyen, B. T., Clark, R. J., and Zhu, L. (2011) Experimental investigation on the mechanism of chelation-assisted, copper(II) acetate-accelerated azide-alkyne cycloaddition, *J Am Chem Soc* *133*, 13984-14001.
128. Yao, J. Z., Uttamapinant, C., Poloukhine, A., Baskin, J. M., Codelli, J. A., Sletten, E. M., Bertozzi, C. R., Popik, V. V., and Ting, A. Y. Fluorophore targeting to cellular proteins

- via enzyme-mediated azide ligation and strain-promoted cycloaddition, *J Am Chem Soc* *134*, 3720-3728.
129. Kim, E. J., Kang, D. W., Leucke, H. F., Bond, M. R., Ghosh, S., Love, D. C., Ahn, J. S., Kang, D. O., and Hanover, J. A. (2013) Optimizing the selectivity of DIFO-based reagents for intracellular bioorthogonal applications, *Carbohydr Res* *377*, 18-27.
 130. Mackinnon, A. L., and Taunton, J. (2009) Target identification by diazirine photo-cross-linking and click chemistry, *Curr Protoc Chem Biol* *1*, 55-73.
 131. Speers, A. E., and Cravatt, B. F. (2004) Profiling enzyme activities in vivo using click chemistry methods, *Chem Biol* *11*, 535-546.
 132. Boyce, M., Carrico, I. S., Ganguli, A. S., Yu, S. H., Hangauer, M. J., Hubbard, S. C., Kohler, J. J., and Bertozzi, C. R. (2011) Metabolic cross-talk allows labeling of O-linked β -*N*-acetylglucosamine-modified proteins via the *N*-acetylgalactosamine salvage pathway, *Proc Natl Acad Sci U S A* *108*, 3141-3146.
 133. Agard, N. J., Baskin, J. M., Prescher, J. A., Lo, A., and Bertozzi, C. R. (2006) A comparative study of bioorthogonal reactions with azides, *ACS Chem Biol* *1*, 644-648.
 134. Grammel, M., and Hang, H. C. (2013) Chemical reporters for biological discovery, *Nat Chem Biol* *9*, 475-484.
 135. Ekkebus, R., van Kasteren, S. I., Kulathu, Y., Scholten, A., Berlin, I., Geurink, P. P., de Jong, A., Goerdal, S., Neefjes, J., Heck, A. J., Komander, D., and Ovaas, H. (2013) On terminal alkynes that can react with active-site cysteine nucleophiles in proteases, *J Am Chem Soc* *135*, 2867-2870.
 136. Dieterich, D. C., Hodas, J. J., Gouzer, G., Shadrin, I. Y., Ngo, J. T., Triller, A., Tirrell, D. A., and Schuman, E. M. (2010) In situ visualization and dynamics of newly synthesized proteins in rat hippocampal neurons, *Nat Neurosci* *13*, 897-905.
 137. Agard, N. J., and Bertozzi, C. R. (2009) Chemical approaches to perturb, profile, and perceive glycans, *Acc Chem Res* *42*, 788-797.
 138. Laughlin, S. T., Baskin, J. M., Amacher, S. L., and Bertozzi, C. R. (2008) In vivo imaging of membrane-associated glycans in developing zebrafish, *Science* *320*, 664-667.

139. Mbuja, N. E., Flanagan-Steet, H., Johnson, S., Wolfert, M. A., Boons, G. J., and Steet, R. (2013) Abnormal accumulation and recycling of glycoproteins visualized in Niemann-Pick type C cells using the chemical reporter strategy, *Proc Natl Acad Sci U S A* 110, 10207-10212.
140. Hang, H. C., Wilson, J. P., and Charron, G. (2011) Bioorthogonal chemical reporters for analyzing protein lipidation and lipid trafficking, *Acc Chem Res* 44, 699-708.
141. Kostiuk, M. A., Corvi, M. M., Keller, B. O., Plummer, G., Prescher, J. A., Hangauer, M. J., Bertozzi, C. R., Rajaiah, G., Falck, J. R., and Berthiaume, L. G. (2008) Identification of palmitoylated mitochondrial proteins using a bio-orthogonal azido-palmitate analogue, *FASEB J* 22, 721-732.
142. Heal, W. P., Jovanovic, B., Bessin, S., Wright, M. H., Magee, A. I., and Tate, E. W. (2011) Bioorthogonal chemical tagging of protein cholesterylation in living cells, *Chem Commun (Camb)* 47, 4081-4083.
143. Hsu, T. L., Hanson, S. R., Kishikawa, K., Wang, S. K., Sawa, M., and Wong, C. H. (2007) Alkynyl sugar analogs for the labeling and visualization of glycoconjugates in cells, *Proc Natl Acad Sci U S A* 104, 2614-2619.
144. Huang, H. W., Chen, C. H., Lin, C. H., Wong, C. H., and Lin, K. I. (2013) B-cell maturation antigen is modified by a single N-glycan chain that modulates ligand binding and surface retention, *Proc Natl Acad Sci U S A* 110, 10928-10933.
145. Anderson, C. T., Wallace, I. S., and Somerville, C. R. (2012) Metabolic click-labeling with a fucose analog reveals pectin delivery, architecture, and dynamics in Arabidopsis cell walls, *Proc Natl Acad Sci U S A* 109, 1329-1334.
146. Liu, Y. C., Yen, H. Y., Chen, C. Y., Chen, C. H., Cheng, P. F., Juan, Y. H., Khoo, K. H., Yu, C. J., Yang, P. C., Hsu, T. L., and Wong, C. H. (2011) Sialylation and fucosylation of epidermal growth factor receptor suppress its dimerization and activation in lung cancer cells, *Proc Natl Acad Sci U S A* 108, 11332-11337.
147. Charron, G., Li, M. M., MacDonald, M. R., and Hang, H. C. (2013) Prenylome profiling reveals S-farnesylation is crucial for membrane targeting and antiviral activity of ZAP long-isoform, *Proc Natl Acad Sci U S A* 110, 11085-11090.
148. Martin, B. R., Wang, C., Adibekian, A., Tully, S. E., and Cravatt, B. F. (2012) Global profiling of dynamic protein palmitoylation, *Nat Methods* 9, 84-89.

149. Niederwieser, A., Spate, A. K., Nguyen, L. D., Jungst, C., Reutter, W., and Wittmann, V. (2013) Two-color glycan labeling of live cells by a combination of Diels-Alder and click chemistry, *Angew Chem Int Ed* 52, 4265-4268.
150. Stockmann, H., Neves, A. A., Stairs, S., Brindle, K. M., and Leeper, F. J. (2011) Exploring isonitrile-based click chemistry for ligation with biomolecules, *Org Biomol Chem* 9, 7303-7305.
151. Wainman, Y. A., Neves, A. A., Stairs, S., Stockmann, H., Ireland-Zecchini, H., Brindle, K. M., and Leeper, F. J. (2013) Dual-sugar imaging using isonitrile and azido-based click chemistries, *Org Biomol Chem* 11, 7297-7300.
152. Stairs, S., Neves, A. A., Stockmann, H., Wainman, Y. A., Ireland-Zecchini, H., Brindle, K. M., and Leeper, F. J. (2013) Metabolic glycan imaging by isonitrile-tetrazine click chemistry, *ChemBioChem* 14, 1063-1067.
153. Han, M. J., Xiong, D. C., and Ye, X. S. (2012) Enabling Wittig reaction on site-specific protein modification, *Chem Commun (Camb)* 48, 11079-11081.
154. Lum, K. M., Xavier, V. J., Ong, M. J., Johannes, C. W., and Chan, K. P. (2013) Stabilized Wittig olefination for bioconjugation, *Chem Commun (Camb)* 49, 11188-11190.
155. Rossin, R., Lappchen, T., van den Bosch, S. M., Laforest, R., and Robillard, M. S. (2013) Diels-Alder reaction for tumor pretargeting: *in vivo* chemistry can boost tumor radiation dose compared with directly labeled antibody, *J Nucl Med* 54, 1989-1995.
156. Vugts, D. J., Vervoort, A., Stigter-van Walsum, M., Visser, G. W., Robillard, M. S., Versteegen, R. M., Vulders, R. C., Herscheid, J. K., and van Dongen, G. A. Synthesis of phosphine and antibody-azide probes for *in vivo* Staudinger ligation in a pretargeted imaging and therapy approach, *Bioconjug Chem* 22, 2072-2081.
157. Hausner, S. H., Carpenter, R. D., Bauer, N., and Sutcliffe, J. L. Evaluation of an integrin $\alpha_v\beta_6$ -specific peptide labeled with [18F]fluorine by copper-free, strain-promoted click chemistry, *Nucl Med Biol* 40, 233-239.
158. Bouvet, V., Wuest, M., and Wuest, F. Copper-free click chemistry with the short-lived positron emitter fluorine-18, *Org Biomol Chem* 9, 7393-7399.

159. Carlson, J. C. T., Meimetis, L. G., Hilderbrand, S. A., and Weissleder, R. (2013) BODIPY-tetrazine derivatives as superbright bioorthogonal turn-on probes, *Angew Chem Int Edit* 52, 6917-6920.
160. Friscourt, F., Fahrni, C. J., and Boons, G. J. (2012) A fluorogenic probe for the catalyst-free detection of azide-tagged molecules, *J Am Chem Soc* 134, 18809-18815.
161. Jewett, J. C., and Bertozzi, C. R. (2011) Synthesis of a fluorogenic cyclooctyne activated by Cu-free click chemistry, *Org Lett* 13, 5937-5939.
162. Devaraj, N. K., Hilderbrand, S., Upadhyay, R., Mazitschek, R., and Weissleder, R. (2010) Bioorthogonal turn-on probes for imaging small molecules inside living cells, *Angew Chem Int Ed* 49, 2869-2872.
163. Shieh, P., Hangauer, M. J., and Bertozzi, C. R. (2012) Fluorogenic azidofluoresceins for biological imaging, *J Am Chem Soc* 134, 17428-17431.
164. Herner, A., Nikic, I., Kallay, M., Lemke, E. A., and Kele, P. (2013) A new family of bioorthogonally applicable fluorogenic labels, *Org Biomol Chem* 11, 3297-3306.
165. Yang, J., Karver, M. R., Li, W., Sahu, S., and Devaraj, N. K. (2012) Metal-catalyzed one-pot synthesis of tetrazines directly from aliphatic nitriles and hydrazine, *Angew Chem Int Ed* 51, 5222-5225.
166. Yao, J. Z., Uttamapinant, C., Poloukhine, A., Baskin, J. M., Codelli, J. A., Sletten, E. M., Bertozzi, C. R., Popik, V. V., and Ting, A. Y. (2012) Fluorophore targeting to cellular proteins via enzyme-mediated azide ligation and strain-promoted cycloaddition, *J Am Chem Soc* 134, 3720-3728.
167. Lin, F. L., Hoyt, H. M., van Halbeek, H., Bergman, R. G., and Bertozzi, C. R. (2005) Mechanistic investigation of the Staudinger ligation, *J Am Chem Soc* 127, 2686-2695.
168. Majkut, P., Bohrsch, V., Serwa, R., Gerrits, M., and Hackenberger, C. P. (2012) Site-specific modification of proteins by the Staudinger-phosphite reaction, *Methods Mol Biol* 794, 241-249.
169. Hangauer, M. J., and Bertozzi, C. R. (2008) A FRET-based fluorogenic phosphine for live-cell imaging with the Staudinger ligation, *Angew Chem Int Ed* 47, 2394-2397.

170. Saxon, E., Armstrong, J. I., and Bertozzi, C. R. (2000) A "traceless" Staudinger ligation for the chemoselective synthesis of amide bonds, *Org Lett* 2, 2141-2143.
171. Soellner, M. B., Tam, A., and Raines, R. T. (2006) Staudinger ligation of peptides at non-glycyl residues, *J Org Chem* 71, 9824-9830.
172. Tam, A., and Raines, R. T. (2009) Protein engineering with the traceless Staudinger ligation, *Method Enzymol* 462, 25-44.
173. Ahad, A. M., Jensen, S. M., and Jewett, J. C. (2013) A traceless Staudinger reagent to deliver diazirines, *Org Lett* 15, 5060-5063.
174. Bertran-Vicente, J., and Hackenberger, C. P. (2013) A supramolecular peptide synthesizer, *Angew Chem Int Ed* 52, 6140-6142.
175. DeForest, C. A., and Anseth, K. S. (2011) Cytocompatible click-based hydrogels with dynamically tunable properties through orthogonal photoconjugation and photocleavage reactions, *Nat Chem* 3, 925-931.
176. Kafri, R., Levy, J., Ginzberg, M. B., Oh, S., Lahav, G., and Kirschner, M. W. (2013) Dynamics extracted from fixed cells reveal feedback linking cell growth to cell cycle, *Nature* 494, 480-483.
177. Chakraborty, A., Wang, D., Ebright, Y. W., Korlann, Y., Kortkhonjia, E., Kim, T., Chowdhury, S., Wigneshweraraj, S., Irschik, H., Jansen, R., Nixon, B. T., Knight, J., Weiss, S., and Ebright, R. H. (2012) Opening and closing of the bacterial RNA polymerase clamp, *Science* 337, 591-595.
178. Liang, G., Ren, H., and Rao, J. (2010) A biocompatible condensation reaction for controlled assembly of nanostructures in living cells, *Nat Chem* 2, 54-60.
179. Nguyen, D. P., Elliott, T., Holt, M., Muir, T. W., and Chin, J. W. (2011) Genetically encoded 1,2-aminothiols facilitate rapid and site-specific protein labeling via a bio-orthogonal cyanobenzothiazole condensation, *J Am Chem Soc* 133, 11418-11421.
180. Lin, Y. A., Boutureira, O., Lercher, L., Bhushan, B., Paton, R. S., and Davis, B. G. (2013) Rapid cross-metathesis for reversible protein modifications via chemical access to Se-allyl-selenocysteine in proteins, *J Am Chem Soc* 135, 12156-12159.

181. Sletten, E. M., and Bertozzi, C. R. (2011) A bioorthogonal quadricyclane ligation, *J Am Chem Soc* 133, 17570-17573.
182. Ho, C. M., Zhang, J. L., Zhou, C. Y., Chan, O. Y., Yan, J. J., Zhang, F. Y., Huang, J. S., and Che, C. M. (2010) A water-soluble ruthenium glycosylated porphyrin catalyst for carbenoid transfer reactions in aqueous media with applications in bioconjugation reactions, *J Am Chem Soc* 132, 1886-1894.
183. Lin, Y. A., Chalker, J. M., and Davis, B. G. (2010) Olefin cross-metathesis on proteins: investigation of allylic chalcogen effects and guiding principles in metathesis partner selection, *J Am Chem Soc* 132, 16805-16811.
184. Chalker, J. M., Wood, C. S., and Davis, B. G. (2009) A convenient catalyst for aqueous and protein Suzuki-Miyaura cross-coupling, *J Am Chem Soc* 131, 16346-16347.
185. Li, N., Lim, R. K., Edwardraja, S., and Lin, Q. (2011) Copper-free Sonogashira cross-coupling for functionalization of alkyne-encoded proteins in aqueous medium and in bacterial cells, *J Am Chem Soc* 133, 15316-15319.
186. Yusop, R. M., Unciti-Broceta, A., Johansson, E. M., Sanchez-Martin, R. M., and Bradley, M. (2011) Palladium-mediated intracellular chemistry, *Nat Chem* 3, 239-243.
187. Spicer, C. D., Triemer, T., and Davis, B. G. (2012) Palladium-mediated cell-surface labeling, *J Am Chem Soc* 134, 800-803.
188. Lercher, L., McGouran, J. F., Kessler, B. M., Schofield, C. J., and Davis, B. G. (2013) DNA modification under mild conditions by Suzuki-Miyaura cross-coupling for the generation of functional probes, *Angew Chem Int Ed* 52, 10553-10558.
189. Li, J., Lin, S., Wang, J., Jia, S., Yang, M., Hao, Z., Zhang, X., and Chen, P. R. (2013) Ligand-free palladium-mediated site-specific protein labeling inside gram-negative bacterial pathogens, *J Am Chem Soc* 135, 7330-7338.
190. Riggsbee, C. W., and Deiters, A. (2010) Recent advances in the photochemical control of protein function, *Trends Biotechnol* 28, 468-475.
191. Pauloehrl, T., Delaittre, G., Winkler, V., Welle, A., Bruns, M., Borner, H. G., Greiner, A. M., Bastmeyer, M., and Barner-Kowollik, C. (2012) Adding spatial control to click

- chemistry: phototriggered Diels-Alder surface (bio)functionalization at ambient temperature, *Angew Chem Int Edit* 51, 1071-1074.
192. Arumugam, S., and Popik, V. V. (2011) Light-induced hetero-Diels-Alder cycloaddition: a facile and selective photoclick reaction, *J Am Chem Soc* 133, 5573-5579.
 193. Adzima, B. J., Tao, Y. H., Kloxin, C. J., DeForest, C. A., Anseth, K. S., and Bowman, C. N. (2011) Spatial and temporal control of the alkyne-azide cycloaddition by photoinitiated Cu(II) reduction, *Nat Chem* 3, 256-259.
 194. Wang, Y., Song, W., Hu, W. J., and Lin, Q. (2009) Fast alkene functionalization in vivo by photoclick chemistry: HOMO lifting of nitrile imine dipoles, *Angew Chem Int Ed* 48, 5330-5333.
 195. Poloukhine, A. A., Mbua, N. E., Wolfert, M. A., Boons, G. J., and Popik, V. V. (2009) Selective labeling of living cells by a photo-triggered click reaction, *J Am Chem Soc* 131, 15769-15776.
 196. Deiters, A. (2010) Principles and applications of the photochemical control of cellular processes, *ChemBioChem* 11, 47-53.
 197. Lim, R. K., and Lin, Q. (2011) Photoinducible bioorthogonal chemistry: a spatiotemporally controllable tool to visualize and perturb proteins in live cells, *Acc Chem Res* 44, 828-839.
 198. McNitt, C. D., and Popik, V. V. (2012) Photochemical generation of oxadibenzocyclooctyne (ODIBO) for metal-free click ligations, *Org Biomol Chem* 10, 8200-8202.
 199. Yu, Z., Ohulchanskyy, T. Y., An, P., Prasad, P. N., and Lin, Q. (2013) Fluorogenic, two-photon triggered photoclick chemistry in live mammalian cells, *J Am Chem Soc* 135, 16766-16769.
 200. Li, Q., Dong, T., Liu, X., and Lei, X. (2013) A bioorthogonal ligation enabled by click cycloaddition of o-quinolinone quinone methide and vinyl thioether, *J Am Chem Soc* 135, 4996-4999.

201. An, P., Yu, Z., and Lin, Q. (2013) Design and synthesis of laser-activatable tetrazoles for a fast and fluorogenic red-emitting 1,3-dipolar cycloaddition reaction, *Org Lett* 15, 5496-5499.
202. Chen, W. X., Wang, D. Z., Dai, C. F., Hamelberg, D., and Wang, B. H. (2012) Clicking 1,2,4,5-tetrazine and cyclooctynes with tunable reaction rates, *Chem Commun (Camb)* 48, 1736-1738.
203. Liang, Y., Mackey, J. L., Lopez, S. A., Liu, F., and Houk, K. N. (2012) Control and design of mutual orthogonality in bioorthogonal cycloadditions, *J Am Chem Soc* 134, 17904-17907.
204. Karver, M. R., Weissleder, R., and Hilderbrand, S. A. (2012) Bioorthogonal reaction pairs enable simultaneous, selective, multi-target imaging, *Angew Chem Int Ed* 51, 920-922.
205. Willems, L. I., Li, N., Florea, B. I., Ruben, M., van der Marel, G. A., and Overkleeft, H. S. (2012) Triple bioorthogonal ligation strategy for simultaneous labeling of multiple enzymatic activities, *Angew Chem Int Ed* 51, 4431-4434.
206. Ess, D. H., Jones, G. O., and Houk, K. N. (2008) Transition states of strain-promoted metal-free click chemistry: 1,3-dipolar cycloadditions of phenyl azide and cyclooctynes, *Org Lett* 10, 1633-1636.
207. Schoenebeck, F., Ess, D. H., Jones, G. O., and Houk, K. N. (2009) Reactivity and regioselectivity in 1,3-dipolar cycloadditions of azides to strained alkynes and alkenes: a computational study, *J Am Chem Soc* 131, 8121-8133.
208. Kamber, D. N., Nazarova, L. A., Liang, Y., Lopez, S. A., Patterson, D. M., Shih, H. W., Houk, K. N., and Prescher, J. A. (2013) Isomeric cyclopropenes exhibit unique bioorthogonal reactivities, *J Am Chem Soc* 135, 13680-13683.
209. Gold, B., Dudley, G. B., and Alabugin, I. V. (2013) Moderating strain without sacrificing reactivity: design of fast and tunable noncatalyzed alkyne-azide cycloadditions via stereoelectronically controlled transition state stabilization, *J Am Chem Soc* 135, 1558-1569.
210. Kolodych, S., Rasolofonjatovo, E., Chaumontet, M., Nevers, M. C., Creminon, C., and Taran, F. (2013) Discovery of chemoselective and biocompatible reactions using a high-throughput immunoassay screening, *Angew Chem Int Ed* 52, 12056-12060.

CHAPTER 2: Functionalized cyclopropenes as bioorthogonal chemical reporters

2.1 Introduction

The bioorthogonal chemical reporter strategy is among the most popular methods to tag biomolecules in live cells and whole animals [1]. This technique relies on the metabolic introduction of a unique functional group (i.e., a chemical reporter) into a biomolecule of interest (Figure 2-1A). The reporter is detected in a second step using highly selective (i.e., bioorthogonal) chemistries [2]. Depending on the type of covalent labeling agent employed, this two-step approach can be used to visualize biomolecules in cellular environments or enrich them for further analyses.

While powerful, the bioorthogonal chemical reporter strategy has been limited to only a handful of broadly functional reporter groups. This select class includes ketones, terminal alkynes, and organic azides [3-6]. Azides, in particular, have been widely utilized in live cells and animals owing to their remarkable biocompatibility and unique reactivity [2, 7, 8]. Azides can be readily affixed to metabolic precursors that target glycans, lipids, and numerous other biomolecules [9-11]. Once installed, these motifs can be selectively reacted with soft nucleophiles (via Staudinger ligation) or activated alkynes (via copper-free “click” chemistry) without detriment to the cell or organism [12-16]. Identifying new chemical reporters remains an important, yet challenging goal, as most functional groups do not meet the stringent criteria required for use in living systems. The scaffolds must remain inert to endogenous biological functionality, yet react robustly with complementary probes in complex environments. Chemical

reporters must also traverse biosynthetic pathways and, thus, be minimally perturbing to the cell's metabolic machinery.

In recent years, strained alkenes and alkynes have been identified that meet several of the criteria for broadly applicable chemical reporters [8]. These scaffolds, including *trans*-cyclooctene (TCO), norbornene (NB), and bicyclononyne (BCN), are abiotic and relatively stable in cellular environs [17-23]. Furthermore, they react rapidly with electron-poor tetrazines via inverse-electron-demand Diels-Alder (IED-DA) reactions. The remarkable speed of these reactions is well suited for sensitive imaging applications, and a variety of TCO- and NB-conjugated nanoparticles and antibodies have been utilized for this purpose [17-23]. More recently, Chin and others have demonstrated that amino acids outfitted with BCN, TCO, or NB can be incorporated into cellular proteins utilizing engineered strains of bacteria; the functionalized proteins can be subsequently targeted with visual probes via IED-DA ligations [21, 24, 25]. While useful, strained alkenes and alkynes have been slow to transition as reporter groups for other metabolic pathways. This is due, in part, to their large size and incompatibility with many endogenous biosynthetic pathways.

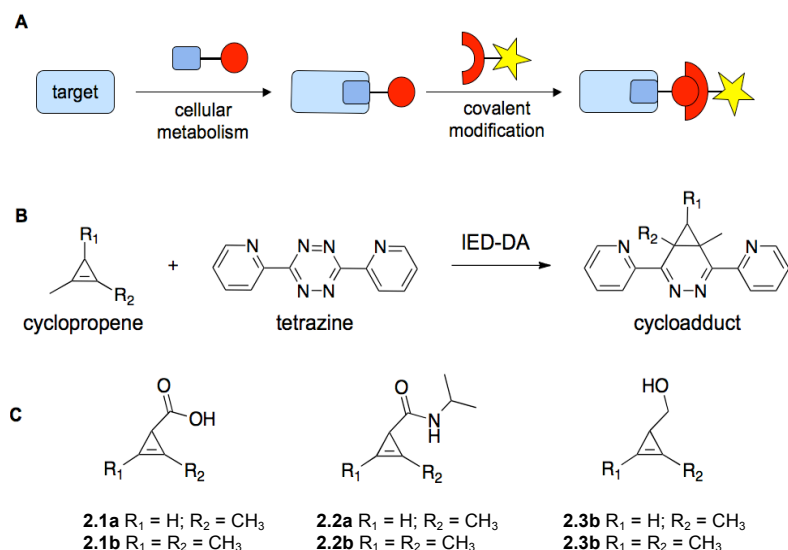
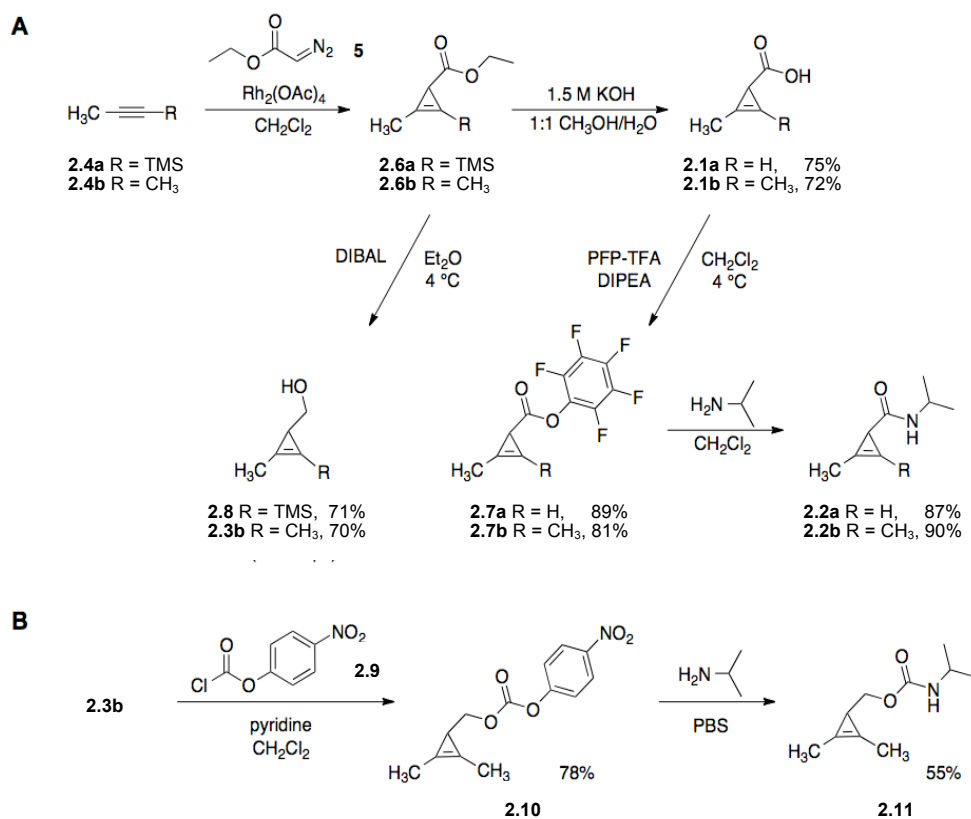


Figure 2-1. Chemical reporters and bioorthogonal chemistries. (A) The bioorthogonal chemical reporter strategy. A biomolecule of interest (light blue rectangle) can be targeted with a chemical reporter group (red circle) appended to a metabolic precursor (dark blue rectangle). Subsequent covalent reaction enables the target biomolecule to be visualized or retrieved. (B) Cyclopropenes undergo cycloaddition reactions with tetrazine scaffolds. (C) Panel of cyclopropene analogs examined in this study.

We aimed to examine a smaller strained olefin—cyclopropene—for use as a bioorthogonal chemical reporter. Cyclopropenes are not present in most eukaryotes, and are likely compatible with a variety of metabolic pathways owing to their small size. In fact, the steric demand of a cyclopropene unit is on par with diazirine, a widely used functional group in cellular labeling and photo-crosslinking studies [26, 27]. Cyclopropenes also possess a large amount of strain energy that can drive IED-DA reactions and other cycloadditions under relatively mild conditions (Figure 2-1B) [28, 29]. These types of transformations are particularly attractive for use in biological settings, and have been the subject of recent work by Devaraj and coworkers [29, 30]. In this chapter, we describe the development and utilization of cyclopropenes as chemical reporters in living systems.

Scheme 2-1. Synthesis of functionalized cyclopropenes.



2.2 Results and Discussion

2.2a Design and synthesis of biocompatible cyclopropenes

While cyclopropenes possess many favorable attributes for cell-based studies, they are not without limitation. Cyclopropene itself is prone to polymerization at room temperature and susceptible to attack by thiols and other biological nucleophiles [31, 32]. However, several lines of evidence suggest that modifications to the cyclopropene core can markedly improve scaffold stability. For example, substituted cyclopropenes are found in both plant and marine natural products, indicating that C-1 and C-2-modified olefins possess some degree of metabolic stability [33-35]. Methyl-substituted cyclopropenes are also produced on the ton-scale in the

agricultural industry and used in produce transport [36]. Additionally, carbonyls and other electron-withdrawing groups positioned at C-3 are known to stabilize cyclopropenes by imparting partial aromatic character to the ring [37-39].

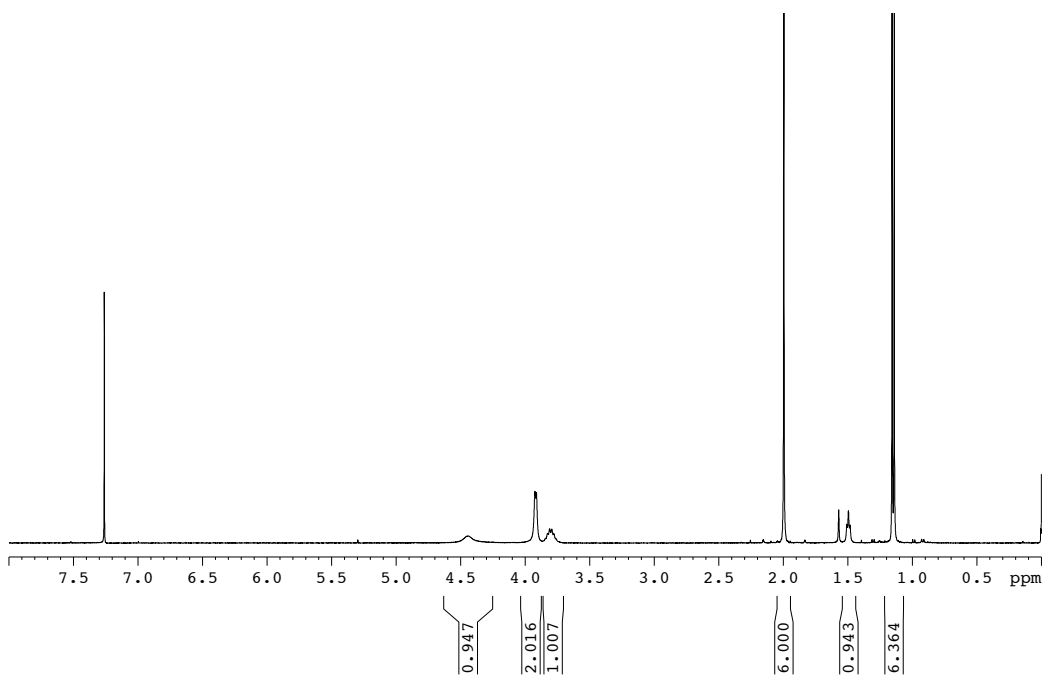
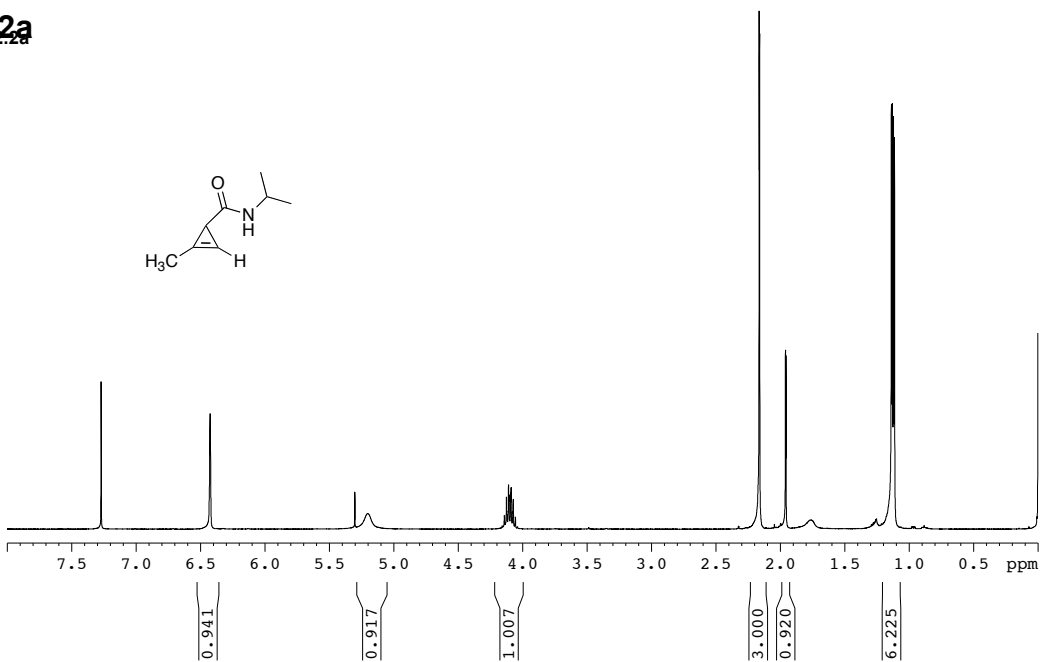
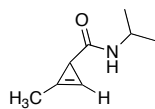
We reasoned that a combination of steric and electronic modifications to the cyclopropene core would provide a chemical reporter suitable for metabolic labeling without compromising cycloaddition reactivity. To test this hypothesis, we designed a panel of cyclopropenes with vinyl methyl substituents and various C-3 appendages (Figure 2-1C). The C-3 groups differed in their electron-withdrawing character and, in some cases, provided handles for eventual attachment to metabolic precursors. We were particularly attracted to the amide- and carbamate-functionalized scaffolds (**2.2** and **2.11**, respectively) as these linkages mimic those found in numerous bioconjugates.

Cyclopropenes can be readily accessed from alkynes, but the synthesis of such low molecular weight compounds presents unique challenges. Many cyclopropenes are volatile and, as mentioned earlier, prone to polymerization upon concentration. To mitigate against these effects, we utilized di-substituted alkynes in the early stages of our syntheses. TMS-protected propyne and 2-butyne were first subjected to rhodium-catalyzed cyclopropenation with ethyl diazoacetate (**2.5**) to provide esters **2.6a-b** (Scheme 2-1A). Subsequent hydrolysis of the isolated esters afforded the free acids **2.1a-b** in good yield.

With **2.1** and **2.6** in hand, we were poised to access the remaining C-3 modified scaffolds. The amide-functionalized cyclopropenes **2.2a-b** were prepared by treating **2.1a-b** with pentafluorophenyl trifluoroacetate (PFP-TFA), followed by isopropylamine. The hydroxy-substituted cyclopropenes **2.3b** and **2.8** were generated via DIBAL-mediated reduction of **2.6**. Unfortunately, attempts to deprotect **2.8** to afford the mono-substituted cyclopropene **2.3a** were

unsuccessful. NMR analyses suggested that **2.3a**—with a single methyl substituent and no electron-withdrawing group—polymerizes rapidly upon concentration (data not shown). Last, the carbamate scaffold **2.11** was isolated in two steps from **2.3b** (Scheme 2-1B). In contrast to **2.3a**, cyclopropenes **2.1**, **2.2**, **2.3b**, and **2.11** exhibited remarkable stability in aqueous buffer and in the presence of biologically relevant thiols. Scaffolds **2.2a** and **2.11**, in particular, were found to be stable for extended periods of time in solution and in the presence of cysteine (Figures 2-2 and 2-3).

2a



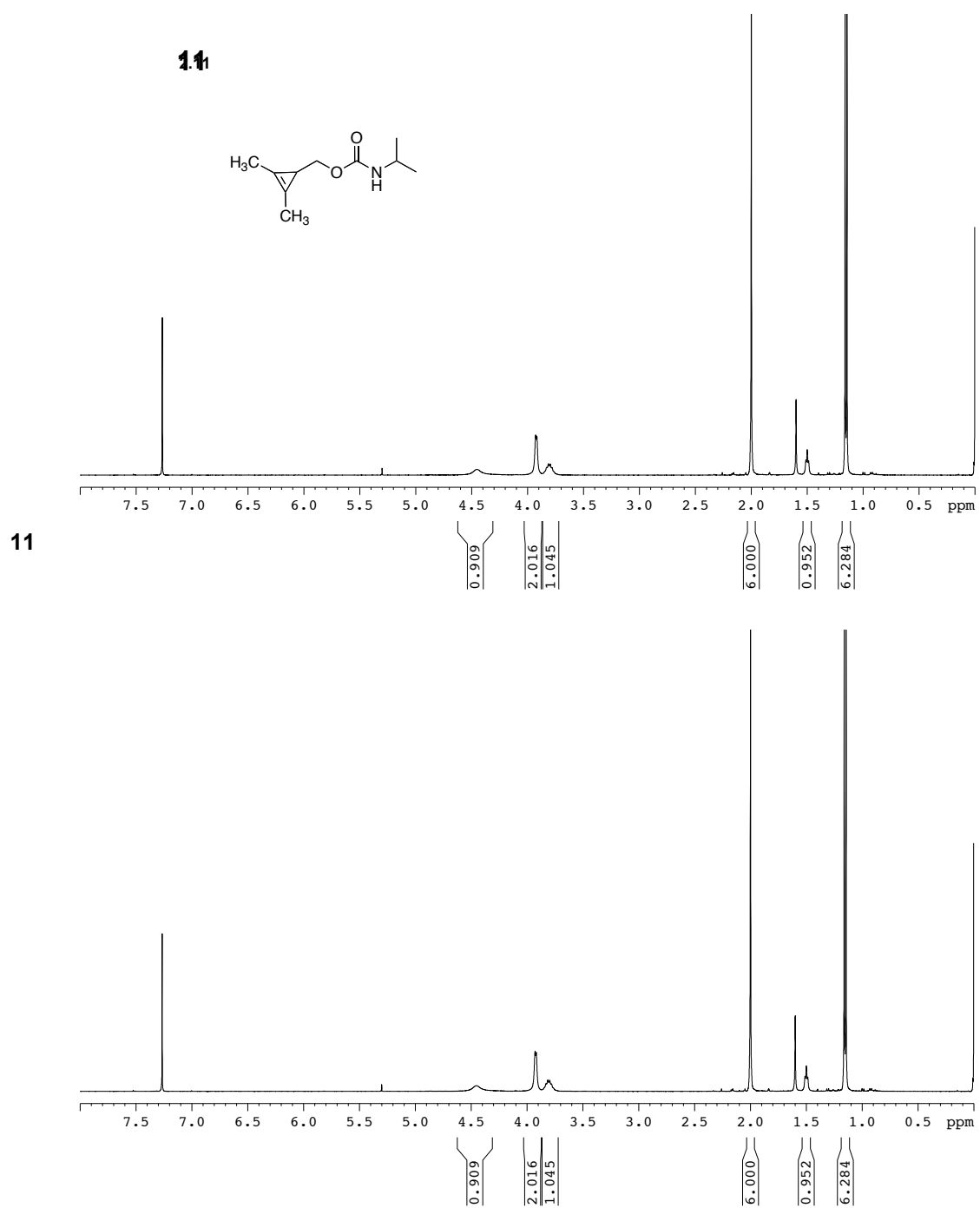
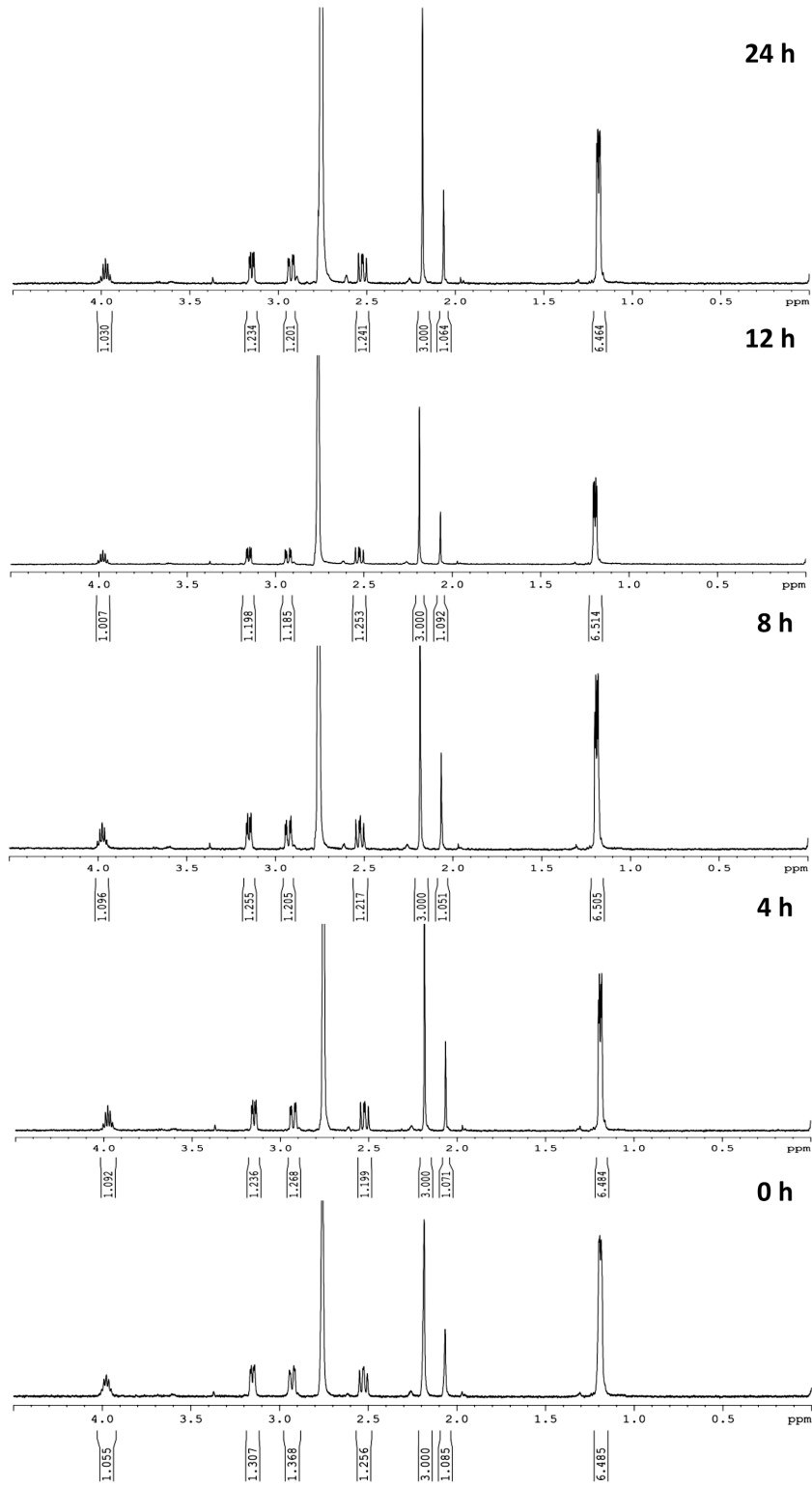


Figure 2-2. Cyclopropenes **2.2a** and **2.11** are stable upon storage. $^1\text{H-NMR}$ spectra of **2.2a** (100 mM in CDCl_3) taken (A) immediately after isolation and (B) 2 months after sample preparation. $^1\text{H-NMR}$ spectra of **2.11** (100 mM in CDCl_3) taken (C) immediately after isolation and (D) 1 week after sample preparation.

A

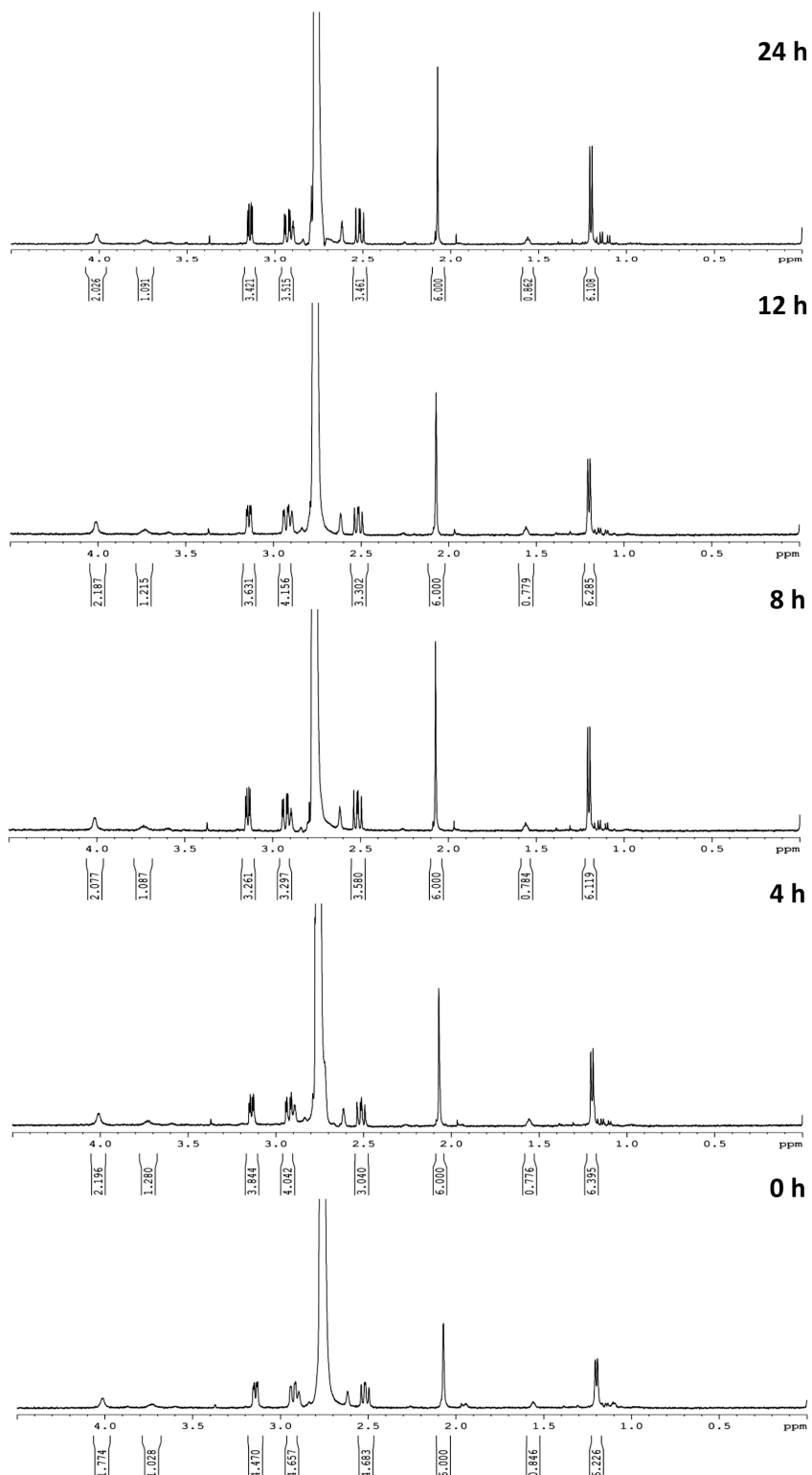


Figure 2-3. Cyclopropenes are stable in the presence of biological nucleophiles. Cyclopropenes (A) **2.2a** and (B) **2.11** (5 mM) were incubated with cysteine (5 mM) in 10% DMSO- d_6 /deuterated PBS and analyzed by $^1\text{H-NMR}$ over 24 h.

2.2b Analysis of cyclopropene-tetrazine reactivity

To examine whether the substituted cyclopropenes were still amenable to facile cycloaddition, we subjected **2.1**, **2.2**, **2.3b**, and **2.11** to the model dipyriddy-tetrazine reagent **2.12**. Cycloadduct formation was observed in all cases when excess cyclopropene was used (Figures 2-4A, 2-5), although the products formed between **2.1** and **2.12** degraded rapidly in solution. The reactions also exhibited distinct fuchsia-to-yellow color changes that were used to calculate second-order rate constants for the transformations (Table 2-1, Figures 2-6 and 2-7). As expected, faster reactions were observed in more polar solvents and with less sterically congested cyclopropenes [29]. Additionally, cyclopropenes with reduced electron-withdrawing character at C-3 were found to react more expediently with **2.12**, in agreement with previous studies [37]. Scaffolds **2.2a** and **2.11** also exhibited comparable reactivity with a functionalized tetrazine probe.

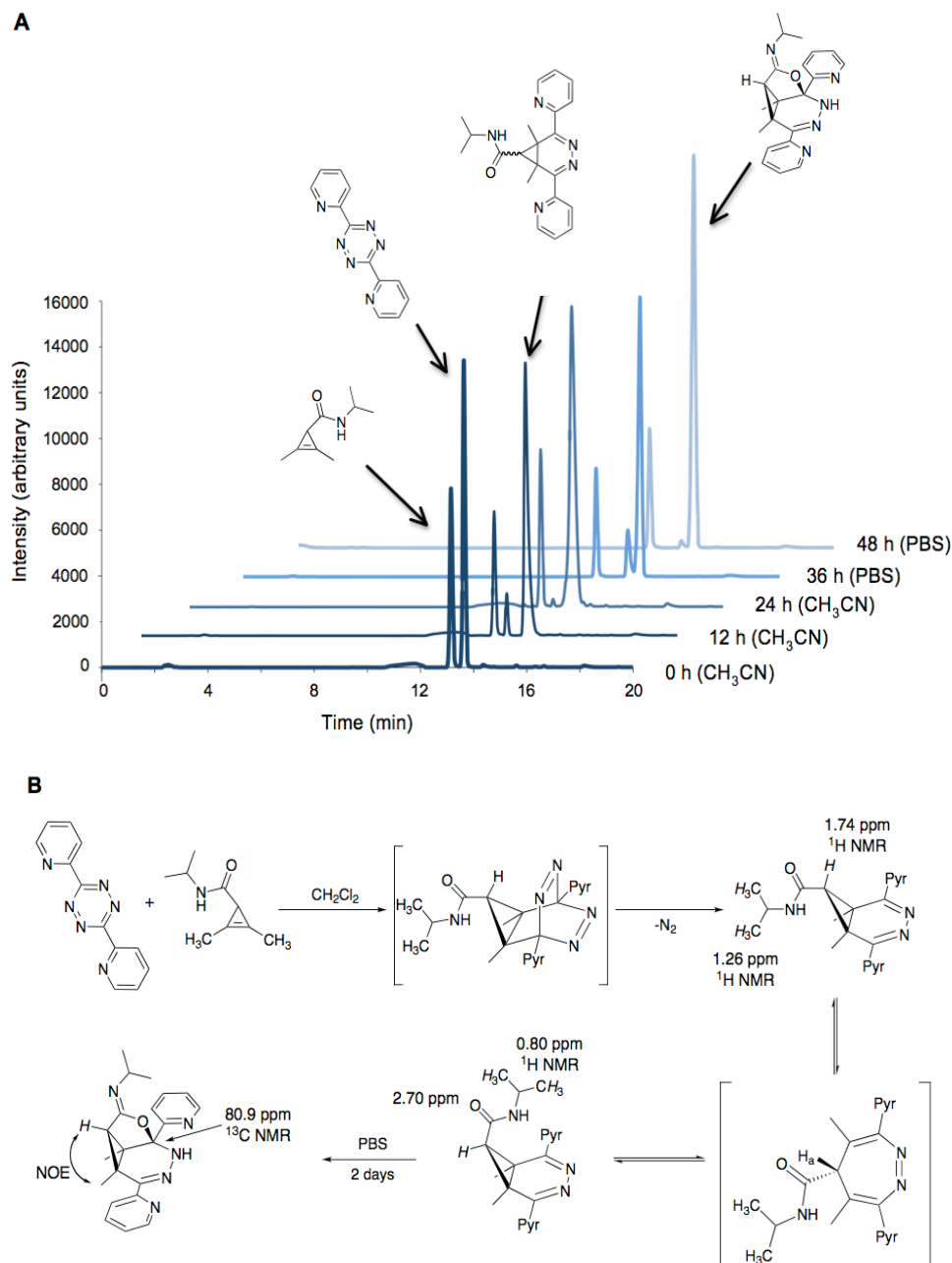
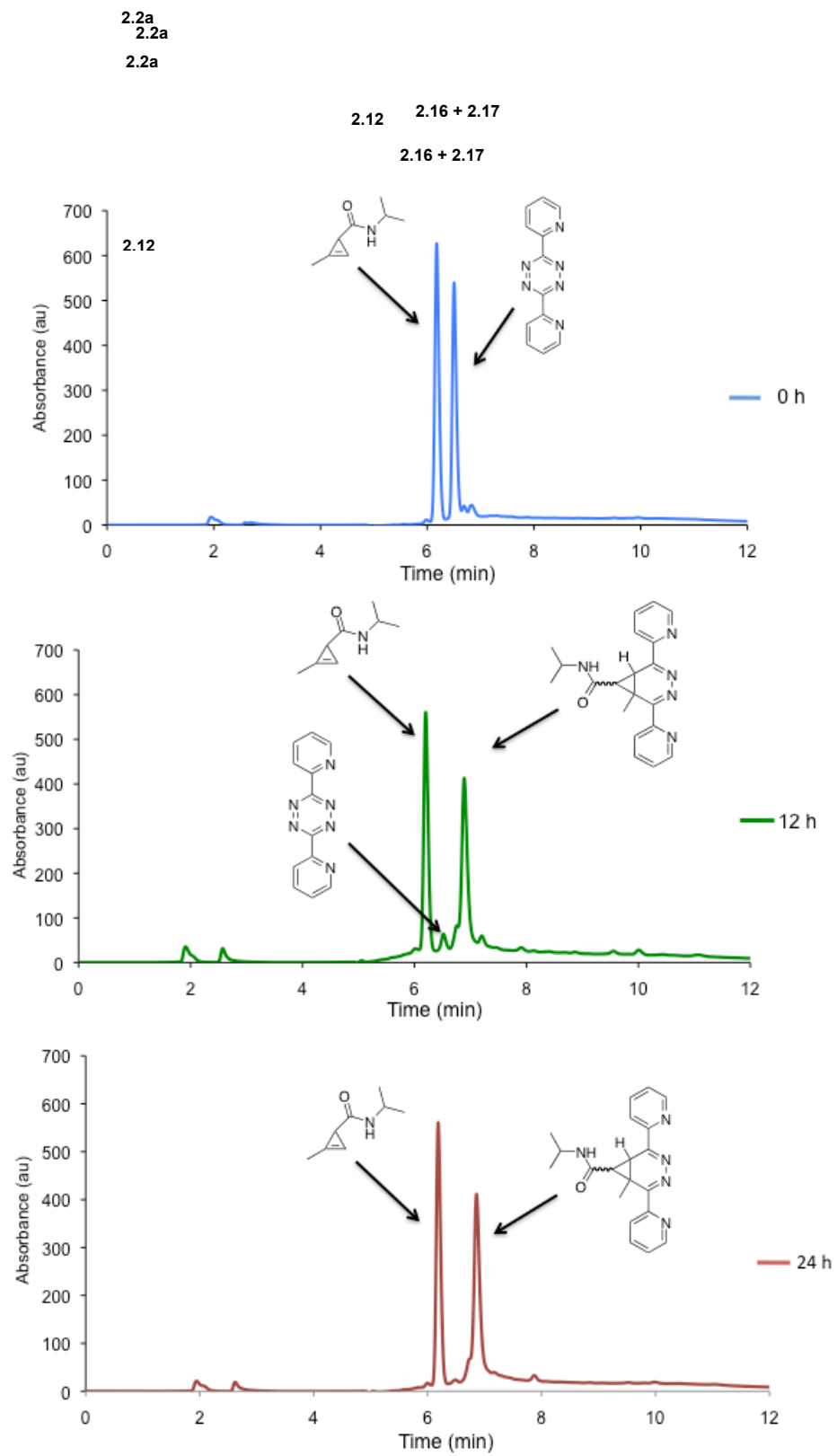
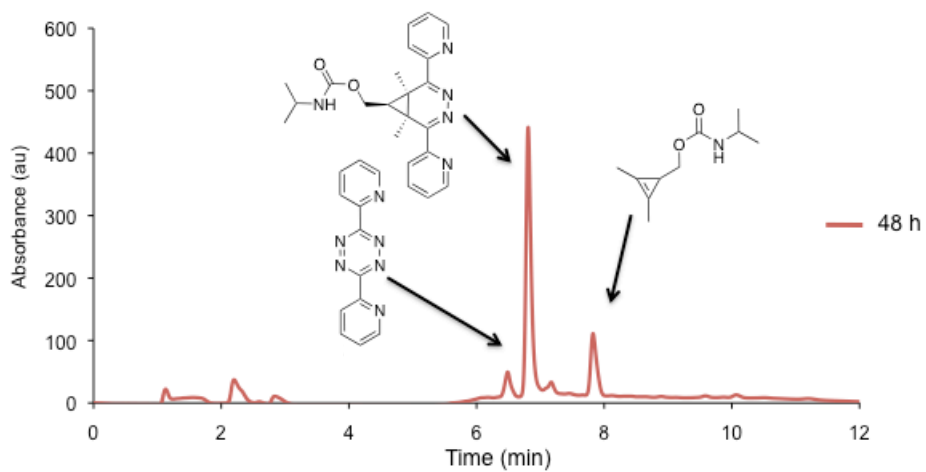
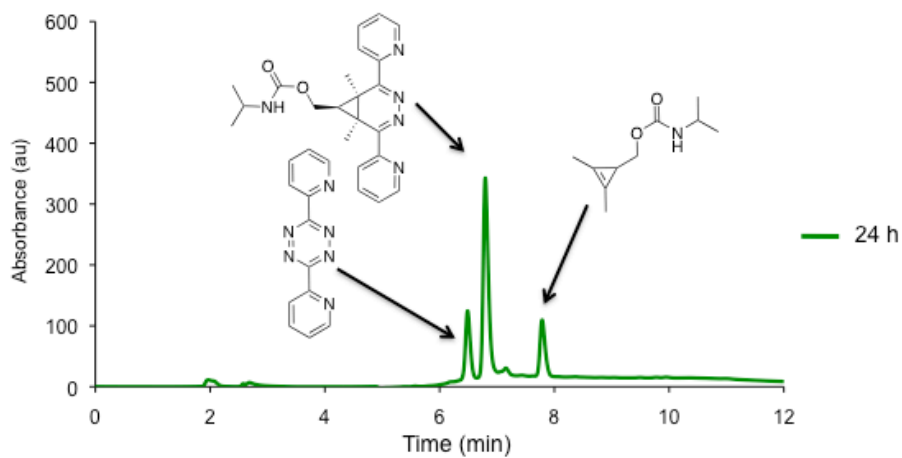
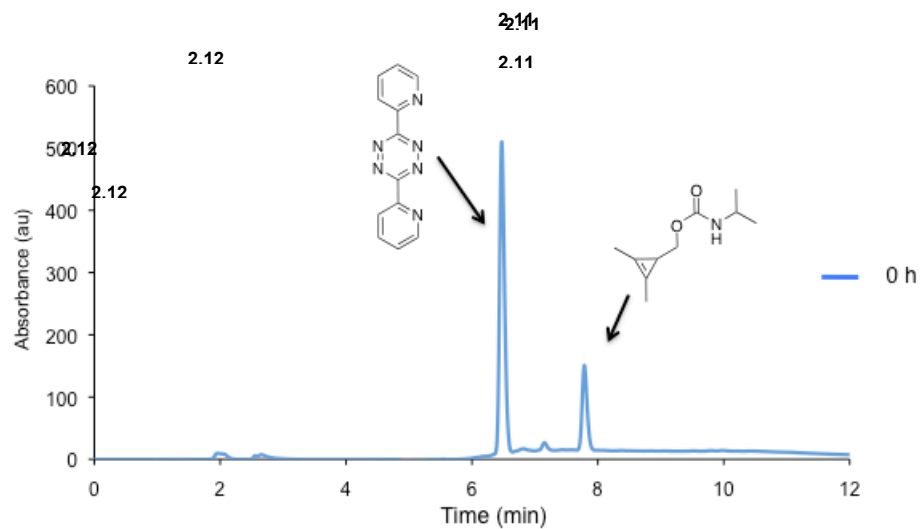


Figure 2-4. Cyclopropenes react with tetrazines to form covalent adducts. (A) HPLC analysis of the cycloaddition between **2.2b** and **2.12**. The reaction was initiated in organic solvent prior to the addition of aqueous buffer. (B) The cyclopropene-tetrazine ligation proceeds via an initial Diels-Alder reaction, followed by N_2 elimination. Subsequent ring opening and closing provides a mixture of diastereomers (**2.13** and **2.14**). Intramolecular cyclization ultimately affords the tricyclic adduct **2.15**. Diagnostic NMR chemical shifts are noted.

A

2. 18



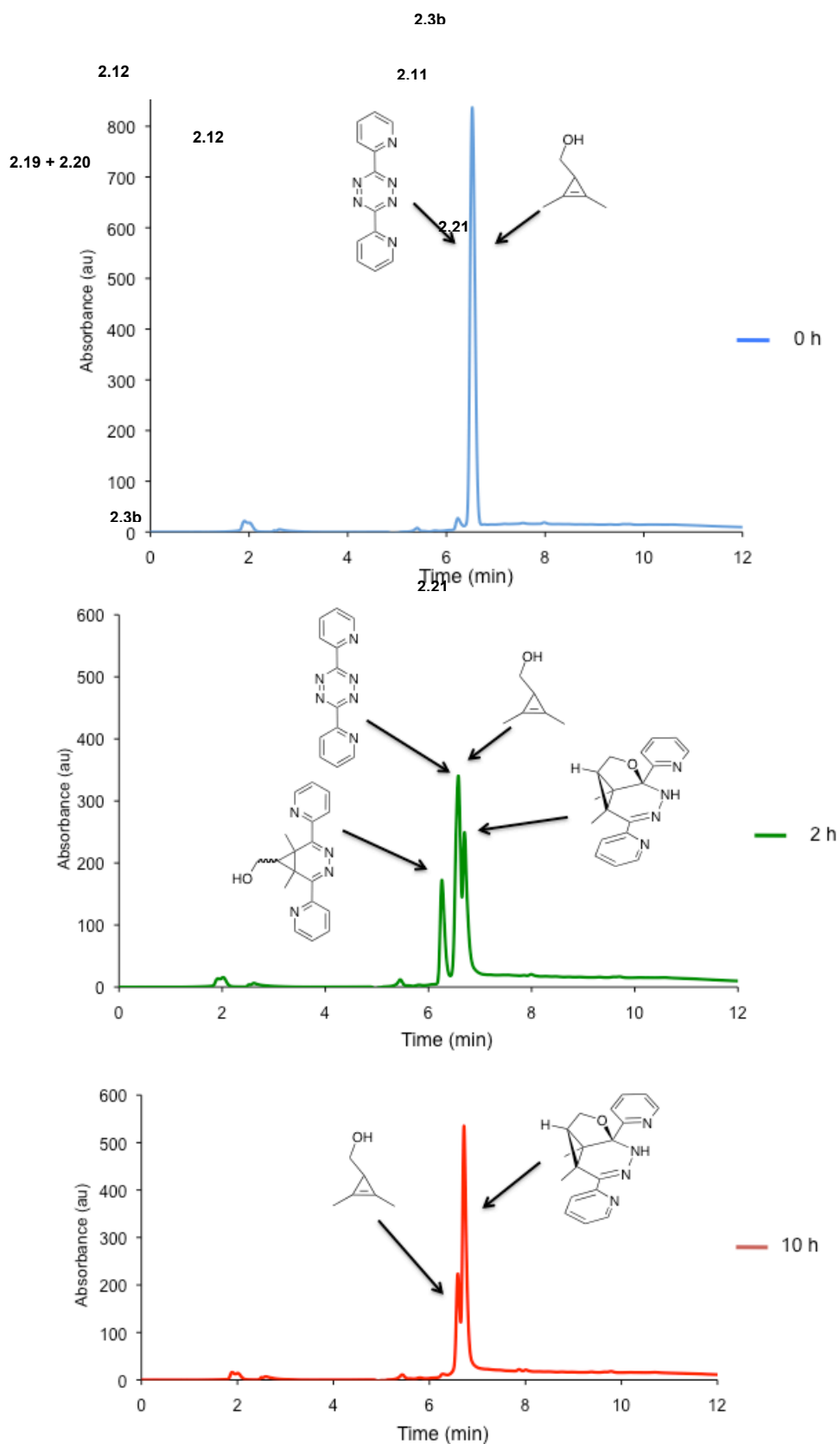
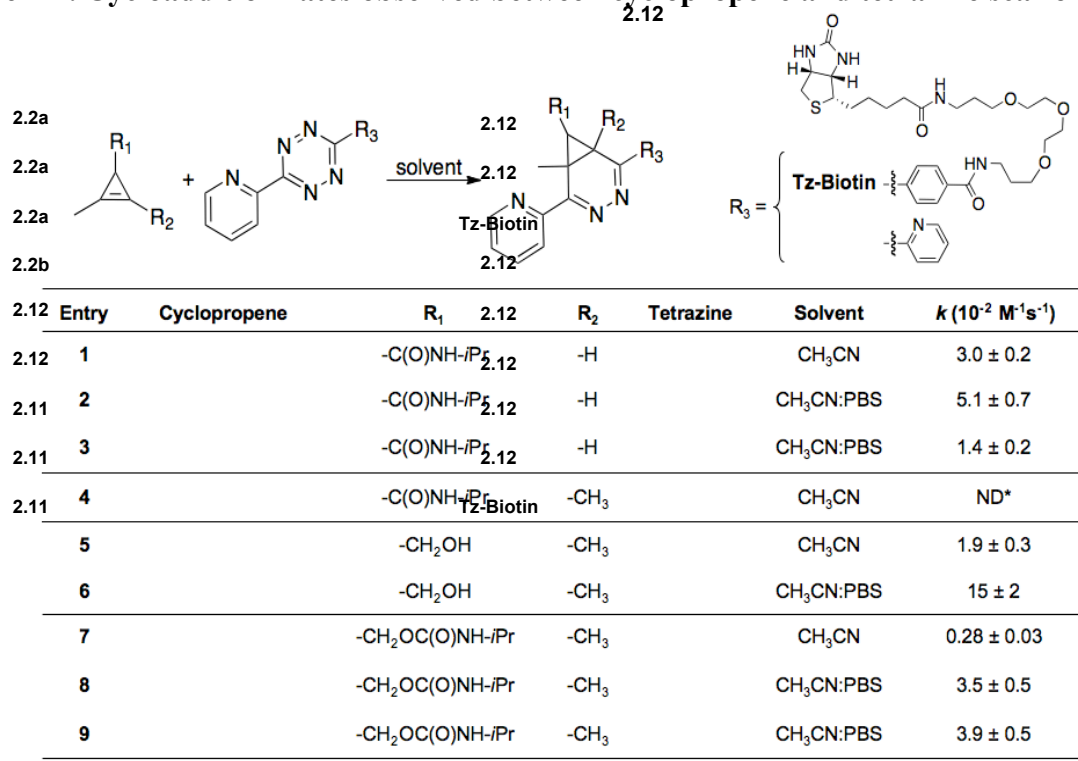
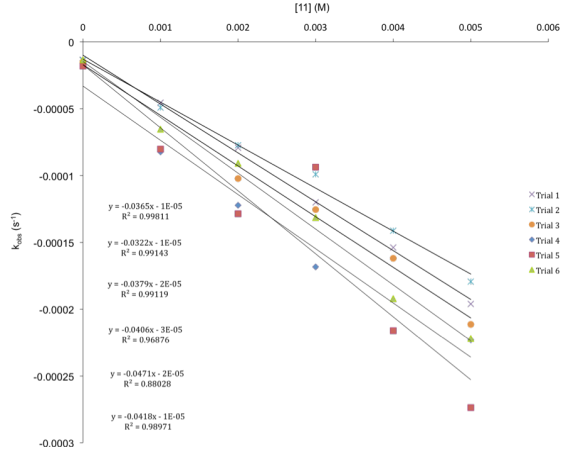
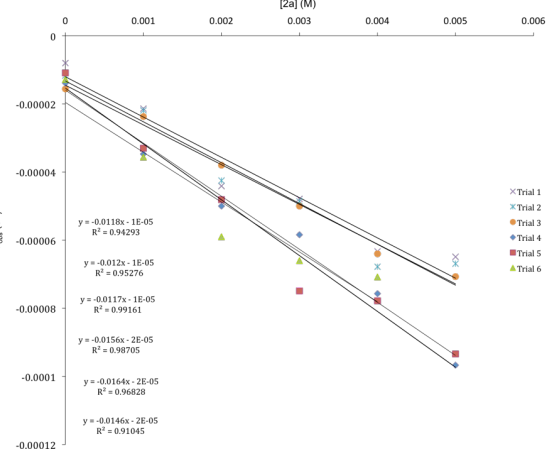
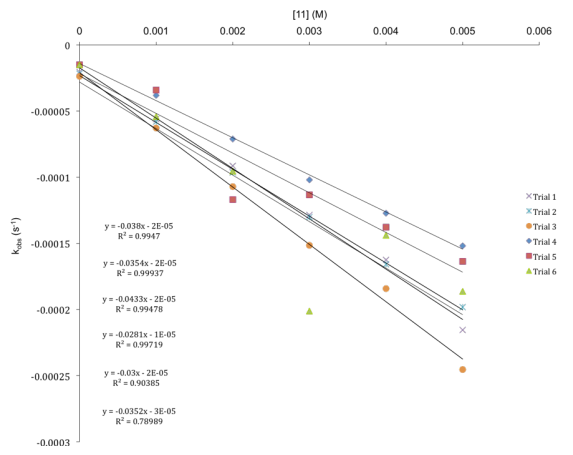
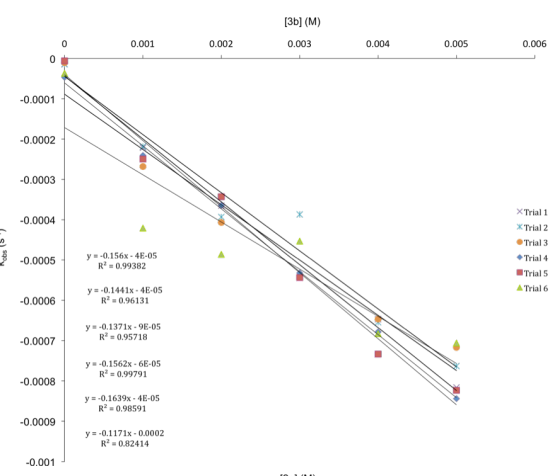
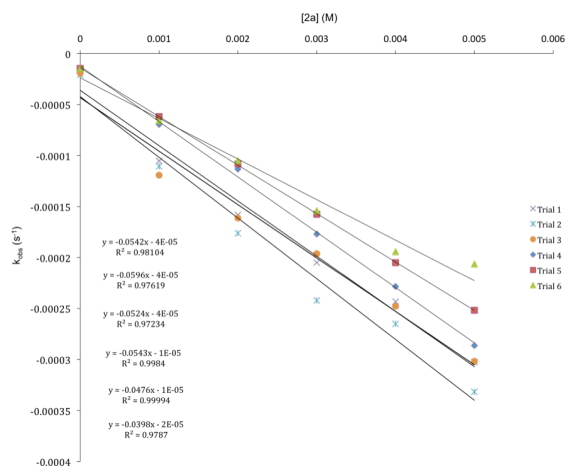


Figure 2-5. HPLC analyses (0-95% CH₃CN/H₂O over 10 min with detection at 214 nm) of the reactions between tetrazine **2.12** and (A) **2.2a** (in excess), (B) **2.11** (in excess), (C) **2.3b** in 1:1 CH₃CN:PBS (**2.3b** and **2.12** co-elute).

Table 2-1. Cycloaddition rates observed between cyclopropene and tetrazine scaffolds





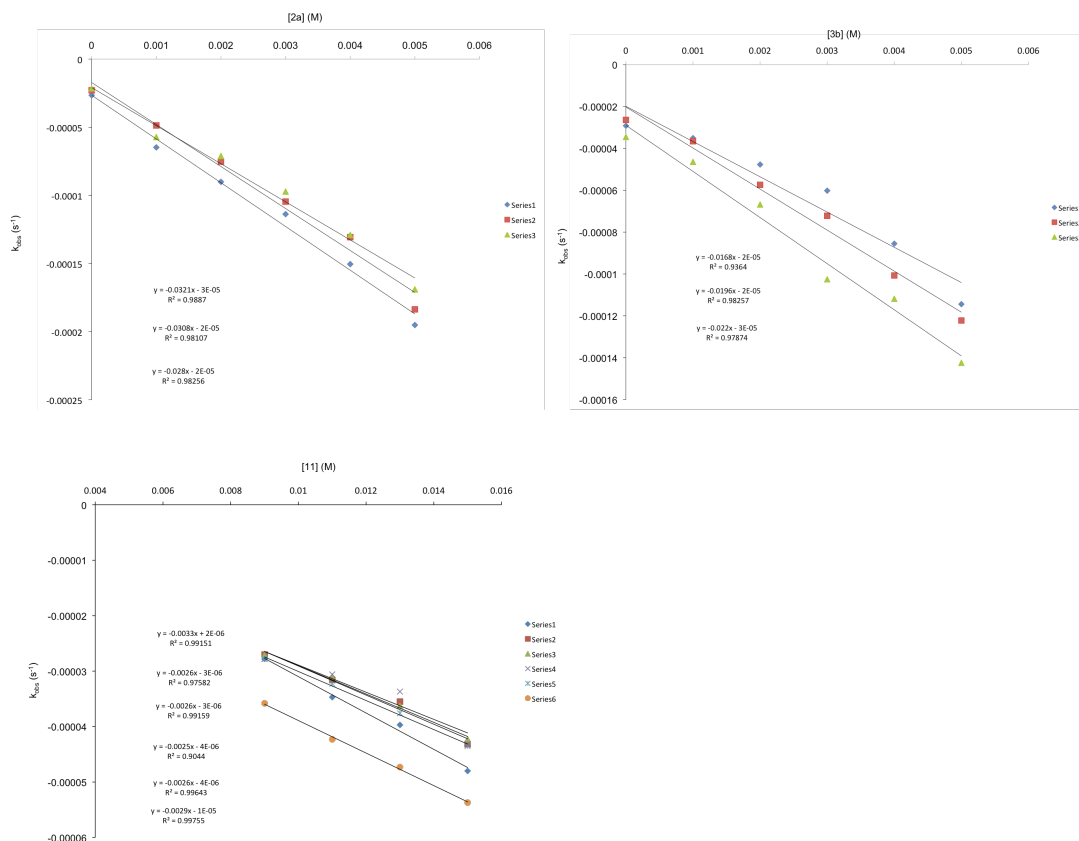


Figure 2-6. Plots used to calculate second-order rate constants of the reaction between (A) **2.2a**, (B) **2.3b**, (C) **2.11** and tetrazine **2.12** in 1:1 CH_3CN :PBS. Second-order rate constants were also calculated for (D) **2.2a** and (E) **2.11** with **Tz-Biotin** in 1:1 CH_3CN :PBS. Second-order rate constants in CH_3CN were also calculated using the plots (F) **2.2a**, (G) **2.3b**, and (H) **2.11** with **2.12**.

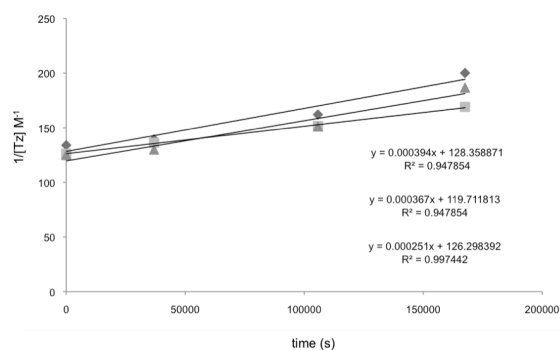


Figure 2-7. Plot used to calculate the rate constant for the cyclopropene **2.2b** - tetrazine **2.12** cycloaddition in CD_3OD .

While the cyclopropene reactions are markedly slower than other tetrazine-based ligations (~4-5 orders of magnitude slower than some TCO reactions) [40], they are still suitable for use in biological systems. In fact, the cycloaddition rates measured for **2.2a** and **2.11** are on par with two bioorthogonal reactions widely utilized in live cells and animals: the Staudinger ligation ($k = 0.25 \times 10^{-2} \text{ M}^{-1}\text{s}^{-1}$ in 5% H₂O/CH₃CN) and the strain-promoted azide-alkyne cycloaddition with a difluorinated cyclooctyne ($k = 7.6 \times 10^{-2} \text{ M}^{-1}\text{s}^{-1}$ in CH₃CN) [14, 41]. These reactions remain popular despite their relatively slow rates, as the need for small, non-perturbing chemical reporters (e.g., azides) can often trump the need for rapid reactivity in living systems.

Our analyses of the cycloaddition reactions also revealed important mechanistic details. Cyclopropene-tetrazine ligations proceed via an initial Diels-Alder cycloaddition, followed by N₂ expulsion. Facial selectivity in the initial cycloadduct is dictated by steric considerations, with the anti-addition product likely predominating for most cyclopropenes (Figures 2-2, 2-8–14) [42]. For di-substituted cyclopropenes, though, the strain associated with multiple suprafacial substituents can drive further electrocyclic ring opening [43, 44]. Subsequent ring closure can ultimately alter the position of the C-3 substituent (placing it over the tetrazine ring, as in **2.14**). Indeed, when dimethyl cyclopropene **2.2b** was treated with **2.12**, resonances for both **2.13** and **2.14** were observed in the ¹H-NMR spectrum. We also noticed that the yellow color of this solution faded over time in aqueous buffer. NMR and HPLC analyses revealed that the initial cycloadduct undergoes further intramolecular attack at the imine carbon to yield **2.15** (Figures 2-2, 2-8–10). This internal cyclization was also observed when cyclopropene **2.3b** was treated with tetrazine **2.12**, although intramolecular attack proceeded at a faster rate (Figures 2-11 and 2-12). By contrast, when **2.11** (lacking a suitable C-3 nucleophile) was treated with **2.12**, no intramolecular cyclization was observed following ring opening (Figure 2-13 and 2-14). While

some cyclopropene-tetrazine adducts are prone to further rearrangement, it is important to note that the starting materials remain covalently linked.

2.2c Protein modification via cyclopropene-tetrazine ligation

In addition to undergoing rapid and selective ligation reactions, chemical reporters must function in complex environments. To evaluate the cyclopropene scaffolds in a biologically relevant setting, we appended the reporters to a model protein (lysozyme or BSA). Standard carbonate- and NHS-ester coupling reactions were used to attach cyclopropene scaffolds **2.10** and **2.24**, respectively, to the protein surface (Figures 2-15A and Scheme 2-2). The modified protein samples were then reacted with a rhodamine-functionalized tetrazine scaffold (**Tz-Rho**, Scheme 2-3) and analyzed via mass spectrometry (Figure 2-16) or in-gel fluorescence imaging (Figures 2-15A and 2-16). As depicted in Figures 2-3B-D and 2-17, the ligations were both time- and dose-dependent, and no reaction was observed in the absence of either **Tz-Rho** or cyclopropene.

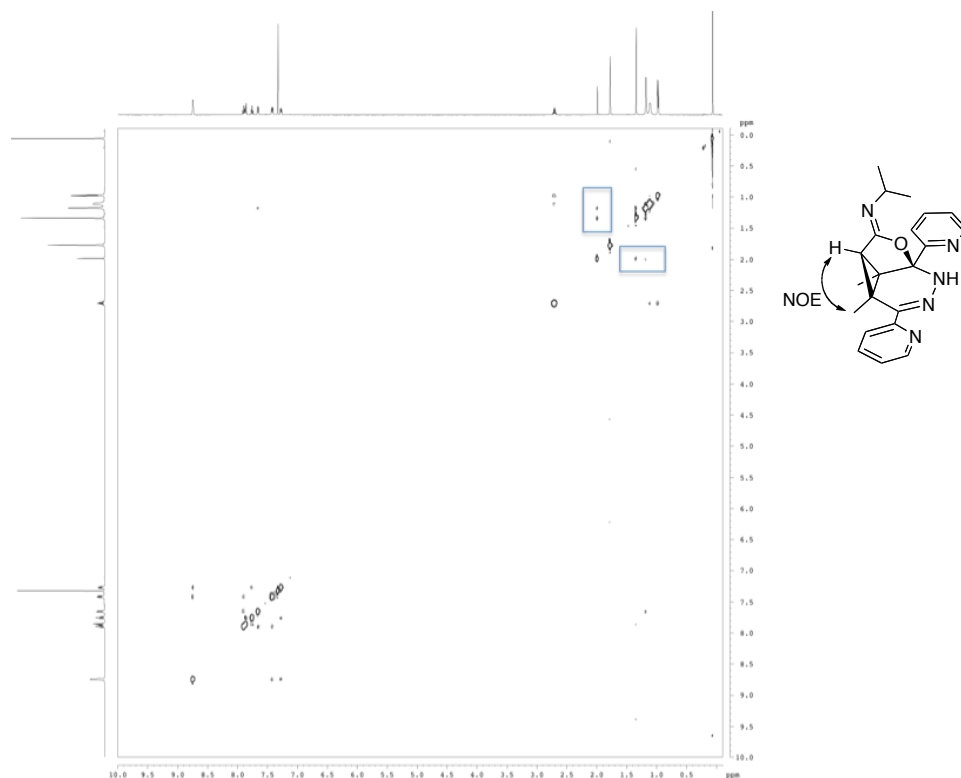


Figure 2-8. NOESY spectrum of cycloadduct **2.15** with relevant cross peaks highlighted.

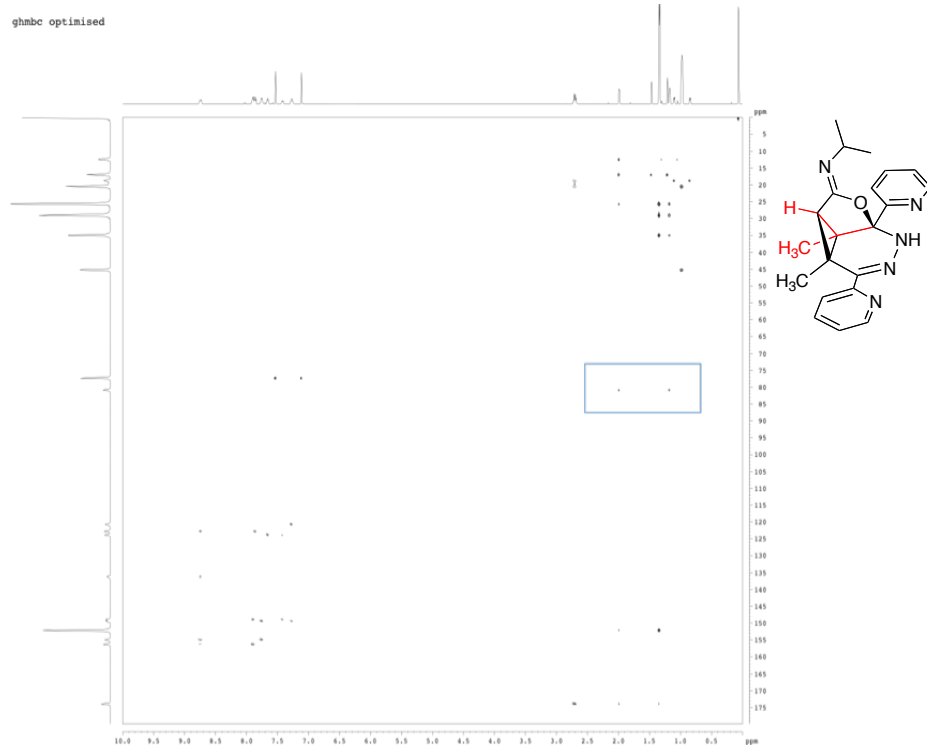


Figure 2-9. HMBC spectrum of cycloadduct **2.15**. Cross peaks highlighting the proximity of the C-3 proton and one methyl substituent to the quaternary center are noted.

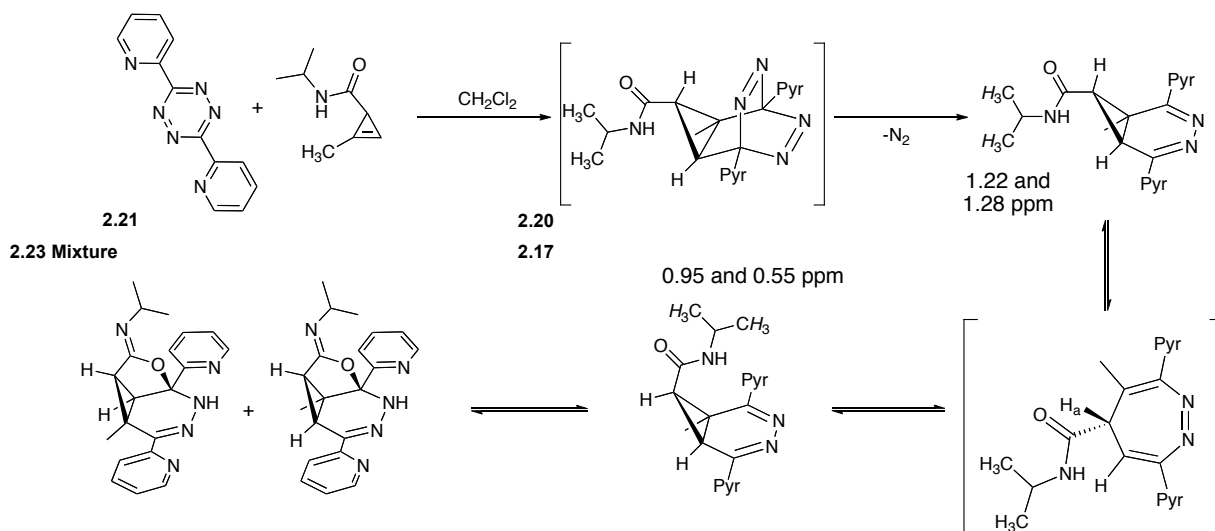


Figure 2-10. The initial cycloadduct **2.16** formed from **2.2a** and **2.12** exists in equilibrium with **2.17** and presumably **2.22**. Diagnostic $^1\text{H-NMR}$ chemical shifts for the italicized methyl protons are provided.

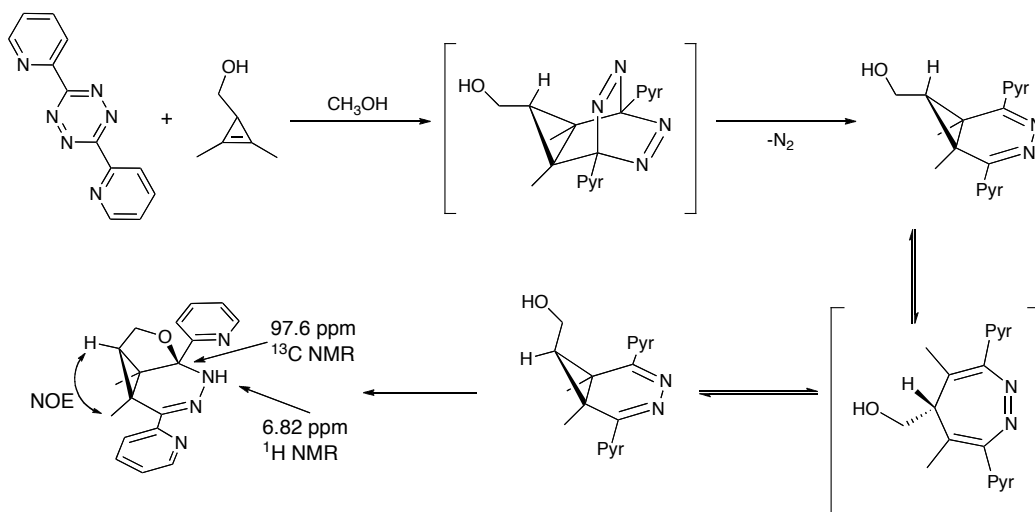


Figure 2-11. Mechanism for cycloadduct formation upon treatment of **2.3b** with **2.12**. The initial cycloadduct further cyclizes to provide **2.21**.

2.12

2.11

2.23

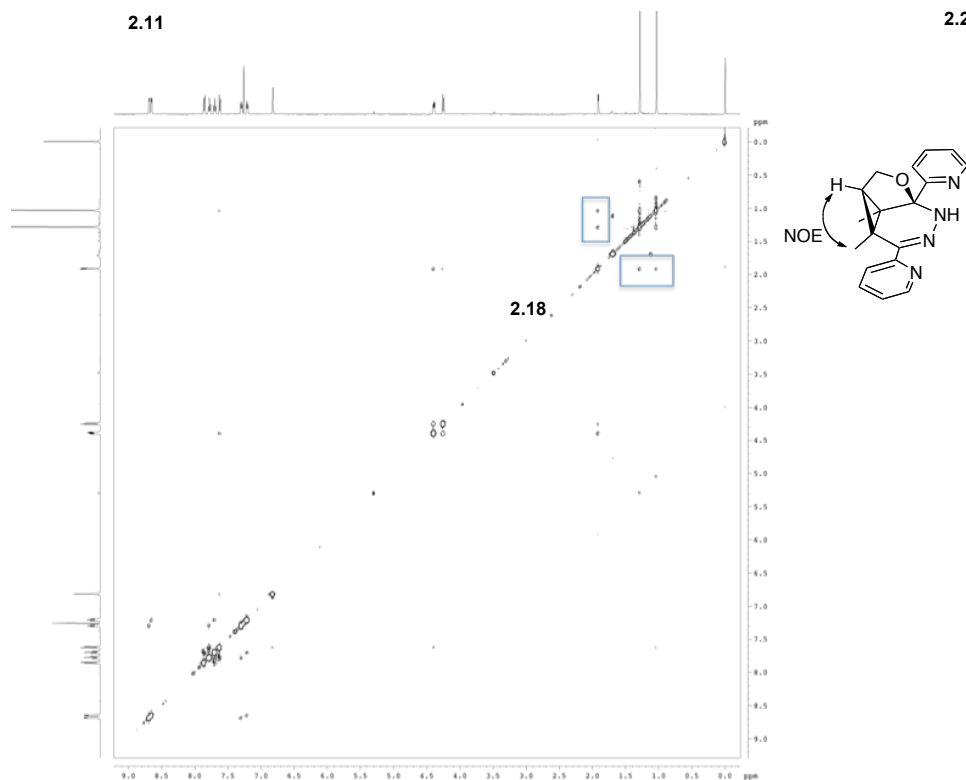


Figure 2-12. NOESY spectrum of cycloadduct **2.21** with relevant cross peaks highlighted.

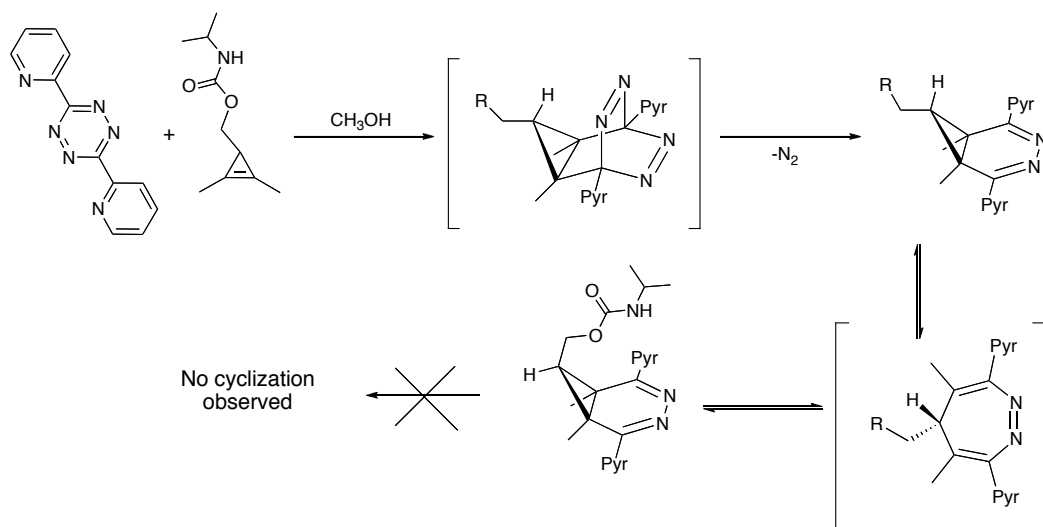


Figure 2-13. Mechanism for cycloadduct formation upon treatment of **2.11** with **2.12**. The ratio of **2.23** to **2.18** is 7:100 by $^1\text{H-NMR}$.

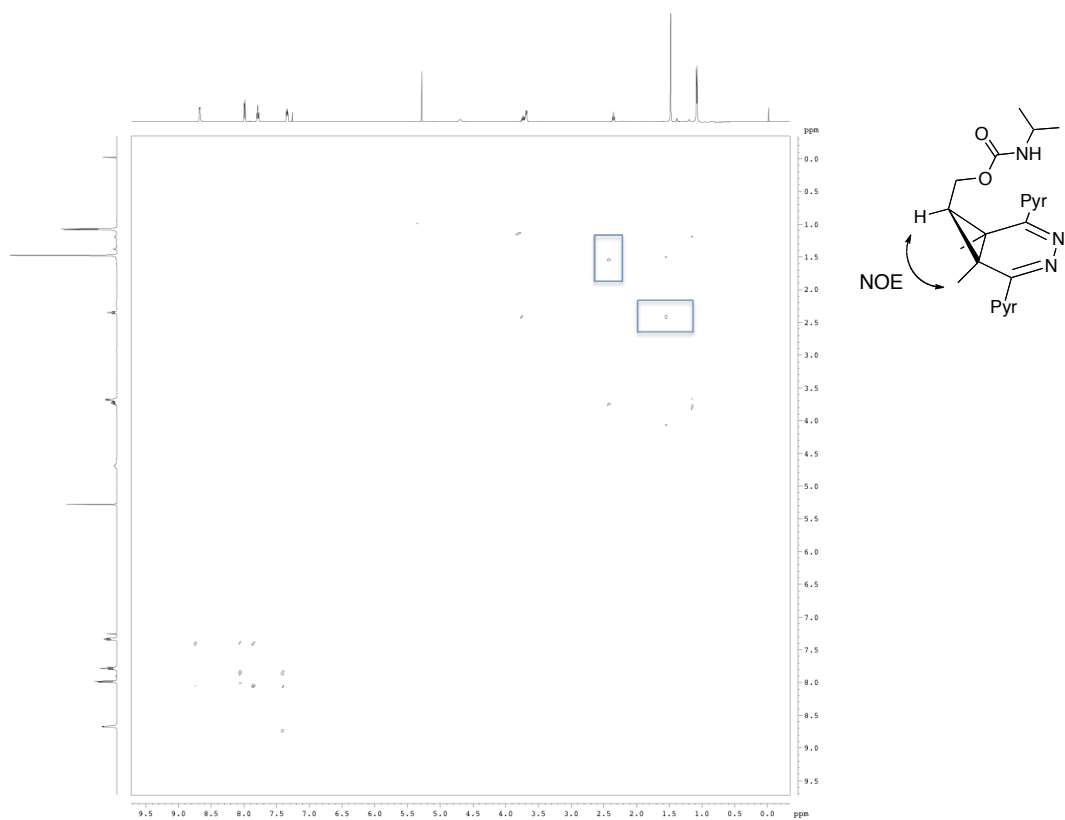


Figure 2-14. NOESY spectrum of cycloadduct **2.18:2.23** mixture with relevant cross peaks highlighted on the major product **2.18**.

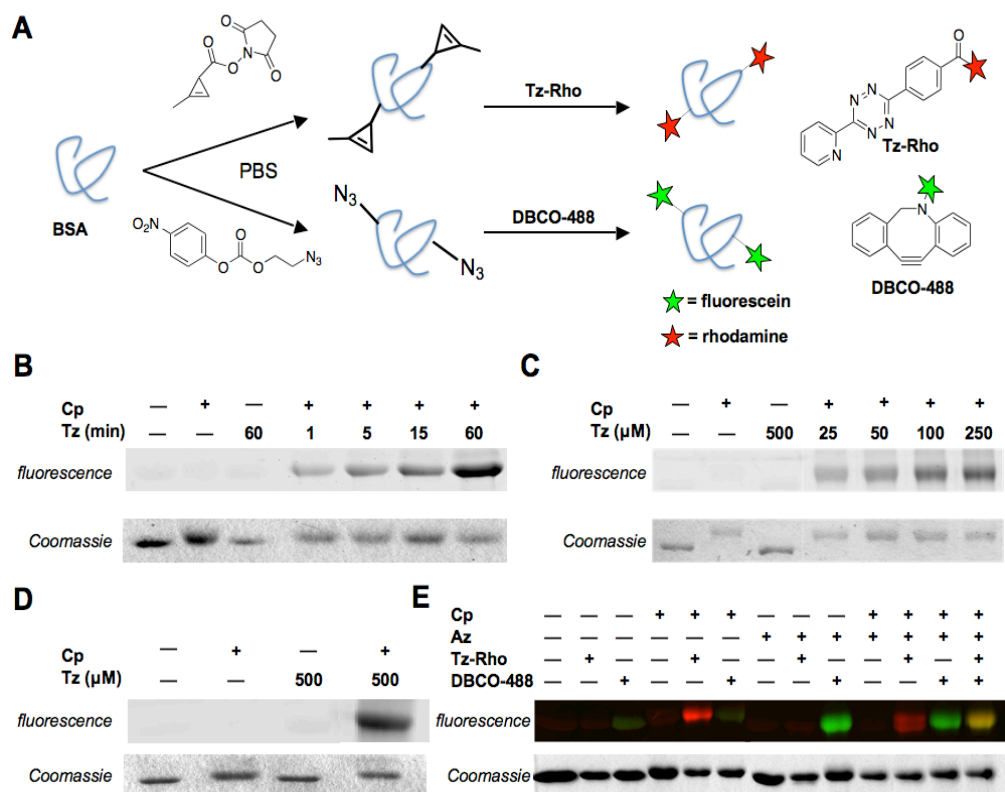
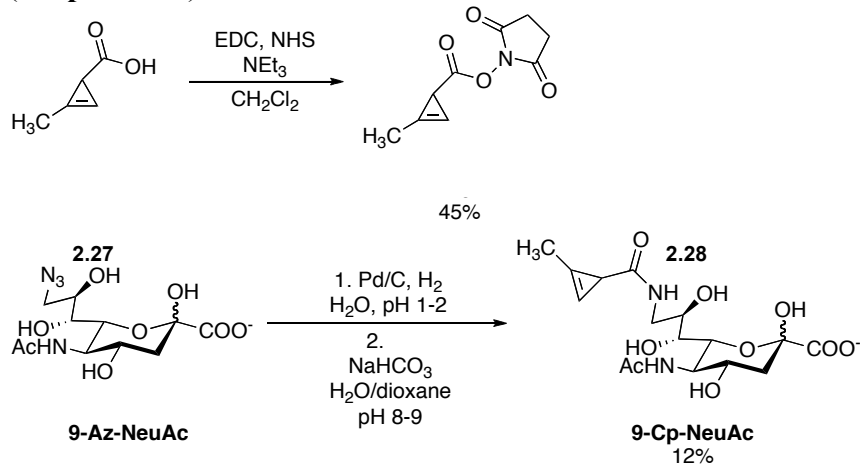


Figure 2-15. Methylcyclopropenes can be selectively modified on protein surfaces. (A) Cyclopropenes (Cp) and azides (Az) were appended to BSA (12.5 mg/mL in PBS) via NHS ester coupling or carbonate activation (8.4 mM labeling reagent). The labeled proteins (2 mg/mL) were subsequently reacted with either a tetrazine-rhodamine (**Tz-Rho**) conjugate or a cyclooctyne-fluorescein conjugate (**DBCO-488**). (B) Gel analysis of cyclopropene-modified BSA incubated with 100 μM **Tz-Rho** for 0-60 min or no reagent (-). (C) Gel analysis of Cp-modified BSA labeled with **Tz-Rho** (0-250 μM) for 1 h. (D) Gel analysis of Cp-modified BSA (+) or BSA only (-) treated with **Tz-Rho** (500 μM) or no reagent (-) at 37 °C for 1 h. (E) Gel analysis of BSA functionalized with Cp, Az, or both chemical reporters (lanes 10-13) and reacted for 1 h with either 100 μM **Tz-Rho**, **DBCO-488**, both reagents simultaneously, or no reagent. For B-E, protein loading was assessed with Coomassie stain (lower panels).

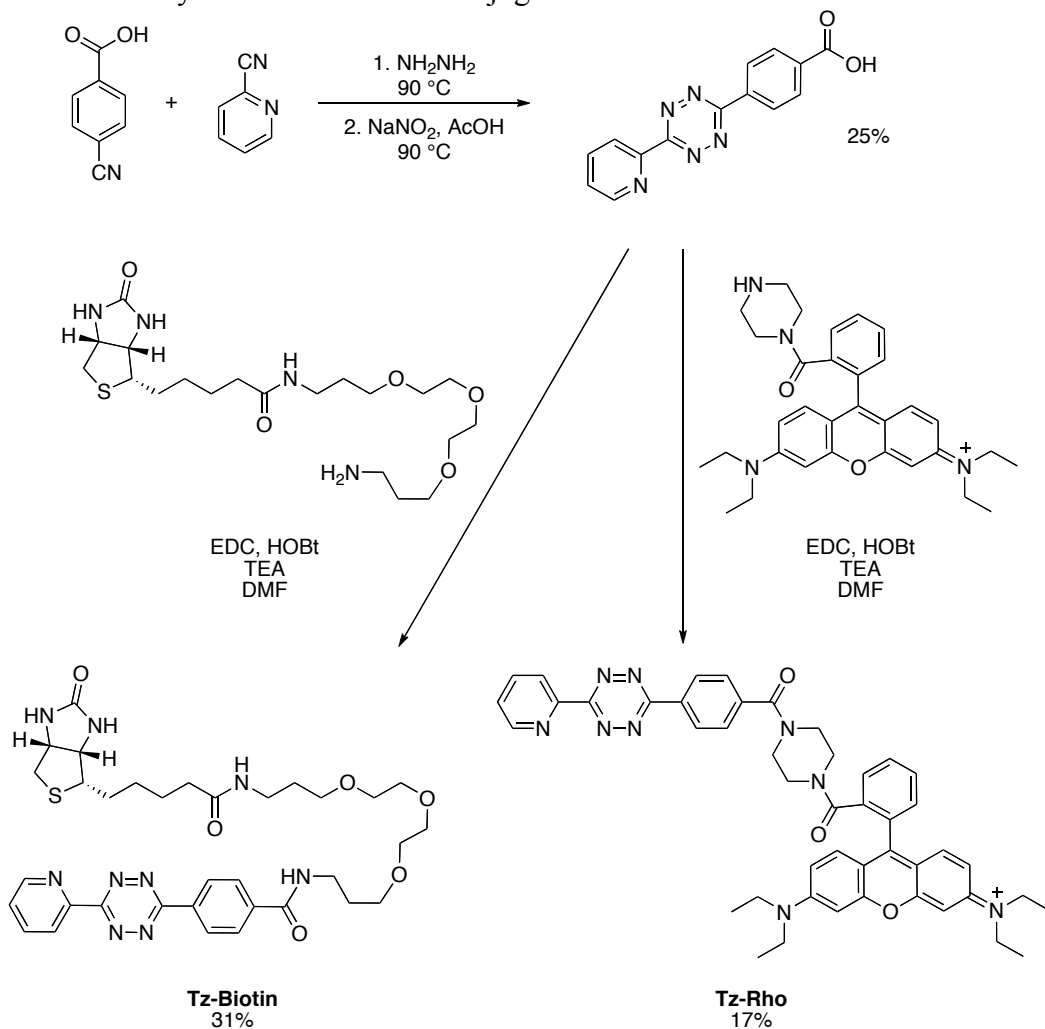
2.24

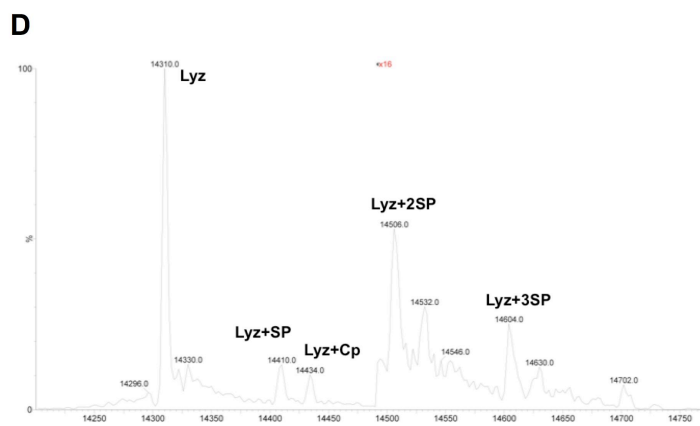
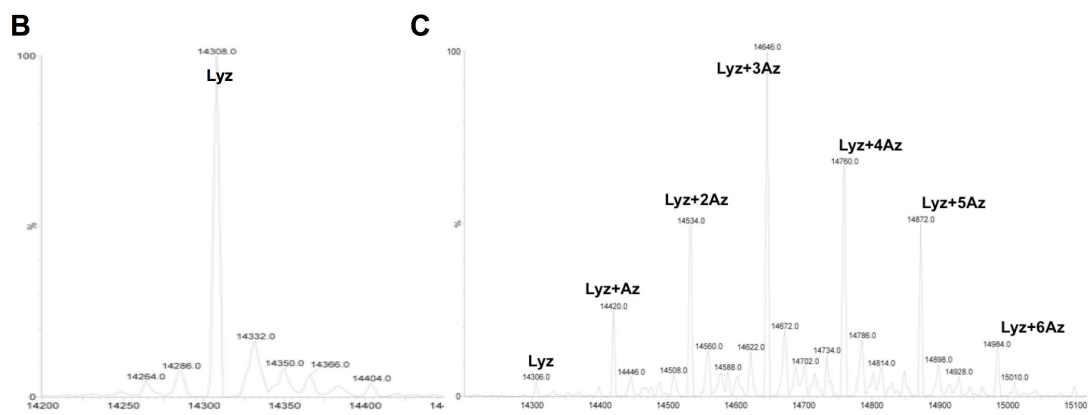
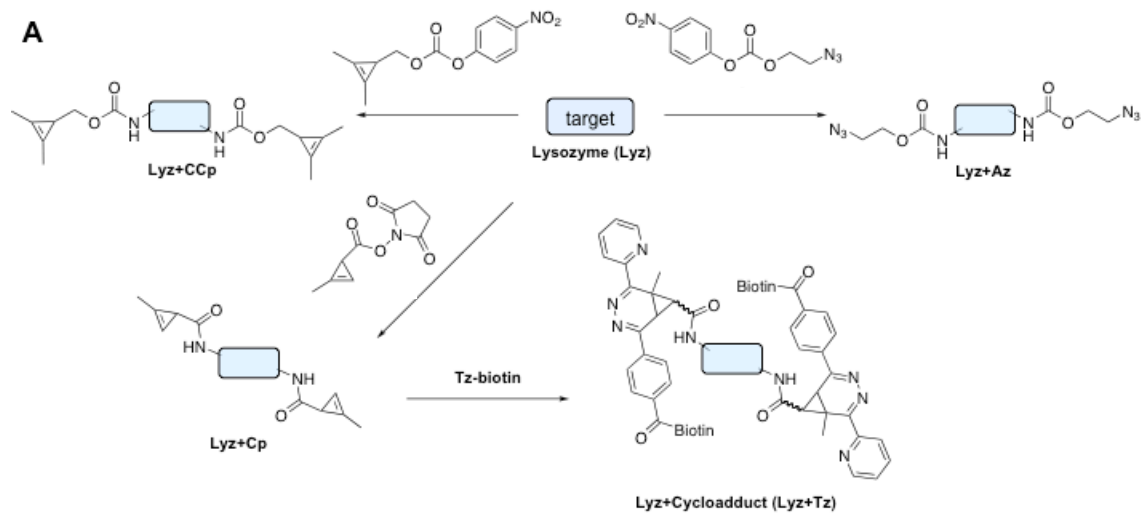
2.24

Scheme 2-2. Synthesis of NHS-cyclopropenyl ester **2.24** and cyclopropene-modified sialic acid (**9-Cp-NeuAc**).



Scheme 2-3. Synthesis of tetrazine conjugates





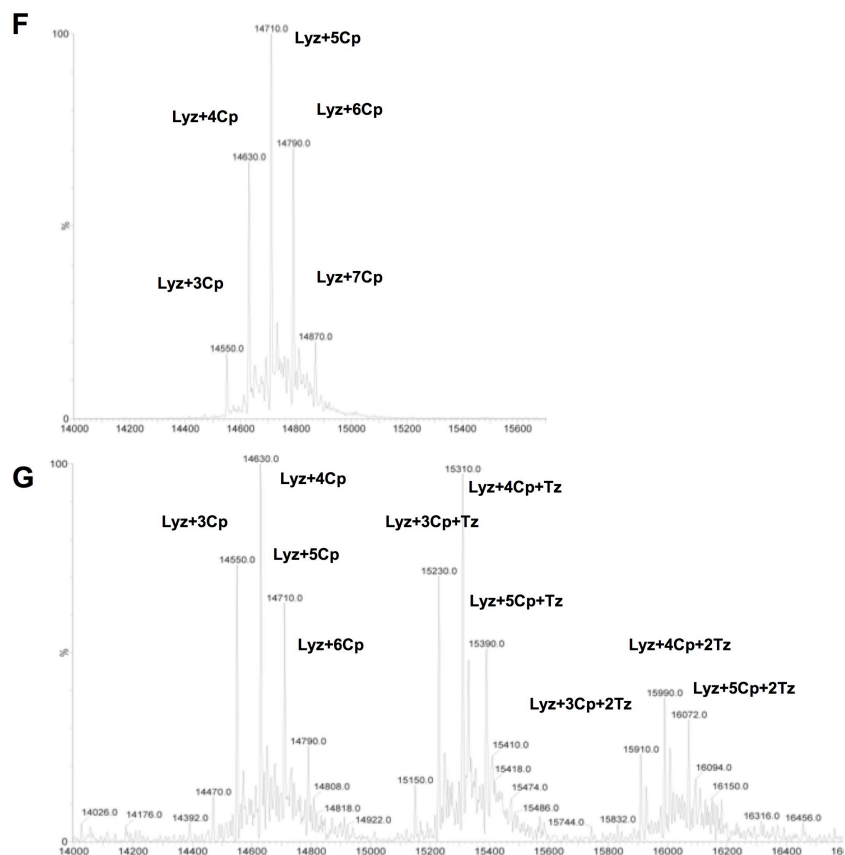


Figure 2-16. Mass spec analysis of protein conjugates. Lysozyme was used as a model protein to verify the extent of cyclopropene and/or-azide modification utilizing NHS-ester or carbonate labeling methods. (A) Lysozyme was treated with carbonates **2.10**, **2.25** or NHS ester **2.24**. A portion of the conjugates was further subjected to covalent labeling with **Tz-Biotin**. (B) Spectrum of unmodified lysozyme. (C) Spectrum of lysozyme modified with **2.25**. (D) Spectrum of lysozyme modified with **2.10**. The lysozyme conjugate also appeared to be modified with an additional group (98 mass units). This could potentially arise via the side reaction shown in E, owing to the large concentration of carbonate probe used. (F) Spectrum of lysozyme modified with **2.24** (G) Spectrum of lysozyme modified with **2.24** and subsequently treated 100 μ M **Tz-Biotin** for 1 h.

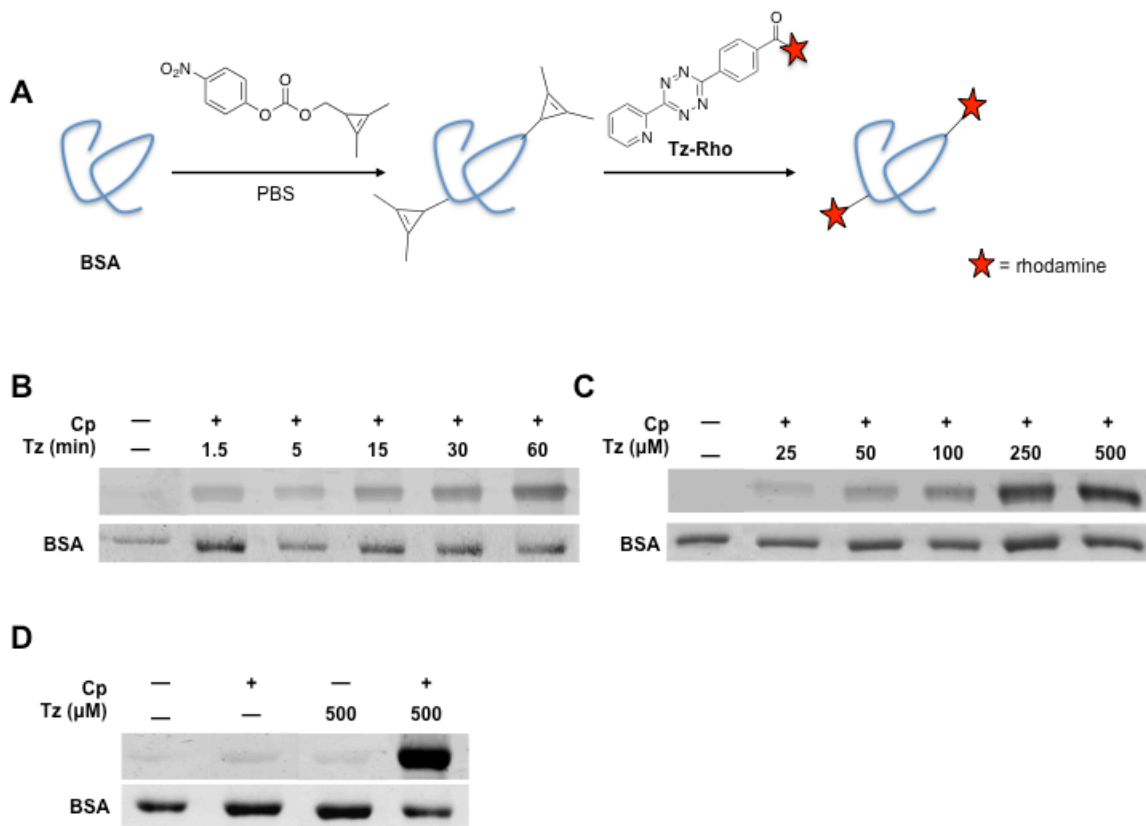


Figure 2-17. Substituted cyclopropenes can be modified on protein surfaces. (A) Cyclopropene (Cp) scaffolds were appended to BSA via carbonate activation. The labeled proteins were subsequently reacted with **Tz-Rho**. (B) Gel analysis of cyclopropene-modified BSA incubated with 100 μM **Tz-Rho** for 0-60 min or no reagent (-). (C) Gel analysis of cyclopropene-modified BSA labeled with **Tz-Rho** (0-500 μM) for 1 h. (D) Gel analysis of cyclopropene-modified BSA (+) or BSA only (-) treated with **Tz-Rho** (500 μM) or no reagent (-) at 37 °C for 2 h. For B-D, protein loading was assessed with Coomassie staining.

We also examined whether the cyclopropene-tetrazine ligation is compatible with azides and strained alkynes. The orthogonality of such reagents would enable cyclopropenes to be used in tandem with established bioorthogonal chemistries for dual labeling experiments. Cyclopropenes are known to react with organic azides and other 1,3-dipoles, but such reactions typically require strong heating [45]. Indeed, when cyclopropenes **2.2a** or **2.11** were subjected to azidoethanol or phenyl azide in organic solvent, no reaction was observed under ambient conditions over 24 h (data not shown). Additionally, when cyclopropene (Cp)- and azide (Az)-modified BSA conjugates were mixed together (providing Cp/Az-BSA), both functional groups could be selectively targeted with covalent probes (either **Tz-Rho** or a dibenzocyclooctyne-fluorophore conjugate, **DBCO-488**) [46], suggesting that Cp and Az can coexist to a certain extent (lanes 11-13, Figure 2-15E). Reduced fluorescence intensities were observed when either **DBCO-488** or **Tz-Rho** was incubated with Cp/Az-BSA (compared to BSA samples modified with either Az or Cp alone), but this was likely due to fewer reporter groups present in the sample itself—Cp-BSA and Az-BSA were combined 1:1 to generate the mixed sample (Cp/Az-BSA), halving the number of available reporter groups (Figure 2-15E).

Cyclopropene reactivity with cyclooctynes and other strained molecules has not been extensively investigated. However, when cyclopropene-modified BSA (Cp-BSA) was treated with **DBCO-488**, no signal above background was observed under the labeling conditions employed (lane 6, Figure 2-15E). The faint fluorescence signal can be attributed to non-specific **DBCO-488** reactivity (lane 3, Figure 2-15E). The compatibility of tetrazine scaffolds with both azides and strained alkynes, by contrast, has been examined in more detail [22, 24, 46]. In a recent study, Hilderbrand and coworkers observed reactivity between a mono-substituted tetrazine and a DBCO conjugate ($k = 6 \times 10^{-2} \text{ M}^{-1}\text{s}^{-1}$). However, no reaction was observed when a di-substituted, deactivated tetrazine was employed [22]. The authors further demonstrated that the kinetically slower tetrazine could be used in tandem with DBCO to label TCOs and azides in cells. In our studies, **Tz-Rho** was expected to react with DBCO (albeit minimally) based on cycloaddition rates measured for similar tetrazines and TCO [39]. However, when **Tz-Rho** was incubated with **DBCO-488**, no reaction was observed over 12 hours in PBS (Figure 2-18). Additionally, co-administration of **Tz-Rho** and **DBCO-488** to Cp/Az-BSA did not significantly diminish covalent protein labeling (Figure 2-15E, Figure 2-19). While a detailed analysis of tetrazine-DBCO reactivity has not been performed, our results suggest that the two reagents can be used concurrently to target cyclopropenes and azides under certain conditions.

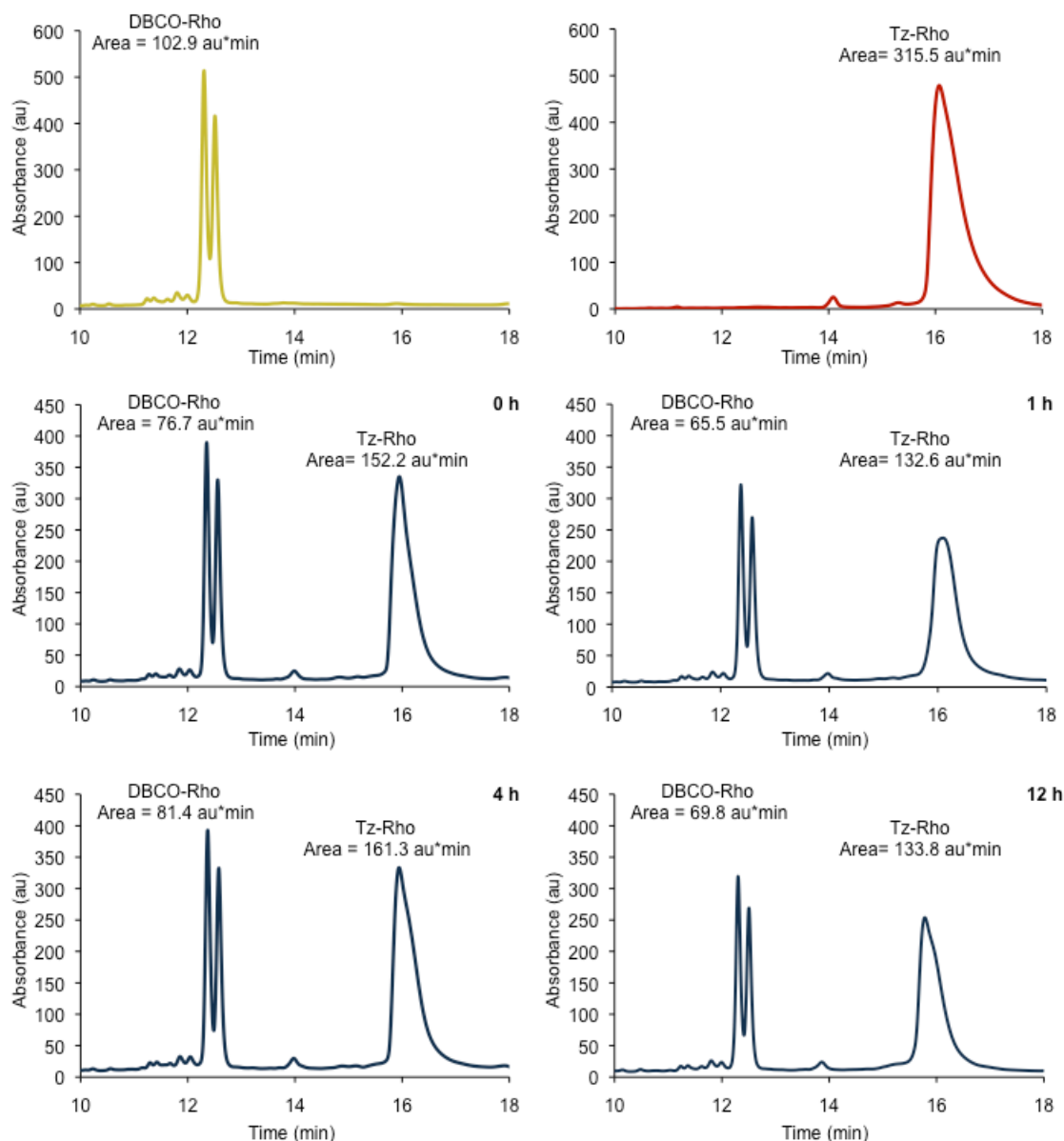


Figure 2-18. No reaction between **DBCO-Rho** and **Tz-Rho** was observed over 12 h. Commercially available **DBCO-Rho** (sold as a mixture of isomers) and **Tz-Rho** were dissolved separately in PBS (2 mM), and 200 μ L of each solution were combined. The final concentration of each reagent in the mixed sample was 1 mM (ten times the concentration used in any protein or cell labeling experiment). Aliquots were drawn from the reaction mixture over time and analyzed by HPLC (eluting with 0-50% CH_3CN in water over 10 min, followed by 50% CH_3CN for 10 min). The peak areas for each reagent are provided in the above plots. The starting traces for DBCO-Rho (yellow) and Tz-Rho (red) were acquired from the initial 2 mM solutions; all other traces were acquired from the mixed sample.

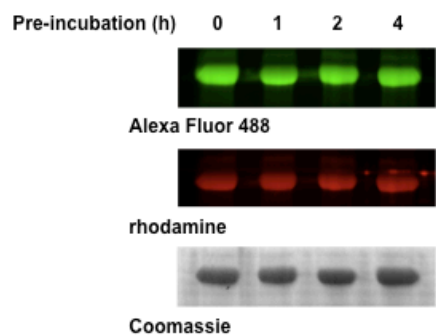


Figure 2-19. Pre-incubation of tetrazine and DBCO scaffolds has no noticeable affect on protein labeling. **DBCO-488** and **Tz-Rho** were incubated together in PBS (1 mM each) for 0-4 h prior to the addition of Az- and Cp-modified BSA. Protein labeling reactions were performed as in Figure 3, and a representative image is shown here. Top panel: **DBCO-488** fluorescence. Middle panel: **Tz-Rho** fluorescence. Lower panel: loading control with Coomassie staining.

2.2d Metabolic incorporation of cyclopropenes onto live cell surfaces

Beyond biomolecule modification *in vitro*, chemical reporters must be able to traverse metabolic pathways *in vivo*. This requires that the scaffolds are stable in living systems and small enough to be tolerated by biosynthetic enzymes [1]. To investigate whether cyclopropenes would be useful for cellular labeling studies, we constructed a methylcyclopropene-sialic acid conjugate (**9-Cp-NeuAc**, Scheme 2-2). Modified sialic acids of this sort are known to be metabolized by cells and incorporated into cell surface glycans [47-50]. Jurkat cells were incubated with various concentrations of **9-Cp-NeuAc** for 24-48 h. The presence of cell surface cyclopropenes was subsequently probed by reaction with a tetrazine-biotin conjugate (**Tz-Biotin**, Scheme 2-3) and avidin staining (Figure 2-20A). The fluorescence of each cell population was measured using flow cytometry. As shown in Figure 2-4B, a dose-dependent increase in signal was observed when cells were incubated with increasing concentrations of **9-Cp-NeuAc**, indicating successful metabolic incorporation of the chemical reporter. The incorporation efficiency of **9-Cp-NeuAc** was lower than that of a similarly functionalized azido sugar (**9-Az-NeuAc**, Scheme 2-2), but on par with other unnatural sialic acids used in metabolic engineering studies (Figure 2-21) [47-50]. Importantly, the fluorescence signal also diminished when **9-Cp-NeuAc**-treated cells were cultured in the presence of unlabeled sugars (sialic acid, NeuAc or peracetylated *N*-acetylmannosamine, Ac₄ManNAc) targeting the same metabolic pathway [47].

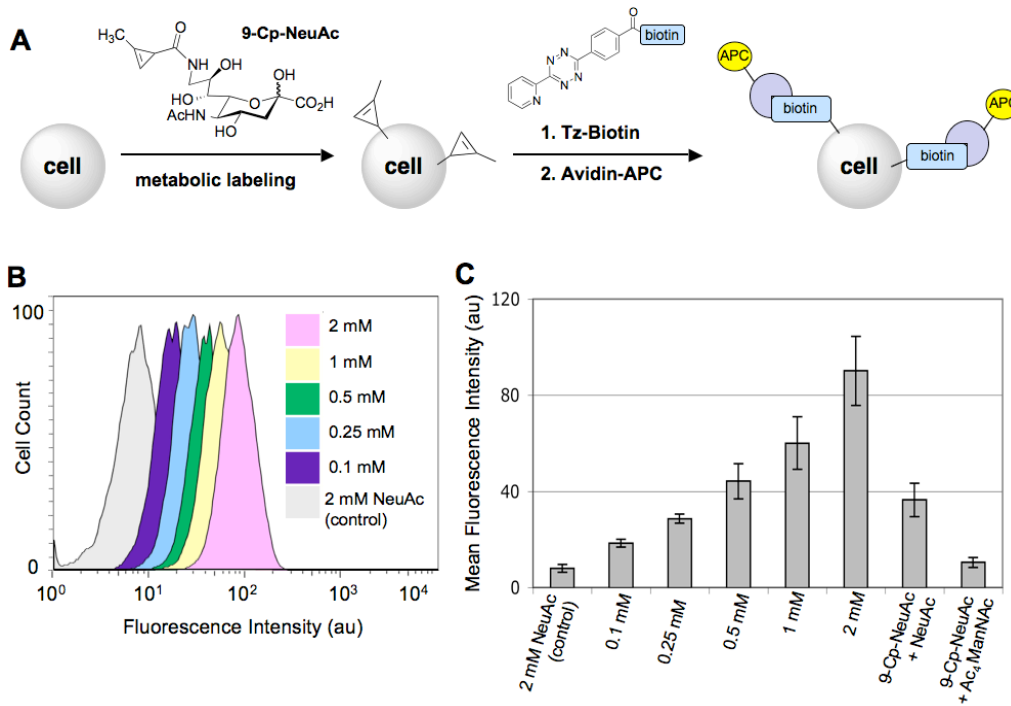


Figure 2-20. Cyclopropenes can be metabolically incorporated onto live cell surfaces. (A) Jurkat cells were incubated with **9-Cp-NeuAc** (0-2 mM), a control sugar (NeuAc, 2 mM) or both **9-Cp-NeuAc** and NeuAc (or Ac₄ManNAc) for 24 h. After washing, the cells were reacted with **Tz-Biotin** (100 μ M) for 1 h at 37 $^{\circ}$ C. Subsequent staining with APC-avidin and flow cytometry analysis provided the plots in (B). (C) Mean fluorescence intensities (in arbitrary units, au) for the histograms in (B). Error bars represent the standard deviation of the mean for three experiments.

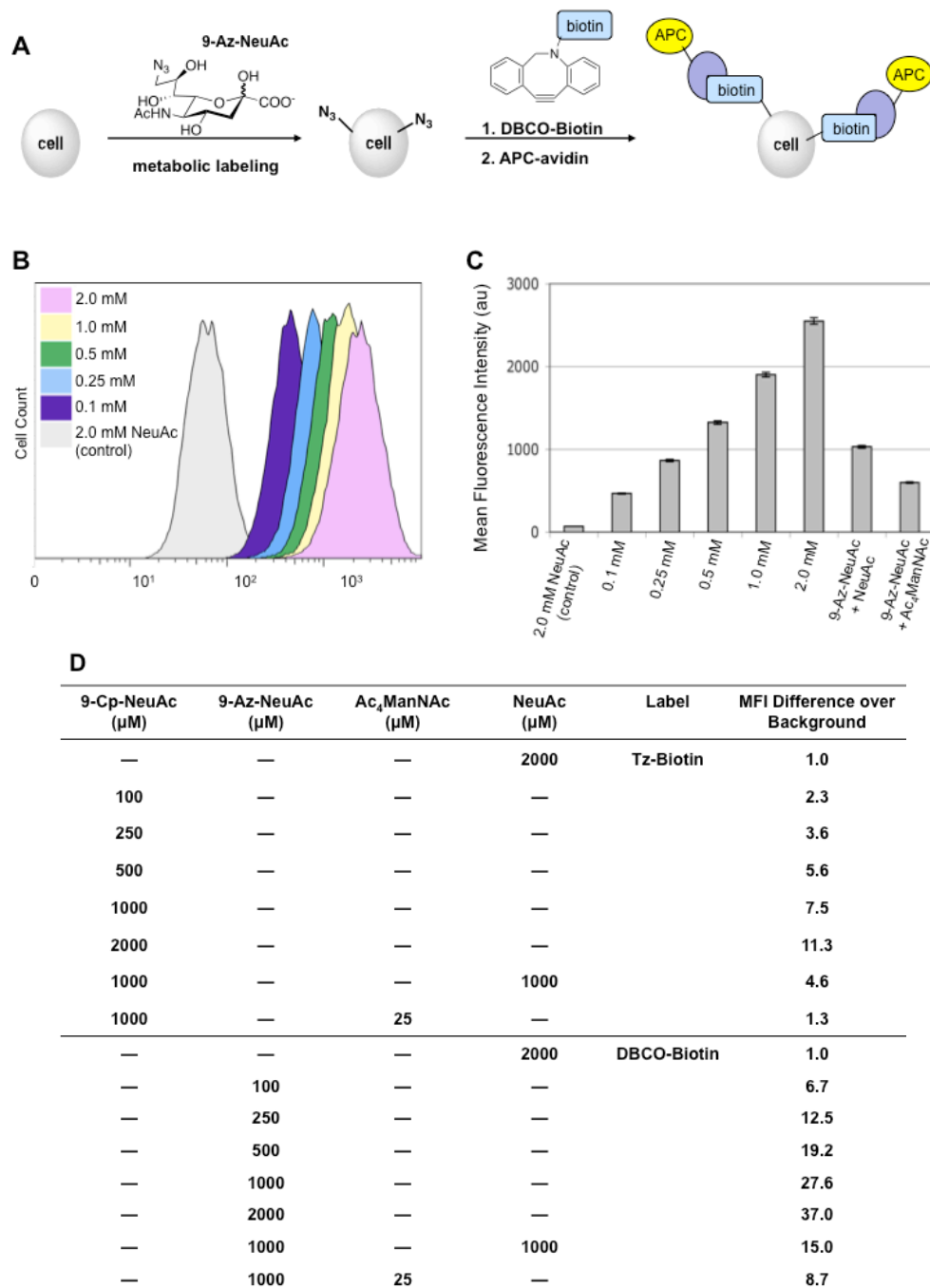


Figure 2-21. Flow cytometry analysis of **9-Az-NeuAc** metabolism in Jurkat cells. (A) Cells incubated with **9-Az-NeuAc** (0-2 mM) were treated with 100 μM **DBCO-Biotin** followed by APC-avidin. (B) Flow cytometry histograms revealing a dose-dependent increase in fluorescence correlating with **9-Az-NeuAc** concentration. (C) Mean fluorescence intensities (in arbitrary units, au) for the histograms in (B). Error bars represent the standard deviation of the mean for three experiments. A reduction in signal was observed when cells were incubated simultaneously with **9-Az-NeuAc** and unlabeled sugars (sialic acid and Ac₄ManNAc). (D) Comparison of the metabolic incorporation efficiencies of **9-Cp-NeuAc** and **9-Az-NeuAc**.

We further investigated whether cyclopropene- and azide-modified sugars could be utilized concurrently for live cell labeling. In one setup, Jurkat cells were incubated with **9-Cp-NeuAc**, **9-Az-NeuAc**, or no sugar. After 24 h, portions of the sugar-treated cells were combined. In a second setup, Jurkat cells were cultured with both sugars simultaneously. All samples were subsequently reacted with either **Tz-Biotin**, a water-soluble cyclooctyne-fluorophore conjugate (**DBCO-Rho**), or both reagents. Cells treated with **Tz-Biotin** were also stained with APC-avidin. The fluorescence of the resulting cell populations was analyzed via two-color flow cytometry, and the corresponding plots are depicted in Figure 2-22. For cells cultured separately with the unnatural sugars prior to mixing and covalent reaction, flow analysis revealed two distinct cell populations—one with robust APC fluorescence (corresponding to the **9-Cp-NeuAc**-treated cells) and one with robust rhodamine fluorescence (corresponding to the **9-Az-NeuAc**-treated cells) (Figure 2-22A). For cells cultured with the cyclopropenyl and azido sugars simultaneously, treatment with both covalent probes and flow analysis revealed a single population of cells labeled with both fluorophores (Figure 2-22B). The overall fluorescence signal attributed to the cyclopropene modification was reduced in this case, though, likely due to the lower incorporation efficiency of **9-Cp-NeuAc** compared to **9-Az-NeuAc**. Non-specific reactivity with **DBCO-Rho** was also observed in the cell labeling studies, but importantly, no cross-reactivity was observed when **9-Az-NeuAc**-treated cells were labeled with **Tz-Biotin** or when **9-Cp-NeuAc**-treated cells were labeled with **DBCO-Rho** (Figure 2-23). Collectively, these results suggest that cyclopropene- and azide-based chemical reporters can be utilized together in live cells and will be useful for multiplexed metabolic engineering strategies.

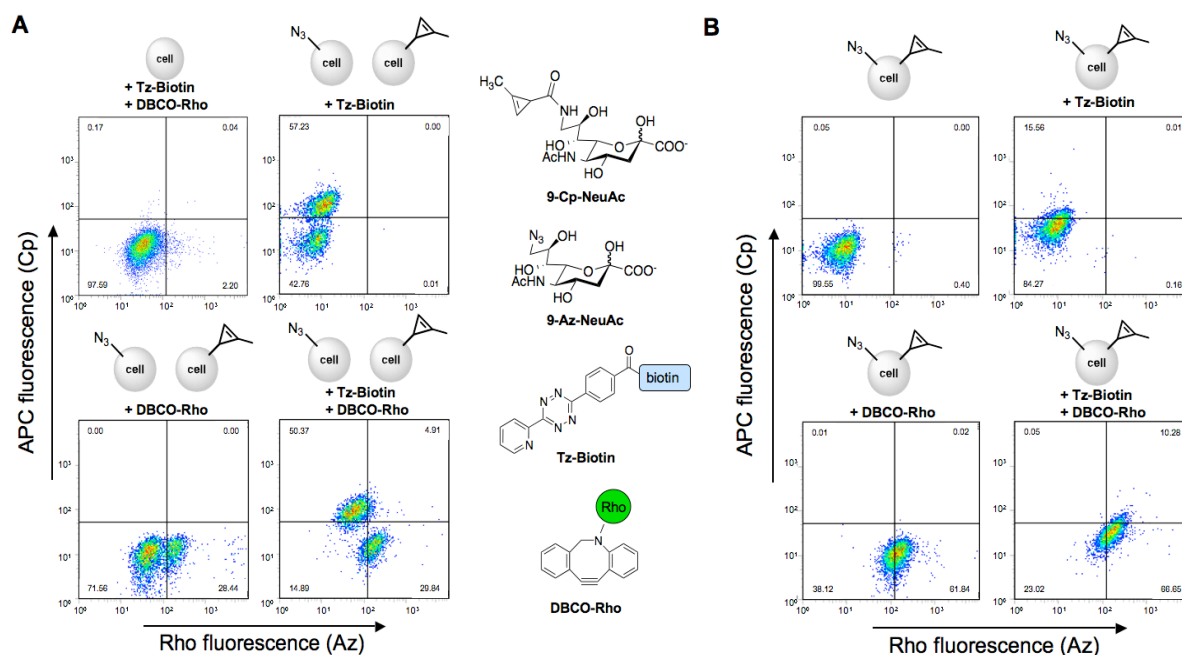


Figure 2-22. Methylcyclopropenes and organic azides can be utilized in tandem for cellular metabolic labeling. (A) Flow cytometry analysis of Jurkat cells treated with **9-Cp-NeuAc** (1 mM), **9-Az-NeuAc** (1 mM), or no sugar for 24 h. After washing, a portion of the **9-Cp-** and **9-Az-NeuAc** cells were mixed. Cell samples were then washed and subsequently reacted with **Tz-biotin** (100 μ M), **DBCO-Rho** (100 μ M) or both reagents for 1 h at 37 $^{\circ}$ C. Following staining with APC-avidin, cellular fluorescence was measured. Plots are shown with Rho (azide) and APC (cyclopropene) levels on the x- and y-axes, respectively. (B) Flow cytometry analysis of Jurkat cells incubated with **9-Cp-NeuAc** (1 mM) and **9-Az-NeuAc** (1 mM) simultaneously. After 24 h, the cells were washed, reacted, and analyzed as in (A). For (A) and (B), the same patterns of labeling were apparent in replicate experiments.

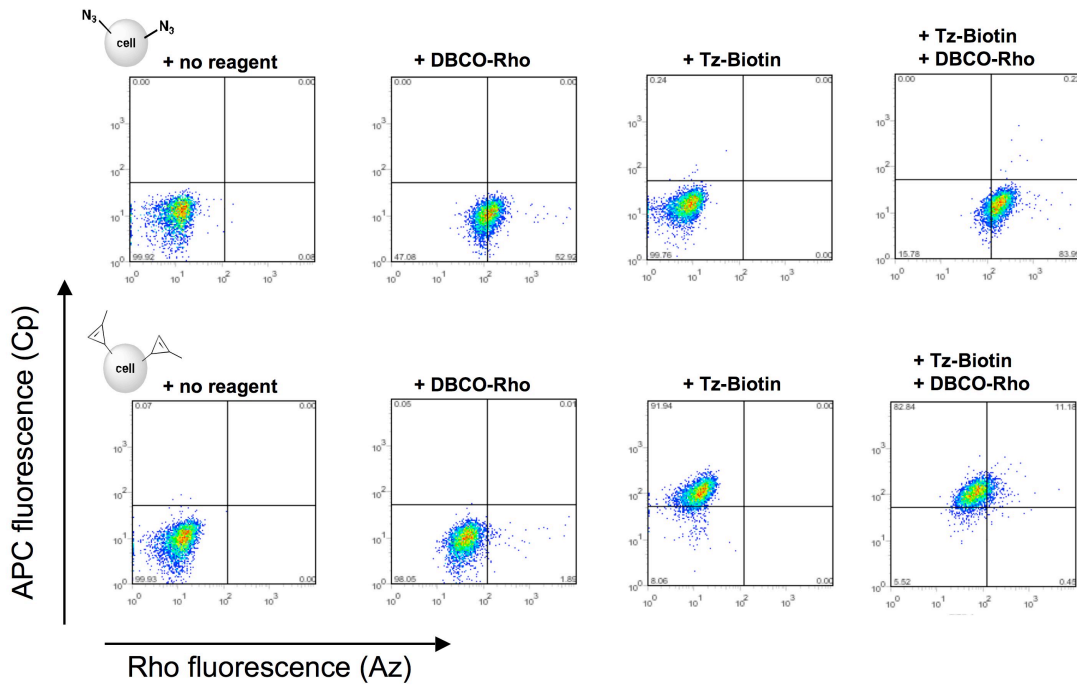


Figure 2-23. Cells incubated with **9-Cp-NeuAc** (lower panels) or **9-Az-NeuAc** (upper panels) (1 mM) were treated with DBCO-Rho (100 μ M), Tz-biotin (100 μ M), both reagents, or no reagent and analyzed as in Figure 2-22.

2.3 Conclusions

In summary, functionalized cyclopropenes have been developed for use as chemical reporters in living systems. These scaffolds react with tetrazines to form covalent adducts in high yield and with rates suitable for biological labeling applications. Our data also indicate that cyclopropenes are stable in biological environs and can be used to derivatize proteins and other biomolecules. Moreover, these functional groups can be metabolically introduced into cellular glycans, suggesting they are small enough to traverse biosynthetic pathways in live cells. Methylcyclopropenes can also be used in tandem with organic azides, and we anticipate that combinations of these and other chemical reporters will be widely used for targeting multiple classes of biomolecules [51].

This work also sets the stage for continued expansion of the bioorthogonal chemistry toolkit. We envision developing a collection of cyclopropene scaffolds suitable for use as both chemical reporters and secondary labeling agents. Toward this end, we are generating cyclopropenes that react more rapidly with tetrazine probes, along with identifying scaffolds with alternative modes of reactivity. These reagents will bolster efforts to monitor multi-component biomolecular processes in living systems.

2.4 Materials and methods

2.4a Cyclopropene stability

The relative stabilities of cyclopropenes **2.2a** and **2.11** were evaluated in two separate assays. To determine shelf stability in solution, the compounds were dissolved in CDCl₃ (100 mM) and monitored over time (at 4 °C) via ¹H-NMR. To analyze cyclopropene stability in the presence of

biological nucleophiles, **2.2a** or **2.11** was incubated with cysteine (5 mM of each reagent in 10% DMSO- d_6 /deuterated PBS, pH 7.4) and the resulting solutions were monitored via $^1\text{H-NMR}$.

2.4b Rate studies

UV-Vis method

The reactions between cyclopropenes **2.2a**, **2.3b**, **2.11** and tetrazine **2.12** or **Tz-Biotin** were monitored by the change in tetrazine absorbance at 536 nm. Reactions were initiated in a 96-well plate by mixing 150 μL of a 0.2 mM tetrazine solution (in CH_3CN or 1:1 CH_3CN :PBS) with 150 μL of cyclopropene solution (2-10 mM in CH_3CN or 1:1 CH_3CN :PBS). The concentration of cyclopropene at the start of each reaction ranged from 1-5 mM, while the tetrazine concentration was held at 0.1 mM. For **2.1** and **2.11**, larger concentrations of cyclopropene (9-15 mM in CH_3CN) were used to overcome slow reaction kinetics. All rate studies were performed in triplicate under pseudo-first order conditions. Absorbance measurements were recorded every 5 min over a 90-min time interval using a BioTek Epoch plate reader equipped with Gen5 software. Pseudo-first order rate constants (k_{obs}) were calculated by plotting the natural log of [**2.12**] or **Tz-Biotin** versus time (in s). Second-order rate constants were determined by plotting k_{obs} vs cyclopropene concentration.

$^1\text{H-NMR}$ method

The cycloaddition reaction between cyclopropene **2.2b** and tetrazine **2.12** was not easily monitored by UV-vis spectroscopy owing to its slow rate. Therefore, $^1\text{H-NMR}$ was used to calculate the rate constant for this transformation. Cyclopropene **2.2b** and tetrazine **2.12** (5 mM

each) were combined in CD₃OD, and the ensuing reaction was monitored over 48 h. An internal standard (TMS) was used to determine peak integration values and, ultimately, the concentrations of the relevant species.

2.4c Reaction analyses by HPLC

To analyze cycloadduct formation and subsequent cyclizations, the reactions between cyclopropenes **2.2a-b**, and **2.11** with tetrazine **2.12** were monitored by HPLC. Cyclopropene **2.2b** (100 mM) was initially reacted with **2.12** (50 mM) in 2 mL CH₂Cl₂. After 24 h, the reaction mixture was concentrated and subsequently dissolved in PBS (3 mL). The reaction was monitored at 12 h intervals by HPLC (0-95% CH₃CN in water over 20 min). The reaction between tetrazine **2.12** and all other cyclopropenes were performed in 1:1 CH₃CN:PBS (2 mM cyclopropene, 0.5 mM tetrazine) and monitored over 10-48 h by HPLC (0-95% CH₃CN in water over 10 min).

2.4d Protein labeling

Bovine serum albumin (BSA) or lysozyme (Lyz) conjugates were prepared by treating the proteins with carbonates **2.10** or **2.17** as described by Sletten, *et al.* [51], or with cyclopropenyl NHS ester **2.16** using standard coupling conditions [52]. In the former case, BSA or Lys (0.5 mL, 20 mg/mL in PBS) was treated with 100 μL carbonate **2.10** or the corresponding azide **2.17** (67 mM in DMSO) and an additional 200 μL DMSO. The final protein solution (12.5 mg/mL protein, 8.4 mM carbonate) was allowed to stand at rt for 3 h. The same procedure was used to label with the NHS ester **2.16**.

In-gel fluorescence analysis of BSA conjugates

The labeled BSA samples were subsequently isolated using P-10 BioGel® (BioRad), eluting with 2 mL PBS (pH 7.4). The derivatized BSA eluents (180 µL, 2 mg/mL) were treated with **Tz-Rho** (1.0 - 20 µL of a 5 mM solution in DMSO) or a dibenzocyclooctyne-fluorescein conjugate (**DBCO-488**, Click Chemistry Tools, Scottsdale, AZ; 2 µL of a 10 mM solution in DMSO), or both reagents. The samples were diluted with additional PBS to total 200 µL. For multi-component labeling, cyclopropene- and azide-derivatized BSA samples were combined 1:1 prior to labeling with fluorophores. After 1-60 min of fluorophore labeling, the modified BSA samples were purified by passage over P-10 BioGel® and eluting with PBS. The concentrations of the isolated protein samples were measured using a DC Protein Assay kit (BioRad). Protein isolates (2-5 µg) were analyzed by gel electrophoresis using 10% or 12% polyacrylamide gels. Gels were rinsed in destain buffer (50% D.I. H₂O, 40% CH₃OH, 10% acetic acid) and analyzed by in-gel fluorescence measurements on a GE Typhoon TRIO+ Variable Mode Imager. **Tz-Rho** fluorescence was measured with a 532 nm excitation wavelength and 580 nm emission. **DBCO-488** was measured with a 488 nm excitation wavelength and 520 nm emission. Total protein loading was confirmed by subsequent staining with Coomassie Brilliant Blue.

Mass spectrometry analysis of lysozyme conjugates

Owing to the heterogeneity of BSA, mass spectrometry analysis was performed on lysozyme. Lysozyme samples modified with **2.10**, **2.16**, and **2.17** (see above) were dialyzed into D.I. water and subsequently analyzed by ESI-MS via direct infusion onto a QTOF2 instrument. A 200 μ L sample of **2.16**-modified lysozyme (1-2 mg/mL) was further reacted with 100 μ M **Tz-Biotin** for 1 h, dialyzed with D.I. water, concentrated and analyzed by ESI-MS.

2.4e Cross-reactivity analysis

The reactivity between DBCO reagents and **Tz-Rho** was assessed by HPLC and protein labeling assays. For the HPLC analyses, **DBCO-Rho** (Click Chemistry Tools, Scottsdale, AZ) and **Tz-Rho** were dissolved separately in PBS (2 mM) and subsequently combined in a 1:1 ratio. The resulting mixture was monitored over time by HPLC (eluting with 0-50% CH₃CN in water over 10 min, followed by 50% CH₃CN for 10 min). For the protein labeling assays, a combined solution of **Tz-Rho** and **DBCO-488** (1 mM each in PBS) was incubated at room temperature for 0-4 h prior to reaction with Az- and Cp-modified BSA. The protein labeling reactions were performed as above (using 1.5 μ g/mL BSA solution and 100 μ M of the Tz-Rho/DBCO-488 solution). Purification and in-gel fluorescence assays were performed as described above.

2.4f Metabolic labeling studies

Jurkat cells were plated at a density of $\sim 1 \times 10^6$ cells/mL in RPMI media (Gibco) supplemented with 10 % fetal bovine serum (FBS), penicillin/streptomycin, and either **9-Cp-NeuAc** (0-2 mM), **9-Az-NeuAc** (0-2 mM), both sugars in tandem (1 mM each) no sugar, or a control sugar (NeuAc, 1-2 mM or peracetylated ManNAc, 25 mM). All cell cultures were incubated for 24-48 h in a 5%

CO₂, water-saturated incubator at 37 °C. The presence of cyclopropenes or azides in cell-surface glycoconjugates was determined by reaction with **Tz-Biotin**, sulfo-dibenzocyclooctyne-biotin (**DBCO-Biotin**; Click Chemistry Tools, Scottsdale, AZ), or dibenzocyclooctyne-PEG-carboxyrhodamine (**DBCO-Rho**, Click Chemistry Tools, Scottsdale, AZ). Briefly, the cells were rinsed with PBS containing 1% bovine serum albumin (FACS buffer), and then reacted with **Tz-Biotin** (100 μM, 1 h, 37 °C), **DBCO-Biotin** (100 μM, 1 h, 37 °C) or **DBCO-Rho** (100 μM, 1 h, 37 °C). The cells were subsequently washed with FACS buffer and, when necessary, stained with APC-avidin (Invitrogen, 1:100 dilution in FACS buffer) for 30 min on ice. The fluorescence of the labeled cells was analyzed by flow cytometry on an LSR-II flow cytometer (BD Biosciences). For each cell population, 10,000 live cells were analyzed for each replicate experiment. Data were analyzed using FloJo software (Tree Star, Inc.).

2.4g General synthetic procedures

Compounds **2.1** [53, 54], **2.6** [53, 54], **2.25** [55], **9-Az-NeuAc** [50], **2.26** [40], **2.27** [56], and **2.28** [57] were synthesized as previously reported. All other reagents were purchased from commercial sources and used as received without further purification. Reactions were carried out under an inert atmosphere of nitrogen or argon in oven- or flame-dried glassware. Dichloromethane (CH₂Cl₂), tetrahydrofuran (THF), diethyl ether (Et₂O), *N,N*-dimethylformamide (DMF), methanol (CH₃OH) and triethylamine (NEt₃) were degassed with argon and passed through two 4 x 36 inch columns of anhydrous neutral A-2 (8 x 14 mesh; LaRoche Chemicals; activated under a flow of argon at 350 °C for 12 h). The remaining solvents were of analytical grade and purchased from commercial suppliers. Thin-layer chromatography

was performed using Silica Gel 60 F₂₅₄ plates. Plates were visualized using UV radiation and/or staining with KMnO₄. Flash column chromatography was performed with 60 Å (240-400 mesh) silica gel from Sorbent Technologies. In some cases, the silica was first deactivated with 1% NEt₃ in the eluting solvent. ¹H, ¹³C, and ¹⁹F NMR spectra were recorded on Bruker GN-500 (500 MHz ¹H, 125.7 MHz ¹³C), CRYO-500 (500 MHz ¹H, 125.7 MHz ¹³C) or DRX-400 (400 MHz ¹H, 100 MHz ¹³C, 376.5 MHz ¹⁹F) spectrometers. All spectra were collected at 298 K unless otherwise noted. NOESY experiments were performed exclusively with the CRYO-500 instrument with mixing times ranging from 0.8-1.0 s. Chemical shifts are reported in ppm values relative to tetramethylsilane or residual non-deuterated NMR solvent, and coupling constants (*J*) are reported in Hertz (Hz). High-resolution mass spectrometry was performed by the University of California, Irvine Mass Spectrometry Center. HPLC runs were conducted on a Varian ProStar equipped with 325 Dual Wavelength UV-Vis Detector. Analytical runs were performed using an Agilent Polaris 5 C18-A column (4.6 x 150 mm, 5 μm) with a 1 mL/min flow rate. Semi-preparative runs were performed using an Agilent Prep-C18 Scalar column (9.4 x 150 mm, 5 μm) with a 5 mL/min flow rate. The elution gradients for the relevant separations are specified below.

2.4h Synthetic procedures

Pentafluorophenyl 2-methylcycloprop-2-enecarboxylate (2.7a). Compound **2.1a** (100 mg, 1.02 mmol) was dissolved in 8 mL CH₂Cl₂. *N,N*-Diisopropylethylamine (0.42 mL, 2.4 mmol) was added and the solution was cooled to 4 °C. Pentafluorophenyltrifluoroacetate (0.35 mL, 2.0 mmol) was then added dropwise over 1 min via syringe. After 1 h, the reaction mixture was

concentrated *in vacuo* to afford a yellow oil. The crude product was purified by flash column chromatography (eluting with CH₂Cl₂) to yield **2.7a** as a white solid (0.259 g, 0.979 mmol, 89%); TLC R_f = 0.5 (10% Et₂O in hexanes, KMnO₄ stain); ¹H NMR (400 MHz, CDCl₃) δ 6.45 (app quint, *J* = 1.4 Hz, 1H), 2.41 (d, *J* = 1.6 Hz, 1H), 2.25 (d, *J* = 1.2 Hz, 3H); ¹³C NMR (125.7 MHz, CDCl₃) δ 172.1, 111.1, 93.9, 19.5, 10.4; ¹⁹F NMR (376.5 MHz, CDCl₃) δ -153.4 (dd, *J* = 22.3, 5.0 Hz, 2F), -159.2 (t, *J* = 21.7 Hz, 1F), -163.1 (dt, *J* = 22.0, 5.0 Hz, 2F) HRMS (GC-Cl) *m/z* calcd for C₁₁H₉O₂F₅N [M+NH₄]⁺ 282.0554, found 282.0555.

Pentafluorophenyl 2,3-dimethylcycloprop-2-enecarboxylate (2.7b). Compound **2.1b** (0.050 g, 0.45 mmol) was dissolved in 5 mL CH₂Cl₂. *N,N*-Diisopropylethylamine (0.260 mL, 1.49 mmol) was added and the solution was cooled to 4 °C. Pentafluorophenyltrifluoroacetate (0.215 mL, 1.25 mmol) was then added dropwise over 1 min via syringe. After 1 h, the reaction mixture was concentrated *in vacuo* to afford a yellow oil. The crude product was purified by flash column chromatography (eluting with CH₂Cl₂) to yield **2.7b** as a white solid (0.102 g, 0.364 mmol, 81%); TLC R_f = 0.5 (10% Et₂O in hexanes, KMnO₄ stain); ¹H NMR (400 MHz, CDCl₃) δ 2.29 (s, 1H), 2.13 (s, 6H); ¹³C NMR (125.7 MHz, CDCl₃) δ 172.4, 101.8, 22.5, 9.6; ¹⁹F NMR (376.5 MHz, CDCl₃) δ -153.6 (d, *J* = 22.9, 4.6 Hz, 2F), -159.5 (t, *J* = 22.0 Hz, 1F), -163.3 (dt, *J* = 21.2, 4.5 Hz, 2F); HRMS (GC-Cl) *m/z* calcd for C₁₂H₈O₂F₅ [M+H]⁺ 279.0444, found 279.0445.

***N*-Isopropyl-2-methylcycloprop-2-enecarboxamide (2.2a).** Cyclopropene **2.7a** (0.170 g, 0.644 mmol) was dissolved in 4 mL CH₂Cl₂. Isopropylamine (0.153 mL, 1.92 mmol) was added to the solution via syringe. After a few minutes, a white precipitate formed. The reaction mixture was

allowed to stir at rt for an additional hour before the white precipitate was removed by filtration. The remaining filtrate was concentrated *in vacuo* to yield **2.2a** as a white powder (75.3 mg, 0.56 mmol, 87%). TLC $R_f = 0.2$ (5% CH₃OH in CH₂Cl₂, KMnO₄ stain); ¹H NMR (400 MHz, CDCl₃) δ 6.41 (app quin, $J = 1.3$ Hz, 1H), 5.18 (br s, 1H), 4.12-4.07 (m, 1H), 2.15 (d, $J = 1.2$ Hz, 3H), 1.95 (d, $J = 1.6$ Hz, 1H), 1.13 (d, $J = 3.0$, 3H), 1.11 (d, $J = 3.0$ Hz, 3H); ¹³C NMR (125 MHz, CDCl₃) δ 175.1, 114.1, 96.2, 41.2, 23.10, 23.08, 22.6, 10.7; HRMS (ESI) calcd for C₈H₁₃NONa [M+Na]⁺ 162.0895, found 162.0889.

***N*-Isopropyl-2,3-dimethylcycloprop-2-enecarboxamide (2.2b).** Cyclopropene **2.7b** (0.202 g, 0.726 mmol) was dissolved in 4 mL CH₂Cl₂. Isopropylamine (179 mg, 3.03 mmol) was added to the solution via syringe. After a few minutes, a white precipitate formed. The reaction mixture was allowed to stir at rt for an additional hour before the white precipitate was removed by filtration. The remaining filtrate was concentrated *in vacuo* to yield **2.2b** as a white powder (0.100 g, 0.653 mmol, 90% yield): TLC $R_f = 0.3$ (5% CH₃OH in CH₂Cl₂, KMnO₄ stain); ¹H NMR (500 MHz, CDCl₃) δ 5.07 (br s, 1H), 4.12–4.08 (m, 1H), 2.03 (s, 6H), 1.83 (s, 1H), 1.11 (d, $J = 6.5$ Hz, 6H); ¹³C NMR (125.7 MHz, CDCl₃) δ 175.6, 104.3, 40.9, 25.5, 23.2, 9.7; HRMS (ESI) m/z calcd for C₉H₁₅NONa [M+Na]⁺ 176.1051, found 176.1057.

3-Hydroxymethyl-1,2-dimethylcyclopropene (2.3b). Diisobutylaluminum hydride (0.213 g, 1.50 mmol) was dissolved in 5 mL Et₂O, and the resulting solution was cooled to 4 °C. Cyclopropene **2.6b** (0.142 g, 1.01 mmol) was added dropwise to the vessel via syringe over 1 min. The resulting solution was stirred for 30 min before the reaction mixture was quenched with

saturated Rochelle's salt and allowed to stir until a white gel formed. The organic layer was separated and the aqueous gel was extracted with Et₂O (2 x 5 mL). The combined organic layers were dried with MgSO₄ and concentrated *in vacuo* to afford the crude product mixture as faint yellow oil. The crude product was purified by flash column chromatography (eluting with 50% Et₂O in hexanes) to yield **2.3b** as a clear oil (0.091 g, 0.92 mmol, 70% two steps): TLC R_f = 0.2 (25% ethyl acetate in hexanes, KMnO₄ stain); ¹H NMR (400 MHz, CDCl₃) δ 3.53 (d, *J* = 4.3 Hz, 2H), 2.03 (s, 6H), 1.53 (t, *J* = 4.3 Hz, 1H); ¹³C NMR (125 MHz, CDCl₃) δ 110.3, 68.6, 22.8, 10.6; HRMS (GC-CI) calcd for C₆H₁₁O [M+H]⁺ 99.0810, found 99.0807.

3-Hydroxymethyl-2-methyl-trimethylsilylcyclopropene (2.8). Diisobutylaluminum hydride (0.213 g, 1.50 mmol) was dissolved in 5 mL Et₂O, and the resulting solution was cooled to 4 °C. Cyclopropene **2.6a** (0.200 g, 1.00 mmol) was added dropwise to the vessel via syringe over 1 min. The resulting solution was stirred for 30 min before the reaction mixture was quenched with saturated Rochelle's salt and allowed to stir until a white gel formed. The organic layer was separated and the aqueous gel was extracted with Et₂O (2 x 10 mL). The combined organic layers were dried with MgSO₄ and concentrated *in vacuo* to afford the crude product mixture as faint yellow oil. The crude product was purified by flash column chromatography (eluting with 20% Et₂O in hexanes) to yield **2.8** as a faint yellow oil (0.138 g, 0.883 mmol, 71% two steps): TLC R_f = 0.2 (10% EtOAc in hexanes, KMnO₄ stain); ¹H NMR (500 MHz, CDCl₃) δ 3.48 (d, *J* = 4.6 Hz, 2H), 2.21 (s, 3H), 1.56 (t, *J* = 4.6 Hz, 1H), 0.17 (s, 9H). This material was subjected to deprotection conditions (2.0 mL of 1 M tetrabutylammonium fluoride in THF) without further purification.

***p*-Nitrophenyl carbonate dimethyl cyclopropene (2.10).** Cyclopropene **2.3b** (59 mg, 0.60 mmol) and dry pyridine (0.30 mL, 3.7 mmol) were dissolved in 5 mL CH₂Cl₂. The resulting solution was stirred and cooled to 4 °C before adding *p*-nitrophenyl chloroformate (0.266 g, 1.32 mmol). The solution was allowed to warm to rt and stir for 2 h before quenching the reaction with D.I. H₂O. The organic layer was separated and the aqueous layer was extracted with CH₂Cl₂ (2 x 15 mL). The organic layers were combined, dried with MgSO₄, and concentrated. The crude mixture was purified via flash column chromatography (eluting with 10-20% Et₂O in hexanes) to afford **2.10** as a white solid (0.123 g, 0.467 mmol, 78% yield): TLC R_f = 0.7 (25% ethyl acetate in hexanes); ¹H NMR (400 MHz, CDCl₃) δ 8.27 (d, *J* = 8.6 Hz, 2H), 7.38 (d, *J* = 8.6 Hz, 2H), 4.18 (d, *J* = 5.3 Hz, 2H), 2.04 (s, 6H), 1.64 (t, *J* = 5.3 Hz, 1H); ¹³C NMR (125 MHz, CDCl₃) δ 155.9, 152.8, 145.3, 125.3, 121.9, 109.5, 77.9, 19.0, 10.5; HRMS (GC-CI) calcd for C₁₃H₁₃NO₅ [M]⁺ 263.0794, found 263.0796.

(2,3-Dimethylcyclopropenyl)methyl isopropylcarbamate (2.11). Carbonate cyclopropene **2.10** (163 mg, 0.619 mmol) was added to a solution of isopropylamine (230 μL, 2.8 mmol) in 5 mL CH₂Cl₂. The solution turns yellow and is allowed to stir overnight. The reaction mixture was rinsed with water (3 x 20 mL). The organic layer was dried with MgSO₄ and concentrated. The crude mixture was purified via flash column chromatography (eluting with 20% Et₂O in hexanes) to afford **11** as a pale yellow oil (82.7 mg, 0.451 mmol, 73% yield): TLC R_f = 0.4 (20% ethyl acetate in hexanes); ¹H NMR (500 MHz, CDCl₃) δ 4.42 (br s, 1H), 3.92 (d, *J* = 4.9 Hz, 2H), 3.79 (app octet, *J* = 6.7 Hz, 1H), 1.99 (s, 6H), 1.50 (t, *J* = 5.0 Hz, 1H), 1.14 (d, *J* = 6.7 Hz, 6H);

^{13}C NMR (500 MHz, CDCl_3) δ 156.3, 109.9, 72.0, 43.0, 23.1, 19.6, 10.3; HRMS (GC-CI) calcd for $\text{C}_{10}\text{H}_{17}\text{NO}_2\text{Na}$ $[\text{M}+\text{Na}]^+$ 206.1157, found 206.1157.

Mixture of cycloadducts 2.13 and 2.14. Cyclopropene **2.2b** (18.0 mg, 0.117 mmol) was added to a solution of 3,6-dipyridyl-1,2,4,5-tetrazine **2.12** (28.2 mg, 0.119 mmol) in 3 mL CH_2Cl_2 . The solution was allowed to stir for 2 d at 37 °C, and the color changed from pink to pale purple. The reaction mixture was concentrated *in vacuo* and purified by flash column chromatography with deactivated silica (eluting with 0-5% CH_3OH in CH_2Cl_2) to afford a 5.5:1 (**2.14** : **2.13**) mixture of diastereomers as a yellow solid (17.4 mg, 0.0481 mmol, 41% yield): TLC R_f = 0.3 (10% CH_3OH in CH_2Cl_2 , UV); ^1H NMR (500 MHz, CDCl_3 , **2.13**) δ 8.69 (app d, J = 4.7 Hz, 2H), 7.94 (app d, J = 7.8 Hz, 2H), 7.83 (dt, J = 7.7, 1.6 Hz, 2H), 7.38 (ddd, J = 7.5, 4.9, 1.0 Hz, 2H), 6.96 (ddd, J = 7.5 Hz, 1H), 4.15 (m, 1H), 1.74 (s, 1H), 1.47 (s, 6H), 1.26 (d, J = 6.5 Hz, 6H); ^1H NMR (500 MHz, CDCl_3 , **2.14**) δ 8.73 (app d, J = 4.8 Hz, 2H), 8.04 (app d, J = 7.8, 2H), 7.83 (dt, J = 7.7, 1.6 Hz, 2H), 7.56 (d, J = 7.5 Hz, 1H), 7.38 (ddd, J = 7.5, 4.9, 1.0 Hz, 2H), 3.75 (m, 1H), 2.70 (s, 1H), 1.43 (s, 6H), 0.80 (d, J = 6.6 Hz, 6H); ^{13}C NMR (125 MHz, CDCl_3 , mixture) δ 165.3, 165.1, 163.8, 163.0, 156.2, 155.6, 148.8, 148.7, 137.1, 137.0, 124.6, 124.4, 124.3, 123.6, 41.6, 41.4, 35.0, 31.0, 28.8, 27.9, 23.0, 22.1, 18.0, 13.5; HRMS (ESI) calcd for $\text{C}_{21}\text{H}_{23}\text{N}_5\text{ONa}$ $[\text{M}+\text{Na}]^+$ 384.1800, found 384.1810.

Cycloadduct 2.15. The cycloadduct mixture of **2.13** and **2.14** (12.0 mg, 0.0326 mmol) was dissolved in water and the reaction progress was monitored by HPLC. After 1 d, the resulting cycloadduct was purified by HPLC (0-95% CH_3CN in water over 20 min) and concentrated *in*

vacuo to yield **2.15** (6.0 mg, 0.017 mmol, 52% yield) as a white solid: ^1H NMR (400 MHz, 318 K , CDCl_3) δ 8.68 (m, 2H), 7.82 (dt, $J = 8.0, 1.8\text{ Hz}$, 1H), 7.81 (app d, $J = 7.9\text{ Hz}$, 1H), 7.68 (dt, $J = 7.8, 1.8\text{ Hz}$, 1H), 7.59 (app d, $J = 8.0\text{ Hz}$, 1H), 7.34 (ddd, $J = 7.5, 5.0, 0.9\text{ Hz}$, 1H), 7.31 (br s, 1H), 7.19 (ddd, $J = 7.4, 4.9, 1.1\text{ Hz}$, 1H), 2.66 (sept, $J = 6.8\text{ Hz}$, 1H), 1.90 (s, 1H), 1.29 (s, 3H), 1.12 (s, 3H), 1.04 (d, $J = 6.8\text{ Hz}$, 3H), 0.91 (d, $J = 6.8\text{ Hz}$, 3H); ^{13}C NMR (125 MHz, CDCl_3) δ 174.0, 156.2, 154.9, 152.1, 149.4, 148.9, 136.5, 136.2, 123.8, 122.7, 120.7, 80.9, 45.2, 34.9, 29.0, 25.6, 20.4, 18.7, 17.0, 12.4; HRMS (ESI) calcd for $\text{C}_{21}\text{H}_{23}\text{N}_5\text{ONa}$ $[\text{M}+\text{Na}]^+$ 384.1800, found 384.1798.

Mixture of cycloadducts 2.16 and 2.17. Cyclopropene **2.2a** (11.8 mg, 0.0847 mmol) was added to a solution of 3,6-dipyridyl-1,2,4,5-tetrazine **2.12** (10.0 mg, 0.0423 mmol) in 4 mL CH_2Cl_2 . The solution was allowed to stir for 3 h at $37\text{ }^\circ\text{C}$, and the color changed from pink to yellow. The reaction mixture was concentrated *in vacuo* and purified by flash column chromatography with deactivated silica (eluting with 0-5% CH_3OH in CH_2Cl_2) to afford a mixture of isomers as a yellow solid (10.0 mg, 0.0288 mmol, 68% yield): ^1H NMR (500 MHz, CDCl_3 , **2.16**) δ 8.76 (app d, $J = 4.2\text{ Hz}$, 1H), 8.68 (app d, $J = 4.6\text{ Hz}$, 1H), 8.43 (d, $J = 7.9\text{ Hz}$, 1H), 8.01 (d, $J = 7.9\text{ Hz}$, 1H), 7.81 (m, 2H), 7.39 (m, 2H), 6.21 (d, $J = 7.8\text{ Hz}$, 1H), 4.21 (m, 1H), 3.94 (d, $J = 5.1\text{ Hz}$, 1H), 1.48 (s, 3H), 1.43 (d, $J = 5.1\text{ Hz}$, 1H), 1.28 (d, $J = 6.5\text{ Hz}$, 3H), 1.22 (d, $J = 6.5\text{ Hz}$, 3H); ^{13}C NMR (125 MHz, CDCl_3 , **2.16**) δ 166.1, 164.3, 161.0, 155.1, 153.9, 149.5, 148.8, 137.1, 136.5, 125.2, 124.8, 123.7, 122.0; HRMS (ESI) calcd for $\text{C}_{20}\text{H}_{22}\text{N}_5\text{O}$ $[\text{M}+\text{H}]^+$ 348.1824, found 348.1815.

Cycloadduct 2.21. Cyclopropene **2.3b** (8.3 mg, 0.085 mmol) was added to a solution of 3,6-dipyridyl-1,2,4,5-tetrazine **2.12** (10.0 mg, 0.0423 mmol) in 5 mL CH₃OH at rt. After 8 h, the resulting yellow solution was concentrated *in vacuo*. The crude mixture was purified by flash column chromatography with deactivated silica (eluting with 0-5% CH₃OH in CH₂Cl₂) to afford **2.21** as a white solid (10.0 mg, 0.0326 mmol, 77% yield): TLC R_f = 0.4 (5% CH₃OH in CH₂Cl₂, UV); ¹H NMR (500 MHz, CDCl₃) δ 8.69-8.67 (m, 1H), 8.65-8.64 (m, 1H), 7.85 (d, *J* = 8.0 Hz, 1H), 7.77 (dt, *J* = 8.0, 1.8 Hz, 1H), 7.69 (dt, *J* = 7.7, 1.7 Hz, 1H), 7.61 (d, *J* = 7.9 Hz, 1H), 7.29 (ddd, *J* = 7.5, 4.9, 1.1 Hz, 1H), 7.20 (ddd, *J* = 7.5, 5.0, 0.9 Hz, 1H), 6.82 (s, 1H), 4.39 (dd, *J* = 8.4, 4.2 Hz, 1H), 4.25 (d, *J* = 8.4 Hz, 1H), 1.91 (d, *J* = 4.0 Hz, 1H), 1.28 (s, 3H), 1.03 (s, 3H); ¹³C NMR (125 MHz, CDCl₃) δ 159.6, 156.7, 152.9, 149.1, 148.7, 136.7, 136.3, 123.4, 122.5, 122.3, 121.2, 97.6, 71.0, 37.2, 31.9, 22.9, 16.8, 13.0; HRMS (ESI) *m/z* calcd for C₁₈H₁₉N₄O [M+H]⁺ 307.1559, found 307.1557.

Cycloadduct 2.18. Cyclopropene **2.11** (46.1 mg, 0.252 mmol) was added to a solution of 3,6-dipyridyl-1,2,4,5-tetrazine **2.12** (29.5 mg, 0.125 mmol) in 3 mL CH₂Cl₂. The solution was allowed to stir for 8 h at 37 °C, and the color changed from pink to yellow. The reaction mixture was concentrated *in vacuo* and purified by flash column chromatography with deactivated silica (eluting with 0-5% CH₃OH in CH₂Cl₂) to afford product in a 100:7 ratio as a yellow solid (42.9 mg, 0.110 mmol, 88% yield): ¹H NMR (500 MHz, CDCl₃) δ 8.67 (d, *J* = 4.0 Hz, 2H), 7.99 (app d, *J* = 7.9 Hz, 2H), 7.78 (dt, *J* = 7.6, 1.4 Hz, 2H), 7.34 (m, 2H), 4.69 (br s, 1H), 3.73 (m, 1H), 3.68 (d, *J* = 7.4 Hz, 2H), 2.35 (t, *J* = 7.5 Hz, 1H), 1.48 (s, 6H), 1.08 (d, *J* = 6.6 Hz, 6H); ¹³C NMR (125 MHz, CDCl₃) δ 163.5, 156.2, 155.7, 148.7, 136.7, 124.4, 124.0, 60.4, 53.5, 42.8,

32.5, 27.0, 23.1, 18.1; HRMS (ESI) m/z calcd for $C_{22}H_{25}N_5O_2Na$ $[M+Na]^+$ 414.1906, found 414.1923.

4-(6-(Pyridin-2-yl)-1,2,4,5-tetrazin-3-yl)benzoic acid (2.26). (Procedure adapted from Karver *et al.*) [40] To a dried round bottom flask was added 2-cyanonitrile (1.071 g, 10.28 mmol) and 4-cyanobenzoic acid (0.3134 g, 2.130 mmol) followed by addition of anhydrous hydrazine (1.2 ml, 25 mmol). The reaction was stirred at 80 °C for 90 min under N_2 . After cooling to rt, the reaction mixture was diluted with acetic acid (7 mL) and cooled to 4 °C in an ice bath. Aqueous $NaNO_2$ (1.40 g in 3 mL D.I. H_2O) was added dropwise to the reaction mixture turning resulting in a purple solution. Once the evolution of gas subsided, the purple solid was isolated by centrifugation (3000g x 1 min) followed by rinsing with copious amounts of acetone until the filtrate was colorless. The resulting solid was dried *in vacuo* yielding the product **2.27** as a purple solid (147 mg, 0.527 mmol, 25% yield): 1H NMR (400 MHz, $DMSO-d_6$) δ 8.95 (d, $J = 4.0$ Hz, 1H), 8.69 (d, $J = 8.5$ Hz, 2H), 8.61 (d, $J = 7.9$ Hz, 1H), 8.25 (d, $J = 8.5$ Hz, 1H), 8.17 (td, 1, $J = 7.7, 1.7$), 7.74 (t, 1, $J = 6.2$).

Tetrazine-biotin conjugate (Tz-Biotin). To a dried round bottom flask was added anhydrous DMF (4 ml), tetrazine **2.26** (60.0 mg, 0.215 mmol), triethylamine (100 μ L, 0.722 mmol), 1-ethyl-3-(3-dimethylaminopropyl) carbodiimide hydrochloride salt (56.0 mg, 0.361 mmol), and hydroxybenzotriazole (24.0 mg, 0.178 mmol). The solution was allowed to stir for 20 min. To this solution was added biotin-PEG- NH_2 **2.27** (80.0 mg, 0.179 mmol). The solution was stirred for 5 h at 50 °C. The product isolated by HPLC (30% CH_3CN in water over 20 min) and

concentrated *in vacuo* to yield a purple solid (39.6 mg, 0.508 mmol, 31%): ^1H NMR (400 MHz, CD_3OD) δ 8.88 (d, $J = 4.5$ Hz, 1H), 8.76 (d, $J = 8.23$ Hz, 3H), 8.16 (t, $J = 7.62$ Hz, 1H), 8.09 (d, $J = 7.9$ Hz, 2H), 7.88 (s, 1H), 7.72 (app t, $J = 5.8$ Hz, 1H), 4.49-4.45 (m, 1H), 4.30-4.25 (m, 1H), 3.65-3.45 (m, 17H), 3.20-3.10 (m, 3H), 2.89 (dd, $J = 12.9, 4.6$ Hz, 1H), 2.68 (d, $J = 12.8$ Hz, 1H), 2.16 (t, $J = 7.3$ Hz, 2H), 1.95-1.52 (m, 10H), 1.44-1.38 (m, 2H); ^{13}C NMR (125 MHz, CD_3OD) δ 174.5, 167.6, 163.2, 150.1, 138.1, 138.1, 134.6, 128.0, 128.0, 126.7, 124.1, 70.2, 70.2, 69.9, 69.9, 68.9, 68.5, 62, 60.2, 55.6, 39.7, 37.6, 36.4, 35.5, 29.0, 29.0, 28.4, 28.1, 25.5. HRMS (ESI) m/z calcd for $\text{C}_{34}\text{H}_{45}\text{N}_9\text{O}_6\text{SNa}$ $[\text{M}+\text{Na}]^+$ 730.3111, found 730.3116.

Tetrazine-rhodamine conjugate (Tz-Rho). Tetrazine **2.26** (15.0 mg, 0.0537 mmol) was dissolved in DMF (5 ml) with triethylamine (30.0 μL , 0.215 mmol), 1-ethyl-3-(3-dimethylaminopropyl)carbodiimide hydrochloride salt (20.7 mg, 0.108 mmol), and *N*-hydroxysuccinimide (8.4 mg, 0.055 mmol). The solution was allowed to stir for 5 min under N_2 . Rhodamine-piperazine **2.28** (27.6 mg, 0.0539 mmol) was then added, and the reaction mixture was stirred overnight at rt. The reaction mixture was concentrated *in vacuo* and the product was isolated by HPLC (0-100% CH_3CN in water over 20 min) as a red solid (7.2 mg, 0.0093 mmol, 17%): HRMS (ESI) m/z calcd for $\text{C}_{46}\text{H}_{46}\text{N}_9\text{O}_3$ $[\text{M}]^+$ 772.3724, found 772.3723.

NHS-cyclopropenyl ester (2.16). Cyclopropene **2.1a** (100 mg, 1.02 mmol) was dissolved in 1 mL of CH_2Cl_2 . *N*-Hydroxysuccinimide (121 mg, 1.05 mmol) was added, followed by 1-ethyl-3-(3-dimethylaminopropyl)carbodiimide hydrochloride salt (128 mg, 1.07 mmol) and NEt_3 (0.3 mL, 2 mmol). The reaction mixture was allowed to stir at rt overnight, then diluted with 50 mL

of ethyl acetate and washed with saturated NH_4Cl (2x20 mL) followed by brine (1x20 mL). The organic layers were combined, dried with MgSO_4 , and concentrated *in vacuo* to afford **2.16** (90.0 mg, 0.461 mmol, 45%) as pale yellow oil. The product was used without further purification; TLC $R_f = 0.6$ (50% ethyl acetate in hexanes); ^1H NMR (400 MHz, CDCl_3) δ 6.38 (t, $J = 1.2$ Hz, 1H), 2.78 (br s, 4H), 2.32 (d, $J = 1.6$ Hz, 1H), 2.20 (d, $J = 1.2$ Hz, 3H); ^{13}C NMR (125 MHz, CDCl_3) δ 171.1, 169.5, 110.5, 93.3, 25.6, 17.5, 10.3; HRMS (ESI) m/z calcd for $\text{C}_9\text{H}_9\text{O}_4\text{NNa}$ $[\text{M}+\text{Na}]^+$ 218.0429, found 218.0427.

Sialic Acid-cyclopropene conjugate (9-Cp-NeuAc). **9-Az-NeuAc** (0.34 g, 1.0 mmol) was dissolved in 11.0 mL water and the pH of the reaction mixture was adjusted to 1-2 with acetic acid. After the addition of Pd/C (33 mg), the reaction mixture was stirred under H_2 at rt overnight. The reaction mixture was then filtered through Celite and concentrated *in vacuo*. The residue was dissolved in 28 mL dioxane:water (3:2) and the pH of the reaction mixture was adjusted to 8-9 with saturated NaHCO_3 . NHS-cyclopropenyl ester **2.16** (0.250 g, 1.26 mmol) was added and the reaction mixture stirred at rt overnight. The resulting reaction mixture was concentrated *in vacuo* and purified via HPLC (0-30% CH_3CN in water over 20 min). Fractions containing product were combined and lyophilized to yield a white solid (44.7 mg, 9% yield, $\alpha:\beta = 1:5$); TLC $R_f = 0.5$ (50% CH_3OH in CH_2Cl_2); ^1H NMR (500 MHz, CD_3OD , β -anomer) δ 6.56 – 6.57 (m, 1H), 4.01 – 4.03 (m, 2H), 3.94 – 3.98 (m, 1H), 3.71 – 3.74 (m, 1H), 3.66 (dt, $J = 5.0$, 14.0 Hz, 1H), 3.32 (app d, $J = 9.0$ Hz, 1H), 3.26 (ddd, $J = 5.5$, 14.0 Hz, 1H), 2.17 – 2.18 (m, 3H), 2.14 (d, $J = 4.5$ Hz, 1H), 2.10 (d, $J = 1.5$ Hz, 1H), 2.04 (s, 3H), 1.90 (app t, $J = 12.5$ Hz, 1H); ^{13}C

NMR (125 MHz, CD₃OD): δ 178.6, 176.1, 172.9, 112.7, 96.3, 95.0, 70.4, 70.2, 69.6, 67.4, 52.6, 43.2, 40.5, 21.5, 21.3, 9.1; HRMS (ESI) m/z calcd C₉H₉O₄N [M-H]⁻ 387.1404, found 387.1412.

References

1. Prescher, J., and Bertozzi, C. (2005) Chemistry in living systems, *Nat Chem Biol* 1, 13-21.
2. Sletten, E. M., and Bertozzi, C. R. (2009) Bioorthogonal chemistry: fishing for selectivity in a sea of functionality, *Angew Chem Int Ed* 48, 6974-6998.
3. Hsu, T. L., Hanson, S. R., Kishikawa, K., Wang, S. K., Sawa, M., and Wong, C. H. (2007) Alkynyl sugar analogs for the labeling and visualization of glycoconjugates in cells, *Proc Natl Acad Sci U S A* 104, 2614-2619.
4. Luchansky, S. J., Hang, H. C., Saxon, E., Grunwell, J. R., Yu, C., Dube, D. H., and Bertozzi, C. R. (2003) Constructing azide-labeled cell surfaces using polysaccharide biosynthetic pathways, *Methods Enzymol* 362, 249-272.
5. Mahal, L. K., Yarema, K. J., and Bertozzi, C. R. (1997) Engineering chemical reactivity on cell surfaces through oligosaccharide biosynthesis, *Science* 276, 1125-1128.
6. Link, A. J., Mock, M. L., and Tirrell, D. A. (2003) Non-canonical amino acids in protein engineering, *Curr Opin Biotechnol* 14, 603-609.
7. Bräse, S., Gil, C., Knepper, K., and Zimmermann, V. (2005) Organic azides: an exploding diversity of a unique class of compounds, *Angew Chem Int Ed* 44, 5188-5240.
8. Debets, M. F., van Berkel, S. S., Dommerholt, J., Dirks, A. T., Rutjes, F. P., and van Delft, F. L. (2011) Bioconjugation with strained alkenes and alkynes, *Acc Chem Res* 44, 805-815.
9. El-Sagheer, A. H., Sanzone, A. P., Gao, R., Tavassoli, A., and Brown, T. (2011) Biocompatible artificial DNA linker that is read through by DNA polymerases and is functional in *Escherichia coli*, *Proc Natl Acad Sci U S A* 108, 11338.

10. Hang, H. C., Wilson, J. P., and Charron, G. (2011) Bioorthogonal chemical reporters for analyzing protein lipidation and lipid trafficking, *Acc Chem Res* 44, 699-708.
11. Ngo, J. T., and Tirrell, D. A. (2011) Noncanonical amino acids in the interrogation of cellular protein synthesis, *Acc Chem Res* 44, 677-685.
12. Saxon, E., and Bertozzi, C. R. (2000) Cell surface engineering by a modified Staudinger reaction, *Science* 287, 2007-2010.
13. Agard, N. J., Prescher, J. A., and Bertozzi, C. R. (2004) A strain-promoted [3 + 2] azide-alkyne cycloaddition for covalent modification of biomolecules in living systems, *J Am Chem Soc* 126, 15046-15047.
14. Baskin, J. M., Prescher, J. A., Laughlin, S. T., Agard, N. J., Chang, P. V., Miller, I. A., Lo, A., Codelli, J. A., and Bertozzi, C. R. (2007) Copper-free click chemistry for dynamic in vivo imaging, *Proc Natl Acad Sci U S A* 104, 16793-16797.
15. Jewett, J. C., Sletten, E. M., and Bertozzi, C. R. (2010) Rapid Cu-free click chemistry with readily synthesized biarylazacyclooctynones, *J Am Chem Soc* 132, 3688-3690.
16. Ning, X., Guo, J., Wolfert, M. A., and Boons, G. J. (2008) Visualizing metabolically labeled glycoconjugates of living cells by copper-free and fast Huisgen cycloadditions, *Angew Chem Int Ed* 47, 2253-2255.
17. Blackman, M. L., Royzen, M., and Fox, J. M. (2008) Tetrazine ligation: fast bioconjugation based on inverse-electron-demand Diels-Alder reactivity, *J Am Chem Soc* 130, 13518-13519.
18. Devaraj, N. K., Weissleder, R., and Hilderbrand, S. A. (2008) Tetrazine-based cycloadditions: application to pretargeted live cell imaging, *Bioconjug Chem* 19, 2297-2299.
19. Dommerholt, J., Schmidt, S., Temming, R., Hendriks, L. J., Rutjes, F. P., van Hest, J. C., Lefeber, D. J., Friedl, P., and van Delft, F. L. (2010) Readily accessible bicyclononynes for bioorthogonal labeling and three-dimensional imaging of living cells, *Angew Chem Int Ed* 49, 9422-9425.

20. Karver, M. R., Weissleder, R., and Hilderbrand, S. A. (2012) Bioorthogonal reaction pairs enable simultaneous, selective, multi-target imaging, *Angew Chem Int Ed* 51, 920-922.
21. Lang, K., Davis, L., Wallace, S., Mahesh, M., Cox, D. J., Blackman, M. L., Fox, J. M., and Chin, J. W. (2012) Genetic Encoding of bicyclononynes and trans-cyclooctenes for site-specific protein labeling in vitro and in live mammalian cells via rapid fluorogenic Diels-Alder reactions, *J Am Chem Soc* 134, 10317-10320.
22. Devaraj, N. K., and Weissleder, R. (2011) Biomedical applications of tetrazine cycloadditions, *Acc Chem Res* 44, 816-827.
23. Willems, L. I., Verdoes, M., Florea, B. I., van der Marel, G. A., and Overkleeft, H. S. (2010) Two-step labeling of endogenous enzymatic activities by Diels-Alder ligation, *ChemBioChem* 11, 1769-1781.
24. Plass, T., Milles, S., Koehler, C., Szymanski, J., Mueller, R., Wiessler, M., Schultz, C., and Lemke, E. A. (2012) Amino acids for Diels-Alder reactions in living cells, *Angew Chem Int Ed* 51, 4166-4170.
25. Seitchik, J. L., Peeler, J. C., Taylor, M. T., Blackman, M. L., Rhoads, T. W., Cooley, R. B., Refakis, C., Fox, J. M., and Mehl, R. A. (2012) Genetically encoded tetrazine amino acid directs rapid site-specific in vivo bioorthogonal ligation with *trans*-cyclooctenes, *J Am Chem Soc* 134, 2898-2901.
26. Suchanek, M., Radzikowska, A., and Thiele, C. (2005) Photo-leucine and photo-methionine allow identification of protein-protein interactions in living cells, *Nat Methods* 2, 261-267.
27. Tanaka, Y., and Kohler, J. J. (2008) Photoactivatable crosslinking sugars for capturing glycoprotein interactions, *J Am Chem Soc* 130, 3278-3279.
28. Zhu, Z. B., Wei, Y., and Shi, M. (2011) Recent developments of cyclopropene chemistry, *Chem Soc Rev* 40, 5534-5563.
29. Temming, R. P., van Scherpenzeel, M., te Brinke, E., Schoffelen, S., Gloerich, J., Lefeber, D. J., and van Delft, F. L. (2012) Protein enrichment by capture-release based on

- strain-promoted cycloaddition of azide with bicyclononyne (BCN), *Bioorg Med Chem* 20, 655-661.
30. Yu, Z., Pan, Y., Wang, Z., Wang, J., and Lin, Q. (2012) Genetically encoded cyclopropene directs rapid, photoclick-chemistry-mediated protein labeling in mammalian cells, *Angew Chem Int Ed* 51, 10600-10604.
 31. Closs, G. L., Boll, W. A., and Closs, L. E. (1963) Base-induced pyrolysis of tosylhydrazones of α,β -unsaturated aldehydes and ketones - a convenient synthesis of some alkylcyclopropenes, *J Am Chem Soc* 85, 3796-3800.
 32. Matsuura, M., Saikawa, Y., Inui, K., Nakae, K., Igarashi, M., Hashimoto, K., and Nakata, M. (2009) Identification of the toxic trigger in mushroom poisoning, *Nat Chem Biol* 5, 465-467.
 33. Doss, G. A., and Djerassi, C. (1988) Sterols in marine-invertebrates. 60. isolation and structure elucidation of 4 new steroidal cyclopropenes from the sponge Calyx-Podatypa, *J Am Chem Soc* 110, 8124-8128.
 34. Li, L. N., Li, H. T., Lang, R. W., Itoh, T., Sica, D., and Djerassi, C. (1982) Minor and trace sterols in marine invertebrates. 31. Isolation and structure elucidation of 23H-isocalysterol, a naturally occurring cyclopropene. Some comparative observations on the course of hydrogenolytic ring opening of steroidal cyclopropenes and cyclopropanes, *J Am Chem Soc* 104, 6726-6732.
 35. Bao, X., Katz, S., Pollard, M., and Ohlrogge, J. (2002) Carbocyclic fatty acids in plants: biochemical and molecular genetic characterization of cyclopropane fatty acid synthesis of *Sterculia foetida*, *Proc Natl Acad Sci U S A* 99, 7172-7177.
 36. Watkins, C. (2006) The use of 1-methylcyclopropene (1-MCP) on fruits and vegetables, *Biotech Adv* 24, 389-409.
 37. Diev, V. V., Kostikov, R. R., Gleiter, R., and Molchanov, A. P. (2006) Cyclopropenes in the 1,3-dipolar cycloaddition with carbonyl ylides: experimental and theoretical evidence for the enhancement of α -withdrawal in 3-substituted-cyclopropenes, *J Org Chem* 71, 4066-4077.

38. Lien, A. (1987) Substituent effects on the structures and strain energies of cyclopropenes, *J Mol Struct* 149, 139-151.
39. Tang, S.-Y., Shi, J., and Guo, Q.-X. (2012) Accurate prediction of rate constants of Diels–Alder reactions and application to design of Diels–Alder ligation, *Org Biomol Chem* 10, 2673.
40. Karver, M. R., Weissleder, R., and Hilderbrand, S. A. (2011) Synthesis and evaluation of a series of 1,2,4,5-tetrazines for bioorthogonal conjugation, *Bioconjug Chem* 22, 2263-2270.
41. Lin, F. L., Hoyt, H. M., Van Halbeek, H., Bergman, R. G., and Bertozzi, C. R. (2005) Mechanistic investigation of the Staudinger ligation, *J Am Chem Soc* 127, 2686-2695.
42. Xidos, J. D., Gosse, T. L., Burke, E. D., Poirier, R. A., and Burnell, D. J. (2001) Endo-exo and facial stereoselectivity in the Diels-Alder reactions of 3-substituted cyclopropenes with butadiene, *J Am Chem Soc* 123, 5482-5488.
43. Sauer, J., Bauerlein, P., Ebenbeck, W., Gousetis, C., Sichert, H., Troll, T., Utz, F., and Wallfaher, U. (2001) [4+2] Cycloadditions of 1,2,4,5-tetrazines and cyclopropenes - Synthesis of 3,4-diazanorcaradienes and tetracyclic aliphatic azo compounds, *Eur J Org Chem*, 2629-2638.
44. Steigel, A., Sauer, J., Binsch, G., and Kleier, D. A. (1972) Nitrogen analogs of cycloheptatrienes and norcaradienes - nuclear magnetic-resonance study of their thermodynamic and kinetic properties, *J Am Chem Soc* 94, 2770-2779.
45. Aue, D., Lorens, R., and Helwig, G. (1979) 1, 3-Dipolar additions to cyclopropenes and methylenecyclopropane, *J Org Chem* 44, 1202-1207.
46. Debets, M. F., van Berkel, S. S., Schoffelen, S., Rutjes, F. P., van Hest, J. C., and van Delft, F. L. (2010) Aza-dibenzocyclooctynes for fast and efficient enzyme PEGylation via copper-free (3+2) cycloaddition, *Chem Commun (Camb)* 46, 97-99.
47. Campbell, C. T., Sampathkumar, S.-G., and Yarema, K. J. (2007) Metabolic oligosaccharide engineering: perspectives, applications, and future directions, *Mol BioSyst* 3, 187-194.

48. Han, S., Collins, B. E., Bengtson, P., and Paulson, J. C. (2005) Homomultimeric complexes of CD22 in B cells revealed by protein-glycan cross-linking, *Nat Chem Biol* 1, 93-97.
49. Luchansky, S. J., Hang, H. C., Saxon, E., Grunwell, J. R., Yu, C., Dube, D. H., Bertozzi, C. R. (2003) Constructing azide-labeled cell surfaces using polysaccharide biosynthetic pathways, *Meth Enzymol* 362, 249-272.
50. Oetke, C., Brossmer, R., Mantey, L. R., Hinderlich, S., Isecke, R., Reutter, W., Keppler, O. T., and Pawlita, M. (2002) Versatile biosynthetic engineering of sialic acid in living cells using synthetic sialic acid analogues, *J Biol Chem* 277, 6688-6695.
51. Sletten, E. M., and Bertozzi, C. R. (2011) A bioorthogonal quadricyclane ligation, *J Am Chem Soc* 133, 17570-17573.
52. Hermanson, G. T. (1996) *Bioconjugate techniques*, Academic Press, San Diego.
53. Liao, L., Zhang, F., Yan, N., Golen, J., and Fox, J. (2004) An efficient and general method for resolving cyclopropene carboxylic acids, *Tetrahedron* 60, 1803-1816.
54. Ko, K. S., Park, G., Yu, Y., and Pohl, N. L. (2008) Protecting-group-based colorimetric monitoring of fluoros-phase and solid-phase synthesis of oligoglucosamines, *Org Lett* 10, 5381-5384.
55. Wilbur, D. S., Hamlin, D. K., Vessella, R. L., James, E., Buhler, K. R., Stayton, P. S., Klumb, L. A., Pathare, P. M., and Weerawarna, S. A. (1996) Antibody fragments in tumor pretargeting. Evaluation of biotinylated Fab' colocalization with recombinant streptavidin and avidin, *Bioconjugate Chem.* 7, 689-702.
56. Nguyen, T., Francis, M. B. (2003) Practical synthetic route to functionalized rhodamine dyes, *Organic Letters* 5, 3245-3248.

Chapter 3: Improved cyclopropene reporters for probing protein glycosylation

3.1 Introduction

The chemical reporter strategy is a popular method to tag biomolecules with probes in live cells and animals [1, 2]. This strategy relies on the metabolic introduction of unique functional groups (i.e., chemical reporters) into target biomolecules [3]. The reporters can be selectively modified in a second step using highly specific (i.e., bioorthogonal) chemistries. This two-step approach has been widely employed to visualize and profile cellular biopolymers, including glycoconjugates [3-8]. For example, sialylated glycans have been targeted with various *N*-acetyl mannosamine (ManNAc) and sialic acid precursors [9-12]. Similarly, mucin-type O-linked glycans and O-GlcNAc-modified proteins have been targeted with *N*-acetyl galactosamine (GalNAc) and *N*-acetyl glucosamine (GlcNAc) analogs, respectively [5, 13]. In most cases, the sugars were equipped with azide or alkyne reporter groups and ultimately detected via Staudinger ligation [14, 15], copper (I)-catalyzed azide-alkyne cycloaddition (CuAAC), or strain-promoted cycloaddition [16].

In recent years, cyclopropenes have gained traction as broadly useful chemical reporters for biomolecule visualization and retrieval [17-21]. Cyclopropenes are small in size and likely compatible with a variety of endogenous biosynthetic pathways. These motifs can also be readily ligated with tetrazine probes via inverse electron-demand Diels-Alder (IED-DA) reactions or nitrile imines via 1,3-dipolar cycloaddition. Importantly, cyclopropenes can be used concurrently with organic azides and alkynes—the most established chemical

reporters to date [17, 19, 22, 23]. Thus, cyclopropenes are well suited for multi-component imaging studies.

We and others have recently utilized cyclopropene-modified sugars (including the ManNAc analog, **Ac₄ManNCyc**, Figure 3-1A) to target sialic acid residues on live cell surfaces [17, 19]. In these previous studies, cells were first incubated with **Ac₄ManNCyc**, and then treated with various tetrazine probes. Cyclopropene-specific signal was observed in all cases, but the intensities were quite low, likely due to poor metabolic conversion of the unnatural sugar, inefficient tetrazine ligation, or both of these issues. Indeed, the N-acyl unit in **Ac₄ManNCyc** is branched at the beta carbon; beta-substituted N-acyl chains are not well tolerated in the sialic acid biosynthetic pathway [24, 25]. Additionally, cyclopropenes with amides or other electron-withdrawing groups at C-3 (see Figure 3-1A) are sluggish IED-DA reactants [17, 21].

Here we report three cyclopropene-modified sugars that enable more facile tagging of mammalian cell glycoconjugates in a variety of assays. These monosaccharides comprise carbamate linkages between the requisite cyclopropene and sugar core (Figure 3-1A). The N-cyclopropenyl carbamate derivative **Ac₄ManCCp** was designed to intercept the sialic acid biosynthetic pathway and target sialylated glycoconjugates [26]. The analogous GalNAc and GlcNAc analogs (**Ac₄GalCCp** and **Ac₄GlcCCp**) were designed to target mucin-type O-linked structures and O-GlcNAcylated proteins, respectively. Carbamates are relatively stable moieties, making them attractive for use in cells and live organisms. Indeed, Pratt and coworkers recently synthesized a set of N-propargyloxycarbamate sugars that can be readily detected via CuAAC for proteomics applications [27]. For the cyclopropene probes, the carbamate linkage also alleviates steric congestion at the beta-position, improving the

likelihood that cellular enzymes will efficiently process the sugars. Moreover, we and others have shown that cyclopropenes outfitted with carbamates (versus amides) at C-3 react ~100 times faster with electron-poor tetrazines [17, 18, 21, 26].

3.2 Results and Discussion

We prepared the desired probes (**Ac₄ManCCp**, **Ac₄GalCCp**, **Ac₄GlcCCp**, Scheme 3-1) via direct conjugation of amino sugars **3.4-3.6** with an activated cyclopropene unit (**3.3**). Carbonate **3.3** was prepared by treating alcohol **3.1** with anhydrous cesium fluoride (to remove the silyl group), followed by nitrophenyl chloroformate (Scheme 3-1A). These transformations were performed sequentially as intermediate **3.2** was not stable upon concentration. Direct activation of **3.1** also resulted in product decomposition. Ultimately, carbonate **3.3** was used to acylate the hydrochloride salts of mannosamine (**3.4**), galactosamine (**3.5**), and glucosamine (**3.6**, Scheme 3-1B). The resulting carbamate sugars were then globally acetylated to provide the desired probes **Ac₄ManCCp**, **Ac₄GlcCCp**, and **Ac₄GalCCp**. Acylation of sugar hydroxyl groups has been previously shown to facilitate probe uptake into mammalian cells [28].

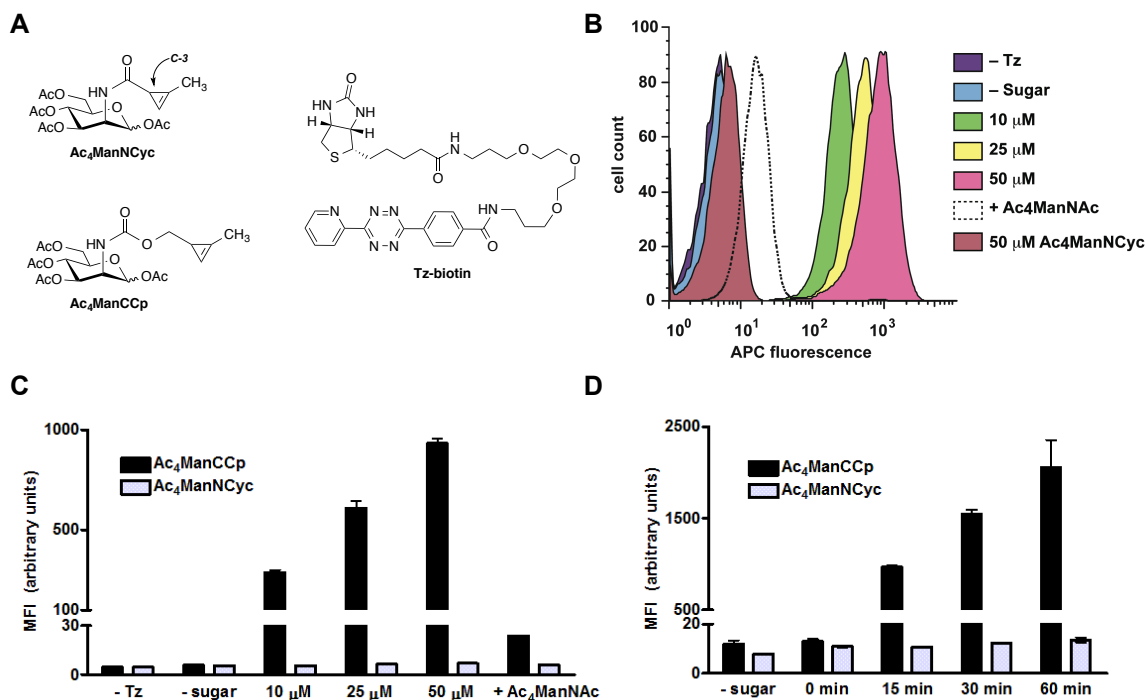
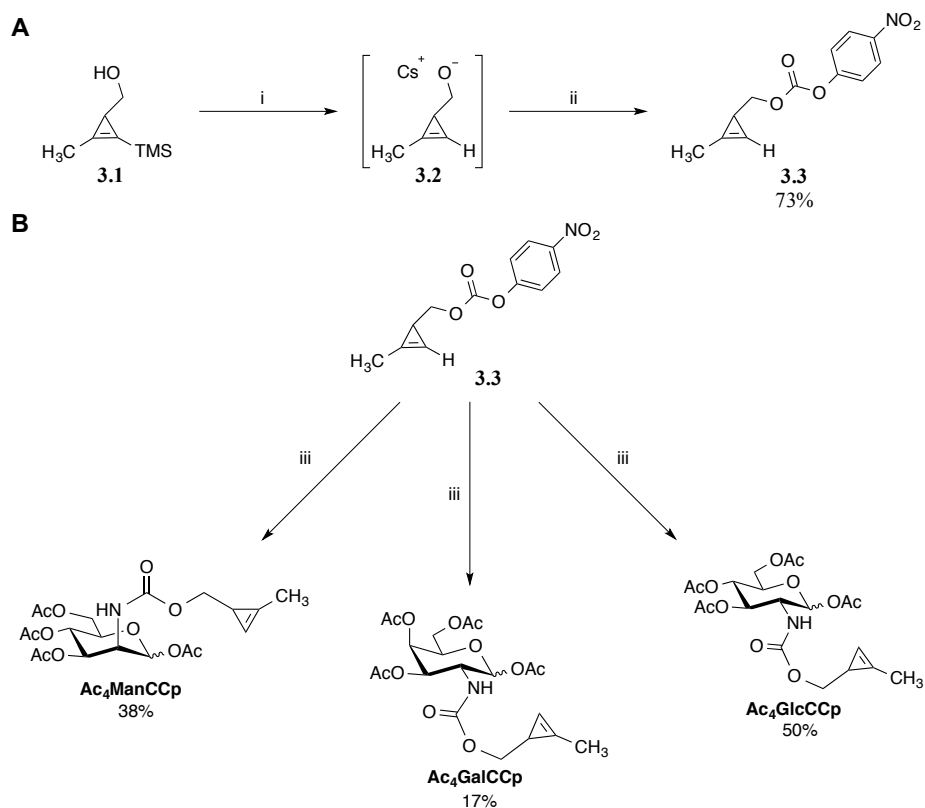


Figure 3-1. Cyclopropene-modified ManNAc derivatives can be metabolically incorporated onto cell surfaces and covalently detected with tetrazine probes. (A) Structures of the ManNAc analogs (**Ac₄ManNCyc** and **Ac₄ManCCp**) and tetrazine reagent (**Tz-biotin**) used in this study. (B) **Ac₄ManCCp** is robustly incorporated onto live cell surfaces. Jurkat cells were incubated with **Ac₄ManCCp** (0-50 μM), **Ac₄ManNCyc** (0-50 μM) **Ac₄ManCCp** (50 μM) plus **Ac₄ManNAc** (10 μM, +**Ac₄ManNAc**) or no sugar (-sugar). Samples were then treated with **Tz-biotin** (10 μM) for 30 min at 37 °C. One **Ac₄ManCCp**-treated sample (10 μM) was not labeled with **Tz-biotin** (-Tz). All cells were then stained with APC-avidin and analyzed by flow cytometry. Representative histograms are shown. (C) and (D) **Ac₄ManCCp** enables more robust cell surface labeling than **Ac₄ManNCyc**. (C) The mean fluorescence intensities (MFI, in arbitrary units) for the histograms in (B) are plotted. MFI values for cells treated with **Ac₄ManNCyc** (10-50 μM) are also shown. (D) **Ac₄ManCCp** can be rapidly detected with **Tz-biotin**. Jurkat cells were incubated with **Ac₄ManCCp** (25 μM) or **Ac₄ManNCyc** (25 μM), then treated with **Tz-biotin** (10 μM) for 0-60 min at 37 °C. The cells were stained with APC-avidin and analyzed by flow cytometry. The mean fluorescence intensities of the cell populations are plotted. In (C) and (D), error bars represent the standard deviation of the mean for three labeling reactions.



Scheme 3-1. (A) Synthesis of carbonate **3.3** via sequential deprotection and activation of **3.1**. (B) Synthesis of carbamate-linked cyclopropene sugars. i) CsF (1.05 equiv), 18-crown-6 (1.10 equiv), THF, rt, 3 h; ii) 4-nitrochloroformate (2 equiv), pyridine (6 equiv), CH₂Cl₂, rt, overnight; iii) mannosamine, galactosamine, or glucosamine hydrochloride (0.25 equiv), *N,N*-diisopropylethylamine (4 equiv), DMF, rt, 4-12 h, followed by Ac₂O, pyridine.

Once in hand, the modified sugars were used to metabolically target glycoconjugates in live cells. Jurkat T cells were first incubated with **Ac₄ManCCp** (0-50 μ M) for 24 h, then reacted with a tetrazine-biotin probe (**Tz-biotin**, 10 μ M, 30 min at 37 °C). Cell surface cycloadducts were detected upon staining with a fluorescent streptavidin conjugate and flow cytometry analysis. As shown in Figures 3-1 B-C, **Ac₄ManCCp**-dependent fluorescence was observed, indicating successful metabolism and cell surface incorporation of the unnatural sugar. Notably, **Ac₄ManCCp** provided enhanced cellular fluorescence compared to the N-acetyl variant **Ac₄ManNCyc** at all reagent concentrations and labeling times investigated, with nearly a 130-fold improvement in signal at the maximal doses and times. This was likely due to the improved incorporation efficiency of the carbamate probe, along with its faster rate of reaction. Similar trends were observed in other cell lines cultured with **Ac₄ManCCp** (Figure 3-2) [26]. The fluorescence signal from **Ac₄ManCCp**-treated cells was also diminished in the presence of Ac₄ManNAc, the native substrate, suggesting that the carbamate probe enters the sialic acid biosynthetic pathway. Furthermore, Western blot analysis of proteins harvested from **Ac₄ManCCp**-treated cells (and reacted with **Tz-biotin**) revealed a similar banding pattern—or “fingerprint”—compared to proteins isolated from cells treated with a previously validated report of sialylation, the azido-ManNAc analog Ac₄ManNAz (Figure 3-3 and 3-4) [29]. In this experiment, Ac₄ManNAz-labeled glycoproteins were detected via CuAAC with an alkyne probe.

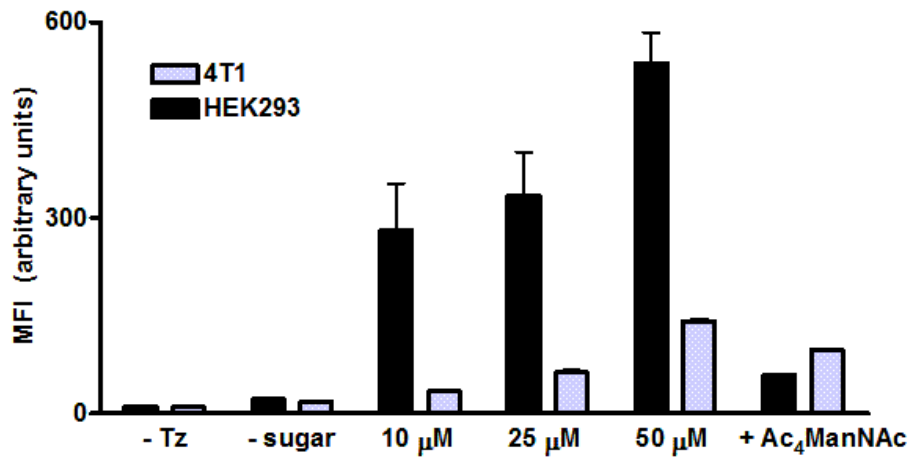


Figure 3-2. Ac₄ManCCp is metabolically incorporated into 4T1 and HEK293 cell surface glycans. Cells were incubated with Ac₄ManCCp (0-50 μ M), Ac₄ManCCp plus a control sugar (+ Ac₄ManNAc, 10 μ M), or no sugar (- sugar) for 24 h. After washing, the cells were treated with Tz-biotin (10 μ M) for 30 min or no secondary reagent (-Tz) at 37 °C, stained with streptavidin-APC, and analyzed by flow cytometry. The mean fluorescence intensity (MFI) values for the cell populations are plotted. Error bars represent the standard deviation of the mean for three experiments.

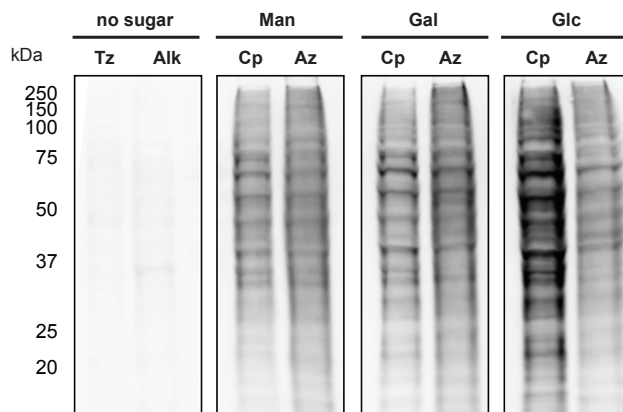


Figure 3-3. Carbamate-linked cyclopropene sugars label cellular glycoproteins. Jurkat cells were incubated with cyclopropene (Cp) or azido (Az) analogs of ManNAc (Man), GalNAc (Gal), or GlcNAc (Glc) (75 μ M) for 36 h, then lysed. Soluble protein isolates were treated with either 100 μ M **Tz-biotin** to tag Cp-modified proteins or an alkyne-modified biotin (structure shown in Figure 3-4, 100 μ M) to tag Az-modified proteins via CuAAC. All samples were separated by gel electrophoresis and analyzed via Western blot. Equivalent protein loading was confirmed using Ponceau S stain (Figure 3-4).

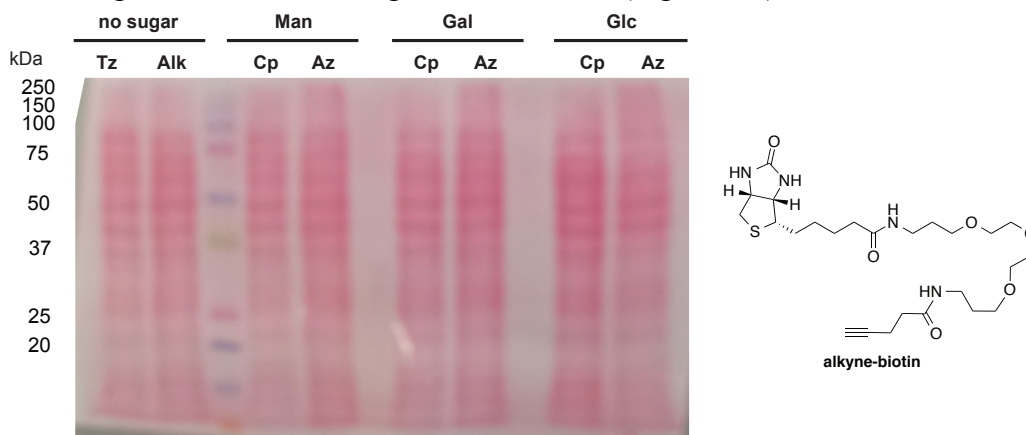


Figure 3-4. Equivalent protein loading was observed via Ponceau S staining. Jurkat cells were incubated with cyclopropene (Cp) or azido (Az) analogs of ManNAc (Man), GalNAc (Gal), or GlcNAc (Glc) (75 μ M) for 36 h, then lysed. Protein isolates were treated with either 100 μ M **Tz-biotin** to tag Cp-modified proteins or **alkyne-biotin** (100 μ M) to tag Az-modified proteins via CuAAC. The labeled proteins were separated by gel electrophoresis and transferred to nitrocellulose prior to Ponceau S staining.

Ac₄GalCCp and **Ac₄GlcCCp**, the putative metabolic reporters for GalNAc and GlcNAc, respectively, were similarly evaluated in cultured cells. Jurkat or HEK293 cells were incubated with the unnatural sugars (0-50 μ M) for 24 h prior to tetrazine ligation and flow cytometry analysis. Cell surface cyclopropenes were detected in all cases (Figure 3-5). The glycoprotein targets of these sugars were also analyzed. Soluble protein isolates from **Ac₄GalCCp**- or **Ac₄GlcCCp**-treated Jurkat cells were reacted with **Tz-biotin**, then separated by gel electrophoresis and analyzed by Western blot. As shown in Figure 3-3, both **Ac₄GalCCp** and **Ac₄GlcCCp** produced “fingerprints” similar to their azido counterparts [30-32]. It should be noted, though, that some N-acyl analogs of GalNAc, GlcNAc, and ManNAc have been observed to target multiple classes of biomolecules due to N-deacetylation and/or enzymatic scrambling [30-32]. The extent to which the carbamate sugars are interconverted remains to be determined, and further biochemical studies will ultimately elucidate their metabolic fates. Based on our work to date, though, the cyclopropene sugars appear to function similarly to the analogous azido probes (Figures 3-3 and 3-6).

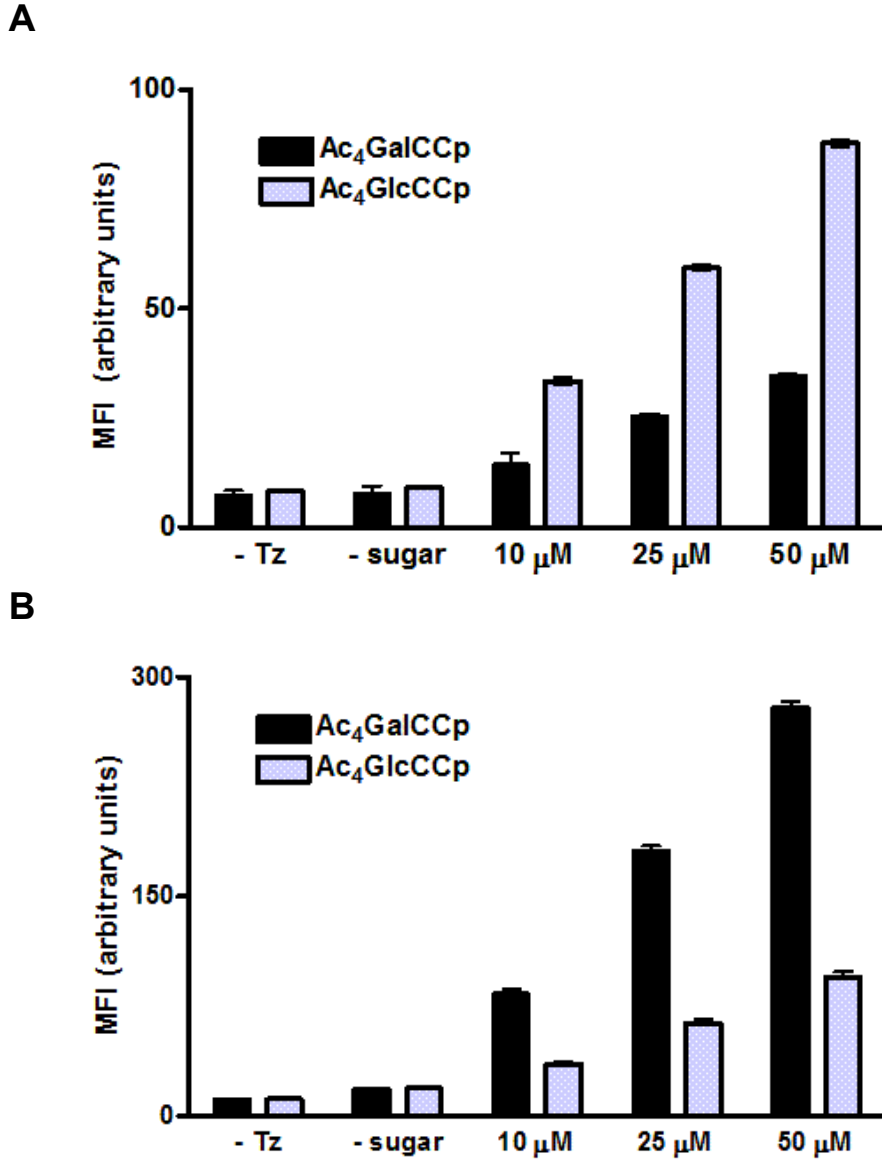


Figure 3-5. Ac₄GalCCp and Ac₄GlcCCp are metabolically incorporated into cell surface glycans. Jurkat (A) and HEK293 (B) cells were incubated in the presence of Ac₄GalCCp (0-50 μM), Ac₄GlcCCp (0-50 μM), or no sugar (-sugar) for 24 h. After washing, the cells were treated with Tz-biotin (10 μM) or no reagent (-Tz) for 30 min at 37 °C, stained with streptavidin-APC, and analyzed by flow cytometry. The mean fluorescence intensity (MFI) values for the cell populations are plotted. Error bars represent the standard deviation of the mean for three experiments.

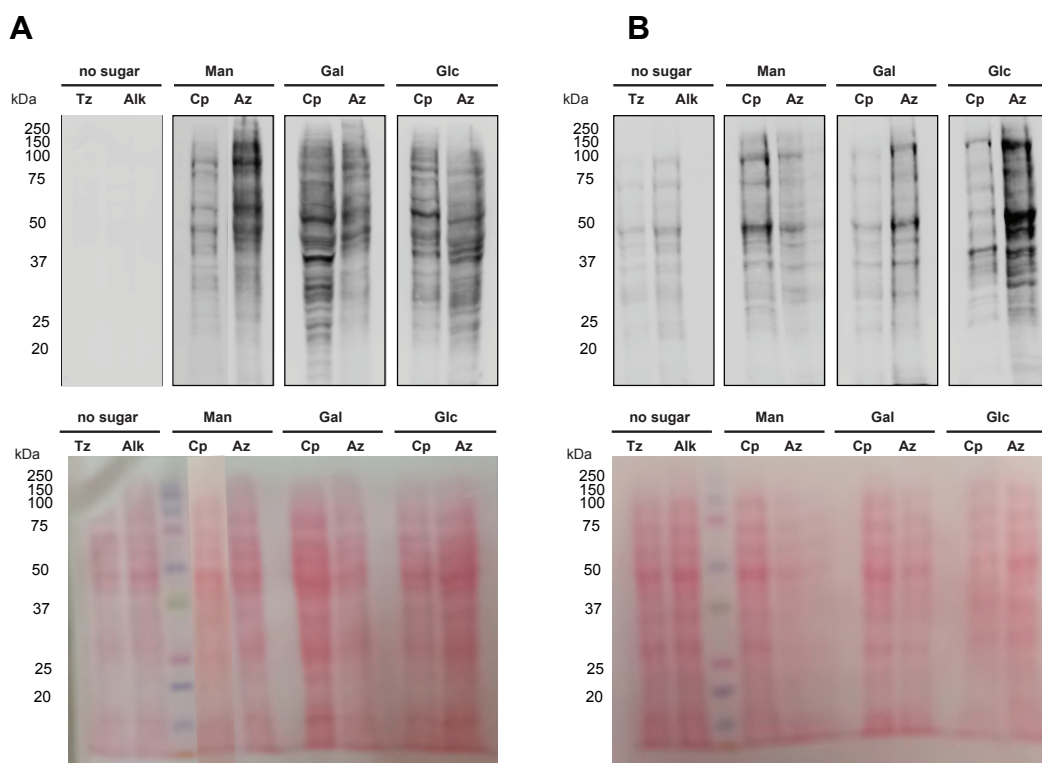


Figure 3-6. Carbamate-linked cyclopropene sugars label cellular glycoproteins. (A) HEK293 and (B) 4T1 cells were incubated with cyclopropene (Cp) or azido (Az) analogs of ManNAc (Man), GalNAc (Gal), or GlcNAc (Glc) (75 μ M) for 36 h, then lysed. Soluble protein isolates were treated with either 100 μ M **Tz-biotin** to tag Cp-modified proteins or 100 μ M **alkyne-biotin** (structure shown in Figure 3-4) to tag Az-modified proteins via CuAAC. All samples were separated by gel electrophoresis and analyzed via Western blot. Protein loading was confirmed using Ponceau S stain.

Azide-alkyne cycloadditions and cyclopropene-tetrazine ligations can be used simultaneously to visualize distinct biomolecules in live cells. However, in most examples to date, the cyclopropene-tagging reactions required either extensive labeling times (>1 h with 100 μ M tetrazine) or large probe concentrations (>100 μ M **Ac₄ManNCyc** or >100 μ M tetrazine). Such conditions resulted in cellular toxicity and higher levels of background labeling. With the carbamate-functionalized sugars, lower concentrations of reagents and shorter reaction times can be employed, facilitating glycan visualization in live cells. Indeed, when 4T1 cells were treated with **Ac₄ManCCp** or **Ac₄GalCCp** (25 μ M), the targeted glycoconjugates could be readily detected with functionalized tetrazines in just 15 min (Figures 3-7 and 3-8). By contrast, no detectable fluorescence was observed in **Ac₄ManNCyc**-treated cells even after extended tetrazine labeling times (1 h, Figure 3-10).

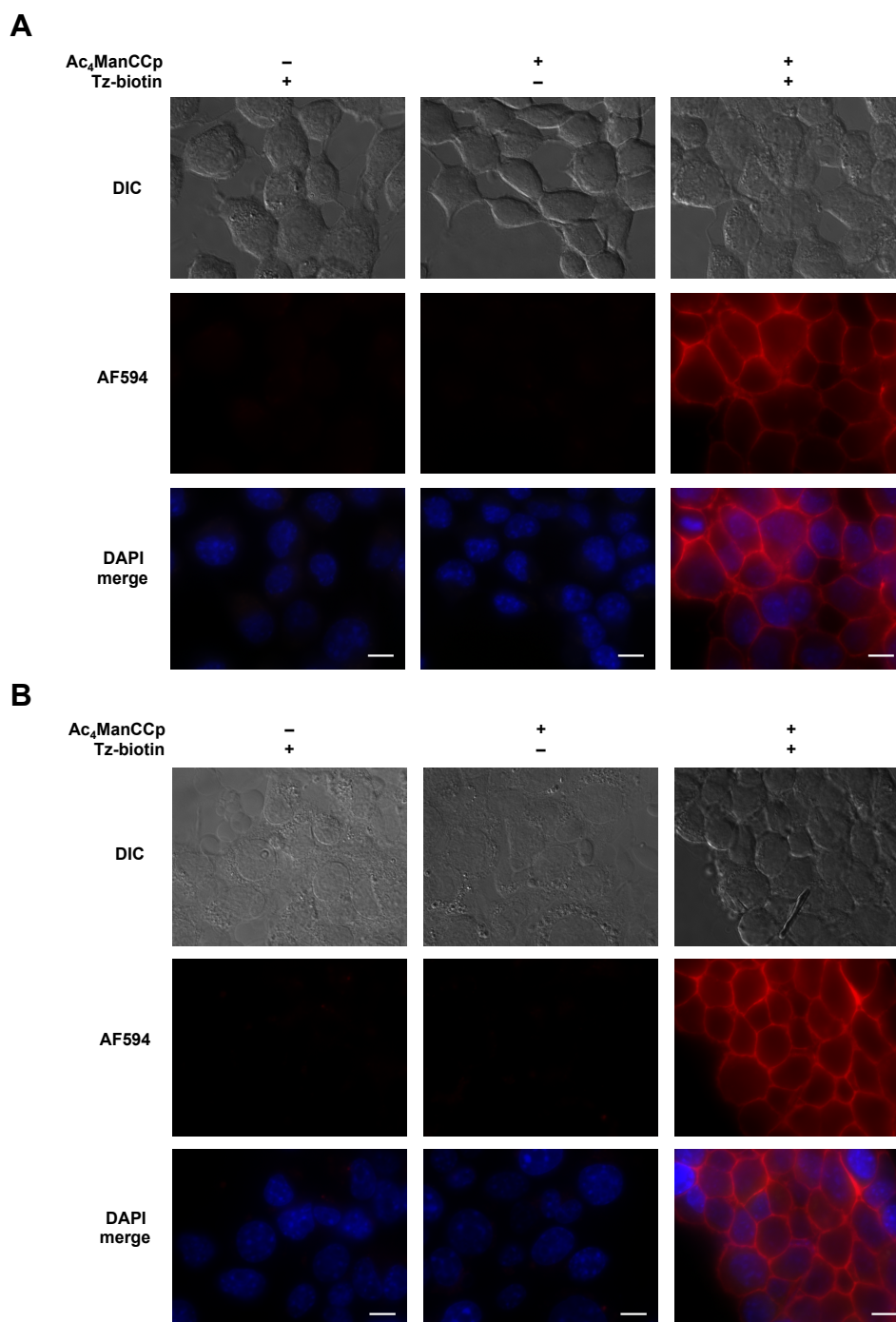


Figure 3-7. Carbamate cyclopropene sugars can be metabolically introduced and visualized in 4T1 mammalian cells. Cells were incubated in the presence of **Ac₄ManCCp** (25 μ M, +) or no sugar (-) for 36 h. After washing, the cells were treated with **Tz-biotin** (25 μ M, +) or no reagent (-) for (A) 1 h or (B) 15 min at 37 °C, stained with streptavidin-APC and DAPI, and analyzed by fluorescence microscopy. Cell surface fluorescence (red) was only observed in samples treated with both **Ac₄ManCCp** and **Tz-biotin**). Representative bright-field (DIC) images AF594 images, and merged images are shown. Scale bar = 10 μ m.

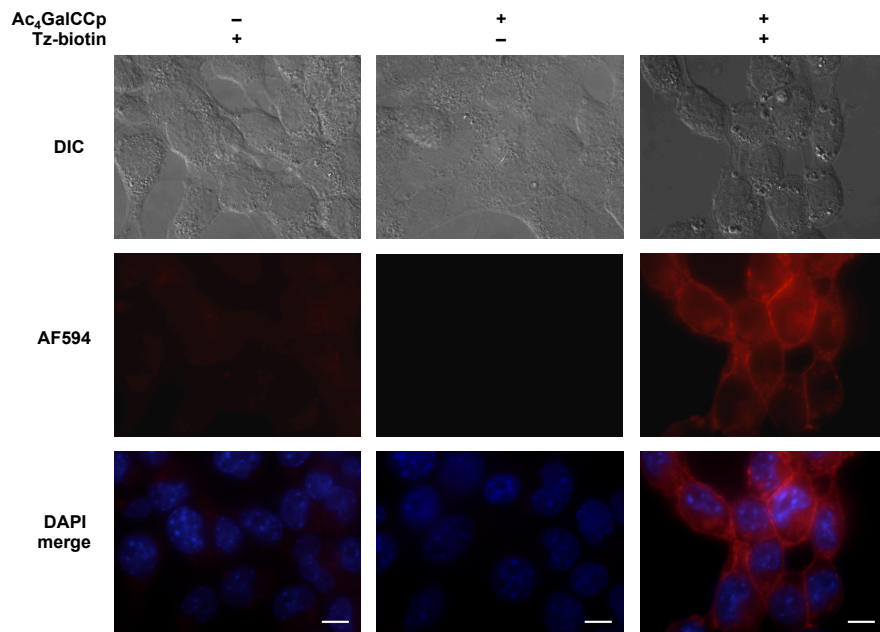


Figure 3-8. Cyclopropene-GalNAc reporters can be metabolically incorporated and visualized in 4T1 cells. Cells were incubated in the presence of **Ac₄GalCCp** (25 μ M, +) or no sugar (-) for 36 h. After washing, the cells were treated with **Tz-biotin** (25 μ M, +) or no reagent (-) for 1 h at 37 °C, stained with streptavidin-APC and DAPI, and analyzed by fluorescence microscopy. Representative bright-field (DIC) images, AF594 images, and merged images are shown. Scale bar = 10 μ m.

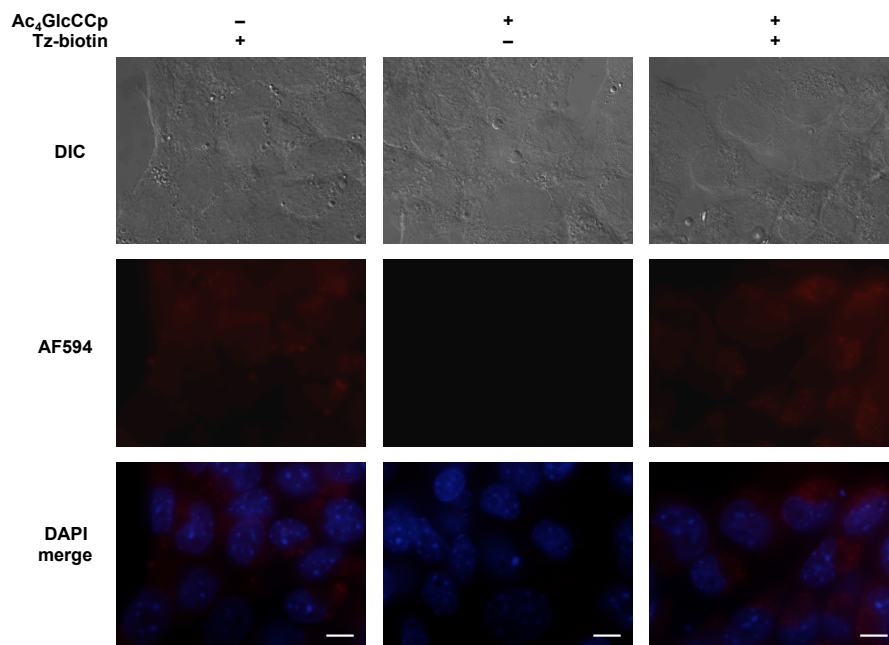


Figure 3-9. Ac₄GlcCCp is incorporated into cellular glycoconjugates (as shown in Figures 3-3, 3-5, and 3-6), but minimal cell surface labeling is observed. Cells were incubated in the presence of Ac₄GlcCCp (25 μM, +) or no sugar (–) for 36 h. After washing, the cells were treated with Tz-biotin (25 μM, +) or no reagent (–) for 1 h at 37 °C, stained with streptavidin-APC and DAPI, and analyzed by fluorescence microscopy. Representative bright-field (DIC) images, AF594 images, and merged images are shown. Scale bar = 10 μm.

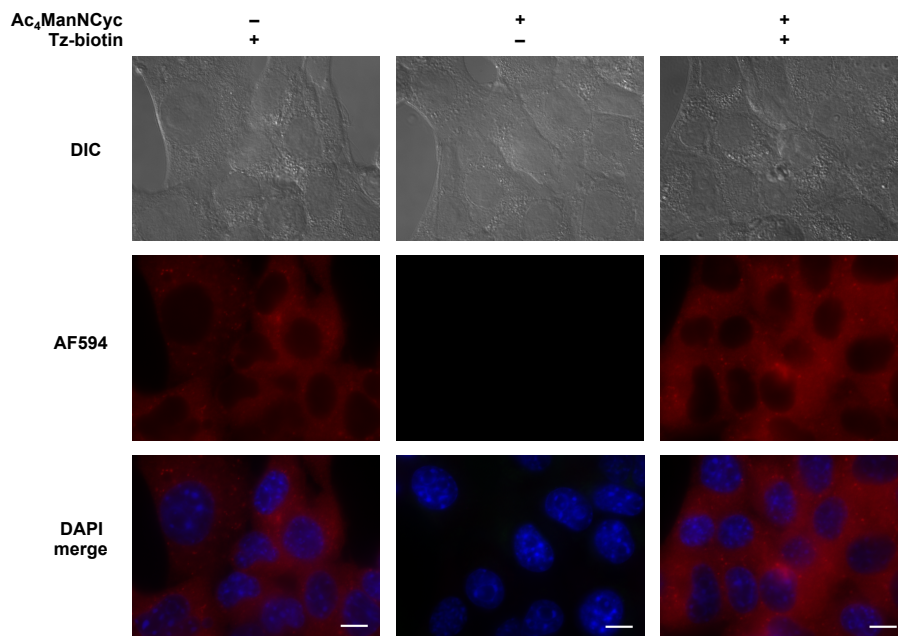


Figure 3-10. No cell surface labeling observed with Ac₄ManNCyc. Cells were incubated with Ac₄ManNCyc (25 μM, +) or no sugar (–) for 36 h. After washing, the cells were treated with Tz-biotin (25 μM, +) or no reagent (–) for 1 h at 37 °C, stained with streptavidin-APC and DAPI, and analyzed by fluorescence microscopy. Representative bright-field (DIC) images, AF594 images, and merged images are shown. Scale bar = 10 μm. (Note: the exposure times used for the AF594 panels in this experiment were ~3X greater than those used to generate the images in Figure 3-7).

We used the optimized carbamate cyclopropenes in tandem with azido reporters to target unique subsets of cellular glycans (Figures 3-11 and 3-12). In brief, cells were treated with either **Ac₄ManCCp** (to target sialylated structures), the azido GalNAc analog (**Ac₄GalNAz**), both unnatural sugars, or no sugar. All cell samples were reacted concurrently with **Tz-biotin** (to tag cell surface cyclopropenes) and a strained alkyne (**DBCO-FLAG**, Scheme 3-2) to tag cell surface azides. Selective labeling of each unnatural sugar was observed with no cross-reactivity. Unique sites of biomolecule co-localization were also observed near cellular junctions. Further insights into these and other multi-component processes will be aided by the cyclopropene chemical reporters described in this work.

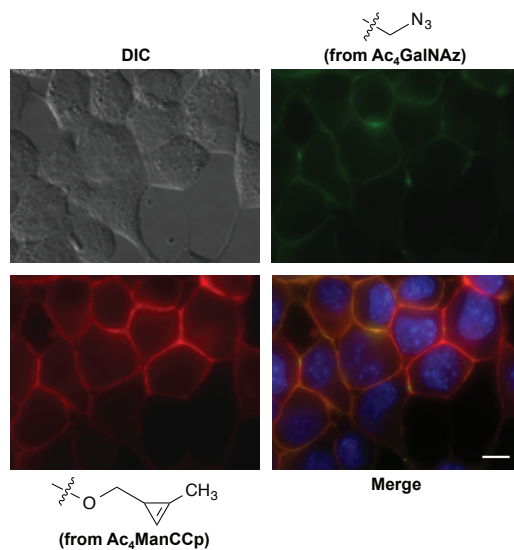


Figure 3-11. Distinct metabolic targets can be simultaneously imaged using cyclopropene and azido reporters. 4T1 cells were cultured in the presence of both **Ac₄ManCCp** (25 μ M) and **Ac₄GalNAz** (25 μ M) for 24 h, followed by concurrent treatment with **Tz-biotin** (25 μ M, 1 h at 37 $^{\circ}$ C) and **DBCO-FLAG** (100 μ M, 1 h at 37 $^{\circ}$ C) to covalently tag cell surface cyclopropenes and azides, respectively. Cells were then stained with streptavidin-AF594 and FITC-a-FLAG and imaged via confocal microscopy. Representative images are shown. Red: AF594, Green: FITC, Blue: DAPI. Scale bar: 10 μ m.

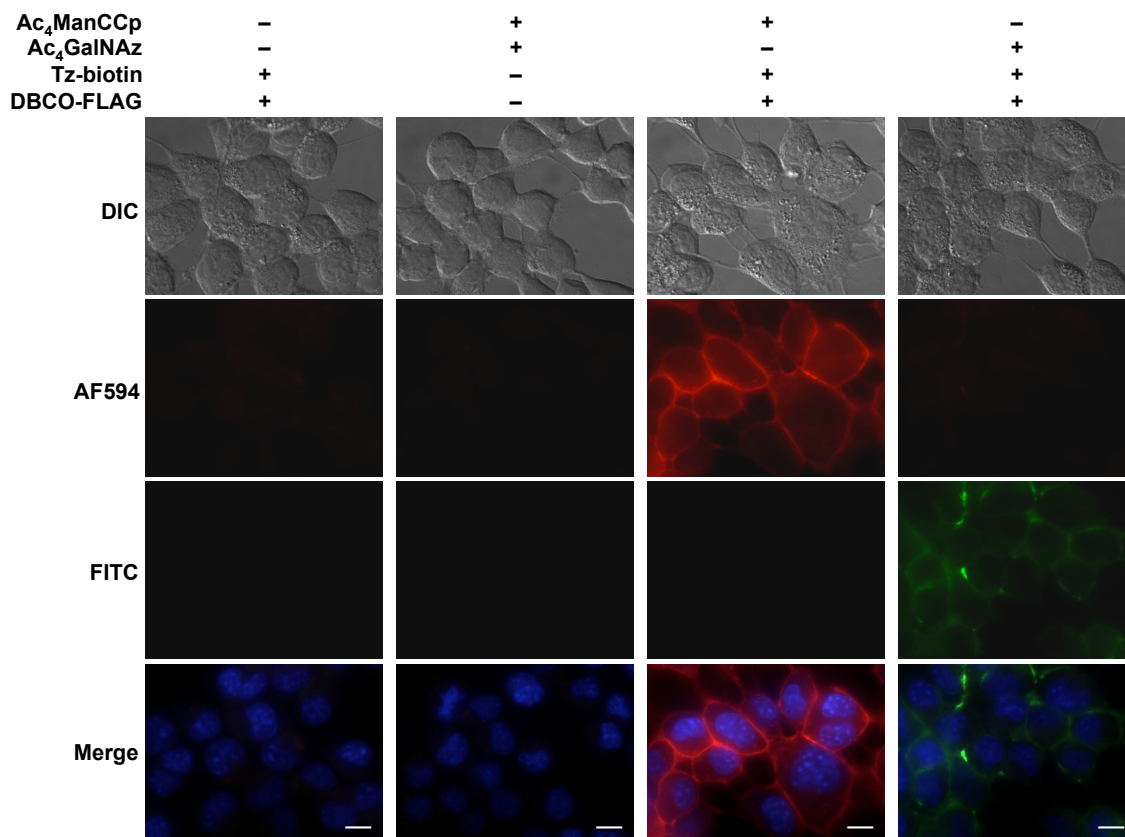
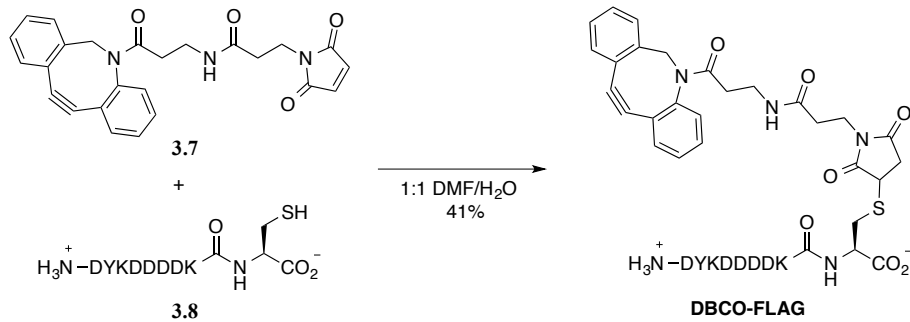


Figure 3-12. Control images for the dual labeling experiment in Figure 3-11. 4T1 cells were cultured in the presence of **Ac₄ManCCp** (25 μ M, +), **Ac₄GalNAz** (25 μ M, +), both sugars (25 μ M each), or no sugar (-) for 36 hours. The cells were then treated with **Tz-biotin** (25 μ M, +), **DBCO-FLAG** (100 μ M, +), both reagents (+) or no reagent (-) for 1 h at 37 °C. Cells were then stained (streptavidin-AF594, FITC- α -FLAG, and DAPI) and imaged by fluorescence microscopy. Representative bright-field (DIC), AF594, FITC, and merged images are shown. Scale bar = 10 μ m.

Scheme 3-2. Synthesis of DBCO-FLAG.



3.3 Conclusions

Cyclopropenes are versatile chemical reporters for biomolecule tagging in live cells. Despite their remarkable cellular compatibilities and unique chemistries, they have been inefficient reports of glycosylation to date. We developed a set of carbamate-functionalized cyclopropenes with improved utility for glycan imaging and profiling. These tools were readily processed in cultured cells and rapidly ligated with tetrazine probes. The carbamate-cyclopropene sugars can also be used in tandem with other chemical reporters including azides and alkynes, and we utilized combinations of these tools to tag two different subsets of glycans in live cells. Future multi-component imaging studies of glycans and related biomolecules will benefit from the versatility of the cyclopropene probes presented here.

3.4 Materials and methods

3.4a Metabolic labeling studies with cultured cells

Jurkat cells were plated at a density of ~500,000 cells/mL in RPMI media (Corning) supplemented with 10% fetal bovine serum (FBS, Life Technologies), penicillin (100 U/mL), and streptomycin (100 mg/mL). HEK293 and 4T1 cells were plated at ~500,000 cells/well in 2 mL DMEM media (Corning) supplemented with 10% FBS, penicillin (100 U/mL), and streptomycin (100 mg/mL). Cells were incubated with **Ac₄ManNCyc**, **Ac₄ManCCp**, **Ac₄GalCCp**, or **Ac₄GlcCCp** (0-50 μ M) for 24 h in a 5% CO₂, water-saturated incubator at 37 °C. The cells were rinsed with PBS containing 1% bovine serum albumin (FACS buffer, 3 x 200 mL), then reacted with **Tz-biotin** (10 μ M, 30 min, 37 °C). The cells were subsequently pelleted (1500 rpm), washed with FACS buffer (3 x 200 mL), and stained with streptavidin-APC (eBioscience, 1:500 dilution in FACS buffer) for 20 min on ice. The cells were pelleted

and washed with additional FACS buffer (3 x 200 mL), then analyzed by flow cytometry on an LSR-II flow cytometer (BD Biosciences). For each sample, data were acquired for 10,000 live cells. Cells were analyzed in triplicate, and three replicate experiments were performed for each study. Cellular fluorescence data were analyzed using FloJo software (Tree Star, Inc.).

3.4b Western blot analyses

Jurkat cells were plated at a density of ~500,000 cells/mL in RPMI media (Corning) supplemented with 10% FBS along with penicillin (100 U/mL) and streptomycin (100 mg/mL). Cells were incubated with azido sugars **Ac₄ManNAz**, **Ac₄GalNAz**, or **Ac₄GlcNAz** (75 μM) or cyclopropene sugars **Ac₄ManCCp**, **Ac₄GalCCp**, or **Ac₄GlcCCp** (75 μM) for 36 h in a 5% CO₂, water-saturated incubator at 37 °C. The cells were pelleted (1500 rpm), rinsed with PBS (3 x 0.5 mL), and then lysed with 100 mL lysis buffer (1% Igepal™ CA-630, 150 mM NaCl, 50 mM triethanolamine, pH 7.4) on ice for 30 min. The lysates were pelleted (13,000 rpm for 10 min at 4 °C) and protein concentrations were measured using a BCA protein assay kit (Pierce). Lysates (~1 mg/mL, 50 mL) were treated with either freshly prepared "click" chemistry cocktail containing **alkyne-biotin** (100 μM); sodium ascorbate (1 mM); tris[(1-benzyl-1-H-1,2,3-triazol-4-yl)methyl]amine (TBTA) (100 μM); CuSO₄•5H₂O (1 mM)] or **Tz-biotin** (100 μM, 1 h, 37 °C). To precipitate the labeled proteins, ice-cold methanol (1 mL) was added and the samples were stored at -80 °C overnight. Protein precipitates were pelleted via centrifugation (13,000 rpm for 10 min at 4 °C), aspirated and dried for 1 h at rt. The protein isolates were then re-suspended in 10 mL buffer (4% SDS, 150 mM NaCl, 50 mM triethanolamine, pH 7.4), then treated with SDS-PAGE loading buffer (10

μ L of a 2X stock containing 20% glycerol, 0.2% bromophenol blue, 1.4% β -mercaptoethanol). The samples were heated at 90 °C for 5–10 min, separated by gel electrophoresis using 12% polyacrylamide gels, and then electroblotted to nitrocellulose membranes (0.2 μ m; Bio-Rad). Transfer efficiency was analyzed with Ponceau S staining. The membranes were rinsed with water and incubated with blocking buffer (7% bovine serum albumin in PBS containing 1% Tween® 20, PBS-T) for 1 h at rt, followed by IRDye® 800CW streptavidin (LI-COR Biosciences; 1:10,000 dilution in blocking buffer) for at least 1 h. The membranes were subsequently washed with PBS-T (5 x 10 min) and imaged using an Odyssey infrared imaging system (Li-Cor, Odyssey version 3.0).

3.4c Microscopy

4T1Luc2 cells were grown on glass cover slips submerged in 0.5 mL DMEM media (Corning) supplemented with 10% FBS, penicillin (100 U/mL), and streptomycin (100 mg/mL) (in 24-well culture dishes). The media also contained **Ac₄ManCCp** (25 μ M), **Ac₄GalCCp** (25 μ M), **Ac₄GlcCCp** (25 μ M), or no sugar. After 36 h, the cells were washed with FACS buffer (3 x 0.25 mL). Cells were then treated with **Tz-biotin** (25 μ M) in media for 15 min at 37 °C. The cells were washed with FACS buffer (3 x 0.25 mL) and fixed with 4% paraformaldehyde in PBS for 15 min at rt. After washing with PBS (3 x 0.25 mL), the cells were blocked for 1 h at rt with PBS + 5% BSA (0.5 mL). The cells were treated with streptavidin-AlexaFluor594 (Jackson Labs; 1:1000 in FACS buffer) for 30 min at rt, then washed with FACS buffer (3 x 0.25 mL). The cover slips were mounted on glass slides with Vectashield® mounting media (Vector Laboratories) for imaging. Images were acquired on a

Nikon Eclipse Ti inverted microscope with NIS-Elements Microscope Imaging Software and analyzed with ImageJ.

For dual labeling experiments, 4T1Luc2 cells were grown on glass cover slips submerged in 0.5 DMEM media (Corning) supplemented with 10% FBS, penicillin (100 U/mL), and streptomycin (100 mg/mL) (in 24-well culture dishes). The media also contained **Ac₄ManCCp** (25 μ M), **Ac₄GalNAz** (25 μ M), both sugars (25 μ M each), or no sugar. After 36 h, the cells were washed with PBS + 1% BSA (3 x 0.25 mL). Cells were then treated with **Tz-Biotin** (25 μ M), **DBCO-FLAG** (100 mM), both reagents, or no reagent in media for 1 h at 37 °C. The cells were then washed with FACS buffer (3 x 0.25 mL) and blocked for 1 h at rt with PBS + 5% BSA (0.5 mL). The cells were treated with streptavidin-AlexaFluor594 (Jackson Labs; 1:1000 in FACS buffer) and FITC-a-FLAG (Sigma-Aldrich; 10 μ g/mL in FACS buffer) for 1 h at rt. The cover slips were washed with FACS buffer (3 x 0.25 mL), then fixed with 4% paraformaldehyde in PBS for 15 min at rt. The cover slips were washed with FACS buffer (3 x 0.25 mL) and mounted on glass slides with Vectashield® mounting media (Vector Laboratories) for imaging. Images were acquired on a Nikon Eclipse Ti inverted microscope with NIS-Elements Microscope Imaging Software and analyzed with ImageJ.

3.4d General synthetic procedures

Compounds **Ac₄ManNCyc** [19], **Tz-biotin** [17], **alkyne-biotin** [33], **3.7** [34], and **3.8** [35] were synthesized as previously reported. All other reagents were purchased from commercial sources and used as received without further purification. Reactions were carried out under an inert atmosphere of nitrogen in oven- or flame-dried glassware. Dichloromethane (CH₂Cl₂), tetrahydrofuran (THF), *N,N*-dimethylformamide (DMF), and triethylamine (NEt₃) were degassed with argon and passed through two 4 x 36 inch columns of anhydrous neutral A-2 (8 x 14 mesh; LaRoche Chemicals; activated under a flow of argon at 350 °C for 12 h). The remaining solvents were of analytical grade and purchased from commercial suppliers. Thin-layer chromatography was performed using Silica Gel 60 F₂₅₄ plates. Plates were visualized with UV radiation or staining with 10% sulfuric acid in ethanol or KMnO₄. Flash column chromatography was performed with SiliaFlash® F60 40-63 mM (230-400 mesh) silica gel from Silicycle. ¹H and ¹³C NMR spectra were recorded on CRYO-500 (500 MHz ¹H, 125.7 MHz ¹³C) or DRX-400 (400 MHz ¹H) spectrometers. All spectra were collected at 298 K. Chemical shifts are reported in ppm values relative to residual non-deuterated NMR solvent and coupling constants (*J*) are reported in Hertz (Hz). High-resolution mass spectrometry was performed by the University of California, Irvine Mass Spectrometry Center. HPLC runs were conducted on a Varian ProStar equipped with 325 Dual Wavelength UV-Vis Detector. Semi-preparative runs were performed using an Agilent Prep-C18 Scalar column (9.4 x 150 mm, 5 μm) with a 5 mL/min flow rate. The elution gradients for the relevant separations are specified below.

3.4e Synthetic Procedures

3-Hydroxymethyl-2-methyl-trimethylsilylcyclopropene (3.1). To a stirring mixture of TMS-propyne (4.0 mL, 27 mmol) and rhodium acetate dimer (15 mg, 0.034 mmol) was slowly added ethyl diazoacetate (1.0 mL, 8.6 mmol) dissolved in 15 mL CH₂Cl₂ at a rate of 0.5-1.0 mL/min. Once the addition was complete, the reaction was stirred for an additional 30 min. The mixture was then partially concentrated under reduced pressure and eluted through a plug of silica gel (eluting with CH₂Cl₂) to remove the rhodium catalyst. The eluant was gently concentrated under reduced pressure and added dropwise (over 1 min) to a solution of DIBAL-H (14.0 mL of a 25% wt/wt solution in hexanes, 17.2 mmol) in 15 mL Et₂O at 4 °C. The reaction was stirred until the cyclopropene ester was consumed (30–60 min). Saturated Rochelle's salt was then added and the mixture was stirred until a white gel formed. The organic layer was isolated and the aqueous layer was further extracted with Et₂O (2 x 20 mL). The combined organic layers were dried with MgSO₄, filtered, and concentrated *in vacuo* to afford the crude product as a faint yellow oil. The product was purified by flash column chromatography (eluting with 30% Et₂O in hexanes) to yield **3.1** as a faint yellow oil (714 mg, 53% two steps): ¹H NMR (500 MHz, CDCl₃) δ 3.48 (d, *J* = 4.6 Hz, 2H), 2.21 (s, 3H), 1.56 (t, *J* = 4.6 Hz, 1H), 0.17 (s, 9H). Data is in agreement with previously reported spectrum [17].

(2-Methylcycloprop-2-enyl)methyl (4-nitrophenyl) carbonate (3.3). Cyclopropene **3.1** (392 mg, 2.51 mmol) was dissolved in 10 mL THF. Anhydrous 18-crown-6 (729 mg, 2.76 mmol) and anhydrous cesium fluoride (400 mg, 2.63 mmol) were added, and the solution was stirred until **3.1** was fully consumed (2.5 h). The reaction was then diluted with CH₂Cl₂ (25

mL). Pyridine (1.2 mL, 15 mmol) was added, followed by 4-nitrophenyl chloroformate (1.01 g, 5.01 mmol), and the reaction was stirred overnight. The reaction mixture was then concentrated *in vacuo*, dissolved in Et₂O (30 mL), rinsed with concentrated NaHCO₃ (3 x 30 mL), and dried with MgSO₄. The crude product was filtered, then gently concentrated and purified by flash column chromatography (eluting with 5% Et₂O in petroleum ether) to afford carbonate **3.3** as a clear oil (459 mg, 73%): ¹H NMR (500 MHz, CDCl₃) δ 8.27 (m, 2H), 7.38 (m, 2H), 6.61 (s, 1H), 4.20 (dd, *J* = 10.9, 5.2 Hz, 1H), 4.13 (dd, *J* = 10.9, 5.5 Hz, 1H), 2.17 (d, *J* = 1.2 Hz, 3H), 1.78 (m, 1H); ¹³C NMR 125 MHz, CDCl₃) δ 155.8, 152.7, 145.3, 125.3, 121.9, 120.2, 101.7, 77.5, 16.7, 11.7; LRMS (ESI) calcd for C₁₂H₁₁O₅NNa [M+Na]⁺ 272.0535, found 272.0460.

General procedure for the synthesis of carbamate sugars

The hydrochloride salt of mannosamine (**3.4**), galactosamine (**3.5**), or glucosamine (**3.6**) (20.1 mg, 0.0932 mmol) was added to a solution of DMF (2 mL) and *N,N*-diisopropylethylamine (65 mL, 0.37 mmol) and heated to 60 °C. The solution was cooled to ambient temperature and treated with a solution of carbonate **3.3** (91.0 mg, 0.365 mmol) dissolved in 0.5 mL DMF. The solution quickly turned yellow, indicating the release of 4-nitrophenol. The reaction was stirred for 4-12 h. The solvent was removed *in vacuo* onto silica gel and was run through a plug of silica gel (flushed with 5% and eluted with 10% MeOH in CH₂Cl₂). The isolated sugar was dissolved in 1 mL pyridine and treated with acetic anhydride (0.5 mL, 4 mmol). The reactions were stirred overnight and concentrated *in vacuo*. The crude acetylated sugar was diluted with CH₂Cl₂ and rinsed with NaHSO₄ (3 x 10 mL) and washed with brine (10 mL). The product was purified by flash column chromatography

(eluting with 3:2 hexanes:ethyl acetate) or HPLC (eluting with 30–70% CH₃CN in H₂O over 20 min). The desired fractions were combined and dried to yield **Ac₄ManCCp**, **Ac₄GalCCp**, or **Ac₄GlcCCp**.

Ac₄ManCCp. Mixture of anomers isolated (16.1 mg, 0.0352, 38%) as a white solid: ¹H NMR (400 MHz, CDCl₃, 2:1 α:β) δ (α anomer) 6.58 (d, *J* = 4.8 Hz, 1H), 6.09 (s, 1H), 5.31 (dd, *J* = 10.2, 4.2 Hz, 1H), 5.20 (app t, *J* = 9.8 Hz, 1H), 5.02 (m, 1H), 4.34 (dd, *J* = 8.6, 2.9 Hz, 1H), 4.25 (dd, *J* = 12.2, 4.2 Hz, 1H), 4.02 (m, 1H), 3.95 (app t, *J* = 5.2 Hz, 2H), 2.17 (s, 3H), 2.14 (s, 3H), 2.10 (s, 3H), 2.05 (s, 3H), 2.02 (s, 3H), 1.65 (m, 1H); (β anomer) 6.58 (d, *J* = 4.8 Hz, 1H), 5.85 (s, 1H), 5.16 (app t, *J* = 9.7 Hz, 1H), 5.09 (d, *J* = 9.2 Hz, 1H), 5.02 (m, 1H), 4.47 (m, 1H), 4.25 (dd, *J* = 12.2, 4.2 Hz, 1H), 4.13-4.04 (m, 2H), 3.78 (ddd, *J* = 9.5, 4.8, 2.6 Hz, 1H), 2.14 (s, 3H), 2.12 (s, 3H), 2.10 (s, 3H), 2.05 (s, 3H), 2.03 (s, 3H), 1.65 (m, 1H); ¹³C NMR (125 MHz, CDCl₃, 298 K) δ 170.7, 170.6, 170.2, 170.2, 169.7, 169.7, 168.5, 168.2, 156.9, 156.3, 120.7, 120.5, 102.3, 102.2, 102.1, 92.0, 90.8, 73.4, 73.2, 73.2, 73.0, 71.6, 70.2, 69.2, 65.4, 65.3, 62.0, 61.9, 51.3, 51.1, 21.0, 20.9, 20.8, 20.8, 20.8, 20.8, 20.7, 20.7, 17.1, 17.1, 11.7, 11.7; ¹³C NMR (125 MHz, CDCl₃, 318 K) δ 170.4, 170.4, 169.9, 169.9, 169.4, 169.4, 168.3, 168.0, 156.2, 120.5, 120.5, 102.2, 102.1, 92.1, 90.9, 73.5, 73.2, 72.9, 71.5, 70.3, 69.2, 65.6, 65.6, 62.1, 62.0, 51.3, 51.3, 20.7, 20.7, 20.6, 20.6, 20.6, 20.6, 20.5, 20.5, 17.2, 17.1, 11.5, 11.5; HRMS (ESI) calcd for C₂₀H₂₇O₁₁NNa [M+Na]⁺ 480.1482, found 480.1460.

Ac₄GalCCp. Mixture of anomers isolated (14.3 mg, 0.0313 mmol, 17%) as a white solid: ¹H NMR (500 MHz, DMSO-*d*₆, 3:1 α:β) δ (α anomer) 7.53 (m, 1H), 6.86 (d, *J* = 9.0 Hz, 1H), 6.08 (dd, *J* = 5.1, 3.6 Hz, 1H), 5.41 (d, *J* = 2.3 Hz, 1H), 5.09 (dd, *J* = 11.7, 3.0 Hz, 1H), 4.34

(app t, $J = 6.2$ Hz, 1H), 4.15-3.97 (m, 3H), 3.92-3.74 (m, 2H), 2.16 (s, 3H), 2.14 (s, 3H), 2.11 (s, 3H), 2.00 (s, 3H), 1.95 (s, 3H), 1.53 (m, 1H); (β anomer) 7.23 (m, 1H), 6.86 (d, $J = 9.0$ Hz, 1H), 5.66 (d, $J = 8.7$ Hz, 1H), 5.29 (d, $J = 3.0$ Hz, 1H), 5.09 (dd, $J = 11.7, 3.0$ Hz, 1H), 4.17 (app t, $J = 6.1$ Hz, 1H), 4.15-3.97 (m, 3H), 3.92-3.74 (m, 2H), 2.14 (s, 3H), 2.11 (s, 3H), 2.07 (s, 3H), 2.01 (s, 3H), 1.94 (s, 3H), 1.53 (m, 1H); ^{13}C NMR (125 MHz, DMSO- d_6 , α anomer) δ 170.5, 170.4, 170.1, 169.7, 156.9, 120.5, 102.7, 90.7, 71.8, 68.7, 67.9, 67.1, 61.8, 48.7, 21.3, 21.0, 21.0, 20.9, 17.1, 11.8; HRMS (ESI) calcd for $\text{C}_{20}\text{H}_{27}\text{O}_{11}\text{NNa}$ $[\text{M}+\text{Na}]^+$ 480.1482, found 480.1466.

Ac₄GlcCCp. Single isomer isolated (57.9 mg, 0.127, 51%) as a white solid: ^1H NMR (500 MHz, DMSO- d_6 , α anomer only) δ 7.51 (d, $J = 8.6$ Hz, 1H), 6.86 (s, 1H), 6.00 (s, 1H), 5.17 (app t, $J = 10.2$ Hz, 1H), 5.01 (app t, $J = 9.8$, 1H) 4.19 (dd, $J = 12.4, 3.8$ Hz, 1H), 4.11 (ddd, $J = 10.3, 3.5, 2.2$ Hz, 1H), 4.01 (dd, $J = 12.0, 1.5$ Hz, 2H), 3.93-3.75 (m, 2H), 2.18 (s, 3H), 2.11 (s, 3H), 2.03 (s, 3H), 2.00 (s, 3H), 1.96 (s, 3H), 1.53 (m, 1H); ^{13}C NMR (125 MHz, DMSO- d_6) δ 170.5, 170.1, 169.7, 169.7, 156.9, 120.6, 102.6, 90.3, 71.8, 70.9, 69.5, 68.5, 61.8, 52.6, 21.3, 21.0, 20.9, 20.9, 17.1, 11.8; HRMS (ESI) calcd for $\text{C}_{20}\text{H}_{27}\text{O}_{11}\text{NNa}$ $[\text{M}+\text{Na}]^+$ 480.1482, found 480.1464.

Dibenzocyclooctyne-FLAG peptide conjugate (DBCO-FLAG). The peptide conjugate was prepared as previously described [35]. Briefly, DYKDDDDKC (20 mg, 0.018 mmol) was dissolved in 0.25 mL H_2O and added to a solution of DBCO-maleimide (Click Chemistry Tools; 5.0 mg, 0.012 mmol) in 0.2 mL DMF. The reaction was stirred overnight. The product was isolated via HPLC (eluting with 20–80% MeCN in H_2O over 20 min). The desired

fractions were combined and lyophilized to yield **DBCO-FLAG** (7.5 mg, 41%) as a white solid; LRMS (ESI) calcd for $C_{69}H_{88}N_{14}O_{25}S [M+2H]^{2+}$ 772.27, found 772.26.

References

1. Prescher, J. A., and Bertozzi, C. R. (2005) Chemistry in living systems, *Nat Chem Biol* 1, 13-21.
2. Sletten, E. M., and Bertozzi, C. R. (2009) Bioorthogonal chemistry: fishing for selectivity in a sea of functionality, *Angew Chem Int Edit* 48, 6974-6998.
3. Grammel, M., and Hang, H. C. (2013) Chemical reporters for biological discovery, *Nat Chem Biol* 9, 475-484.
4. Debets, M. F., van Hest, J. C., and Rutjes, F. P. (2013) Bioorthogonal labeling of biomolecules: new functional handles and ligation methods, *Org Biomol Chem* 11, 6439-6455.
5. Prescher, J. A., and Bertozzi, C. R. (2006) Chemical technologies for probing glycans, *Cell* 126, 851-854.
6. Liu, Y. C., Yen, H. Y., Chen, C. Y., Chen, C. H., Cheng, P. F., Juan, Y. H., Khoo, K. H., Yu, C. J., Yang, P. C., Hsu, T. L., and Wong, C. H. (2011) Sialylation and fucosylation of epidermal growth factor receptor suppress its dimerization and activation in lung cancer cells, *Proc Natl Acad Sci U S A* 108, 11332-11337.
7. Neef, A. B., and Luedtke, N. W. (2011) Dynamic metabolic labeling of DNA in vivo with arabinosyl nucleosides, *Proc Natl Acad Sci U S A* 108, 20404-20409.
8. Rabuka, D., Hubbard, S. C., Laughlin, S. T., Argade, S. P., and Bertozzi, C. R. (2006) A chemical reporter strategy to probe glycoprotein fucosylation, *J Am Chem Soc* 128, 12078-12079.
9. Yarema, K. J., Mahal, L. K., Bruehl, R. E., Rodriguez, E. C., and Bertozzi, C. R. (1998) Metabolic delivery of ketone groups to sialic acid residues. Application to cell surface glycoform engineering, *J Biol Chem* 273, 31168-31179.

10. Han, S., Collins, B. E., Bengtson, P., and Paulson, J. C. (2005) Homomultimeric complexes of CD22 in B cells revealed by protein-glycan cross-linking, *Nat Chem Biol* 1, 93-97.
11. Luchansky, S. J., Hang, H. C., Saxon, E., Grunwell, J. R., Yu, C., Dube, D. H., and Bertozzi, C. R. (2003) Constructing azide-labeled cell surfaces using polysaccharide biosynthetic pathways, *Methods Enzymol* 362, 249-272.
12. Oetke, C., Brossmer, R., Mantey, L. R., Hinderlich, S., Isecke, R., Reutter, W., Keppler, O. T., and Pawlita, M. (2002) Versatile biosynthetic engineering of sialic acid in living cells using synthetic sialic acid analogues, *J Biol Chem* 277, 6688-6695.
13. Rouhanifard, S. H., Nordstrom, L. U., Zheng, T., and Wu, P. (2013) Chemical probing of glycans in cells and organisms, *Chem Soc Rev* 42, 4284-4296.
14. van Berkel, S. S., van Eldijk, M. B., and van Hest, J. C. (2011) Staudinger ligation as a method for bioconjugation, *Angew Chem Int Ed* 50, 8806-8827.
15. Schilling, C. I., Jung, N., Biskup, M., Schepers, U., and Brase, S. (2011) Bioconjugation via azide-Staudinger ligation: an overview, *Chem Soc Rev* 40, 4840-4871.
16. Debets, M. F., van der Doelen, C. W., Rutjes, F. P., and van Delft, F. L. (2010) Azide: a unique dipole for metal-free bioorthogonal ligations, *ChemBiochem* 11, 1168-1184.
17. Patterson, D. M., Nazarova, L. A., Xie, B., Kamber, D. N., and Prescher, J. A. (2012) Functionalized cyclopropenes as bioorthogonal chemical reporters, *J Am Chem Soc* 134, 18638-18643.
18. Yang, J., Seckute, J., Cole, C. M., and Devaraj, N. K. (2012) Live-cell imaging of cyclopropene tags with fluorogenic tetrazine cycloadditions, *Angew Chem Int Ed* 51, 7476-7479.
19. Cole, C. M., Yang, J., Seckute, J., and Devaraj, N. K. (2013) Fluorescent live-cell imaging of metabolically incorporated unnatural cyclopropene-mannosamine derivatives, *ChemBioChem* 14, 205-208.

20. Yu, Z., Pan, Y., Wang, Z., Wang, J., and Lin, Q. (2012) Genetically encoded cyclopropene directs rapid, photoclick-chemistry-mediated protein labeling in mammalian cells, *Angew Chem Int Ed* 51, 10600-10604.
21. Kamber, D. N., Nazarova, L. A., Liang, Y., Lopez, S. A., Patterson, D. M., Shih, H. W., Houk, K. N., and Prescher, J. A. (2013) Isomeric cyclopropenes exhibit unique bioorthogonal reactivities, *J Am Chem Soc* 135, 13680-13683.
22. Wainman, Y. A., Neves, A. A., Stairs, S., Stockmann, H., Ireland-Zecchini, H., Brindle, K. M., and Leeper, F. J. (2013) Dual-sugar imaging using isonitrile and azido-based click chemistries, *Org Biomol Chem* 11, 7297-7300.
23. Niederwieser, A., Spate, A. K., Nguyen, L. D., Jungst, C., Reutter, W., and Wittmann, V. (2013) Two-color glycan labeling of live cells by a combination of Diels-Alder and click chemistry, *Angew Chem Int Ed* 52, 4265-4268.
24. Bond, M. R., Zhang, H. C., Kim, J., Yu, S. H., Yang, F., Patrie, S. M., and Kohler, J. J. (2011) Metabolism of diazirine-modified *N*-acetylmannosamine analogues to photo-cross-linking sialosides, *Bioconjugate Chem* 22, 1811-1823.
25. Jacobs, C. L., Goon, S., Yarema, K. J., Hinderlich, S., Hang, H. C., Chai, D. H., and Bertozzi, C. R. (2001) Substrate specificity of the sialic acid biosynthetic pathway, *Biochemistry* 40, 12864-12874.
26. Spate, A. K., Busskamp, H., Niederwieser, A., Schart, V. F., Marx, A., and Wittmann, V. (2013) Rapid labeling of metabolically engineered cell-surface glycoconjugates with a carbamate-linked cyclopropene reporter, *Bioconjugate Chem* 25, 147-154.
27. Bateman, L. A., Zaro, B. W., Chuh, K. N., and Pratt, M. R. (2013) *N*-Propargyloxycarbamate monosaccharides as metabolic chemical reporters of carbohydrate salvage pathways and protein glycosylation, *Chem Commun (Camb)* 49, 4328-4330.
28. Sarkar, A. K., Fritz, T. A., Taylor, W. H., and Esko, J. D. (1995) Disaccharide uptake and priming in animal cells: inhibition of sialyl Lewis X by acetylated Gal β 1-4GlcNAc β -O-naphthalenemethanol, *Proc Natl Acad Sci U S A* 92, 3323-3327.
29. Saxon, E., and Bertozzi, C. R. (2000) Cell surface engineering by a modified Staudinger reaction, *Science* 287, 2007-2010.

30. Boyce, M., Carrico, I. S., Ganguli, A. S., Yu, S. H., Hangauer, M. J., Hubbard, S. C., Kohler, J. J., and Bertozzi, C. R. (2011) Metabolic cross-talk allows labeling of O-linked beta-N-acetylglucosamine-modified proteins via the *N*-acetylgalactosamine salvage pathway, *Proc Natl Acad Sci U S A* 108, 3141-3146.
31. Vocadlo, D. J., Hang, H. C., Kim, E. J., Hanover, J. A., and Bertozzi, C. R. (2003) A chemical approach for identifying O-GlcNAc-modified proteins in cells, *Proc Natl Acad Sci U S A* 100, 9116-9121.
32. Zaro, B. W., Yang, Y. Y., Hang, H. C., and Pratt, M. R. (2011) Chemical reporters for fluorescent detection and identification of O-GlcNAc-modified proteins reveal glycosylation of the ubiquitin ligase NEDD4-1, *Proc Natl Acad Sci U S A* 108, 8146-8151.
33. Charron, G., Zhang, M. M., Yount, J. S., Wilson, J., Raghavan, A. S., Shamir, E., and Hang, H. C. (2009) Robust fluorescent detection of protein fatty-acylation with chemical reporters, *J Am Chem Soc* 131, 4967-4975.
34. Wilbur, D. S., Hamlin, D. K., Vessella, R. L., Stray, J. E., Buhler, K. R., Stayton, P. S., Klumb, L. A., Pathare, P. M., and Weerawarna, S. A. (1996) Antibody fragments in tumor pretargeting. Evaluation of biotinylated Fab' colocalization with recombinant streptavidin and avidin, *Bioconjugate Chem* 7, 689-702.
35. Chang, P. V., Prescher, J. A., Sletten, E. M., Baskin, J. M., Miller, I. A., Agard, N. J., Lo, A., and Bertozzi, C. R. (2010) Copper-free click chemistry in living animals, *Proc Natl Acad Sci U S A* 107, 1821-1826.

CHAPTER 4: Orthogonal bioorthogonal chemistries

4.1 Introduction

Bioorthogonal reactions provide a versatile platform to probe and manipulate biomolecules. These reactions employ unique functional groups that are relatively inert to life's diverse chemical functionality, but react expediently with one another in complex environments. Bioorthogonal chemistries have been used extensively to image proteins and other biomolecules in living systems [1], retrieve active enzymes from tissues [2], identify drug targets *in vivo* [3], and even build designer antibody conjugates [4]. Additional creative applications are anticipated as new reactions are developed.

While the bioorthogonal toolbox is rapidly expanding, notable voids have emerged. For example, many of the most well known bioorthogonal reagents—including organic azides and strained reagents—are incompatible with one another and cannot be used in tandem to probe biological systems. Thus, it has been historically difficult to image multiple biomolecules in live cells and craft multi-functional proteins using distinct bioorthogonal chemistries. Multi-component studies require not only reliable transformations, but also *combinations* of transformations that are compatible with one another –i.e., *mutually orthogonal* bioorthogonal chemistries (Figure 4-1).

Identifying “orthogonal bioorthogonal” transformations is a formidable challenge. The barrier to developing a single biocompatible reaction remains high: the reactants must remain inert to biological functionality while maintaining robust reactivity with their complementary reagent [5]. Applications *in vivo* typically impose further restrictions on reagent size, reactivity rates, and product stability [6]. Mutually orthogonal reactions must meet these same demands and also remain inert to each other. This chapter highlights recent efforts to identify such

4.2 Mutually orthogonal bioorthogonal reactions

4.2a Unique reaction mechanisms

One straightforward method to identify compatible reactions is to search for transformations with unique mechanisms. Two of the earliest reported bioorthogonal reactions—keto/aldehyde condensations and the Staudinger ligation—are orthogonal in this regard [7]. Keto/aldehyde condensations are polar reactions involving a hard electrophile (ketone or aldehyde) and hard nucleophile (hydrazide or aminoxy group). By contrast, the Staudinger ligation exploits a soft electrophile (azide) and a soft nucleophile (phosphine) to form an amide linkage. These mechanistic features mitigate cross-reactivities among the reagents and enable the ligations to be performed in concert in biological settings [7]. Keto/aldehyde condensations can also be performed in tandem with other azide-specific chemistries, including the venerable copper-catalyzed azide-alkyne cycloaddition (CuAAC). CuAAC is among the most rapid ($10^5 \text{ M}^{-1} \text{ s}^{-1}$ per mole of catalyst) and most accessible bioorthogonal transformations [8], making it attractive for numerous applications. Distefano and coworkers recently utilized CuAAC in combination with the oxime ligation to craft bifunctional proteins for imaging and therapeutic applications [9]. These researchers used farnesyl transferase to append alkyne- and aldehyde-modified farnesyl groups to proteins bearing a C-terminal CaaX recognition sequence. The alkyne and aldehyde motifs were subsequently modified with a variety of imaging and targeting agents via simultaneous bioorthogonal ligation.

Another class of azide-specific ligations - strain-promoted azide-alkyne cycloadditions (SPAAC) - is also compatible with ketone/aldehyde condensations. SPAAC reactions exploit strained cycloalkynes; these molecules react with organic azides under mild conditions (and in the absence of copper) in a variety of biological environments. SPAAC has been used

extensively in combination with keto/aldehyde ligations to assemble defined antibody conjugates (Figure 4-2A and B) [10-12]. In one recent example, Schultz and coworkers exploited these reactions to assemble bispecific antigen-binding fragments (biFabs). BiFabs are capable of binding two distinct targets and can control immune cell recruitment to cancer cells [11]. In this study, antibody fragments targeting either human C-type lectin-like molecule-1 (CCL1) or CD3 were modified with keto groups installed via non-canonical amino acid (ncAA) mutagenesis. The keto groups were then reacted with aminoxy linkers bearing an azide or strained cyclooctyne. SPAAC ligation between the two fragments provided the desired biFab. This conjugate exhibited potent antitumor activity in mice via T cell recruitment (via CD3 binding) to cancer cell grafts (via CCL1 binding). BiFabs and other protein conjugates have numerous biomedical applications, and further developments in bifunctional synthesis are expected with improved ligation chemistries [13-15].

Strained *alkenes*, similar to their alkyne counterparts, are also widely used in bioorthogonal reaction development. Recent examples include *trans*-cyclooctene (TCO), norbornene, and cyclopropene [16]. These motifs react efficiently with electron-poor dienes (e.g., 1,2,4,5-tetrazines) via strain-promoted inverse-electron-demand Diels-Alder cycloaddition (SPIEDAC) [17]. Importantly, most strained alkenes and tetrazines are unreactive with organic azides and terminal alkynes; thus, SPIEDAC ligations can often be used in tandem with CuAAC (Figure 4-2C) [18-20]. The TCO-tetrazine ligation and CuAAC are especially well suited for dual and quantitative protein labeling owing to their fast rates. The Chin group recently capitalized on these features to append FRET fluorophores to calmodulin (Figure 4-2D) [18]. Alkynyl and cyclopropenyl ncAA's were site-specifically into the protein and subsequently

tagged with azide and tetrazine fluorophores simultaneously. Quantitative, dual labeling of calmodulin was achieved in only 30 min.

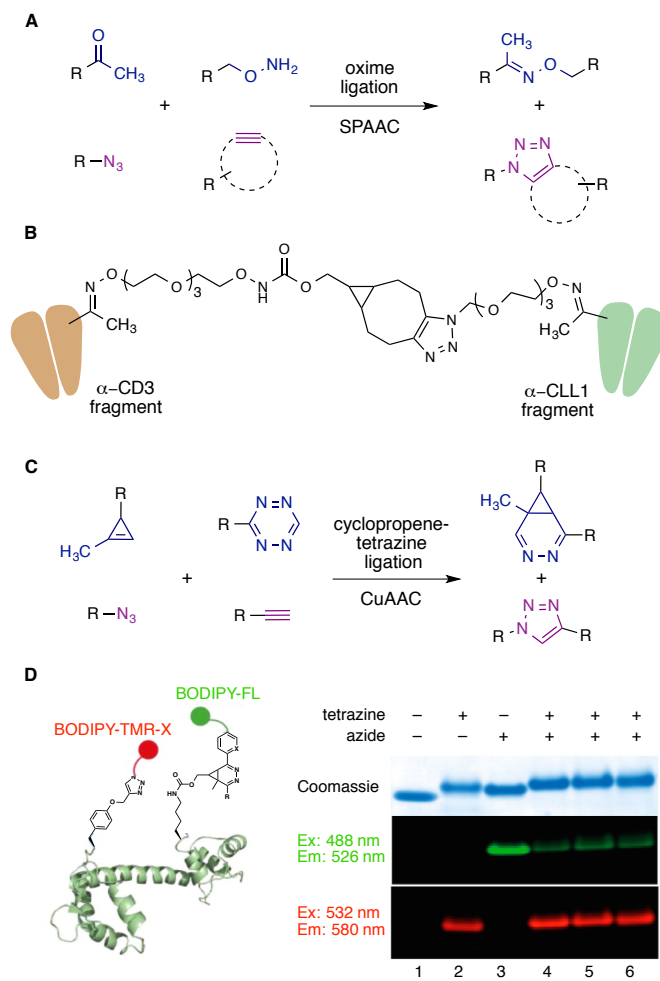


Figure 4-2. Orthogonal bioorthogonal ligations with distinct reaction mechanisms. (A) Keto/aldehyde condensations and strain-promoted azide-alkyne cycloadditions (SPAAC) can be used simultaneously. (B) Keto-functionalized Fabs (α CLL1 and α CD3) were modified via oxime ligation to install azide or bicyclononyne linkers, respectively. These modified Fabs were mixed, to form a covalently linked bispecific Fab via SPAAC. (Reprinted in part with permission from Ref [11]. Copyright 2014 Wiley) (C) The cyclopropene-tetrazine ligation is mutually orthogonal to CuAAC. (D) Alkynyl and cyclopropenyl ncAAs were installed in calmodulin. These residues were covalently targeted with matched fluorophores (via CuAAC and SPIEDAC) for FRET studies. Efficient labeling was observed when the reactions were performed sequentially (with or without purification, lanes 4 and 5, respectively) or simultaneously (lane 6). Reprinted in part with permission from Ref [18]. Copyright 2014 ACS Publications

4.2b Tuning reactions for orthogonality

While strained-promoted cycloadditions are ubiquitous in chemical biology, many of the reagents cross-react with one another. For example, several tetrazines react robustly with strained alkynes, precluding many tandem applications of SPIEDAC and SPAAC [21, 22]. This is detrimental for many live cell imaging applications, where the two reaction classes have traditionally excelled. Fortunately, most SPAAC and SPIEDAC reagents can be “tuned” to access desired reactivities. For example, tetrazines can be outfitted with electron-withdrawing or donating groups to modulate reactivity [23]. Bulky appendages to the tetrazine core can similarly influence reactivity [24]. Cyclooctyne reactivities can also be tuned via steric or electronic modification [25, 26]. For example, bicyclononyne reacts readily with both azides and tetrazines [21, 22, 27]. By contrast, dibenzylcyclooctyne (DBCO) and other bulky cycloalkynes are reactive with azides, but inert to di-substituted tetrazines due to predicted steric clashes (Figure 4-3D) [24]. This sterically-driven orthogonality has been exploited by many groups for biological applications [27-36]. In one example, the Weissleder group used DBCO and a bis-alkyl tetrazine in tandem to label multiple cell lines with visual probes via SPAAC and SPIEDAC [28].

Cycloalkynes, while suitable for some dual labeling applications, are relatively large in size and can perturb native biomolecule function. Lemke and coworkers recently attempted to study viral particle assembly, where small tags are necessary to preserve critical protein interactions. Toward this end, the group developed a smaller, “minimal” cyclooctyne scaffold (SCO) that reacts efficiently with mono-substituted tetrazines and can be used in combination with some TCO ligations [27]. TCO reacts readily with nearly all tetrazines (Figure 4-3C), but SCO remains inert to di-substituted tetrazines. This is likely due to steric clashes between the

tetrazine substituents and SCO's propargylic linker. The researchers exploited this differential by labeling viral proteins with TCO, followed by SCO, in a pulse-chase type experiment. The motifs were ultimately visualized via reaction with a di-substituted tetrazine (to tag TCO), followed by a mono-substituted tetrazine (to label SCO). These orthogonal reactions enabled the dynamics of virus-like protein assemblies to be examined via super-resolution microscopy.

Strained alkenes can also be tuned to elicit specific reactivities. While TCO exhibits remarkably fast reaction rates with tetrazines in SPIEDAC ($>10^5 \text{ M}^{-1}\text{s}^{-1}$), its large size and modest stability can be limiting in some applications [37]. TCO can also react with organic azides, making certain applications with these two popular reagents inaccessible [28]. To address some of these limitations, our group turned to a smaller strained alkene for bioorthogonal reaction development: cyclopropene. The small size of the cyclopropene has proven useful for metabolic targeting of biomolecules *in vitro* and *in vivo* [29-31, 33, 38, 39]. Additionally, cyclopropene is completely unreactive to azides and alkynes under ambient conditions, and thus orthogonal to SPAAC reagents (Figure 4-3A). We capitalized on this selective reactivity by targeting unique glycans with cyclopropene- and azide-bearing sialic acid derivatives. The biomolecules were ultimately visualized with DBCO and bis-aryl tetrazine, simultaneously, on live cells (Figure 4-3B) [29, 30].

Cyclopropene itself offers unique opportunities for orthogonal bioorthogonal reaction development. The motif can be tuned both sterically and electronically to access collections of mutually orthogonal transformations. In one example, we collaborated with the Houk lab to design a cyclopropene that remains inert to tetrazines, but exhibits rapid reactivity with 1,3-dipoles [40]. This cyclopropene differs from others by the position of a single methyl group: tetrazine-reactive cyclopropenes harbor a single substituent at C3. Installing a second methyl

group at this position thwarts cyclopropene-tetrazine reactivity by preventing effective orbital overlap between the diene and dienophile (Figure 4-4). While recalcitrant to tetrazine reactions, 3,3-disubstituted cyclopropenes, undergo rapid cycloadditions with nitrile imines [41, 42]. We exploited this reaction differential to label proteins bearing both 1,3- and 3,3-cyclopropenes [40].

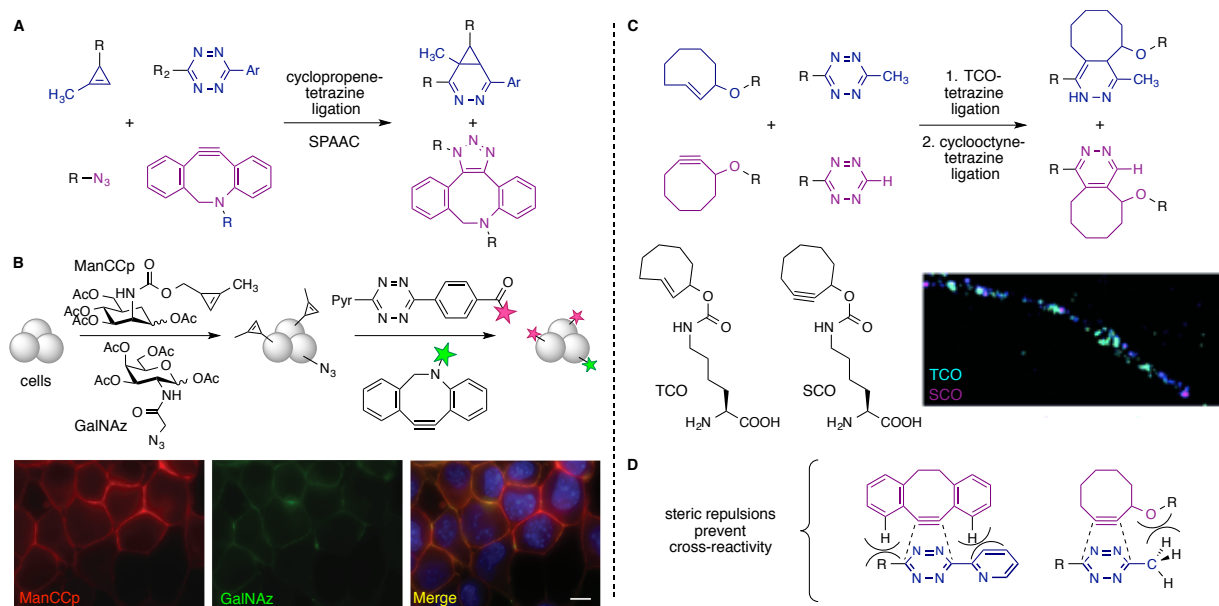


Figure 4-3. Tetrazines and cyclooctynes can be tuned to generate mutually orthogonal reaction pairs. (A) Cyclopropene-tetrazine and azide-DBCO cycloadditions can be performed simultaneously. (B) Orthogonal reactions were used to visualize distinct classes of glycoconjugates. Cells were incubated with a cyclopropenyl-ManNAc analog (ManCCp), an azido-GalNAc analog (GalNAz), or both sugars. The distinct biomolecules targeted with these probes were subsequently visualized via simultaneous treatment with tetrazine and DBCO probes. Scale bar: 10 μm. [30] – Reproduced by permission of the Royal Society of Chemistry. (C) Sequential ligations can be used to detect *trans*-cyclooctene (TCO) and a cyclooctyne variant (SCO). TCO reacts with both mono- and di-substituted tetrazines, while SCO reacts only with mono-substituted tetrazines. In a pulse-chase experiment, TCO- and SCO-bearing amino acids were incorporated into viral hemagglutinin. The protein conjugates were co-expressed with matrix protein 1 in mammalian cells, and ultimately visualized via reaction with a fluorescent di-substituted tetrazine (cyan, to tag TCO), followed by a mono-substituted tetrazine probe (magenta, to tag SCO). (D) Steric clashes preclude reactions between di-substituted tetrazines and cyclooctynes with propargylic substituents. Reprinted in part with permission from Ref [27]. Copyright 2014 Wiley.

4.3 Orthogonal reactivity via controlled reagent activation

Several bioorthogonal reactions rely on strained or otherwise highly reactive molecules that are often incompatible with one another. In such cases, masking one reagent in an inactive form and liberating it on demand can render the motif orthogonal. Thus, after an initial ligation proceeds to completion, liberation of the masked functional group provides a second competent bioorthogonal reagent for reaction. Such ‘activation’ methods exploited in recent years include metal-catalysis, photolysis, and chemical transformation. Examples are provided below.

4.3a Metal-catalyzed reactions

The most well-known bioorthogonal reaction, CuAAC, serves as an example of a metal-activated reaction. In the absence of copper (I), terminal alkynes and azides do not react under ambient conditions. When copper ions are present, the dipolar cycloaddition ensues [43]. The activatable nature of this reaction enables azides and alkynes to be used concurrently—targeting different species—and covalently detected via control over copper addition. For example, azide-labeled biomolecules can be reacted via Staudinger ligation or SPAAC; the alkyne can be subsequently detected via CuAAC [44-47]. An early demonstration of SPAAC/CuAAC compatibility was reported by Wolfbeis and coworkers to craft protease sensors. This group designed an MMP II substrate bearing cyclooctyne or terminal alkyne handles. The peptide was appended to an azido-labeled nanoparticle (via SPAAC) and then modified with an azido-fluorophore (via CuAAC). This sensor was used to report on protease activity [47].

Note that reverse sequential labeling approach – reacting the alkyne first via CuAAC, followed by SPAAC or Staudinger ligation to target azides – is problematic. Azides will cross-react with alkynes during the initial CuAAC reaction. This side-reactivity can be circumvented

using alternative 1,3-dipoles in place of azides. The Raines group reported an elegant example of this approach with diazo units [48]. Diazos are small, remarkably bioinert functional groups that do not react with terminal alkynes under CuAAC conditions. These groups can be efficiently ligated with strained alkynes, though. This unique reactivity enabled the researchers to perform sequential CuAAC and strain-promoted diazo-alkyne cycloadditions to detect alkynyl and diazo-labeled glycans. Excitingly, the labeling reactions could be performed in either order with no cross-reactivities observed. Sequential azide-alkyne cycloadditions are also possible using unique alkyne protecting groups [49, 50] or asymmetric azides with differential reactivity [51]. Further advances in metal-activated orthogonal bioorthogonal chemistries are anticipated with several recent reports on transition metal-mediated reactions that are biocompatible [52, 53]. In particular, advances in bioorthogonal palladium-catalyzed reactions have enabled cross-couplings on proteins *in vitro* and in live cells [54-58].

4.3b Light-activated reactions

Similar to metal catalysis, light can be used to liberate bioorthogonal functional groups and thus control reagent activation for dual labeling experiments. In one example, Popik and colleagues utilized cyclopropenone as a photolabile protecting group for cyclooctyne in constructing protein-nanoparticle conjugates [59]. The researchers synthesized a bifunctional linker comprising azadibenzocyclooctyne (ADIBO) and a masked dibenzocyclooctyne (photo-DIBO). ADIBO was reacted with azide-functionalized nanoparticles to append the linker to the surface. The nanoparticles were subsequently photolyzed to unveil a cyclooctyne for reaction with azide-modified bovine serum albumin (as a model protein). Similarly, the Lin group pioneered the use of tetrazoles as photolabile masks for nitrile imines. Nitrile imines are 1,3-

dipoles that react readily with 3,3-disubstituted cyclopropenes and other alkenes [60]. However, these dipoles must be liberated on demand owing to their aqueous instabilities and short lifetimes. Our group employed tetrazole photolysis and nitrile imine generation for cyclopropene detection discussed above (Figure 4-4) [40]. While they have differential tetrazine reactivity (vide supra), both 1,3- and 3,3-disubstituted cyclopropenes undergo rapid dipolar cycloaddition with nitrile imines. Thus, dual labeling of proteins with 1,3- and 3,3-disubstituted cyclopropenes requires that the tetrazine ligation be performed first to target the 1,3-disubstituted variants, followed by nitrile imine liberation via tetrazole photolysis to tag proteins bearing 3,3-disubstituted cyclopropenes. Ongoing work to develop new photoactivatable reactions and masking groups responsive to unique wavelengths of light [61, 62] will offer new paths to mutually orthogonal reactions.

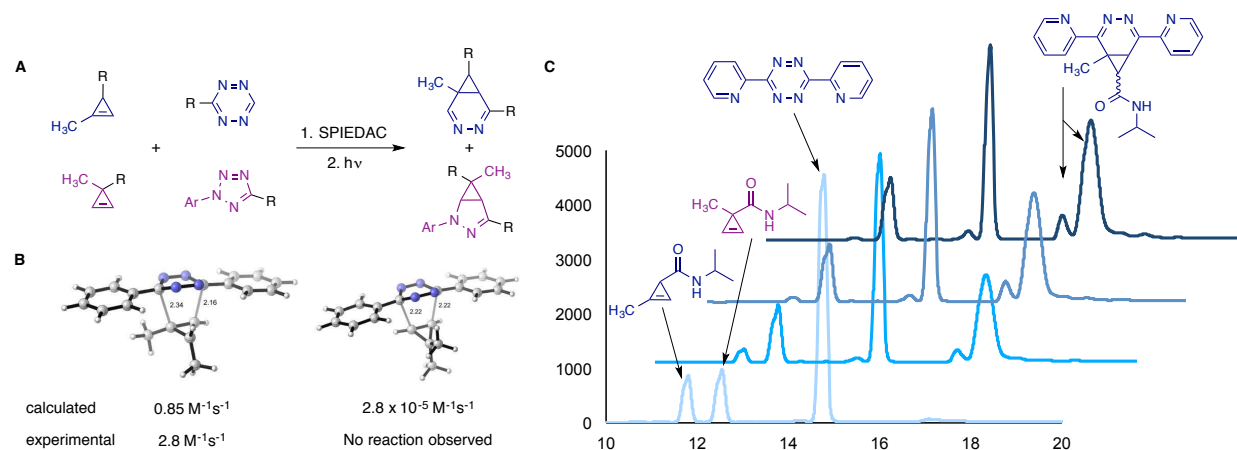


Figure 4-4. Isomeric cyclopropenes exhibit unique bioorthogonal reactivities. (A) 1,3-Disubstituted cyclopropenes react readily with tetrazines. 3,3-Disubstituted cyclopropenes, by contrast, do not react with tetrazines, but react efficiently with nitrile imines (available from tetrazole photolysis). These differential reactivities can be exploited for dual labeling applications. (B) Predicted transition state geometries for the tetrazine-cyclopropene ligations account for the observed reactivity differences. The C3 methyl substituent (in the 3,3-disubstituted cyclopropene) blocks the approach of tetrazine. In the 1,3-disubstituted regioisomer, this position is occupied by a smaller H atom. (C) Both 1,3- and 3,3-disubstituted cyclopropene (5 mM in 15% MeCN/PBS) were treated with dipyrityl tetrazine (10 mM) and monitored by HPLC. Dipyrityl tetrazine reacted exclusively with the 1,3-disubstituted cyclopropene. Reprinted in part with permission from Ref [40]. Copyright 2014 ACS Publications

4.3c Chemical activation

Controlled reactivity can also be achieved through *in situ* formation of bioorthogonal functional groups. Boons, Pezacki and others have established that nitrones and nitrile oxides react rapidly with strained alkynes in 1,3-dipolar cycloadditions [63-67]. Both nitrones and nitrile oxides have limited stability under biological conditions, though, and they cross-react with multiple strained reagents. Fortunately, both can be formed *in situ* from aldehydes and oximes, respectively, under relatively mild conditions. Using these conditions, Boons and coworkers were able to assemble a bifunctional glycan dendrimer utilizing a bifunctional azide-oxime linker [63]. The azide reacts selectively with DIBO modified with biotin or a fluorophore. Subsequently, the oxime group was activated through mild oxidation with hypervalent iodide, to

a nitrile oxide, which reacts rapidly with a second DIBO reagent modified with a glycan dendrimer. The on-demand generation of nitrile oxides and nitrones enables sequential strain-promoted cycloadditions.

4.4 Identifying new mutually orthogonal reactions

A comprehensive understanding of biological systems requires studying many biomolecules and pathways simultaneously. While impressive strides have been made in developing mutually orthogonal reactions for this purpose, additional groups of compatible reagents are necessary. To date, only one example using three bioorthogonal reactions on a single biological system has been described [20]. Analyses of multiple enzyme activities and signaling pathways require more mutually orthogonal bioorthogonal ligations. Fortunately, many recently reported bioorthogonal reagents and reactions are potentially useful for multi-component applications. These include those based on sydnone [68-70], quinone methide [71, 72], isonitrile [36, 73], acyltrifluoroborate [74], azetidine [75], and 1,2-quinones [76]. Additionally, several new metal-catalyzed bioorthogonal reactions based on palladium, ruthenium, and nickel may offer compatible reactivity based on selective metal activation [53].

Identifying reaction combinations for mutual orthogonality has typically been through empirical testing of established bioorthogonal reactions or by developing clever activating/uncaging strategies. Such efforts could be greatly accelerated using computational modeling to compare established bioorthogonal reagents for reactivity. Computation is extensively used for identifying and improving bioorthogonal reactions and is quickly becoming invaluable for developing compatible reactions. In a recent paper, the Houk group predicted an orthogonal pair of di-substituted tetrazines and 1,3-cyclopropene with azide and

tetramethylthiocycloheptyne [32]. Our group independently confirmed a similar orthogonal pair and applied them to live cell glycan imaging (described in chapters 2 and 3).

In an effort to identify new orthogonal pairs, we collaborated with the Houk group to develop a computational model capable of predicting reactivity between known bioorthogonal reagents. They identified potential reaction pairs using their distortion-interaction model to predict transition state energies. These transition state energies can be used to calculate a relative rate constant (Figure 4-5). Our group then synthesized several of these reagents to experimentally verify predicted orthogonal pairs. This led to identification of potential mutually orthogonal pairs, including a new pair based on cyclooctyne-nitrone and norbornene-tetrazine ligations. To date, orthogonality between cyclooctyne and tetrazine reactions has been driven through steric repulsions that prevent orbital overlap between the alkyne and tetrazine π -electrons (Figure 4-3D) [24, 32]. The Houk group predicted that an electron-deficient cyclooctyne, difluorocyclooctyne (DIFO), would be unreactive towards electron-poor tetrazines, likely resulting from the electronic “mismatch” between the reagents.

A popular cyclooctyne for use in living systems, DIFO was predicted to react readily with two commonly used nitrone scaffolds, a cyclic nitrone (cyc-nitrone) and glyoxylate-derived nitrone (gly-nitrone). Nitrones, as noted above, are 1,3-dipoles that react with cyclooctynes and typically display faster kinetics than azides. Both were experimentally determined to have rate constants of $\sim 3 \text{ M}^{-1} \text{ s}^{-1}$ with DIFO via ^1H NMR (Figure 4-5, 4-6A, and 4-6B). While this closely matched the computationally predicted rate constant for the DIFO–gly-nitrone, the DIFO–cyc-nitrone rate constant was smaller by roughly two orders of magnitude. The Houk group is investigating the source of this discrepancy.

Importantly, both nitrones are largely unreactive towards norbornene, which is a commonly used strained alkene in SPIEDAC with tetrazines. Expectedly, norbornene was shown to react readily with dipyrindyl tetrazine ($k_2 = 3.3 \text{ M}^{-1} \text{ s}^{-1}$). This was slightly larger than the predicted rate constant of $0.1 \text{ M}^{-1} \text{ s}^{-1}$. Finally, DIFO was tested for reactivity with tetrazine. Interestingly, the expected rate constant between DIFO and mono-substituted tetrazines is $1 \text{ M}^{-1} \text{ s}^{-1}$, but only $10^{-4} \text{ M}^{-1} \text{ s}^{-1}$ with di-substituted tetrazines (Figure 4-5, 4-6C and 4-6D). This suggests the differential might also be sterically driven in addition to the assumption that DIFO would be electronically “mismatched” with tetrazine in an IED-DA cycloaddition. The experimental data matched the rate predictions very closely in both cases, verifying the computational analysis.

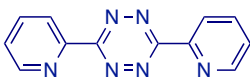
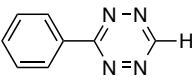
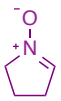
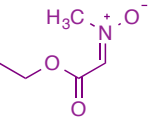
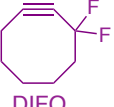

		 dipyrindyl tetrazine	 phenyl tetrazine	 cyc-nitron	 gly-nitron
 DIFO	calc	10^{-4}	1	10^2	1
	exp	$(3.7 \pm 0.5) \times 10^{-4}$	0.49 ± 0.03	3.0 ± 0.3	2.9 ± 0.9
 norbornene	calc	10^{-1}	10^{-1}	10^{-5}	10^{-4}
	exp	3.3 ± 0.3	not determined	$(1.2 \pm 0.7) \times 10^{-7}$	no reaction*

Figure 4-5. Difluorinated cyclooctyne and norbornene react preferentially with nitrones and di-substituted tetrazines, respectively. M06-2X/6-311+G(d,p)//6-31G(d)-computed relative rate constants were obtained by the Houk group and rate constants were determined experimentally by ^1H NMR in CD_3CN . All rate constants are reported in $\text{M}^{-1} \text{ s}^{-1}$. Standard deviation is reported for 2–3 experiments. *No reaction seen over ~ 2 days.

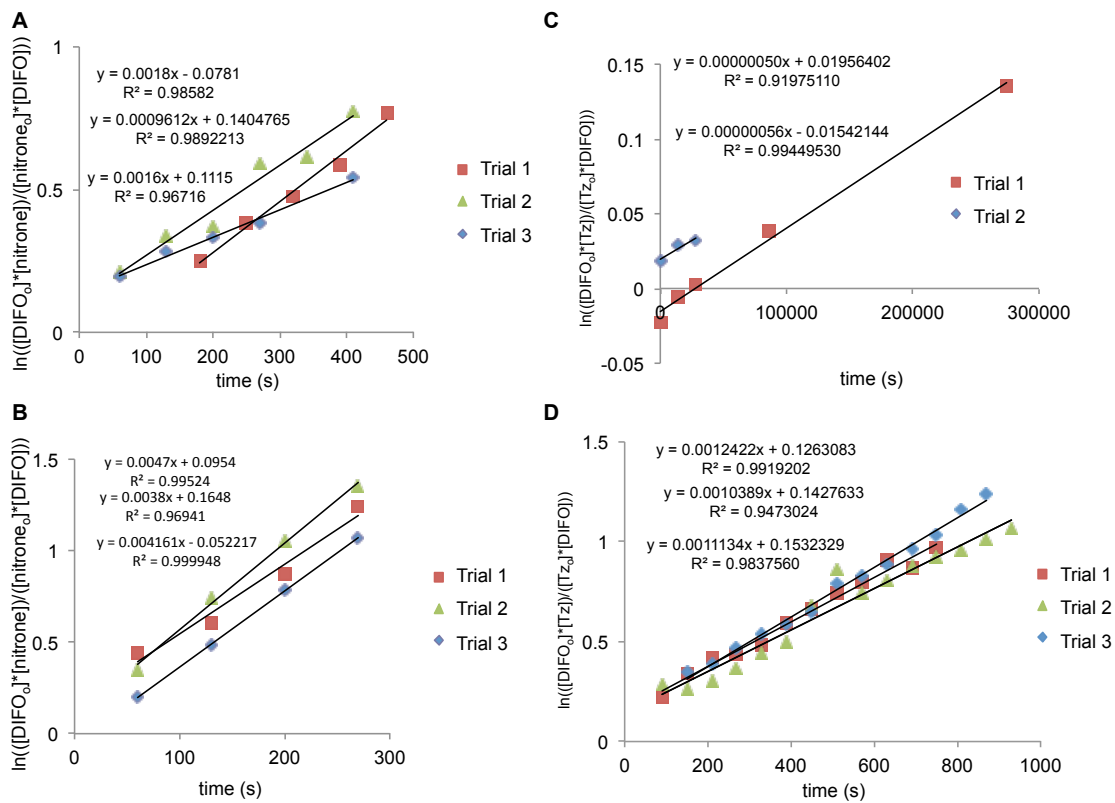
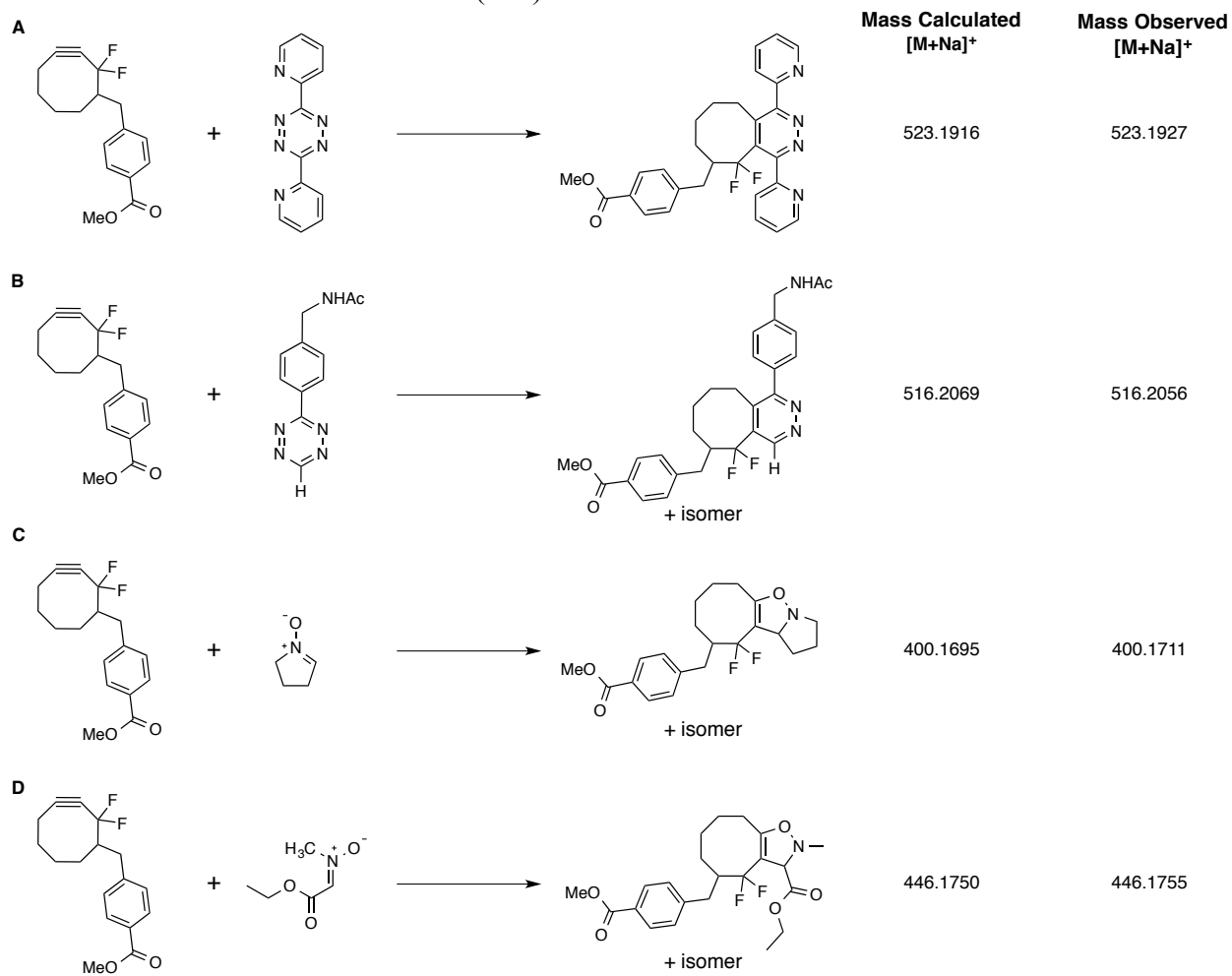


Figure 4-6. Plots used to calculate second-order rate constants of the reaction between DIFO and (A) gly-nitron, (B) cyc-nitron, (C) dipyridyl tetrazine, and (D) phenyl tetrazine in CD_3CN .

Scheme 4-1. Reactions between DIFO and (A) gly-nitrone, (B) cyc-nitrone, (C) dipyridyl tetrazine, and (D) phenyl tetrazine in CD₃CN. Structures of adducts are shown along with calculated and observed HRMS data (ESI).



4.5 Conclusions

Finding the right bioorthogonal chemistry for a given task has become increasingly easier as the bioorthogonal toolbox grows. However, cross-reactivity between reagents of many of the most popular chemistries has limited their utility for multi-component applications. Imaging multiple biomolecules and forming complex biomolecular assemblies, for example, will require identifying compatible combinations of these chemistries. Recently, several orthogonal bioorthogonal reactions have been developed through mechanistic insight, synthetic tuning and caged reagents. Moving forward, new and better mutually orthogonal bioorthogonal reactions are necessary as some of the approaches outlined here suffer from slow kinetics, multiple steps, or poor specificity. A combination of empirical and computational methods, as well as the continued discovery of novel bioorthogonal reactions, will aid in the hunt for mutually orthogonal reactions.

We successfully identified a novel mutually orthogonal bioorthogonal pair in DIFO-nitrone and norbornene-diaryl tetrazine. The Houk group is continuing to refine their model as we provide additional experimental data to guide their calculations. This should prove to be a useful tool to evaluate the expanding bioorthogonal reaction toolkit for new mutually orthogonal pairs.

4.6 Materials and methods

4.6a Rate studies [77]

UV-Vis method

The reactions between cyclopropenes and dipyriddy tetrazine were conducted in 96-well plates and monitored by the change in tetrazine absorbance at 536 nm. All runs were conducted in triplicate under pseudo-first order conditions and repeated at least two times. For each measurement, 150 μ L of a 0.2 mM tetrazine solution (in 15% DMSO/PBS) was added to a well containing 150 μ L of cyclopropene solution (2-10 mM in 15% DMSO/PBS). The cyclopropene concentration at the start of each reaction ranged from 1.0-5.0 mM, while the tetrazine concentration was held at 0.1 mM. Absorbance values were recorded every 5 min over a 90 min interval or every 4 seconds over a 30 min interval for faster reactions (using a BioTek Epoch plate reader).

¹H-NMR method

All DIFO reactions were monitored by ¹H-NMR spectroscopy. Each reagent was dissolved in CD₃CN at 10 mM and combined in a 1:1 ratio immediately prior to the first acquisition (~5 mM final concentrations of each reagent). The reaction of DIFO with nitrones and phenyl tetrazine was monitored continuously with an acquisition every minute for 15 min. The reaction between DIFO and dipyriddy tetrazine was monitored over 24 or 48 h with acquisition times every few hours. An internal standard (1,3-benzodioxole) was used to determine peak integration values and, ultimately, the concentrations of relevant species. Second-order rate plots were made by plotting $\ln\left(\frac{[A_0][B]}{[B_0][A]}\right)$ versus time. The slope was converted to a second-order rate

constant using the following equation: $k = |\text{slope}/([B_0] - A_0)|$. Adducts were confirmed by HRMS (ESI).

4.6b HPLC analysis

The 1,3- and 3,3-disubstituted cyclopropenes (5 mM in 15% MeCN/PBS) were treated with commercially available dipyrindyl tetrazine (10 mM) and monitored by HPLC over 3 h. A gradient of 100% H₂O with 0.1% TFA to 100% MeCN with 0.1% TFA over 15 min was used.

4.6c Synthetic procedures

Compounds DIFO [78], gly-nitrone [79], cyc-nitrone [80], 1,3-disubstituted cyclopropene [29,40], and 3,3-disubstituted cyclopropene [40] were synthesized as previously reported, and spectroscopic data were consistent with literature values. All other reagents were obtained from commercial sources and used without further purification. Reactions were run under an inert atmosphere of nitrogen, unless otherwise indicated. Tetrahydrofuran (THF), diethyl ether (Et₂O), triethylamine (NEt₃), dichloromethane (CH₂Cl₂), N,N-dimethylformamide (DMF), and methanol (CH₃OH) were degassed with argon and run through two 4 x 36 inch columns of anhydrous neutral A-2 (8 x 14 mesh; LaRoche Chemicals; activated under a flow of argon at 350 °C for 12 h). Thin-layer chromatography was performed using Silica Gel 60 F254-coated glass plates (0.25 mm thickness), and visualization was realized with KMnO₄ stain, CAM stain, and/or UV irradiation. Chromatography was accomplished with 60 Å (240-400 mesh) silica gel, commercially available from Sorbent Technologies. HPLC purifications were performed on a Varian ProStar equipped with 325 Dual Wavelength UV-Vis Detector. Analytical runs were performed using an Agilent C18 Scalar column (4.6 x 150 mm, 5 μm) with a 1 mL/min flow

rate. Semi-preparative runs were performed using an Agilent Prep-C18 Scalar column (9.4 x 150 mm, 5 μ m) with a 5 mL/min flow rate. NMR spectra were collected on a Bruker DRX-400 (400 MHz ^1H , 100 MHz ^{13}C , 376.5 MHz ^{19}F) or CRYO-500 (500 MHz ^1H , 125.7 MHz ^{13}C) instrument. All spectra were collected at 298 K. Chemical shifts are reported in ppm values relative to tetramethylsilane or residual non-deuterated NMR solvent, and coupling constants (J) are reported in Hertz (Hz). High-resolution mass spectrometry was performed by the University of California, Irvine Mass Spectrometry Center.

***N*-(4-(1,2,4,5-tetrazin-3-yl)benzyl)acetamide** (phenyl tetrazine): (4-(1,2,4,5-Tetrazin-3-yl)phenyl)methanamine hydrochloride was synthesized as previously reported.[23] The hydrochloride salt (10.1 mg, 0.0335 mmol) was dissolved in CH_2Cl_2 (2 mL) containing pyridine (0.5 mL). To this solution was added acetic anhydride (0.25 mL) followed by stirring for 1 h. The reaction mixture was diluted with 10 mL CH_2Cl_2 and rinsed with 1 M NaHSO_4 (3 x 20 mL). The organic layer was dried over MgSO_4 and concentrated under reduced pressure to afford 10.1 mg (95% yield) of pure phenyl tetrazine: ^1H NMR (500 MHz, CDCl_3) δ 10.28 (s, 1H), 8.66 (d, J = 8.1 Hz, 2H), 7.58 (d, J = 7.9 Hz, 2H), 5.95 (br s, 1H), 4.63 (d, J = 5.8 Hz, 2H), 2.15 (s, 3H); ^{13}C NMR (125 MHz, CDCl_3) δ 170.2, 166.3, 157.9, 143.9, 130.8, 128.8, 128.7, 43.4, 23.4; HRMS (ESI) m/z calcd for $\text{C}_{11}\text{H}_{12}\text{N}_5\text{O}$ $[\text{M}+\text{H}]^+$ 230.1042, found.

References

1. Grammel, M., and Hang, H. C. (2013) Chemical reporters for biological discovery, *Nat Chem Biol* 9, 475-484.
2. Willems, L. I., van der Linden, W. A., Li, N., Li, K. Y., Liu, N., Hoogendoorn, S., van der Marel, G. A., Florea, B. I., and Overkleeft, H. S. (2011) Bioorthogonal chemistry: applications in activity-based protein profiling, *Acc Chem Res* 44, 718-729.
3. Li, Z., Wang, D., Li, L., Pan, S., Na, Z., Tan, C. Y., and Yao, S. Q. (2014) "Minimalist" cyclopropene-containing photo-cross-linkers suitable for live-cell imaging and affinity-based protein labeling, *J Am Chem Soc* 136, 9990-9998.
4. Agarwal, P., and Bertozzi, C. R. (2015) Site-specific antibody-drug conjugates: the nexus of bioorthogonal chemistry, protein engineering, and drug development, *Bioconjug Chem* 26, 176-192.
5. Shih, H. W., Kamber, D. N., and Prescher, J. A. (2014) Building better bioorthogonal reactions, *Curr Opin Chem Biol* 21, 103-111.
6. Patterson, D. M., Nazarova, L. A., and Prescher, J. A. (2014) Finding the right (bioorthogonal) chemistry, *ACS Chem Biol* 9, 592-605.
7. Chang, P. V., Prescher, J. A., Hangauer, M. J., and Bertozzi, C. R. (2007) Imaging cell surface glycans with bioorthogonal chemical reporters, *J Am Chem Soc* 129, 8400-8401.
8. Presolski, S. I., Hong, V., Cho, S. H., and Finn, M. G. (2010) Tailored ligand acceleration of the Cu-catalyzed azide-alkyne cycloaddition reaction: practical and mechanistic implications, *J Am Chem Soc* 132, 14570-14576.
9. Rashidian, M., Kumarapperuma, S. C., Gabrielse, K., Fegan, A., Wagner, C. R., and Distefano, M. D. (2013) Simultaneous dual protein labeling using a triorthogonal reagent, *J Am Chem Soc* 135, 16388-16396.
10. Kim, C. H., Axup, J. Y., Dubrovskaya, A., Kazane, S. A., Hutchins, B. A., Wold, E. D., Smider, V. V., and Schultz, P. G. (2012) Synthesis of bispecific antibodies using genetically encoded unnatural amino acids, *J Am Chem Soc* 134, 9918-9921.

11. Lu, H., Zhou, Q., Deshmukh, V., Phull, H., Ma, J., Tardif, V., Naik, R. R., Bouvard, C., Zhang, Y., Choi, S., Lawson, B. R., Zhu, S., Kim, C. H., and Schultz, P. G. (2014) Targeting human C-type lectin-like molecule-1 (CLL1) with a bispecific antibody for immunotherapy of acute myeloid leukemia, *Angew Chem Int Ed* 53, 9841-9845.
12. Hudak, J. E., Barfield, R. M., de Hart, G. W., Grob, P., Nogales, E., Bertozzi, C. R., and Rabuka, D. (2012) Synthesis of heterobifunctional protein fusions using copper-free click chemistry and the aldehyde tag, *Angew Chem Int Ed* 51, 4161-4165.
13. Ramadoss, N. S., Schulman, A. D., Choi, S. H., Rodgers, D. T., Kazane, S. A., Kim, C. H., Lawson, B. R., and Young, T. S. (2015) An anti-B cell maturation antigen bispecific antibody for multiple myeloma, *J Am Chem Soc* 137, 5288-5291.
14. Agarwal, P., Kudirka, R., Albers, A. E., Barfield, R. M., de Hart, G. W., Drake, P. M., Jones, L. C., and Rabuka, D. (2013) Hydrazino-Pictet-Spengler ligation as a biocompatible method for the generation of stable protein conjugates, *Bioconjug Chem* 24, 846-851.
15. Agarwal, P., van der Weijden, J., Sletten, E. M., Rabuka, D., and Bertozzi, C. R. (2013) A Pictet-Spengler ligation for protein chemical modification, *Proc Natl Acad Sci U S A* 110, 46-51.
16. Seckute, J., and Devaraj, N. K. (2013) Expanding room for tetrazine ligations in the in vivo chemistry toolbox, *Curr Opin Chem Biol* 17, 761-767.
17. Blackman, M. L., Royzen, M., and Fox, J. M. (2008) Tetrazine ligation: fast bioconjugation based on inverse-electron-demand Diels-Alder reactivity, *J Am Chem Soc* 130, 13518-13519.
18. Sachdeva, A., Wang, K., Elliott, T., and Chin, J. W. (2014) Concerted, rapid, quantitative, and site-specific dual labeling of proteins, *J Am Chem Soc* 136, 7785-7788.
19. Schoch, J., Staudt, M., Samanta, A., Wiessler, M., and Jaschke, A. (2012) Site-specific one-pot dual labeling of DNA by orthogonal cycloaddition chemistry, *Bioconjug Chem* 23, 1382-1386.
20. Willems, L. I., Li, N., Florea, B. I., Ruben, M., van der Marel, G. A., and Overkleeft, H. S. (2012) Triple bioorthogonal ligation strategy for simultaneous labeling of multiple enzymatic activities, *Angew Chem Int Ed* 51, 4431-4434.

21. Borrmann, A., Milles, S., Plass, T., Dommerholt, J., Verkade, J. M., Wiessler, M., Schultz, C., van Hest, J. C., van Delft, F. L., and Lemke, E. A. (2012) Genetic encoding of a bicyclo[6.1.0]nonyne-charged amino acid enables fast cellular protein imaging by metal-free ligation, *ChemBioChem* 13, 2094-2099.
22. Lang, K., Davis, L., Wallace, S., Mahesh, M., Cox, D. J., Blackman, M. L., Fox, J. M., and Chin, J. W. (2012) Genetic Encoding of bicyclononynes and *trans*-cyclooctenes for site-specific protein labeling in vitro and in live mammalian cells via rapid fluorogenic Diels-Alder reactions, *J Am Chem Soc* 134, 10317-10320.
23. Karver, M. R., Weissleder, R., and Hilderbrand, S. A. (2011) Synthesis and evaluation of a series of 1,2,4,5-tetrazines for bioorthogonal conjugation, *Bioconjug Chem* 22, 2263-2270.
24. Liu, F., Liang, Y., and Houk, K. N. (2014) Theoretical elucidation of the origins of substituent and strain effects on the rates of Diels-Alder reactions of 1,2,4,5-tetrazines, *J Am Chem Soc* 136, 11483-11493.
25. Ramil, C. P., and Lin, Q. (2013) Bioorthogonal chemistry: strategies and recent developments, *Chem Commun (Camb)* 49, 11007-11022.
26. Jewett, J. C., and Bertozzi, C. R. (2010) Cu-free click cycloaddition reactions in chemical biology, *Chem Soc Rev* 39, 1272-1279.
27. Nikic, I., Plass, T., Schraidt, O., Szymanski, J., Briggs, J. A., Schultz, C., and Lemke, E. A. (2014) Minimal tags for rapid dual-color live-cell labeling and super-resolution microscopy, *Angew Chem Int Ed* 53, 2245-2249.
28. Karver, M. R., Weissleder, R., and Hilderbrand, S. A. (2012) Bioorthogonal reaction pairs enable simultaneous, selective, multi-target imaging, *Angew Chem Int Ed* 51, 920-922.
29. Patterson, D. M., Nazarova, L. A., Xie, B., Kamber, D. N., and Prescher, J. A. (2012) Functionalized cyclopropenes as bioorthogonal chemical reporters, *J Am Chem Soc* 134, 18638-18643.
30. Patterson, D. M., Jones, K. A., and Prescher, J. A. (2014) Improved cyclopropene reporters for probing protein glycosylation, *Mol Biosyst* 10, 1693-1697.

31. Cole, C. M., Yang, J., Seckute, J., and Devaraj, N. K. (2013) Fluorescent live-cell imaging of metabolically incorporated unnatural cyclopropene-mannosamine derivatives, *ChemBioChem* 14, 205-208.
32. Liang, Y., Mackey, J. L., Lopez, S. A., Liu, F., and Houk, K. N. (2012) Control and design of mutual orthogonality in bioorthogonal cycloadditions, *J Am Chem Soc* 134, 17904-17907.
33. Spate, A. K., Busskamp, H., Niederwieser, A., Schart, V. F., Marx, A., and Wittmann, V. (2014) Rapid labeling of metabolically engineered cell-surface glycoconjugates with a carbamate-linked cyclopropene reporter, *Bioconjug Chem* 25, 147-154.
34. Niederwieser, A., Spate, A. K., Nguyen, L. D., Jungst, C., Reutter, W., and Wittmann, V. (2013) Two-color glycan labeling of live cells by a combination of Diels-Alder and click chemistry, *Angew Chem Int Ed* 52, 4265-4268.
35. Neves, A. A., Stockmann, H., Wainman, Y. A., Kuo, J. C., Fawcett, S., Leeper, F. J., and Brindle, K. M. (2013) Imaging cell surface glycosylation in vivo using "double click" chemistry, *Bioconjug Chem* 24, 934-941.
36. Wainman, Y. A., Neves, A. A., Stairs, S., Stockmann, H., Ireland-Zecchini, H., Brindle, K. M., and Leeper, F. J. (2013) Dual-sugar imaging using isonitrile and azido-based click chemistries, *Org Biomol Chem* 11, 7297-7300.
37. Rossin, R., van den Bosch, S. M., Ten Hoeve, W., Carvelli, M., Versteegen, R. M., Lub, J., and Robillard, M. S. (2013) Highly reactive trans-cyclooctene tags with improved stability for Diels-Alder chemistry in living systems, *Bioconjug Chem* 24, 1210-1217.
38. Elliott, T. S., Townsley, F. M., Bianco, A., Ernst, R. J., Sachdeva, A., Elsasser, S. J., Davis, L., Lang, K., Pisa, R., Greiss, S., Lilley, K. S., and Chin, J. W. (2014) Proteome labeling and protein identification in specific tissues and at specific developmental stages in an animal, *Nat Biotechnol* 32, 465-472.
39. Xiong, D. C., Zhu, J., Han, M. J., Luo, H. X., Wang, C., Yu, Y., Ye, Y., Tai, G., and Ye, X. S. (2015) Rapid probing of sialylated glycoproteins in vitro and in vivo via metabolic oligosaccharide engineering of a minimal cyclopropene reporter, *Org Biomol Chem* 13, 3911-3917.

40. Kamber, D. N., Nazarova, L. A., Liang, Y., Lopez, S. A., Patterson, D. M., Shih, H. W., Houk, K. N., and Prescher, J. A. (2013) Isomeric cyclopropenes exhibit unique bioorthogonal reactivities, *J Am Chem Soc* *135*, 13680-13683.
41. Yu, Z., Pan, Y., Wang, Z., Wang, J., and Lin, Q. (2012) Genetically encoded cyclopropene directs rapid, photoclick-chemistry-mediated protein labeling in mammalian cells, *Angew Chem Int Ed* *51*, 10600-10604.
42. Yu, Z., and Lin, Q. (2014) Design of spiro[2.3]hex-1-ene, a genetically encodable double-strained alkene for superfast photoclick chemistry, *J Am Chem Soc* *136*, 4153-4156.
43. Worrell, B. T., Malik, J. A., and Fokin, V. V. (2013) Direct evidence of a dinuclear copper intermediate in Cu(I)-catalyzed azide-alkyne cycloadditions, *Science* *340*, 457-460.
44. Feng, L., Hong, S., Rong, J., You, Q., Dai, P., Huang, R., Tan, Y., Hong, W., Xie, C., Zhao, J., and Chen, X. (2013) Bifunctional unnatural sialic acids for dual metabolic labeling of cell-surface sialylated glycans, *J Am Chem Soc* *135*, 9244-9247.
45. Galibert, M., Dumy, P., and Boturyn, D. (2009) One-pot approach to well-defined biomolecular assemblies by orthogonal chemoselective ligations, *Angew Chem Int Ed* *48*, 2576-2579.
46. Kele, P., Mezo, G., Achatz, D., and Wolfbeis, O. S. (2009) Dual labeling of biomolecules by using click chemistry: a sequential approach, *Angew Chem Int Ed* *48*, 344-347.
47. Achatz, D. E., Mezo, G., Kele, P., and Wolfbeis, O. S. (2009) Probing the activity of matrix metalloproteinase II with a sequentially click-labeled silica nanoparticle FRET probe, *ChemBioChem* *10*, 2316-2320.
48. Andersen, K. A., Aronoff, M. R., McGrath, N. A., and Raines, R. T. (2015) Diazo groups endure metabolism and enable chemoselectivity in cellulose, *J Am Chem Soc* *137*, 2412-2415.
49. Gobbo, P., Romagnoli, T., Barbon, S. M., Price, J. T., Keir, J., Gilroy, J. B., and Workentin, M. S. (2015) Expanding the scope of strained-alkyne chemistry: a protection-deprotection strategy via the formation of a dicobalt-hexacarbonyl complex, *Chem Commun (Camb)* *51*, 6647-6650.

50. Yoshida, S., Hatakeyama, Y., Johmoto, K., Uekusa, H., and Hosoya, T. (2014) Transient protection of strained alkynes from click reaction via complexation with copper, *J Am Chem Soc* *136*, 13590-13593.
51. Yuan, Z., Kuang, G. C., Clark, R. J., and Zhu, L. (2012) Chemoselective sequential "click" ligation using unsymmetrical bisazides, *Org Lett* *14*, 2590-2593.
52. Sletten, E. M., and Bertozzi, C. R. (2011) A bioorthogonal quadricyclane ligation, *J Am Chem Soc* *133*, 17570-17573.
53. Yang, M., Li, J., and Chen, P. R. (2014) Transition metal-mediated bioorthogonal protein chemistry in living cells, *Chem Soc Rev* *43*, 6511-6526.
54. Yusop, R. M., Unciti-Broceta, A., Johansson, E. M., Sanchez-Martin, R. M., and Bradley, M. (2011) Palladium-mediated intracellular chemistry, *Nat Chem* *3*, 239-243.
55. Chankeshwara, S. V., Indrigo, E., and Bradley, M. (2014) Palladium-mediated chemistry in living cells, *Curr Opin Chem Biol* *21*, 128-135.
56. Spicer, C. D., Triemer, T., and Davis, B. G. (2012) Palladium-mediated cell-surface labeling, *J Am Chem Soc* *134*, 800-803.
57. Li, J., Lin, S., Wang, J., Jia, S., Yang, M., Hao, Z., Zhang, X., and Chen, P. R. (2013) Ligand-free palladium-mediated site-specific protein labeling inside gram-negative bacterial pathogens, *J Am Chem Soc* *135*, 7330-7338.
58. Li, N., Ramil, C. P., Lim, R. K., and Lin, Q. (2015) A genetically encoded alkyne directs palladium-mediated protein labeling on live mammalian cell surface, *ACS Chem Biol* *10*, 379-384.
59. Arumugam, S., and Popik, V. V. (2014) Sequential "click" - "photo-click" cross-linker for catalyst-free ligation of azide-tagged substrates, *J Org Chem* *79*, 2702-2708.
60. Ramil, C. P., and Lin, Q. (2014) Photoclick chemistry: a fluorogenic light-triggered in vivo ligation reaction, *Curr Opin Chem Biol* *21*, 89-95.

61. Yu, Z., Ohulchanskyy, T. Y., An, P., Prasad, P. N., and Lin, Q. (2013) Fluorogenic, two-photon-triggered photoclick chemistry in live mammalian cells, *J Am Chem Soc* 135, 16766-16769.
62. An, P., Yu, Z., and Lin, Q. (2013) Design of oligothiophene-based tetrazoles for laser-triggered photoclick chemistry in living cells, *Chem Commun (Camb)* 49, 9920-9922.
63. Sanders, B. C., Friscourt, F., Ledin, P. A., Mbua, N. E., Arumugam, S., Guo, J., Boltje, T. J., Popik, V. V., and Boons, G. J. (2011) Metal-free sequential [3+2]-dipolar cycloadditions using cyclooctynes and 1,3-dipoles of different reactivity, *J Am Chem Soc* 133, 949-957.
64. Ledin, P. A., Kolishetti, N., and Boons, G. J. (2013) Multi-functionalization of polymers by strain-promoted cycloadditions, *Macromolecules* 46, 7759-7768.
65. Wendeln, C., Singh, I., Rinnen, S., Schulz, C., Arlinghaus, H. F., Burley, G. A., and Ravoo, B. J. (2012) Orthogonal, metal-free surface modification by strain-promoted azide-alkyne and nitrile oxide-alkene/alkyne cycloadditions, *Chem Sci* 3, 2479-2484.
66. MacKenzie, D. A., and Pezacki, J. P. (2014) Kinetics studies of rapid strain-promoted [3+2] cycloadditions of nitrones with bicyclo[6.1.0]nonyne, *Can J Chem* 92, 337-340.
67. MacKenzie, D. A., Sherratt, A. R., Chigrinova, M., Cheung, L. L., and Pezacki, J. P. (2014) Strain-promoted cycloadditions involving nitrones and alkynes--rapid tunable reactions for bioorthogonal labeling, *Curr Opin Chem Biol* 21, 81-88.
68. Wallace, S., and Chin, J. W. (2014) Strain-promoted sydnone bicyclo-[6.1.0]-nonyne cycloaddition, *Chem Sci* 5, 1742-1744.
69. Plougastel, L., Koniev, O., Specklin, S., Decuypere, E., Creminon, C., Buisson, D. A., Wagner, A., Kolodych, S., and Taran, F. (2014) 4-Halogeno-sydnes for fast strain promoted cycloaddition with bicyclo-[6.1.0]-nonyne, *Chem Commun (Camb)* 50, 9376-9378.
70. Kolodych, S., Rasolofonjatovo, E., Chaumontet, M., Nevers, M. C., Creminon, C., and Taran, F. (2013) Discovery of chemoselective and biocompatible reactions using a high-throughput immunoassay screening, *Angew Chem Int Ed* 52, 12056-12060.

71. Li, Q., Dong, T., Liu, X., and Lei, X. (2013) A bioorthogonal ligation enabled by click cycloaddition of o-quinolinone quinone methide and vinyl thioether, *J Am Chem Soc* *135*, 4996-4999.
72. Zhang, X., Dong, T., Li, Q., Liu, X., Li, L., Chen, S., and Lei, X. (2015) Second generation TQ-ligation for cell organelle imaging, *ACS Chem Biol*. ASAP
73. Stockmann, H., Neves, A. A., Stairs, S., Brindle, K. M., and Leeper, F. J. (2011) Exploring isonitrile-based click chemistry for ligation with biomolecules, *Org Biomol Chem* *9*, 7303-7305.
74. Noda, H., Eros, G., and Bode, J. W. (2014) Rapid ligations with equimolar reactants in water with the potassium acyltrifluoroborate (KAT) amide formation, *J Am Chem Soc* *136*, 5611-5614.
75. Engelsma, S. B., Willems, L. I., van Paaschen, C. E., van Kasteren, S. I., van der Marel, G. A., Overkleeft, H. S., and Filippov, D. V. (2014) Acylazetine as a dienophile in bioorthogonal inverse electron-demand Diels-Alder ligation, *Org Lett* *16*, 2744-2747.
76. Borrmann, A., Fatunsin, O., Dommerholt, J., Jonker, A. M., Lowik, D. W., van Hest, J. C., and van Delft, F. L. (2015) Strain-promoted oxidation-controlled cyclooctyne-1,2-quinone cycloaddition (SPOCQ) for fast and activatable protein conjugation, *Bioconjug Chem* *26*, 257-261.
77. Norbornene rates were measured by David N. Kamber. Computational analyses were performed by the Houk group at UCLA.
78. Sletten, E. M., de Almeida, G., Bertozzi, C. R. (2014) A homologation approach to the synthesis of difluorinated cycloalkynes, *Org Lett* *16*, 1634-1637.
79. Dicken, C. M., DeShong, P., (1982) Reactions at high pressure. [3+2] Dipolar cycloadditions of nitrones and vinyl ethers, *J Org Chem* *47*, 2047-2051.
80. Gella, C., Ferrer, È., Alibés, R., Busqué, F., de March, P., Figueredo, M., Font, J. (2009) A metal-free general procedure for oxidation of secondary amines to nitrones, *J Org Chem* *74*, 6365-6367.

Chapter 5: Progress towards an “off-the-shelf” luciferase for imaging implanted cells

5.1 Introduction

Cell-based therapies, such as immunotherapies and regenerative stem-cell treatments, hold great promise for the treatment of injuries, degenerative diseases and cancer [1-3]. Successful implementation of these therapies requires a complete understanding of the fates of transplanted cells. Imaging technologies are well suited to non-invasively track cell proliferation and migration through a whole organism [4, 5]. In many labs, access to expensive equipment and short-lived reagents make methods such as MRI or PET imaging infeasible. More user-friendly fluorescent strategies are not ideal for *in vivo* imaging owing to high background absorbance from tissue and requisite knowledge of cell location within the organism [6, 7].

Bioluminescence imaging is better suited to noninvasively imaging whole organisms. This technique relies on enzymes (luciferases) that generate light via oxidation of small molecule substrates (luciferins) [8]. Cells expressing luciferase (and incubated with luciferin) generate light that can be detected using sensitive cameras. Bioluminescence techniques are, comparatively, easy to use, offer high signal-to-noise, and provide a snapshot of the entire organism [8, 9].

In addition to enabling sensitive imaging, bioluminescence is suitable for serial imaging. Typically, luciferases are genetically encoded into a desired cell line or expressed as a “reporter gene” to identify changes in gene-expression. Such applications require transfection of the requisite luciferase gene into cells, which can be time-consuming and incompatible with certain cell types [10, 11]. To circumvent these issues, we aimed to develop an “off-the-shelf” luciferase

reporter than can be rapidly appended to a cell of interest immediately prior to implantation (Figure 5-1A). Similar strategies are used to incorporate small molecule fluorophores onto live cell surfaces. These typically rely on membrane fusion or non-specific NHS-coupling to cell surface proteins to append the fluorophores [10, 12, 13]. Once attached, they can be used to track cells in the hours post-implantation.

We chose to use a similar approach to chemically append the luciferase from *Gaussia princeps* (Gluc) to model cell surfaces. Gluc emits a photon of light through oxidation of the small molecule coelenterazine to coelenteramide (Figure 5-1B) [8]. Unlike other luciferases, Gluc requires only molecular oxygen to catalyze the oxidation of coelenterazine, thus, it can function in extracellular environments [14, 15]. Gluc is also one of the brightest and most stable luciferases — maximizing the signal given a limited cell surface area. However, there are no general methods to append this protein to cells in a facile manner. Moreover, Gluc is not compatible with intracellular delivery strategies due its five disulfide bonds [16]. Thus, we sought mild chemical methods to append Gluc to the cell surface. Several strategies could be envisioned, but we initially focused on a bioorthogonal chemistry attachment strategy. Herein, we report progress towards a membrane-bound Gluc for noninvasive cell tracking *in vivo*.

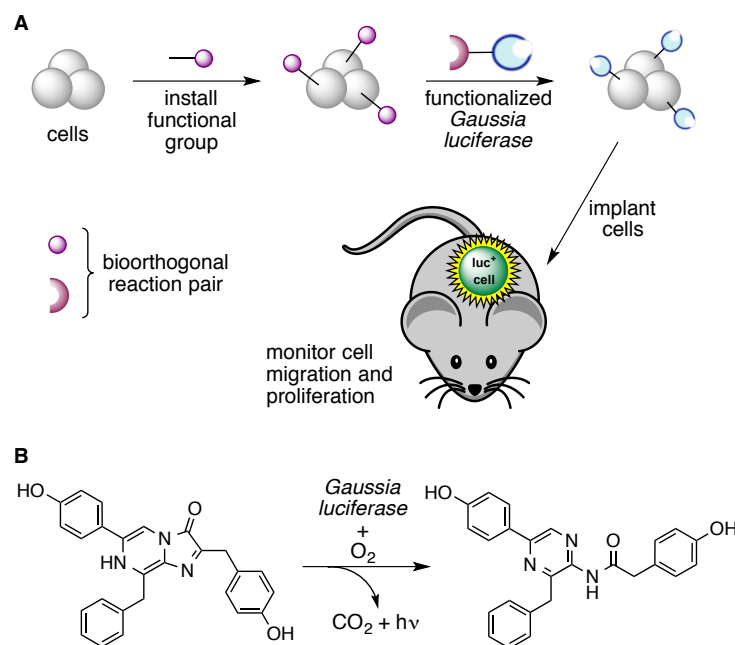


Figure 5-1. Design for “off-the-shelf” bioluminescent cell tracking. (A) Cells are first outfitted with a bioorthogonal functional group. The cells are then treated with a functionalized luciferase (Gluc) bearing the complementary bioorthogonal probe to outfit them with the bioluminescent probe. Cells are then implanted into a live animal for immediate monitoring. (B) Gluc oxidizes coelenterazine to coelenteramide, releasing a photon of light.

5.2 Results and Discussion

We envisioned using bioorthogonal chemistry to selectively attach Gluc to the cell surface (Figure 5-1A). In this approach, one functional group must be installed onto Gluc, while the complementary probe is attached to the cell surface. The functionalized cells and Gluc are then mixed to install the bioluminescent probe. Several attachment strategies were explored and herein we discuss two promising methods.

5.2a Aldehyde-tagged Gluc

In one method, we utilized the formylglycine generating enzyme (FGE) to enzymatically install an aldehyde onto Gluc [17]. FGE is a sulfatase that recognizes the sequence LCTPSR and converts the thiol side chain of cysteine into an aldehyde [18]. The aldehyde is a small non-

perturbing functional group that can be modified bioorthogonally via the oxime ligation, as well as other selective ligation chemistries [19, 20]. Additionally, aldehydes can be installed on cell surfaces by mild oxidation of sialic acid with sodium periodate [21]. We envisioned linking the aldehyde-tagged Gluc to cell surface aldehydes with a bis(aminoxy) linker. This linker could first be attached to the protein and then to the cell surface (Figure 5-2A-B).

We generated an LCTPSR-Gluc fusion and co-expressed it with FGE in *E. coli*, but encountered several issues. First, we were unable to successfully identify the incorporation of the aldehyde tag via mass spectrometry. Moreover, Gluc expression in *E. coli* can lead to misfolded and inactive enzyme (Joanna Laird, *pers. comm.*). Thus, we decided to express LCTPSR-Gluc and FGE in mammalian cells [17]. Others have shown improved Gluc expression through mammalian cell culture [14, 16]. We inserted the gene encoding LCTPSR-Gluc into a pBMN destination vector downstream of the CD8 leader sequence. The fusion protein would ultimately be destined for secretion and isolable from the media for further conjugation. Toward this end, HEK293 cells stably expressing LCTPSR-Gluc were transiently transfected with FGE in pcDNA. After several days, the media—containing the putative aldehyde-modified Gluc—was collected. Cells stably expressing both LCTPSR-Gluc and FGE are currently being prepared and efforts are currently underway to purify, quantify and characterize the resulting protein.

With the aldehyde-tagged Gluc in hand, we aimed to append the enzyme to cell surfaces via oxime ligation. The sample was treated with 1 mM of the bis(aminoxy) linker and dialyzed to remove excess linker. Cells treated with periodate were then incubated with media containing the aminoxy-Gluc (AO-Gluc) sample for 90 min [21]. As shown in Figure 5-2C, the Jurkat and HEK293 cells treated with the LCTPSR-Gluc demonstrate a 5-7-fold signal above Gluc lacking

formylglycine. These results are encouraging and the signal-to-noise should improve with optimized labeling conditions, including the use of cells stably expressing FGE.

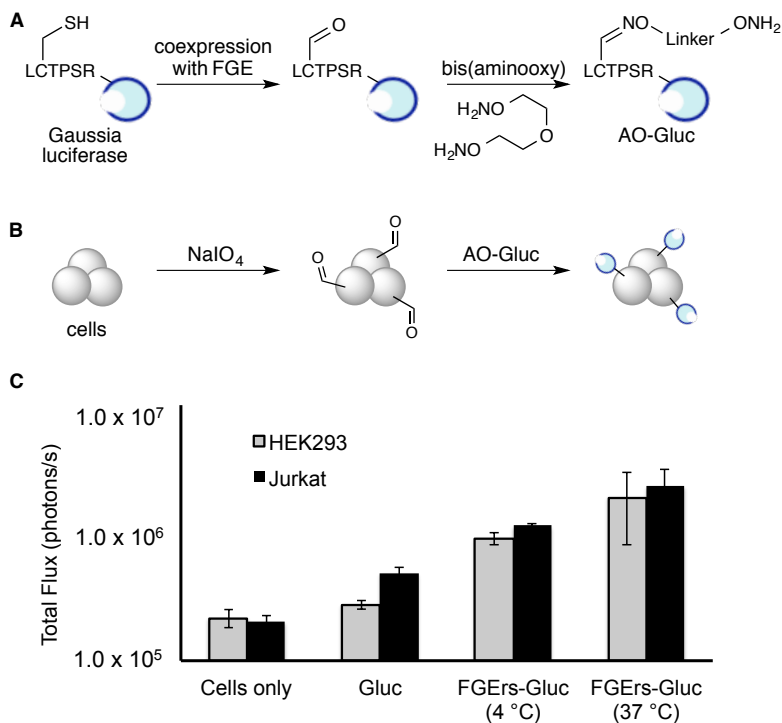


Figure 2. Gluc attachment strategy utilizing the oxime ligation. (A) An aldehyde is incorporated into Gluc using FGE, which is subsequently modified with a bis(aminooxy) linker to generate AO-Gluc. (B) Cells are treated with sodium periodate to generate cell surface aldehydes. Cells are then treated with AO-Gluc to covalently append Gluc to the cell surface. (C) After modification, cells were plated and compared to cells treated with unmodified Gluc. Both HEK293 and Jurkat cells were plated (50,000 cells/well) in a black 96-well plate followed by addition of coelenterazine. The total flux was then recorded. Cells treated with AO-Gluc showed a 5- to 7-fold increase in total flux compared to cells treated with unmodified Gluc.

5.2b Sortagging of Gluc

In an alternative approach, we aimed to incorporate bioorthogonal functional groups into Gluc utilizing the sortagging method (Figure 5-3). Sortagging employs a bacterial transpeptidase enzyme, sortase A, to append peptide probes to proteins bearing the consensus sequence LPETG [22-24]. Sortase A cleaves the amide bond between the threonine and glycine residues and creates a new linkage between the now sortase-bound threonine and exogenous N-terminal glycine motifs [24]. Based on strong literature precedent, we surmised that sortagging would be a viable strategy to append bioorthogonal functional groups to Gluc for cell surface attachment. Sortagging has been exploited by the Ploegh group to append a broad array of substrates to proteins, including bioorthogonal functional groups [25-27]. Toward this end, we generated a Gluc-LPETG construct and expressed the fusion protein in *E. coli*. The isolated protein demonstrated bioluminescent activity, although we have evidence that only a portion is properly folded (Joanna Laird, *pers. comm.*).

The Gluc-LPETG protein allows us to use sortagging to readily insert our bioorthogonal functional group of choice. We chose to install tetrazine, owing to its synthetic accessibility, rapid kinetics with strained alkenes, and suitable stability [19]. By appending tetrazine motifs to the C-terminus of a triglycine peptide (**G₃Tz**), we could use sortagging to functionalize Gluc-LPETG (Figure 5-3A, and Scheme 5-1A) [25]. The resulting conjugate (Gluc-Tz) could then be attached to cyclopropene-labeled cell surfaces. Toward this end, Gluc-LPETG was converted to Gluc-Tz by treatment with sortase A and **G₃Tz** for 24 h at 4 °C. (Figure 5-3D). We were able to detect the ~2 kDa mass change via SDS-PAGE (Figure 5-3E). Gluc-Tz was then purified and dialyzed to remove sortase and excess **G₃Tz**. After modification, the luciferase conjugate also maintained its bioluminescent activity (Figure 5-3E).

Purified Gluc-Tz was then ready for live cell attachment. We investigated two methods to achieve cell surface cyclopropene incorporation using either a lipid-cyclopropene conjugate (**DPPE-Cp**) or an amine reactive cyclopropene (**NHS-Cp**). Lipid derivatives have previously been utilized to insert many chemical moieties into cell membranes, such as DNA [28], fluorophores [10], and bioorthogonal functional groups [29, 30]. Amine reactive NHS esters are also commonly used to install fluorophores non-specifically to cell surface proteins for cell tracking [12, 13]. Both derivatives were synthesized using standard bioconjugation chemistries (Scheme 5-1B).

Unfortunately, initial attempts with both **NHS-Cp** and **DPPE-Cp** proved intractable for labeling. For example, treatment of cells with varying concentrations (1-20 μM) of **NHS-Cp** led to significant cell death. This is likely due to either excessive labeling or the need to perform the labeling in protein-free media. The former could be minimized by using a more polar reagent to prevent intracellular labeling [31]. **DPPE-Cp** was minimally soluble in DMSO or aqueous buffers, hampering initial labeling attempts. After sonication to partially solubilize the lipid, cell labeling was performed on Jurkat cells, which saw a very slight signal over background (Figure 5-3F), but further characterization and optimization is required before this approach can be fully realized. Aside from optimizing conditions, a switch from cyclopropene to bicyclononyne could offer a significant increase in labeling. Bicyclononyne exhibits >100 fold faster reaction kinetics with tetrazine compared to cyclopropene and is commercially available [32]. It has recently been utilized in a similar sortagging approach recently reported by Ploegh and Weissleder [25].

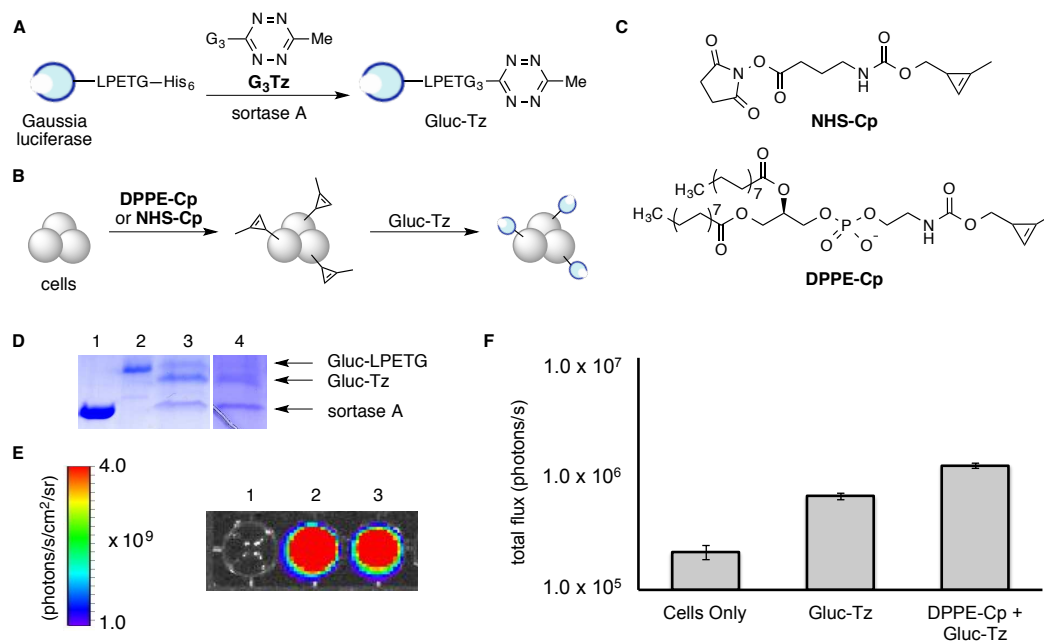
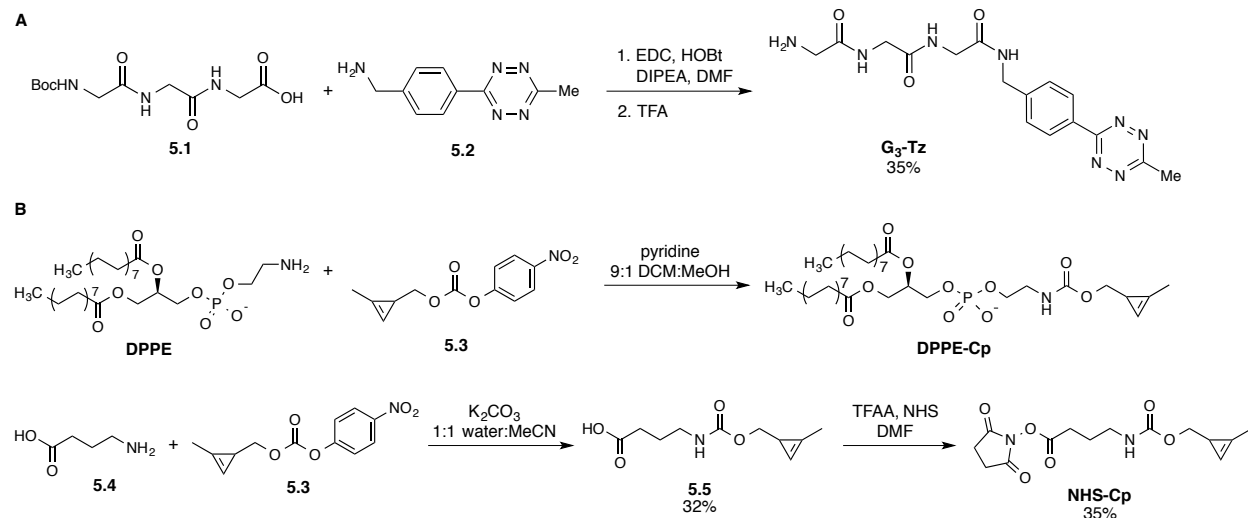


Figure 3. Gluc cell surface attachment method via sortagging. (A) Tetrazine is incorporated via sortase-mediated transpeptidation of **G₃Tz** onto the Gluc-LPETG protein. (B) Cell surfaces are modified with cyclopropene groups through lipid insertion (**DPPE-Cp**) or non-specific amine attachment (**NHS-Cp**). The cells are then treated with Gluc-Tz to functionalize the cells with the bioluminescent protein for *in vivo* tracking. (C) Structure of the two cyclopropene probes. (D) Expressed Gluc (100 μ M) was treated with sortase A (20-40 μ M) and **G₃Tz** (750 μ M) for 24 h at 4 °C. Lane 1 and 2 are the sortase A and Gluc-LPETG controls. Lane 3 and 4 are sortagging with 20 μ M and 40 μ M sortase A, respectively. (E) Gluc-Tz (lane 3) shows comparable bioluminescence activity when compared to the parent Gluc-LPETG (lane 2). Lane 1 contains no Gluc. (F) Jurkat cells were briefly incubated with **DPPE-Cp** (0 or 2 μ M) for 5 min with mild agitation. After washing, the cells were reacted with Gluc-Tz (20 μ M) for 60 min at 37 °C. Upon treatment with coelenterazine, cells treated with **DPPE-Cp** and Gluc-Tz showed slightly higher bioluminescence signal than cells treated with Gluc-Tz only.

Scheme 1. Synthesis of reagents for sortase-mediated cell surface attachment. (A) Synthesis of **G₃Tz** for Gluc functionalization. (B) Synthesis of reagents for attachment of cyclopropene moieties to cell surfaces.



5.3 Conclusions and future directions

Selective, cell surface attachment of luciferases onto live cell surfaces offer obvious advantages for tracking applications. The approaches outlines in this chapter show promise in terms of their modularity, but significant improvements are necessary. For example, current cyclopropene incorporation strategies are currently insufficient due to solubility issues (**DPPE-Cp**) and toxicity (**NHS-Cp**). Alternate probes, such as alternate lipids or more polar NHS probes could improve labeling. Additionally, bicyclononyne offers faster kinetics and could further reduce labeling time.

In addition to optimizing current strategies, alternative approaches for Gluc attachment can be explored. For example, enzymatic attachment methods such as the SpyCatcher:SpyTag system [33] or SNAP tags [34] have recently been utilized for cell surface modification. Upon optimization of the attachment chemistry *in vitro*, the bioluminescence signal strength and lifetime will have to be evaluated *in vivo*. We are also exploring bioorthogonal ligation strategies to attach Gluc to antibodies for *in vivo* imaging of cell contacts. Recent work by our lab has

demonstrated the utility of genetically-encoded split *Gaussia* luciferase for imaging cell proximity [35]. We hope to utilize bioorthogonal chemistry to attach these splits to cells and antibodies to image cell contacts *in vivo* using our “off-the-shelf” bioluminescent probes.

5.4 Materials and methods

5.4a Plasmids

Construction of Gaussia luciferase vectors containing N-term formylglycine generating enzyme recognition (LCTPSR) motif (LCTPSR). PCR was used to generate the gene containing LCTPSR from a previously described *Gaussia* luciferase gene (courtesy of Grant Walkup). The LCTPSR-Gluc gene was then inserted into pET28a(+) using the following primers:

5' - TATACATATGCTGTGTACCCCGTCTCGTAAACCGACCGAAAACAACG - 3'

5' - TATAGAATTCCCTAGTCACCACCCGCAC - 3'

The gene was then moved into pBMN using the following primers:

5' - ATAGAATTCCATCACCATCACCATCACCTGTGTACCCCATCAAGACTCGAGATA - 3'

5' - AACTCGAGTCTTGATGGGGTACACAGGTGATGGTGATGGTGATGGAATTCATA - 3'

Construction of Gaussia luciferase vectors containing C-term sortase recognition (Srt_{rs}) motif (LPETG). Overlap PCR was used to generate the gene containing G₄S linked Srt_{rs} from a previously cloned *Gaussia* luciferase gene. The Gluc-LPETG gene was then inserted into pET28a(+) using the following primers:

5' - TATACCATGGATAAACCGACCGAAAACAACGAAGACTTCAACATCGTTGCG - 3'

5' - TATAGAATTCCCGCCGGTTTCCGGCAGGCTACCGCCGCCACCGCTACC - 3'

Formylglycine generating enzyme. Formylglycine generating enzyme (FGE) gene (courtesy of David Rabuka - Redwood Biosciences) was inserted into pcDNA using the following primers:

5' - TATAGCTAGCATGCTGACCGAGTTGGTTGACCTGC - 3'

5' - TATACTCGAGCTACCCGGACACCGGGTTCG - 3'

5.4b Expression of Guassia luciferase [36]

Both GLuc fusion proteins were expressed in *E. coli* BL21 cells. The cells were cultured in 10 mL Luria-Bertani (LB) medium containing ampicillin (50 µg/ml) at 37 °C for 8-12 h. The starter culture was then transferred into 1 L LB and incubated at 37 °C with shaking (225 rpm) until the O.D. (590 nm) reached 0.7–0.9. Protein expression was induced with 1 mM isopropyl-β-D-1-thiogalactopyranoside (IPTG). After addition of IPTG, *E. coli* cells were cultured for 24 h at 18 °C and harvested by centrifugation. All GLuc variants were purified exclusively from the supernatant (soluble fraction) by using Ni²⁺-NTA affinity chromatography.

5.4c Cell culture

HEK293 cells (American Type Cell Culture) were cultured in DMEM (Corning) supplemented with 10% (vol/vol) fetal bovine serum (FBS, Life Technologies), penicillin (100 U/mL), and streptomycin (100 µg/mL). Jurkat cells were cultured in RPMI media (Corning) supplemented with 10% (v/v) FBS, penicillin (100 U/mL), and streptomycin (100 µg/mL). Cells were maintained in a 5% CO₂, water-saturated incubator at 37 °C. Transient transfections of the LCTPSR-Gluc construct were performed with cationic lipids (Lipofectamine 2000; Invitrogen). HEK293 cells stably expressing the LCTPSR-Gluc were selected with puromycin (10 µg/mL; Corning). HEK293 cells stably expressing LCTPSR-Gluc were transfected with FGE construct

using cationic lipids. Cells stably expressing both constructs were selected with G418 (250 µg/mL; Corning).

5.4d Sortase mediated *Gaussia luciferase* modification

The heptamutant sortase A with enhanced catalytic activity and Ca²⁺-independent activity was used [26]. The reaction mixture contained expressed Gluc-LPETG (100 µM) in Tris-buffered saline (50 mM Tris base, 150 mM NaCl, pH 8.0) with **G₃Tz** (750 µM) and sortase A (20-40 µM). The reaction was rocked for 24 hours at 4 °C before analysis by SDS-PAGE. Gluc-Tz was purified via Ni²⁺-NTA affinity chromatography as previously described [23] followed by dialysis to remove excess **G₃-Tz**.

5.4e Cell surface attachment of *Gaussia luciferase*

Oxime ligation method

Media was collected (4 mL at pH 6.5) from ~6 x 10⁶ HEK293 cells stably expressing LCTPSR-Gluc and transiently expressing FGE. The media was rocked gently overnight with 1 mM bis(aminooxy) linker at 4 °C. The samples were dialyzed into PBS (4 L, pH 6.5) to remove excess linker. HEK293 and Jurkat cells (1.5 x 10⁶ cells) were each treated with 1 mM NaIO₄ for 30 min at 4 °C followed by quenching with 1 mM glycerol and rinsing with PBS (2 x 1 mL, pH 6.5) [21]. Cells were then incubated at 37 °C with media only, media containing unmodified LCTPSR-Gluc, or media containing AO-Gluc and 100 mM aniline (at 4 °C or 37 °C) for 90 min. Cells were rinsed extensively with 1% BSA in PBS (7.4) and transferred to a 96-well black-well plate (50,000 cells/well). A stock solution of coelenterazine (Nanolight Technology, 5 mg/mL in

ethanol) was diluted 1:500 in water and 20 μL was added to each well. Bioluminescence images were acquired using an IVIS Lumina II (Xenogen).

Tetrazine ligation method

Jurkat cells ($\sim 2 \times 10^6$ cells) were pelleted and rinsed (3 x 4 mL) with PBS (pH 7.4) containing 1% bovine serum albumin (BSA). Cells were resuspended in 200 μL PBS and divided into three 50 μL aliquots (0.5×10^6 cells/reaction). To one aliquot was added 0.2 μL **DPPE-Cp** (500 μM). Each sample was agitated with gentle vortexing for 5 min followed by washing with 1% BSA in PBS. Cells were resuspended in 50 μL of Gluc-Tz (0-20 μM) in DMEM media. Samples were incubated at 37 $^\circ\text{C}$ for 1 h before rinsing with 5% BSA in PBS. Cells were then suspended in DMEM media (80 μL) transferred to a 96-well clear-bottom black-well plate (50,000 cells/well). A stock solution of coelenterazine (Nanolight Technology, 5 mg/mL in ethanol) was diluted 1:500 in water and 20 μL was added to each well. Bioluminescence images were acquired using an IVIS Lumina II (Xenogen).

5.4f General synthetic procedures

Compounds bis(aminooxy) linker [37], **5.2** [38], and **5.3** [39] were synthesized as previously reported. All other reagents were purchased from commercial sources and used as received without further purification. Reactions were carried out under an inert atmosphere of nitrogen or argon in oven- or flame-dried glassware. Dichloromethane (CH_2Cl_2), tetrahydrofuran (THF), diethyl ether (Et_2O), *N,N*-dimethylformamide (DMF), methanol (CH_3OH) and triethylamine (NEt_3) were degassed with argon and passed through two 4 x 36 inch columns of anhydrous neutral A-2 (8 x 14 mesh; LaRoche Chemicals; activated under a flow of argon at 350 $^\circ\text{C}$ for 12

h). The remaining solvents were of analytical grade and purchased from commercial suppliers. Thin-layer chromatography was performed using Silica Gel 60 F₂₅₄ plates. Plates were visualized using UV radiation and/or staining with KMnO₄. Flash column chromatography was performed with 60 Å (240-400 mesh) silica gel from Sorbent Technologies. In some cases, the silica was first deactivated with 1% NEt₃ in the eluting solvent. ¹H, ¹³C, and ¹⁹F NMR spectra were recorded on Bruker GN-500 (500 MHz ¹H, 125.7 MHz ¹³C), CRYO-500 (500 MHz ¹H, 125.7 MHz ¹³C) or DRX-400 (400 MHz ¹H, 100 MHz ¹³C, 376.5 MHz ¹⁹F) spectrometers. All spectra were collected at 298 K unless otherwise noted. NOESY experiments were performed exclusively with the CRYO-500 instrument with mixing times ranging from 0.8-1.0 s. Chemical shifts are reported in ppm values relative to tetramethylsilane or residual non-deuterated NMR solvent, and coupling constants (*J*) are reported in Hertz (Hz). High-resolution mass spectrometry was performed by the University of California, Irvine Mass Spectrometry Center. HPLC runs were conducted on a Varian ProStar equipped with 325 Dual Wavelength UV-Vis Detector. Analytical runs were performed using an Agilent Polaris 5 C18-A column (4.6 x 150 mm, 5 μm) with a 1 mL/min flow rate. Semi-preparative runs were performed using an Agilent Prep-C18 Scalar column (9.4 x 150 mm, 5 μm) with a 5 mL/min flow rate. The elution gradients for the relevant separations are specified below.

2.4g Synthetic procedures

Triglycine tetrazine conjugate (G₃Tz). To a solution of Boc-Gly-Gly-Gly-OH (**5.1**) (100 mg, 0.35 mmol) in DMF (0.5 mL) was added *N,N*-diisopropylethylamine (300 μL, 1.7 mmol) and hydroxybenzotriazole (53 mg, 0.35 mmol). The solution was cooled to 4 °C on ice followed by addition of *N*-(3-dimethylaminopropyl)-*N*-ethylcarbodiimide hydrochloride (133 mg, 0.692

mmol). The solution was removed from ice and allowed to stir for 15 min. Tetrazine (**5.2**) (104 mg, 0.347 mmol) in DMF (0.5 mL) was then added to the reaction, and the solution was allowed to stir overnight. The reaction mixture was diluted with CH₂Cl₂ (10 mL) and rinsed with 1 M NaHSO₄ (2 x 20 mL). The organic layer was dried with MgSO₄ and filtered. The organic layer was cooled on ice before addition of triisopropylsilane (0.5 mL) and trifluoroacetic acid (10 mL). The reaction was stirred at rt for 1 h, then concentrated under reduced pressure. The crude mixture was purified via HPLC (5-20% CH₃CN in water with 0.1% TFA over 4 min and 20% over 6 min) to afford **G₃Tz** as a red solid (45.4 mg, 0.122 mmol, 35% yield): ¹H NMR (400 MHz, CDCl₃) δ 8.59 (br s, 1H), 8.49 (d, *J* = 8.5 Hz, 2H), 7.53 (d, *J* = 8.6 Hz, 2H), 4.52 (d, *J* = 6.0 Hz, 1H), 4.00 (s, 2H), 3.95 (s, 2H), 3.74 (s, 2H), 3.02 (s, 2H); ¹³C NMR (500 MHz, CDCl₃) δ 170.4, 170.3, 167.4, 166.7, 163.8, 143.4, 131.0, 127.8, 127.5, 42.3, 42.1, 41.9, 40.1, 19.6; HRMS (ESI) calcd for C₁₆H₂₀N₈O₃Na [M+Na]⁺ 395.1556, found 395.1542.

Dipalmitoyl-cyclopropene conjugate (DPPE-Cp). 1,2-Dipalmitoyl-*sn*-glycero-3-phosphoethanolamine (**DPPE**) (100 mg, 0.14 mmol) was dissolved in 9:1 CH₂Cl₂:CH₃OH (20 mL) at 30 °C. To this solution was added triethylamine (100 μL, 0.72 mmol) followed by carbonate **5.3** (45.6 mg, 0.183 mmol). The reaction mixture was allowed to stir at 30 °C for 30 h before being concentrated onto silica gel under reduced pressure. The product was purified by flash column chromatography (eluting with 5-10% CH₃OH in CH₂Cl₂) to afford product **DPPE-Cp** (41 mg) in ~70% purity with unknown **DPPE** byproduct: HRMS (ESI) calcd for C₄₃H₈₀NO₁₀Na [M+Na]⁺ 824.5417, found 824.5398.

4-(((2-Methylcycloprop-2-en-1-yl)methoxy)carbonyl)amino)butanoic acid (5.5). To a solution of 4-aminobutyric acid (**5.4**) (41 mg, 0.40 mmol) and potassium carbonate (166 mg, 1.20 mmol) in 1 mL of water was added **5.3** (150 mg, 0.60 mmol) in 1 mL CH₃CN. The solution turned yellow immediately and the reaction was allowed to stir overnight. The reaction mixture was diluted with 10 mL water and rinsed with ethyl acetate (2 x 20 mL). The organic layer was discarded, the aqueous layer was acidified with 1 M NaHSO₄ to pH ~2, and extracted with ethyl acetate (3 x 20 mL). The organic layer was dried with MgSO₄, filtered, and purified via flash column chromatography (eluting with 30% ethyl acetate in hexanes) to afford **5.4** as a clear oil (41 mg, 32% yield): ¹H NMR (400 MHz, CDCl₃) δ 6.56 (s, 1H), 4.86 (br s, 1H), 3.93 (d, *J* = 3.9 Hz, 2H), 3.25 (q, *J* = 12.7, 6.3 Hz, 2H), 2.42 (t, *J* = 7.2 Hz, 2H), 2.13 (s, 3H), 1.85 (m, 2H), 1.64 (s, 1H); HRMS (ESI) calcd for C₁₀H₁₅NO₄Na [M+Na]⁺ 236.0899, found 236.0891.

NHS-cyclopropenyl ester (NHS-Cp). To a solution of **5.5** (40 mg, 0.19 mmol) in 1 mL CH₂Cl₂ was added N-hydroxysuccinimide (43 mg, 0.37 mmol) and pyridine (60 μL, 0.75 mmol). The solution was cooled to 4 °C on ice before dropwise addition of trifluoroacetic anhydride (52 μL, 0.37 mmol) with stirring. The reaction mixture was allowed to warm to rt and stir for 1.5 h. The reaction mixture was diluted with 10 mL CH₂Cl₂ and rinsed with 1 M NaHSO₄ (3 x 10 mL) and saturated NaHCO₃ (2 x 10 mL). The organic layer was dried with MgSO₄ and concentrated under reduced pressure. The product was purified by flash column chromatography (eluting with 30-60% ethyl acetate in hexanes) to afford the **NHS-Cp** as a clear oil (20 mg, 35% yield): ¹H NMR (400 MHz, CDCl₃) δ 6.57 (s, 1H), 4.89 (br s, 1H), 3.93 (m, 2H), 3.29 (q, *J* = 13.0, 6.5 Hz, 2H), 2.84 (s, 4H), 2.68 (t, *J* = 7.3 Hz, 2H), 2.14 (s, 3H), 1.98 (m, 2H), 1.64 (s, 1H); HRMS (ESI) calcd for C₁₄H₁₈N₂O₆Na [M+Na]⁺ 333.1063, found 333.1066.

References

1. Chen, F. M., Zhao, Y. M., Jin, Y., and Shi, S. T. (2012) Prospects for translational regenerative medicine, *Biotechnol Adv* 30, 658-672.
2. June, C. H., Maus, M. V., Plesa, G., Johnson, L. A., Zhao, Y. B., Levine, B. L., Grupp, S. A., and Porter, D. L. (2014) Engineered T cells for cancer therapy, *Cancer Immunol Immunother* 63, 969-975.
3. June, C. H. (2007) Adoptive T cell therapy: Grand challenges and opportunities, *J Immunother* 30, 858-858.
4. Hong, H., Yang, Y. A., Zhang, Y., and Cai, W. B. (2010) Non-invasive cell tracking in cancer and cancer therapy, *Curr Top Med Chem* 10, 1237-1248.
5. Hong, H., Yang, Y. N., Zhang, Y., and Cai, W. B. (2010) Non-invasive imaging of human embryonic stem cells, *Curr Pharm Biotechnol* 11, 685-692.
6. Pittet, M. J., and Weissleder, R. (2011) Intravital imaging, *Cell* 147, 983-991.
7. Hilderbrand, S. A., and Weissleder, R. (2010) Near-infrared fluorescence: application to in vivo molecular imaging, *Curr Opin Chem Biol* 14, 71-79.
8. Paley, M. A., and Prescher, J. A. (2014) Bioluminescence: a versatile technique for imaging cellular and molecular features, *MedChemComm* 5, 255-267.
9. Prescher, J. A., and Contag, C. H. (2010) Guided by the light: visualizing biomolecular processes in living animals with bioluminescence, *Curr Opin Chem Biol* 14, 80-89.
10. Lassailly, F., Griessinger, E., and Bonnet, D. (2010) "Microenvironmental contaminations" induced by fluorescent lipophilic dyes used for noninvasive in vitro and in vivo cell tracking, *Blood* 115, 5347-5354.
11. Contag, C. H. (2007) In vivo pathology: Seeing with molecular specificity and cellular resolution in the living body, *Annu Rev Pathol-Mech* 2, 277-305.
12. Foster, A. E., Kwon, S., Ke, S., Lu, A., Eldin, K., Sevick-Muraca, E., and Rooney, C. M. (2008) In vivo fluorescent optical imaging of cytotoxic T lymphocyte migration using IRDye800CW near-infrared dye, *Appl Optics* 47, 5944-5952.
13. Swirski, F. K., Berger, C. R., Figueiredo, J. L., Mempel, T. R., von Andrian, U. H., Pittet, M. J., and Weissleder, R. (2007) A near-infrared cell tracker reagent for multiscopic in vivo imaging and quantification of leukocyte immune responses, *Plos One* 2, e1075.

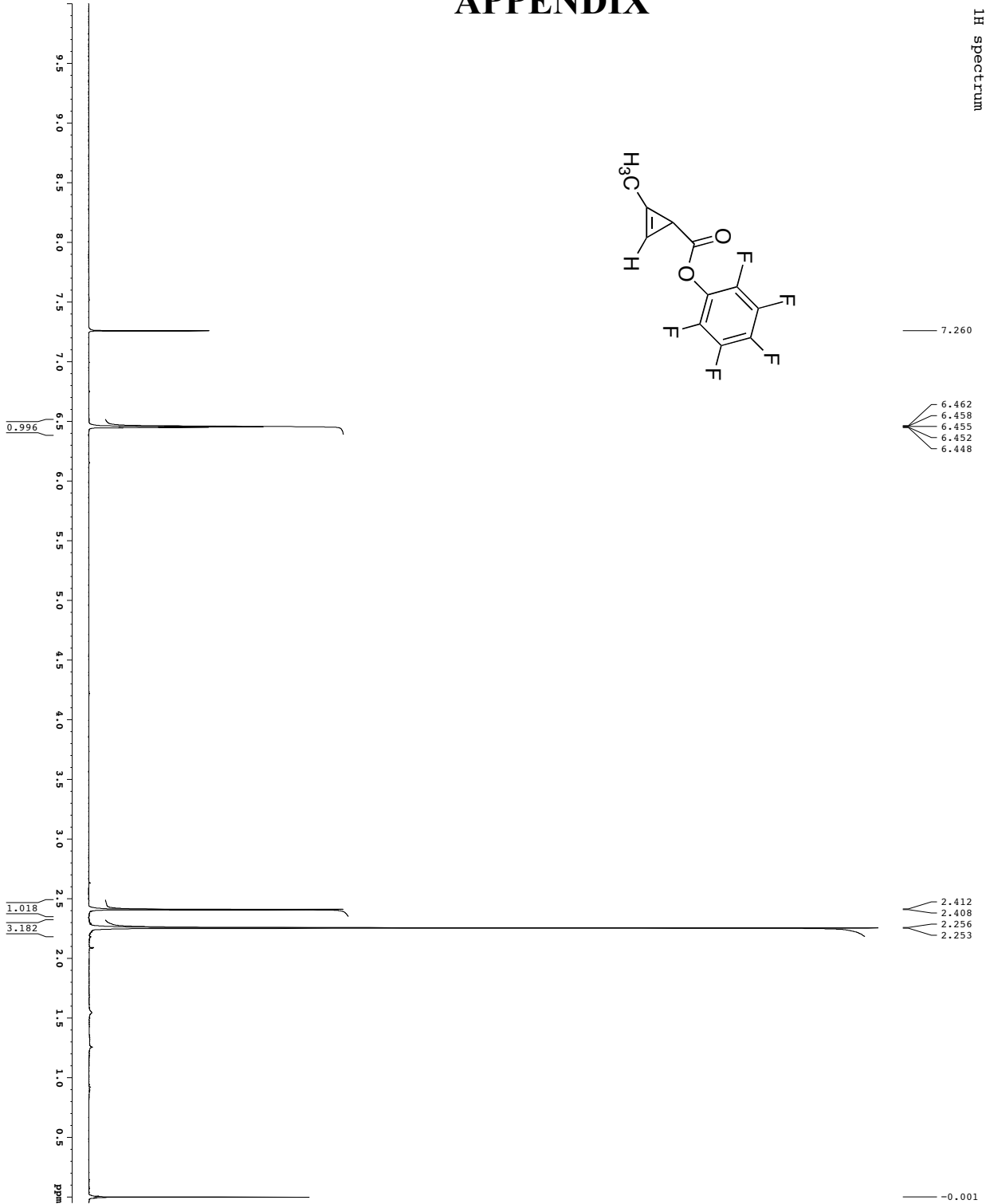
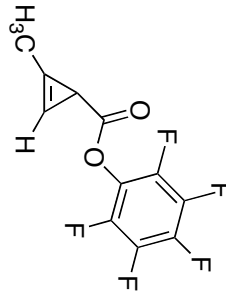
14. Tannous, B. A., Kim, D. E., Fernandez, J. L., Weissleder, R., and Breakefield, X. O. (2005) Codon-optimized *Gaussia luciferase* cDNA for mammalian gene expression in culture and in vivo, *Mol Ther* 11, 435-443.
15. Tannous, B. A. (2009) *Gaussia luciferase* reporter assay for monitoring biological processes in culture and in vivo, *Nat Protoc* 4, 582-591.
16. Santos, E. B., Yeh, R., Lee, J., Nikhamin, Y., Punzalan, B., Punzalan, B., La Perle, K., Larson, S. M., Sadelain, M., and Brentjens, R. J. (2009) Sensitive in vivo imaging of T cells using a membrane-bound *Gaussia princeps luciferase*, *Nat Med* 15, 338-344.
17. Rabuka, D., Rush, J. S., deHart, G. W., Wu, P., and Bertozzi, C. R. (2012) Site-specific chemical protein conjugation using genetically encoded aldehyde tags, *Nat Protoc* 7, 1052-1067.
18. Carlson, B. L., Ballister, E. R., Skordalakes, E., King, D. S., Breidenbach, M. A., Gilmore, S. A., Berger, J. M., and Bertozzi, C. R. (2008) Function and structure of a prokaryotic formylglycine-generating enzyme, *J Biol Chem* 283, 20117-20125.
19. Patterson, D. M., Nazarova, L. A., and Prescher, J. A. (2014) Finding the right (bioorthogonal) chemistry, *ACS Chem Biol* 9, 592-605.
20. Ulrich, S., Boturyn, D., Marra, A., Renaudet, O., and Dumy, P. (2014) Oxime ligation: A chemoselective click-type reaction for accessing multifunctional biomolecular constructs, *Chem Eur J* 20, 34-41.
21. Zeng, Y., Ramya, T. N. C., Dirksen, A., Dawson, P. E., and Paulson, J. C. (2009) High-efficiency labeling of sialylated glycoproteins on living cells, *Nat Methods* 6, 207-209.
22. Popp, M. W. L., and Ploegh, H. L. (2011) Making and breaking peptide bonds: protein engineering using sortase, *Angew Chem Int Edit* 50, 5024-5032.
23. Guimaraes, C. P., Witte, M. D., Theile, C. S., Bozkurt, G., Kundrat, L., Blom, A. E. M., and Ploegh, H. L. (2013) Site-specific C-terminal and internal loop labeling of proteins using sortase-mediated reactions, *Nat Protoc* 8, 1787-1799.
24. Popp, M. W., Antos, J. M., Grotenbreg, G. M., Spooner, E., and Ploegh, H. L. (2007) Sortagging: a versatile method for protein labeling, *Nat Chem Biol* 3, 707-708.
25. Rashidian, M., Keliher, E. J., Bilate, A. M., Duarte, J. N., Wojtkiewicz, G. R., Jacobsen, J. T., Cragolini, J., Swee, L. K., Vitoria, G. D., Weissleder, R., and Ploegh, H. L. (2015) Noninvasive imaging of immune responses, *Proc Natl Acad Sci U S A* 112, 6146-6151.

26. Swee, L. K., Lourido, S., Bell, G. W., Ingram, J. R., and Ploegh, H. L. (2015) One-step enzymatic modification of the cell surface redirects cellular cytotoxicity and parasite tropism, *ACS Chem Biol* 10, 460-465.
27. Wagner, K., Kwakkenbos, M. J., Claassen, Y. B., Maijoor, K., Bohne, M., van der Sluijs, K. F., Witte, M. D., van Zoelen, D. J., Cornelissen, L. A., Beaumont, T., Bakker, A. Q., Ploegh, H. L., and Spits, H. (2014) Bispecific antibody generated with sortase and click chemistry has broad antiinfluenza virus activity, *Proc Natl Acad Sci USA* 111, 16820-16825.
28. Selden, N. S., Todhunter, M. E., Jee, N. Y., Liu, J. S., Broaders, K. E., and Gartner, Z. J. (2012) Chemically programmed cell adhesion with membrane-anchored oligonucleotides, *J Am Chem Soc* 134, 765-768.
29. Hang, H. C., Wilson, J. P., and Charron, G. (2011) Bioorthogonal chemical reporters for analyzing protein lipidation and lipid trafficking, *Acc Chem Res* 44, 699-708.
30. Yang, J., Seckute, J., Cole, C. M., and Devaraj, N. K. (2012) Live-cell imaging of cyclopropene tags with fluorogenic tetrazine cycloadditions, *Angew Chem Int Edit* 51, 7476-7479.
31. Friscourt, F., Ledin, P. A., Mbua, N. E., Flanagan-Steet, H. R., Wolfert, M. A., Steet, R., and Boons, G. J. (2012) Polar dibenzocyclooctynes for selective labeling of extracellular glycoconjugates of living cells, *J Am Chem Soc* 134, 5381-5389.
32. Borrmann, A., Milles, S., Plass, T., Dommerholt, J., Verkade, J. M. M., Wiessler, M., Schultz, C., van Hest, J. C. M., van Delft, F. L., and Lemke, E. A. (2012) Genetic encoding of a bicyclo[6.1.0]nonyne-charged amino acid enables fast cellular protein imaging by metal-free ligation, *ChemBioChem* 13, 2094-2099.
33. Zakeri, B., Fierer, J. O., Celik, E., Chittock, E. C., Schwarz-Linek, U., Moy, V. T., and Howarth, M. (2012) Peptide tag forming a rapid covalent bond to a protein, through engineering a bacterial adhesin, *Proc Natl Acad Sci U S A* 109, E690-697.
34. Rudd, A. K., Valls Cuevas, J. M., and Devaraj, N. K. (2015) SNAP-tag-reactive lipid anchors enable targeted and spatiotemporally controlled localization of proteins to phospholipid membranes, *J Am Chem Soc* 137, 4884-4887.
35. Jones, K. A., Li, D. J., Hui, E., Sellmyer, M. A., and Prescher, J. A. (2015) Visualizing cell proximity with genetically encoded bioluminescent reporters, *ACS Chem Biol* 10, 933-938.

36. Rathnayaka, T., Tawa, M., Nakamura, T., Sohya, S., Kuwajima, K., Yohda, M., Kuroda, Y. (2011) Solubilization and folding of a fully active recombinant *Gaussia* luciferase with native disulfide bonds by using a SEP-Tag, *Biochim Biophys Acta* 1814, 1775-1778.
37. Sadamoto, R., Niikura, K., Ueda, T., Monde, K., Fukuhara, N., Nishimura, S-I. (2004) Control of bacterial adhesion by cell-wall adhesion, *J Am Chem Soc* 126, 3755-3761.
38. Patterson, D. M., Jones, K. A., and Prescher, J. A. (2014) Improved cyclopropene reporters for probing protein glycosylation, *Mol Biosyst* 10, 1693-1697.
39. Karver, M. R., Weissleder, R., and Hilderbrand, S. A. (2011) Synthesis and evaluation of a series of 1,2,4,5-tetrazines for bioorthogonal conjugation, *Bioconjug Chem* 22, 2263-2270.

APPENDIX

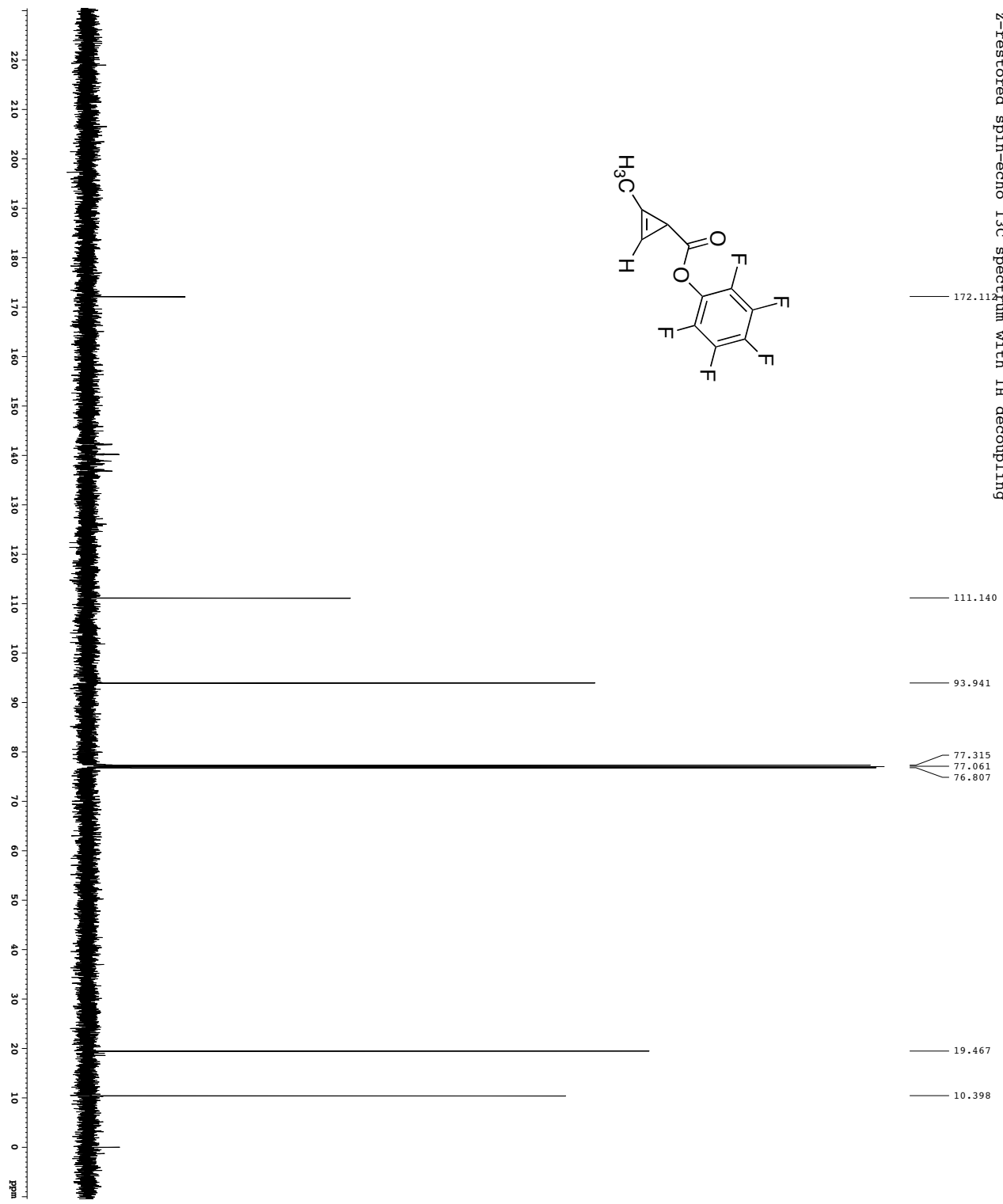
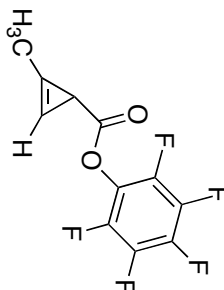
¹H spectrum



Current Data Parameters

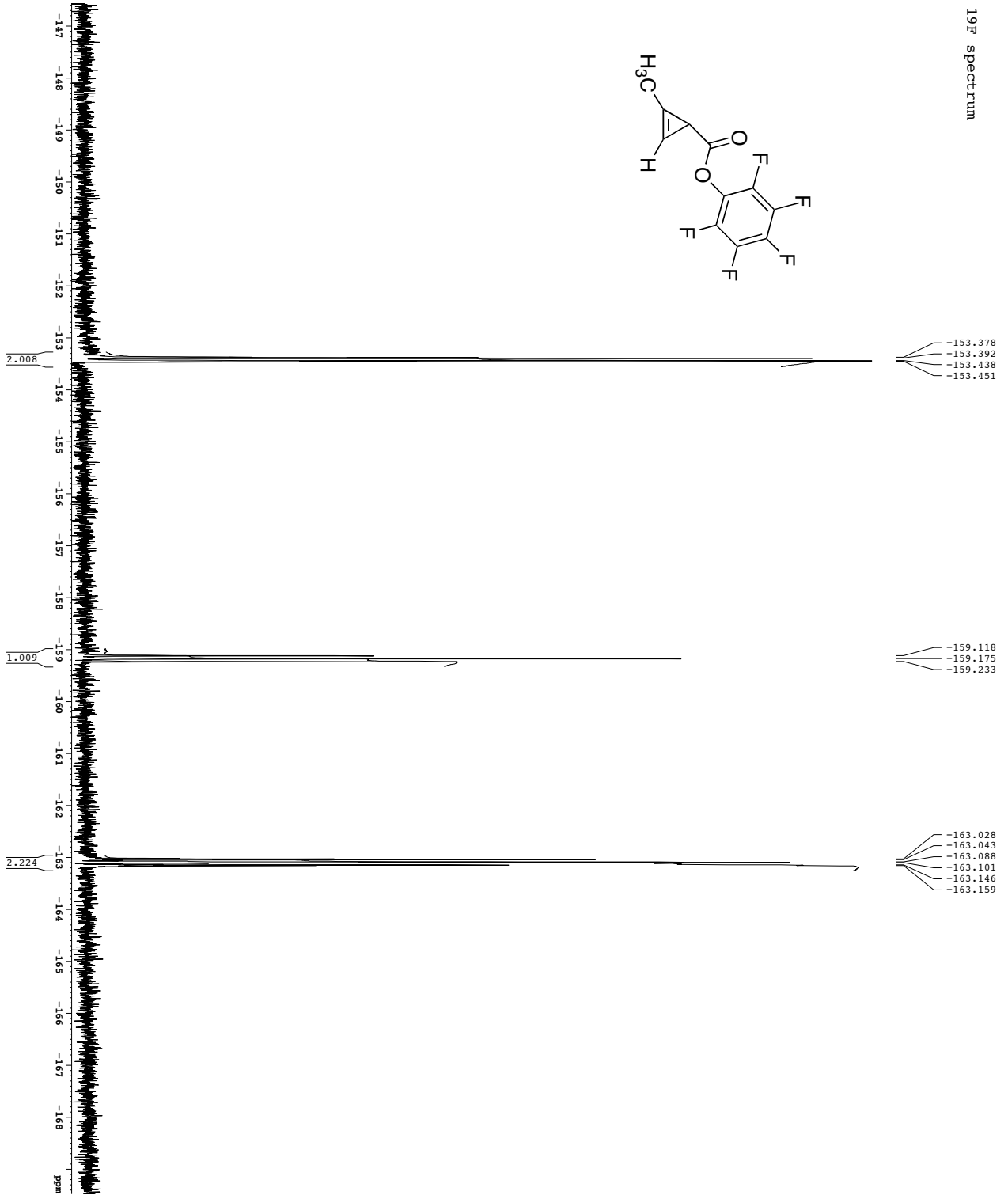
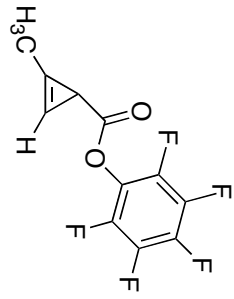
USER	BYRNK
EXPNO	1
PROCNO	1
F2 - Acquisition Parameters	
Date_	2010228
Time	12:40
PROBHD	5 mm QNP 1H/13
PROG	zgpg30
TD	65536
NO	NOVENT
NUC1	13C
NUC2	1H
NUC3	13C
NUC4	13C
NUC5	13C
NUC6	13C
NUC7	13C
NUC8	13C
NUC9	13C
NUC10	13C
NUC11	13C
NUC12	13C
NUC13	13C
NUC14	13C
NUC15	13C
NUC16	13C
NUC17	13C
NUC18	13C
NUC19	13C
NUC20	13C
NUC21	13C
NUC22	13C
NUC23	13C
NUC24	13C
NUC25	13C
NUC26	13C
NUC27	13C
NUC28	13C
NUC29	13C
NUC30	13C
NUC31	13C
NUC32	13C
NUC33	13C
NUC34	13C
NUC35	13C
NUC36	13C
NUC37	13C
NUC38	13C
NUC39	13C
NUC40	13C
NUC41	13C
NUC42	13C
NUC43	13C
NUC44	13C
NUC45	13C
NUC46	13C
NUC47	13C
NUC48	13C
NUC49	13C
NUC50	13C
NUC51	13C
NUC52	13C
NUC53	13C
NUC54	13C
NUC55	13C
NUC56	13C
NUC57	13C
NUC58	13C
NUC59	13C
NUC60	13C
NUC61	13C
NUC62	13C
NUC63	13C
NUC64	13C
NUC65	13C
NUC66	13C
NUC67	13C
NUC68	13C
NUC69	13C
NUC70	13C
NUC71	13C
NUC72	13C
NUC73	13C
NUC74	13C
NUC75	13C
NUC76	13C
NUC77	13C
NUC78	13C
NUC79	13C
NUC80	13C
NUC81	13C
NUC82	13C
NUC83	13C
NUC84	13C
NUC85	13C
NUC86	13C
NUC87	13C
NUC88	13C
NUC89	13C
NUC90	13C
NUC91	13C
NUC92	13C
NUC93	13C
NUC94	13C
NUC95	13C
NUC96	13C
NUC97	13C
NUC98	13C
NUC99	13C
NUC100	13C

Z-restored spin-echo 13C spectrum with 1H decoupling



Current Data Parameters
 USER: BRYAN
 EXPTNO: 1
 PROCNO: 1
 F2 - Acquisition Parameters
 Date_: 201228
 Time: 10:24
 INSTRUM: cryo500
 PROCDM: 5 mm CPDCL 1H-
 PULPROG: zgpg30
 TD: 65536
 SFO: 125.761953
 SOLVENT: CDCl3
 NS: 16
 DS: 4
 SWH: 30343.16 Hz
 SF: 101262.818 Hz
 AQ: 1.0813940 sec
 RG: 656
 FIDRES: 16.500 usec
 DE: 6.00 usec
 DI: 0.23000000 sec
 d11: 0.43000000 sec
 d17: 0.00019600 sec
 ACQRES1: 0.40000000 sec
 ACQRES2: 0.01313100 sec
 F2 - Processing parameters
 SF: 125.7604190 MHz
 DS: 4
 AS: 32768
 LA: 1.00 Hz
 GB: 0
 PC: 2.00

19F spectrum



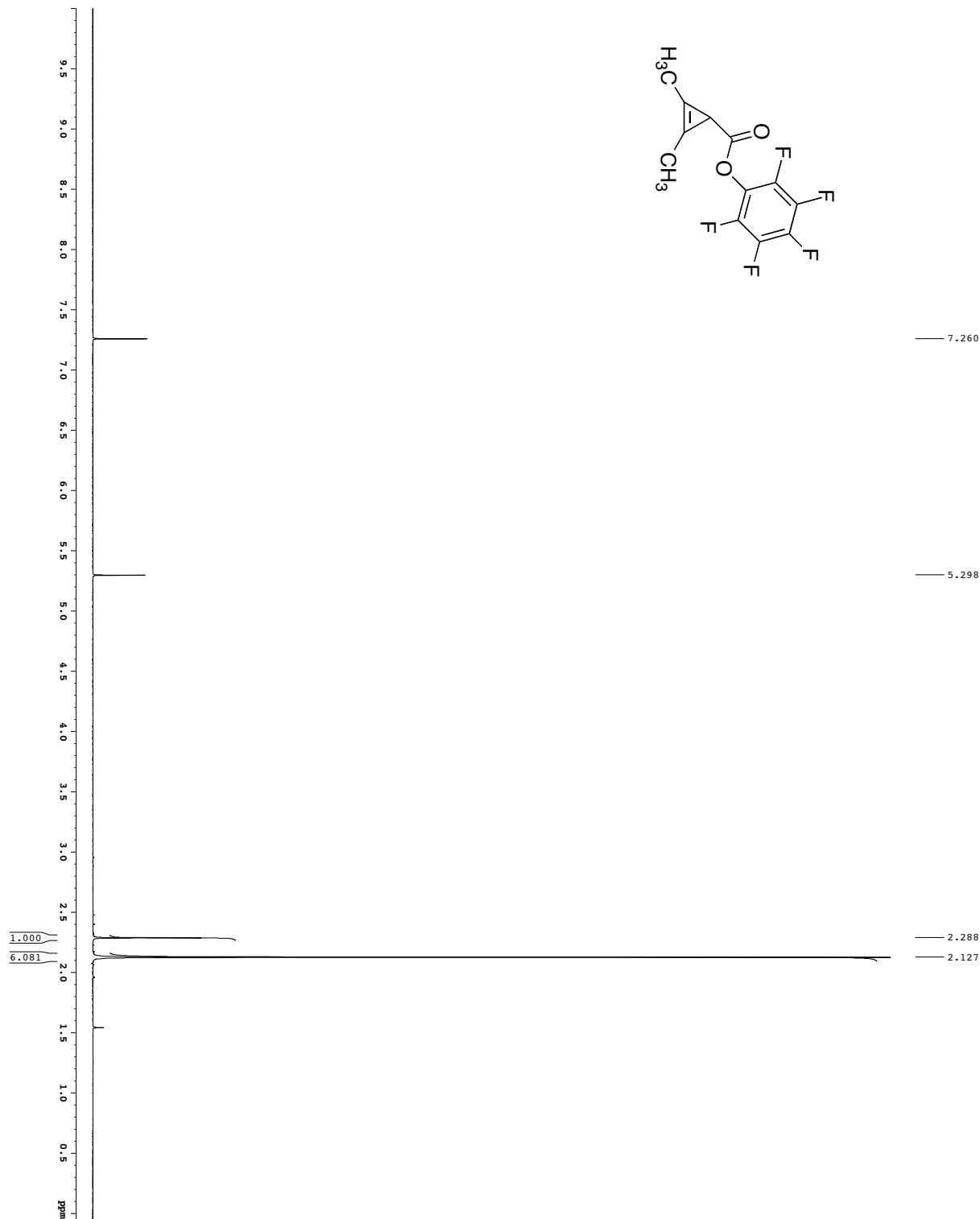
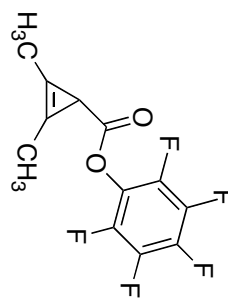
-153.378
-153.392
-153.436
-153.451

-159.118
-159.175
-159.233

-163.028
-163.043
-163.088
-163.101
-163.146
-163.159

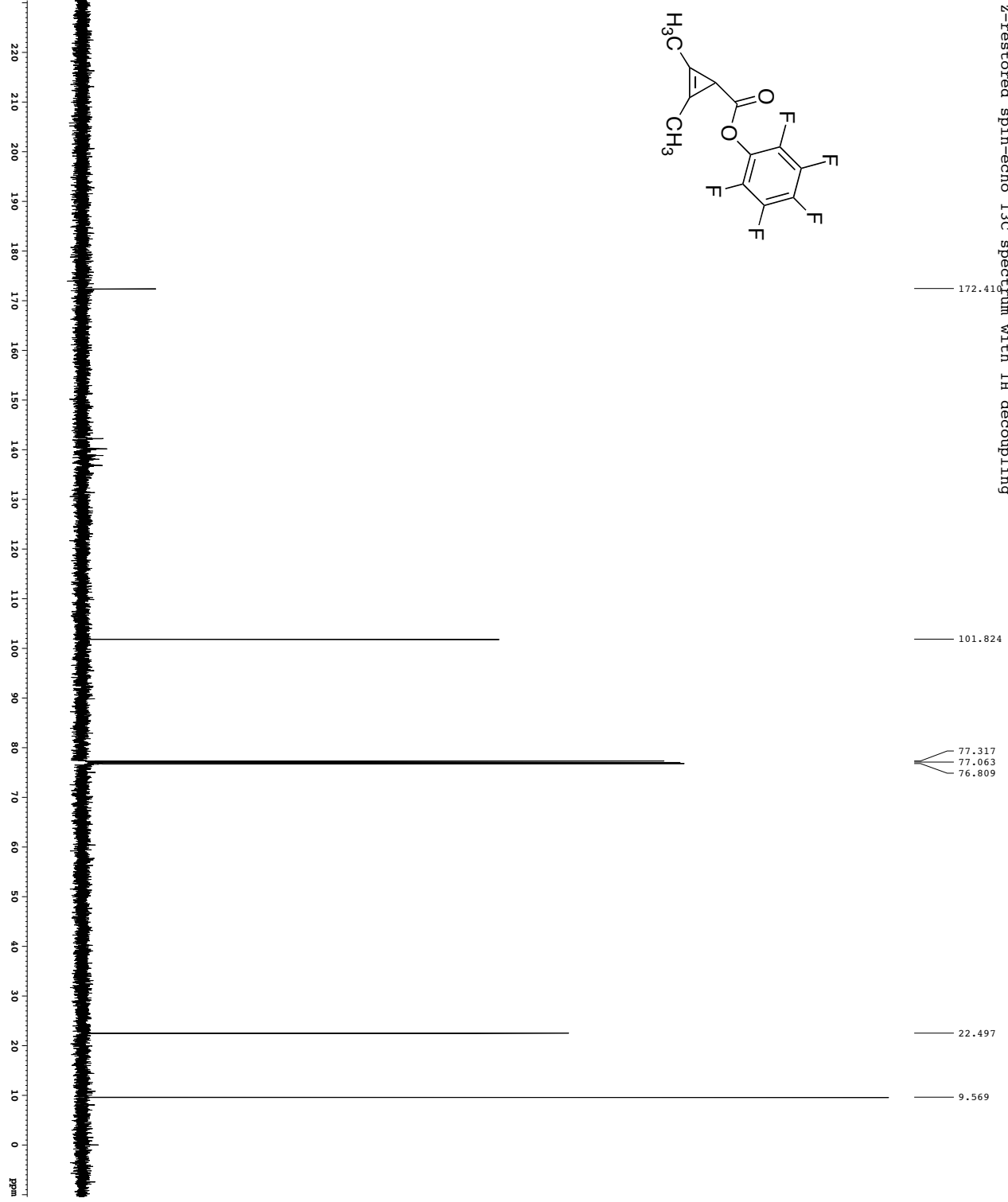
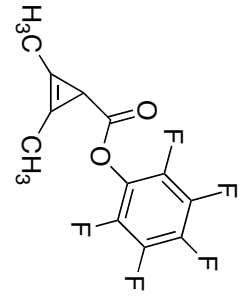
Current Data Parameters
 USER Bruker
 EXPNO 3
 PROCNO 1
 F2 - Acquisition Parameters
 Date_ 20110228
 Time 09:40
 INSTRUM 5 mm QNP HX 77P
 PROBRID 5 mm QNP HX 77P
 P1 12.00000000
 TO 65536
 SOLVENT CDCl3
 NS 2
 DS 72187.427 Hz
 SFORES 11177279 Hz
 AQ 0.4358644 sec
 RG 296.650 usec
 DE 9.46 usec
 DI 2.00000000 sec
 CHANNEL F1 19F
 NUC1 19F
 P1 55.00 usec
 SFO1 376.4232183 MHz
 F2 - Processing parameters
 SI 65536
 SF 376.4984640 MHz
 FIDRES 0
 SSB 0.30 Hz
 GB 0
 PC 1.00

¹H spectrum



Current Data Parameters
 USER: gmark
 SAMPLE: 2501
 EXPTNO: 1
 PROCNO: 1
 F2 - Acquisition Parameters
 Date_: 20110929
 Time: 14:40:44
 INSTRUM: spect
 PROBP1: 5 mm QNP 1H/2
 P1: 12.00
 P1 DELTA: 6.5536
 SOLVENT: CDCl3
 NS: 2
 DS: 4
 SWH: 6418.242 Hz
 SFO: 400.7618 MHz
 AQ: 5.118579 sec
 RG: 78.002
 DE: 4.50 usec
 DI: 0.10000000 sec
 D1 DELTA: 0.00000000 sec
 ACQ: 0.01500000 sec
 CHANNEL: F1
 P1: 12.00 usec
 P1 DELTA: -0.60 dB
 SFO1: 400.132809 MHz
 F2 - Processing Parameters
 SF: 400.130218 MHz
 MDW: EM
 LB: 0.30 Hz
 GB: 0
 PC: 2.00

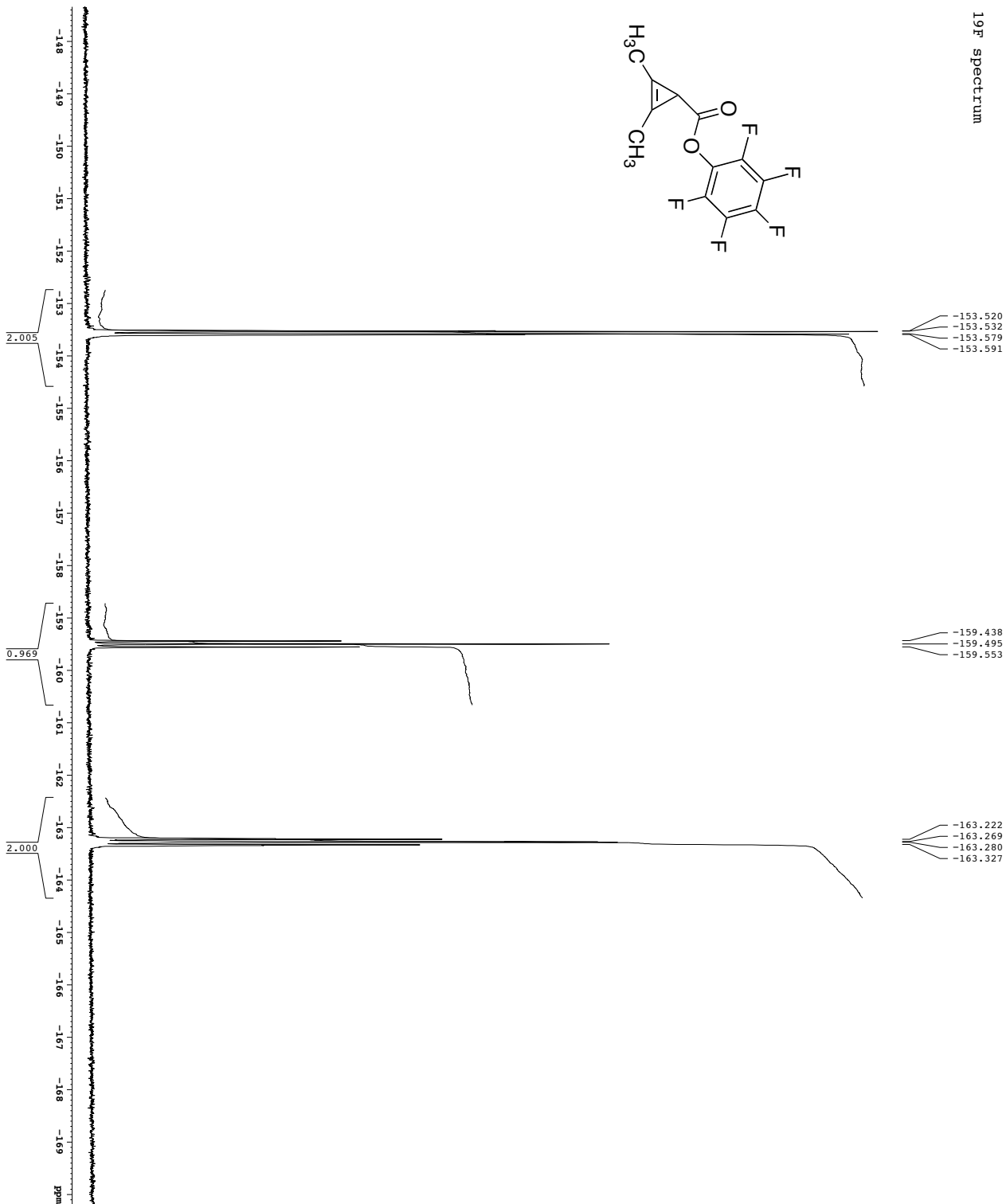
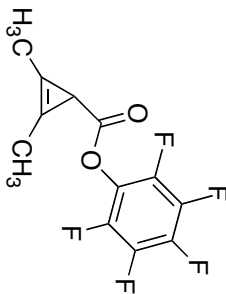
Z-restored spin-echo 13C spectrum with 1H decoupling



Current Data Parameters
 USER galle
 EXPNO 2
 PROCNO 1
 F2 - Acquisition Parameters
 Date_ 20121227
 Time 12:23:13
 INSTRUM cryo500
 PROBRD 5 mm CPYX 1H-13
 PULPROG zgpg30
 TD 65536
 SFO 125.760
 SOLVENT CDCl3
 DS 4
 SWH 16183.16 Hz
 SF 125760.136 MHz
 SFR 1.00000000 sec
 AQ 1.0813940 sec
 RG 655
 FIDRES 0.490 Hz
 AQ 16.500 usec
 DE 6.00 usec
 DI 0.25000000 sec
 D1 0.43000000 sec
 d11 0.43000000 sec
 d17 0.00019600 sec
 MCXRES* 0.00000000 sec
 P2 0.01331000 usec
 P2 0.01331000 usec

===== CHANNEL f1 =====
 NUC1 13C
 P1 15.50 usec
 PL1 0.00 dB
 P2 2000.00 usec
 PL2 120.00 dB
 SFO1 125.7603548 MHz
 SP1 3.20 dB
 SP2 3.20 dB
 SPANM1 CPM60,0.5,20.1 Hz
 SPANM2 CPM60comp,4 Hz
 SFOF2 0.00 Hz
 ===== CHANNEL f2 =====
 CPDPRG2 waltz16
 NUC2 1H
 P1 100.00 usec
 PL1 0.00 dB
 P2 1.00 dB
 SFO2 500.2625191 MHz
 ===== GRADIENT CHANNEL =====
 SPANM3 SINE,100 Hz
 GPMX2 0.00 %
 GPMX1 0.00 %
 GPY1 0.00 %
 GPX2 30.00 %
 GPY2 30.00 %
 GPZ2 50.00 %
 P1.5 1000.00 usec
 P1.6 1000.00 usec
 F2 - Processing parameters
 SF 125.7604190 MHz
 DS 4
 ASB 0
 LA 1.00 Hz
 PC 2.00

19F spectrum



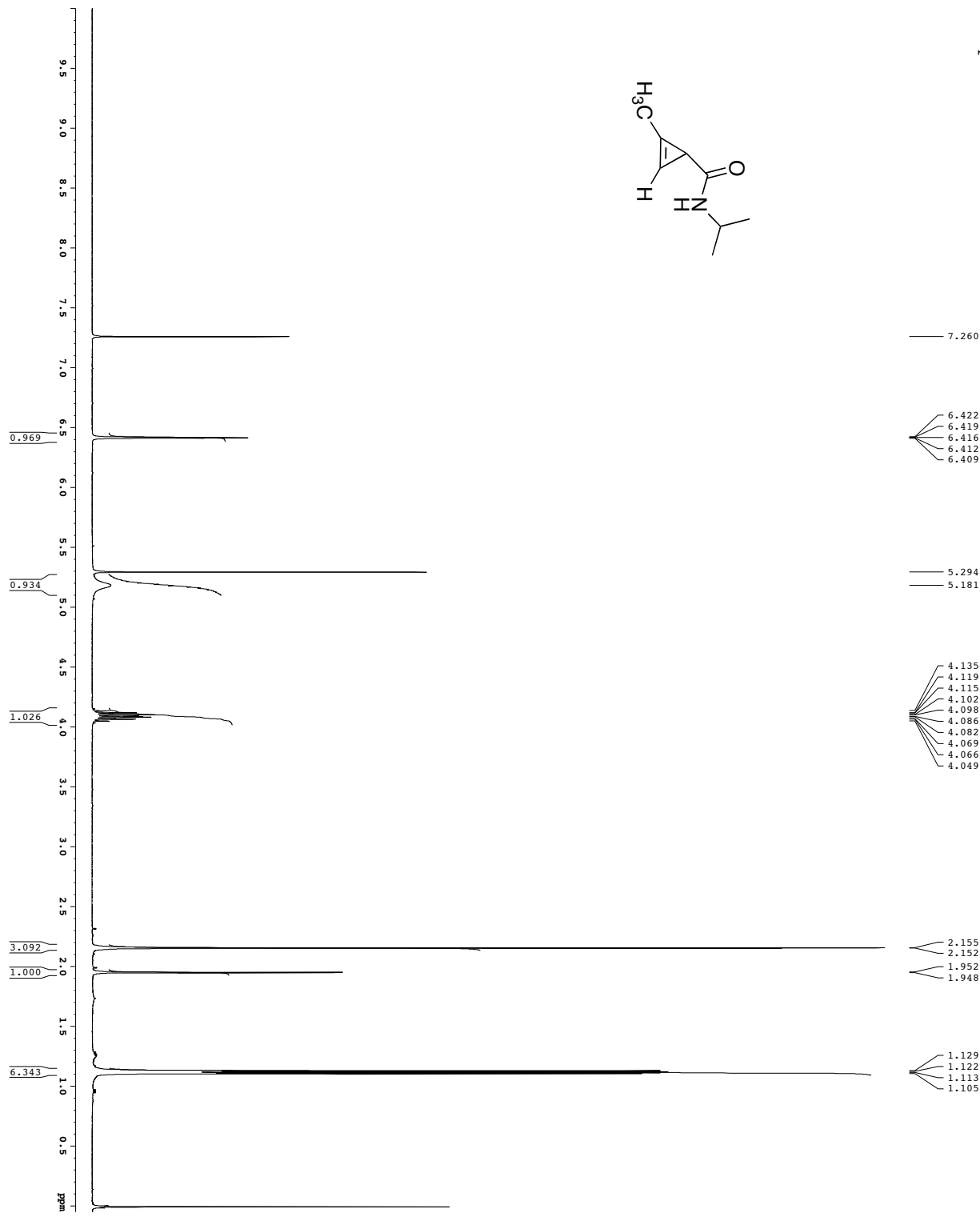
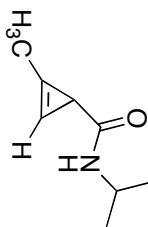
-153.520
-153.532
-153.579
-153.591

-159.438
-159.495
-159.553

-163.222
-163.269
-163.280
-163.327

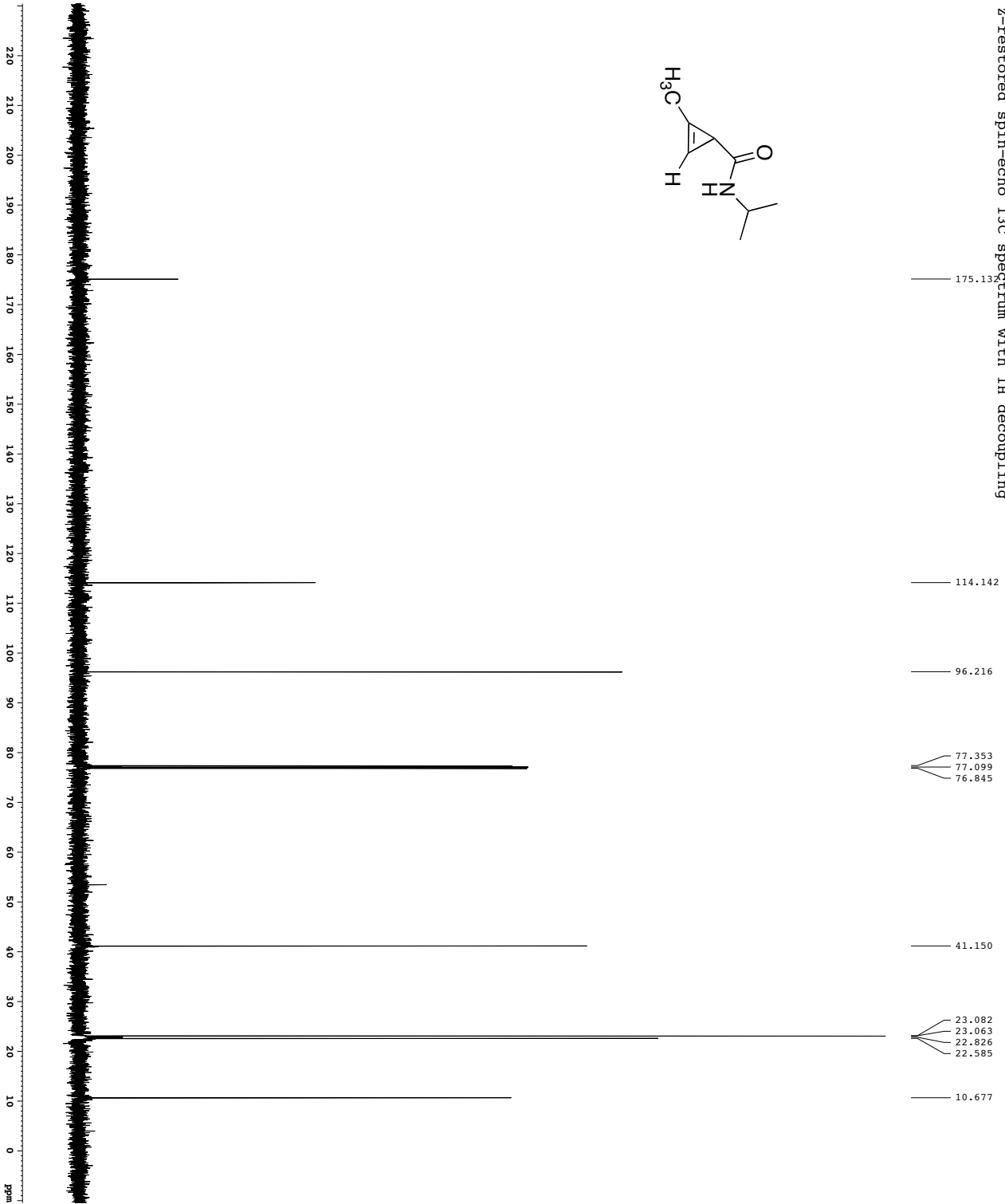
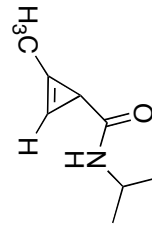
Current Data Parameters
 USER: b7max
 INSTRUM: EXNO
 EXNO: 2
 PROCNM: 1
 P2 - Acquisition Parameters
 Date_: 20110929
 Time: 11:27:29
 INSTRUM: 5 mm QNP HX 750
 PROBNM: dms-d400
 P1: 12.00000000
 TO: 6.5536
 SOLVENT: CDCl3
 NS: 2
 DS: 2
 SWH: 751.87429 Hz
 SFO: 121.272727 MHz
 AQ: 0.4338644 sec
 RG: 6.650
 DE: 9.46 usec
 DI: 2.00000000 sec
 CHANNE1: E1
 NIQC1: 19F
 P1: 55.00 usec
 SFO1: 376.4664491 MHz
 P2 - Processing parameters
 SI: 65536
 SF: 376.4984640 MHz
 SSF: 0
 SSB: 1.00 Hz
 GB: 0
 PC: 1.00

1H spectrum



Current Data Parameters
 USER: bpaux
 INSTRUM: EXNO
 EXNO: 1
 PROCNO: 1
 Date_: 201229
 Time: 22:40
 INSTRUM: 5 mm QNP HZ PZ
 PROBRD: d4-400
 P1: 12.00
 TO: 65536
 SOLVENT: CDCl3
 DS: 2
 SWH: 6418.242 Hz
 SFO: 64097.618 MHz
 AQ: 5.118579 sec
 RG: 655.36
 DE: 78.00 us
 DI: 4.50 us
 DE: 4.50 us
 DI: 0.10000000 sec
 ACQ: 0.00000000 sec
 PCW: 0.01500000 sec
 CHANNE1: F1
 P1: 12.00 us
 P1: -3.60 dB
 SFO1: 400.132809 MHz
 P2 - Processing Parameters
 SF: 400.130217 MHz
 MDW: EM
 LB: 0.30 Hz
 GB: 0
 PC: 2.00

Z-restored spin-echo 13C spectrum with 1H decoupling

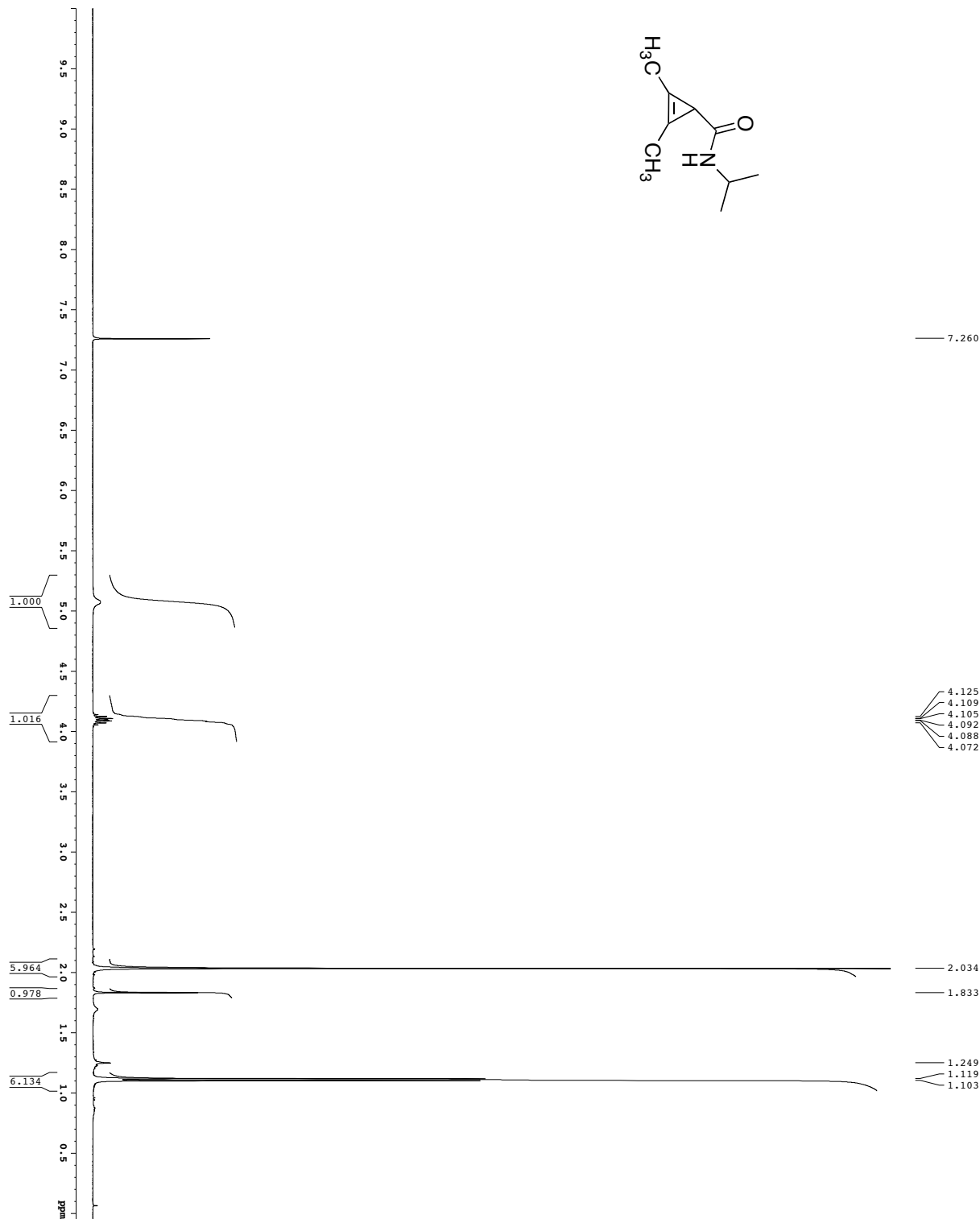
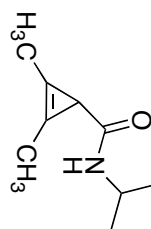


175.132
114.142
96.216
77.353
77.099
76.845
41.150
23.082
23.063
23.029
22.585
10.677

```

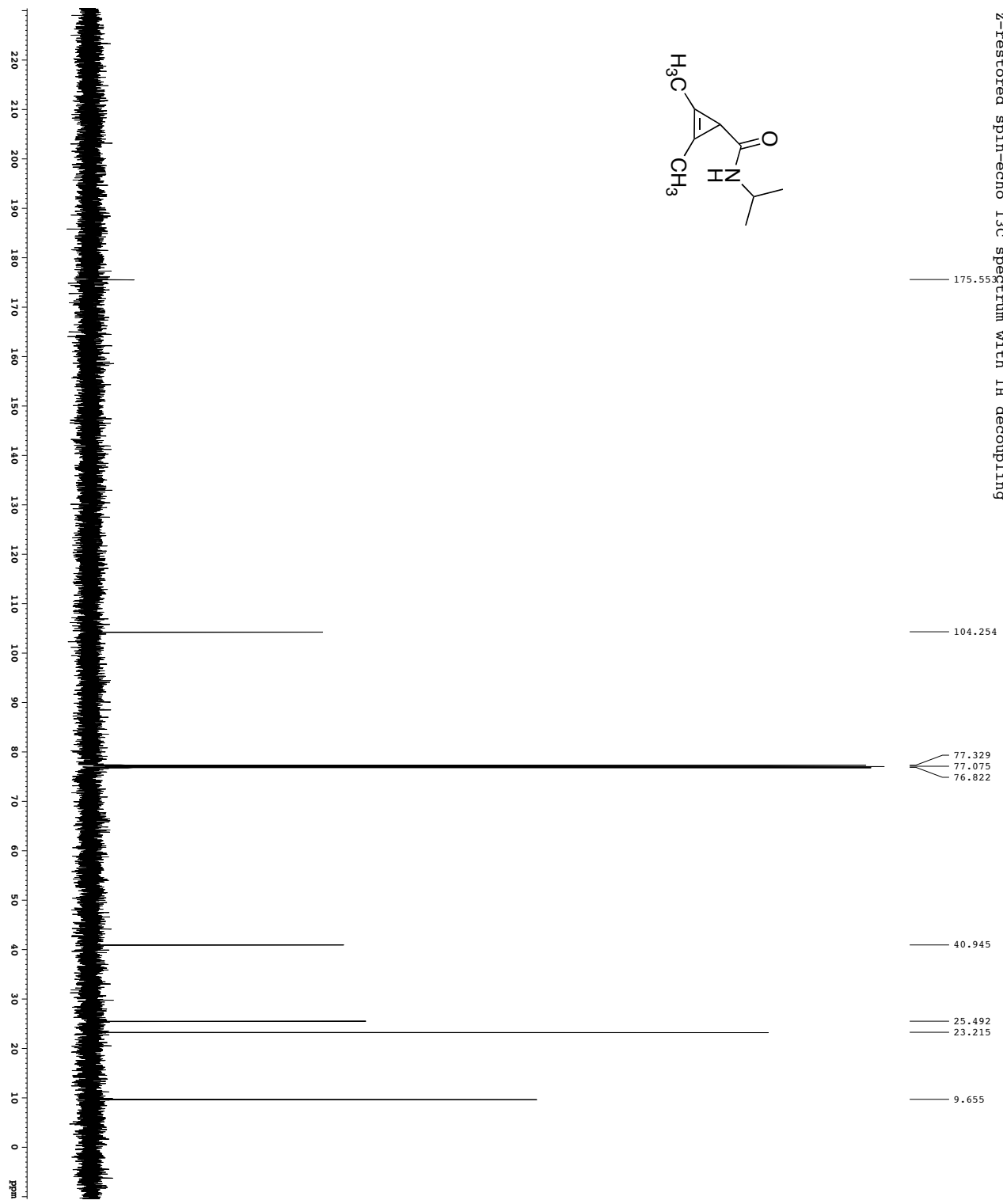
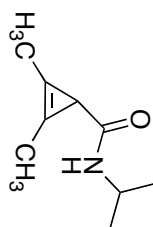
Current Data Parameters
=====
USER          :
DATE         :
TIME        :
EXPNO       : 9
PROCNO      : 1
F2 - Acquisition Parameters
=====
Date_        : 20111111
Time        : 17:11
INSTRUM     : cryo500
PROBHD     : 5 mm CPXI 1H-
PULPROG    : zgpg30
TD         : 65536
SOLVENT    : CDCl3
NS         : 16
DS         : 4
SWH        : 30181.16 Hz
FIDRES    : 0.462381 Hz
AQ        : 1.0813940 sec
RG        : 364.501
RG2       : 364.501
DE        : 6.00 usec
DI        : 0.23000000 sec
d11       : 0.43000000 sec
d12       : 0.00000000 sec
d17       : 0.00019600 sec
MCBRES7   : 0.00000000 sec
PC        : 0.01000000 sec
P2        : 0.01000000 sec
=====
===== CHANNEL f1 13C =====
NUC1       : 13C
P1         : 15.00 usec
PL1        : 0.00 dB
P2         : 2000.00 usec
PL2        : 1.00 dB
SFO1      : 125.7942548 MHz
SFO2      : 125.7942548 MHz
SF         : 125.7942548 MHz
WDW        : EM
SSB        : 0.00 Hz
GB         : 0.00 Hz
PC        : 2.00
===== CHANNEL f2 1H =====
NAME      : WATER16
NUC2       : 1H
P1         : 100.00 usec
PL1        : 1.00 dB
P2         : 1.00 dB
SFO1      : 500.2625111 MHz
===== GRADIENT CHANNEL =====
GPNAM1    : SINE-100
GPNAM2    : SINE-100
GB1X      : 0.00 %
GB2X      : 0.00 %
GB1Y      : 0.00 %
GB2Y      : 0.00 %
GB1Z      : 30.00 %
GB2Z      : 50.00 %
P15       : 100.00 usec
PC        : 100.00 usec
===== Processing parameters =====
SF        : 125.7804190 MHz
RG        : 364
AQ        : 1.00 Hz
PC        : 2.00
    
```

¹H spectrum



Current Data Parameters
 USER: b7mk
 EXPNO: 2571
 PROCNO: 1
 F2 - Acquisition Parameters
 Date_ : 20111011
 Time : 11:41
 INSTRUM: spect
 PROBMOD: 5 mm QNP H₂/P
 PULPROG: zgpg30
 TD: 65536
 TO: 6.556
 SOLVENT: CDCl₃
 NS: 2
 DS: 2
 SWH: 6418.242 Hz
 SFO: 400.7618 MHz
 AQ: 5.118579 sec
 RG: 327.5
 PFG: 78.002 usec
 DE: 4.50 usec
 DI: 4.00 usec
 D1: 0.10000000 sec
 ACQRES: 0.40000000 sec
 PCYCLE: 0.01500000 sec
 CHANNEL: f1
 P1: 12.00 usec
 P1C1: -4.60 dB
 SFO1: 400.125809 MHz
 F2 - Processing Parameters
 SF: 400.130216 MHz
 MDW: EM
 LB: 0.30 Hz
 GB: 0
 PC: 2.00

Z-restored spin-echo 13C spectrum with 1H decoupling

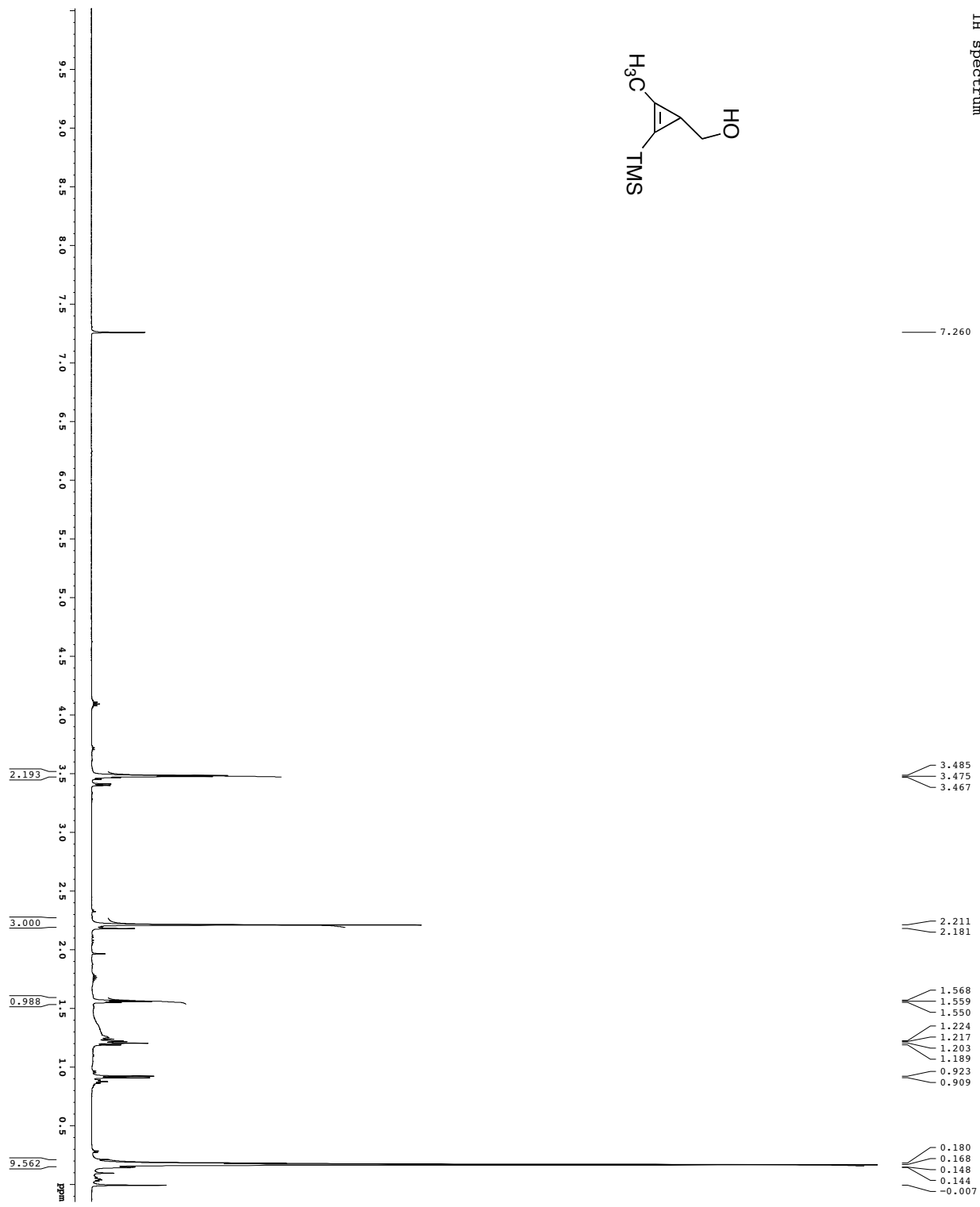
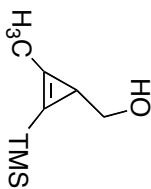


175.558
104.254
77.329
77.075
76.822
40.945
25.492
23.215
9.655

```

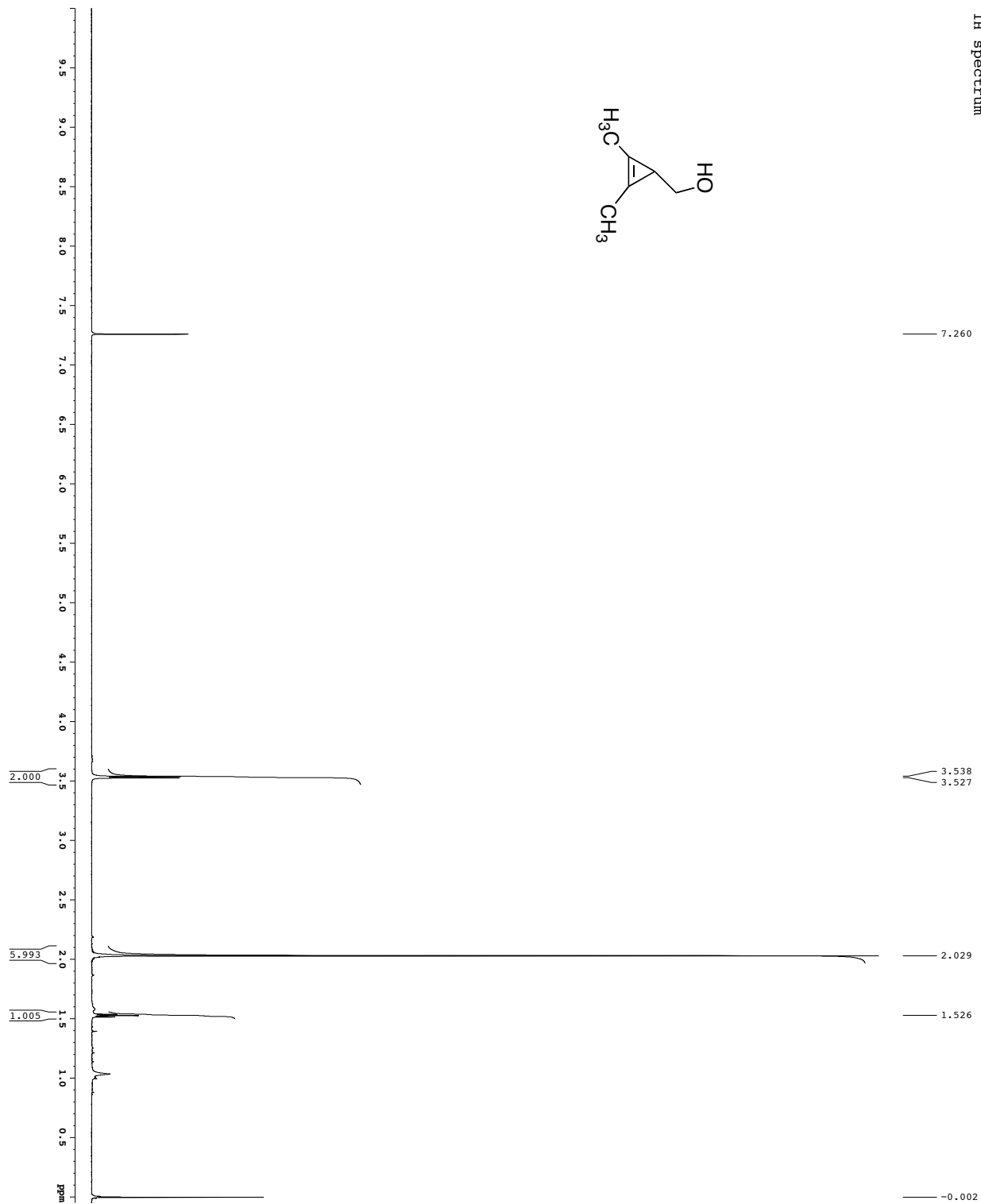
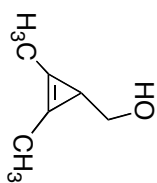
Current Data Parameters
=====
USER          gatte
DATE          2011
EXNO          0911
PROCNO       1
F2 - Acquisition Parameters
=====
Date_         2011011
Time_         14:43
INSTRUM      cryo500
PROBHD       5 mm CPY131
PULPROG      zgpg30
TD            65536
SOLVENT      CDCl3
NS           16
DS            16
SWH          30340.16 Hz
SF           125.760378 Hz
AQ           1.0813940 sec
RG           146.970
RG2          146.970
RG3          146.970
DE           6.00 usec
DI           0.25000000 sec
d11          0.43000000 sec
d17          0.00019600 sec
MCNRES7     0.00000000 sec
PC           0.01313100 usec
=====
===== CHANNEL F1 =====
NUC1         13C
P1           15.50 usec
PL1         -2.00 dB
PL2         2000.00 usec
PL3         120.00 dB
SFO1        125.760378 MHz
SP1         3.20 dB
SP2         3.20 dB
SFO2        CPD60,0.520,1
SFO3        CPD60comp,4
SFO4        0.00 Hz
SFO5        0.00 Hz
===== CHANNEL F2 =====
CPDPRG2     waltz16
NUC2         1H
P2           100.00 usec
PL2         -1.00 dB
PL3         50.262911 MHz
=====
===== GRADIENT CHANNEL =====
GPNAM1      SINE.100
GPNAM2      SINE.100
GB1         0.00 %
GB2         0.00 %
GB3         0.00 %
GB4         0.00 %
GB5         0.00 %
GB6         0.00 %
GB7         30.00 %
GB8         30.00 %
GB9         50.00 %
P1.5        100.00 usec
P1.6        100.00 usec
=====
F2 - Processing parameters
=====
SF           125.7604190 MHz
AQ           20
RG           147
PC           2.00
  
```


¹H spectrum



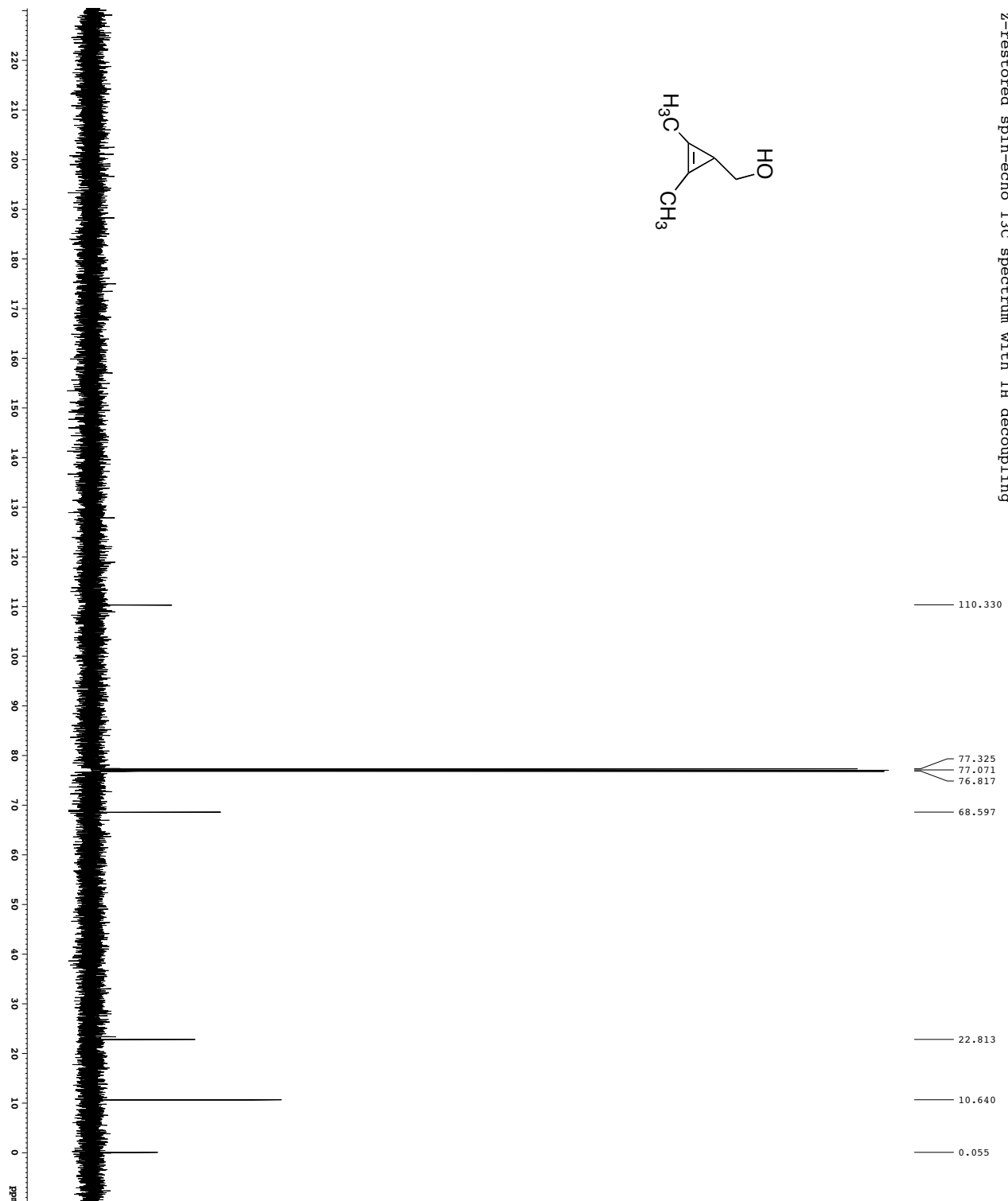
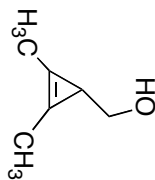
Current Data Parameters
 USER: gpatte
 DATE: 08/15/00
 EXNO: 1
 PROCNO: 1
 F2 - Acquisition Parameters
 Date_: 2011110
 Time: 11.24
 INSTRUM: cryo500
 PROBMOD: 5 mm CPY-500
 PULPROG: zgpg30
 TD: 65536
 FIDRES: 0.1728
 AQ: 81.728
 SOLVENT: CDCl3
 DS: 2
 SWH: 8812.420 Hz
 SFO: 500.136199 MHz
 SFRES: 0.000604 Hz
 AQ: 5.0998774 sec
 RG: 655.360
 RW: 62.400 usec
 DE: 6.00 usec
 DI: 8 usec
 D1: 0.10000000 sec
 ACQRES: 0.40000000 sec
 FIDRES: 0.01500000 sec
 CHANNEL: F1
 P1: 7.50 usec
 P1C1: 1.60 dB
 SFO1: 500.225015 MHz
 F2 - Processing parameters
 SF: 500.2260221 MHz
 MDW: EM
 LB: 0.30 Hz
 GB: 0
 PC: 4.00

¹H spectrum



Current Data Parameters
 USER: h2yax
 EXPNO: 1
 PROCNO: 1
 F2 - Acquisition Parameters
 Date_: 2012/03/06
 Time: 12:46
 INSTRUM: h2yax
 PROBMOD: 5 mm QNP 1H/2
 PULPROG: zgpg30
 TO: 65536
 SOLVENT: CDCl3
 NS: 2
 DS: 2
 SWH: 6418.242 Hz
 SF: 400.7618 MHz
 AQ: 5.118579 sec
 RG: 44.01 usec
 RW: 78.00 usec
 DE: 4.50 usec
 DI: 0.10000000 sec
 D1: 0.10000000 sec
 ACQRES: 0.01500000 sec
 CHANNEL: f1
 P1: 12.00 usec
 P1C1: -9.60 dB
 SFO1: 400.125809 MHz
 F2 - Processing Parameters
 SF: 400.130217 MHz
 MDW: EM
 LB: 0.30 Hz
 GB: 0
 PC: 2.00

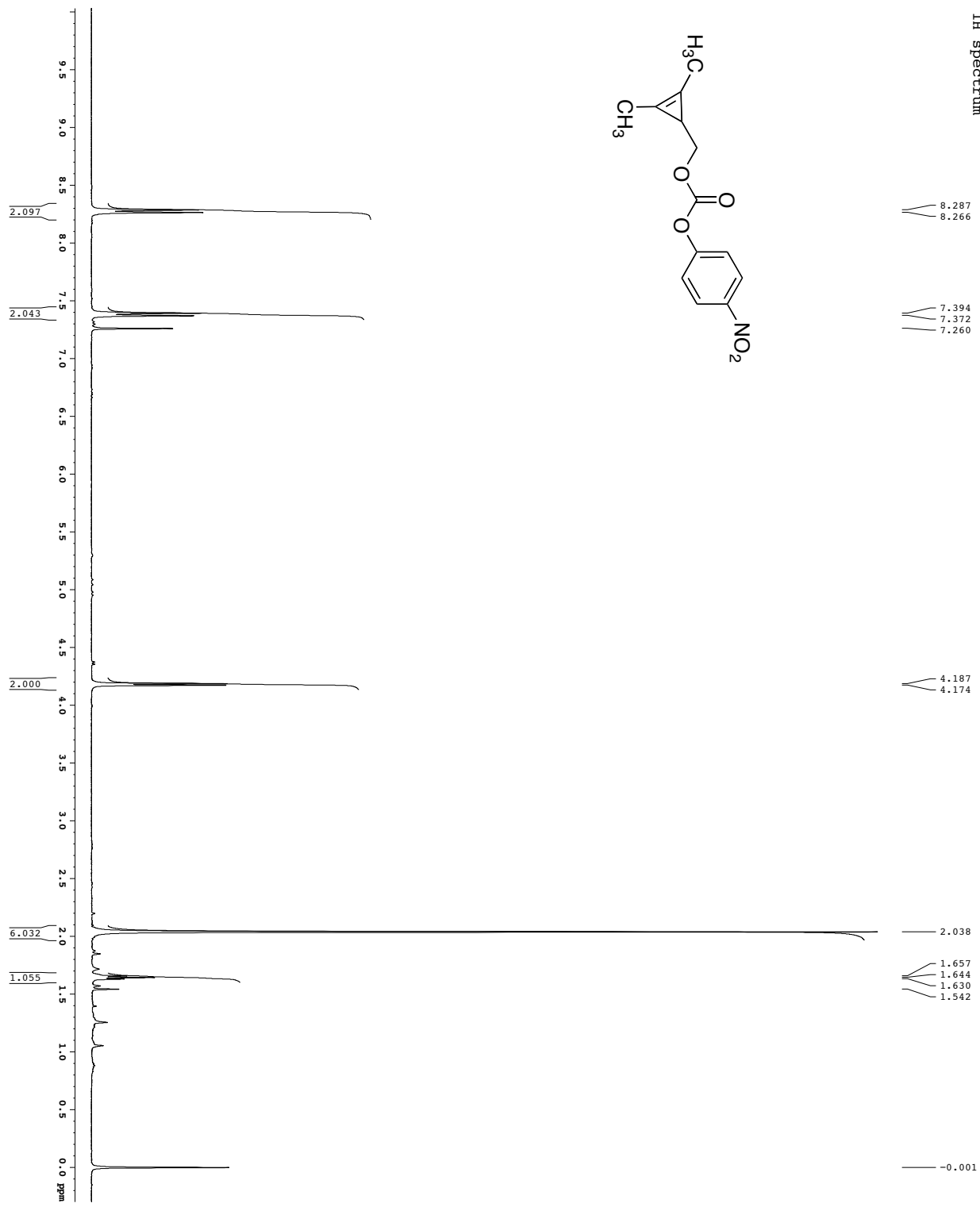
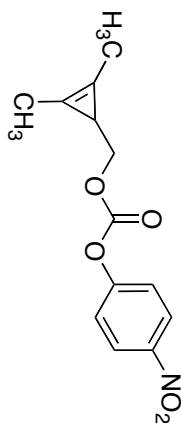
Z-restored spin-echo 13C spectrum with 1H decoupling



110.330
 77.325
 77.071
 76.817
 68.597
 22.813
 10.640
 0.055

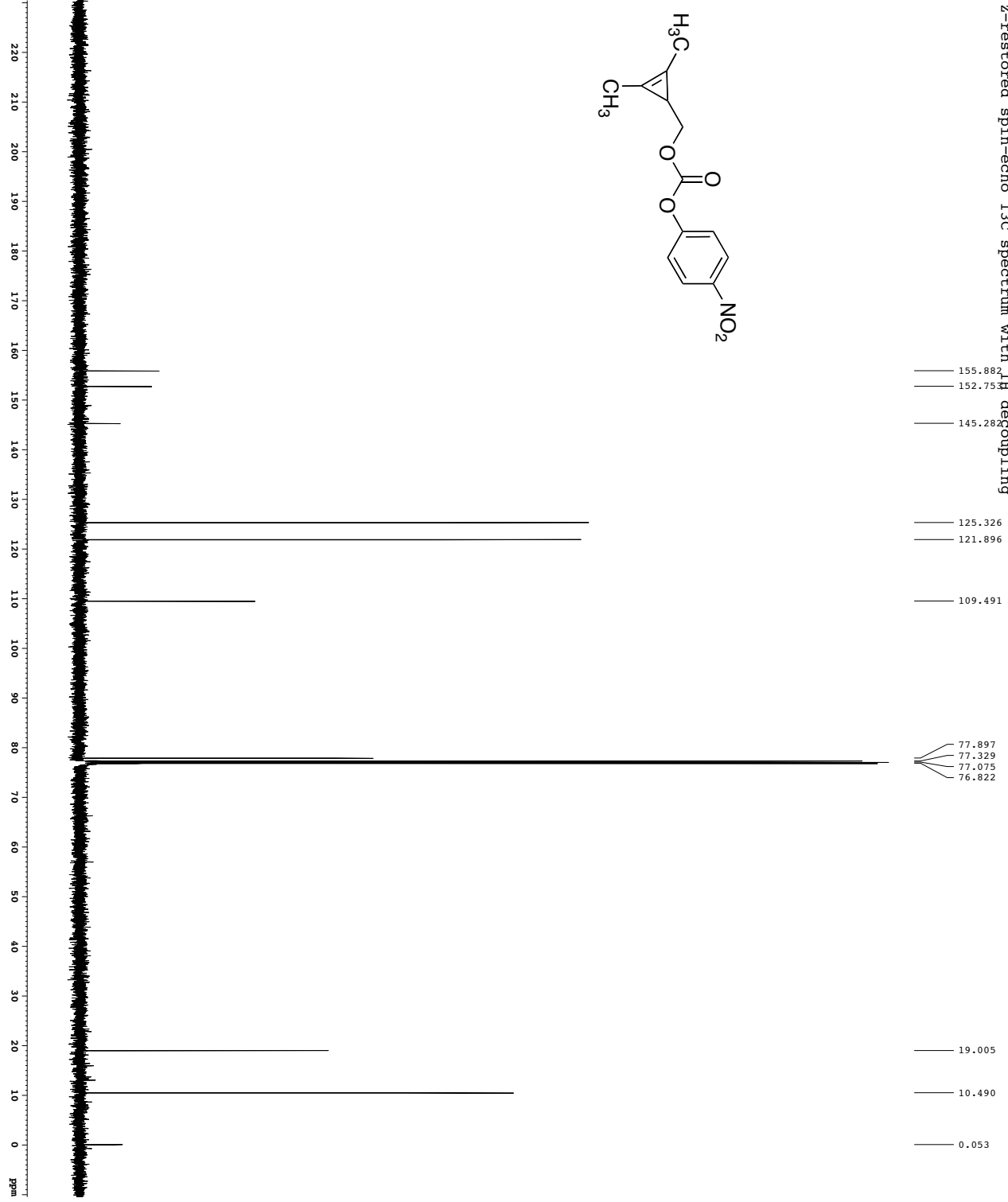
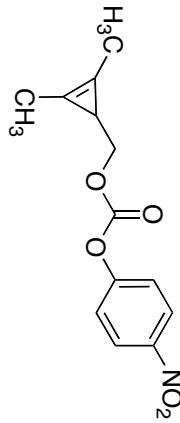
Current Data Parameters
 USER galle
 DATE 8/12
 EXPTNO 12
 PROCNO 1
 F2 - Acquisition Parameters
 Data_ 2011110
 INSTRUM cryo500
 PROBMOD zgpg30
 PULPROG zgpg30
 TD 65536
 SFO 125.760
 SOLVENT CDCl3
 DS 16
 SWH 30342.16 Hz
 SF 125760.000 MHz
 SFR 780.000000 MHz
 AQ 1.0813940 sec
 RG 1328
 RB 1.00000000
 W 1.00000000
 DE 6.00 usec
 DI 8.00 usec
 D1 0.25000000 sec
 d11 0.43000000 sec
 d17 0.00019600 sec
 MCHRES* 0.40000000 sec
 F2 MARK 0.01319100 usec
 ***** CHANNEL f1 *****
 NUC1 13C
 P1 15.00 usec
 PL1 0.00 dB
 P2 2000.00 usec
 PL2 0.00 dB
 SFO1 125.760000 MHz
 SFO2 125.760000 MHz
 SP1 3.20 dB
 SP2 3.20 dB
 SPANM1 C160,0.5,20.1 Hz
 SPANM2 C160,0.5,20.1 Hz
 SFOF2 0.00 Hz
 ***** CHANNEL f2 *****
 CPDPRG2 waltz16
 NUC2 1H
 P1 100.00 usec
 PL1 0.00 dB
 P2 1.00 dB
 PL12 2.00 dB
 SFO 500.262511 MHz
 ***** CHANNEL f3 *****
 CHANNEL GRADIENT CHANNEL
 SPANM3 SINE,100
 GPC1 0.00 %
 GPC2 0.00 %
 GPC3 0.00 %
 GPC4 0.00 %
 GPC5 0.00 %
 GPC6 0.00 %
 GPC7 0.00 %
 GPC8 0.00 %
 GPC9 0.00 %
 GPC10 0.00 %
 GPC11 0.00 %
 GPC12 0.00 %
 GPC13 0.00 %
 GPC14 0.00 %
 GPC15 0.00 %
 P1 50.00 %
 P1.5 50.00 usec
 P1.6 100.00 usec
 F2 - Processing parameters
 SF 125.7604190 MHz
 DS 16
 AS 32
 LA 1.00 Hz
 GB 2.00

¹H spectrum



Current Data Parameters
 USER: BRYAN
 EXPNO: 1
 PROCNO: 1
 F2 - Acquisition Parameters
 Date_: 20120309
 Time: 12:40:40
 INSTRUM: hz400
 PROBMOD: 5 mm QNP H²/P
 P1: 12.00
 TO: 65536
 SOLVENT: CDCl₃
 NS: 2
 DS: 2
 SWH: 6418.242 Hz
 SF: 400761.618 MHz
 AQ: 5.118579 sec
 RG: 78.0072
 DE: 4.50 usec
 DI: 0.10000000 sec
 ACQRES: 0.10000000 sec
 FIDRES: 0.01500000 sec
 CHANNEL: f1
 P1: 12.00 usec
 P1C1: -4.60 dB
 SFO1: 400.122809 MHz
 F2 - Processing Parameters
 SF: 400.130216 MHz
 MDW: EM
 LB: 0.30 Hz
 GB: 0
 PC: 2.00

Z-restored spin-echo 13C spectrum with 1H decoupling

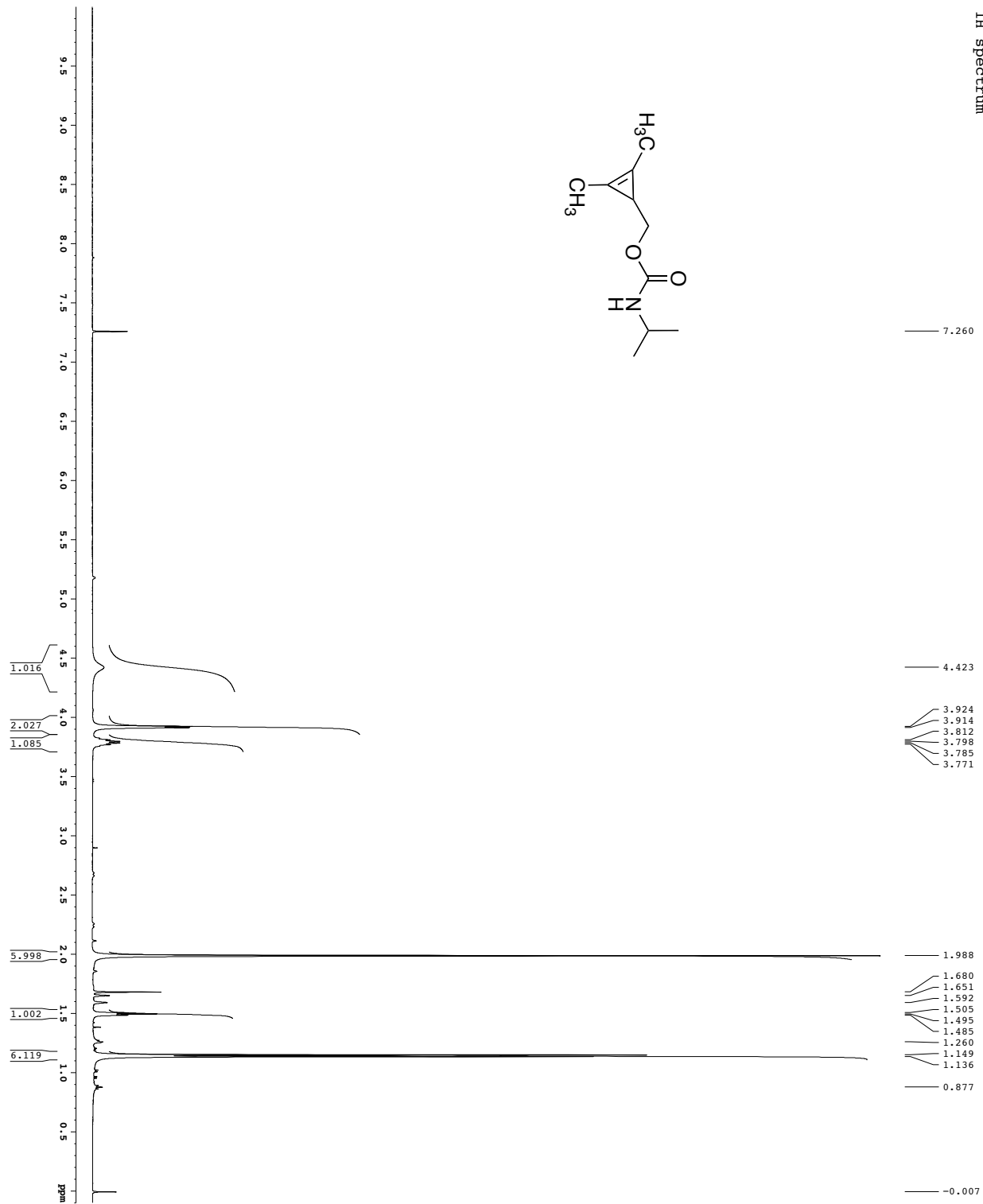
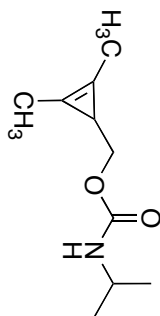


155.882
152.753
145.282
125.326
121.896
109.491
77.897
77.329
77.075
76.822

19.005
10.490
0.053

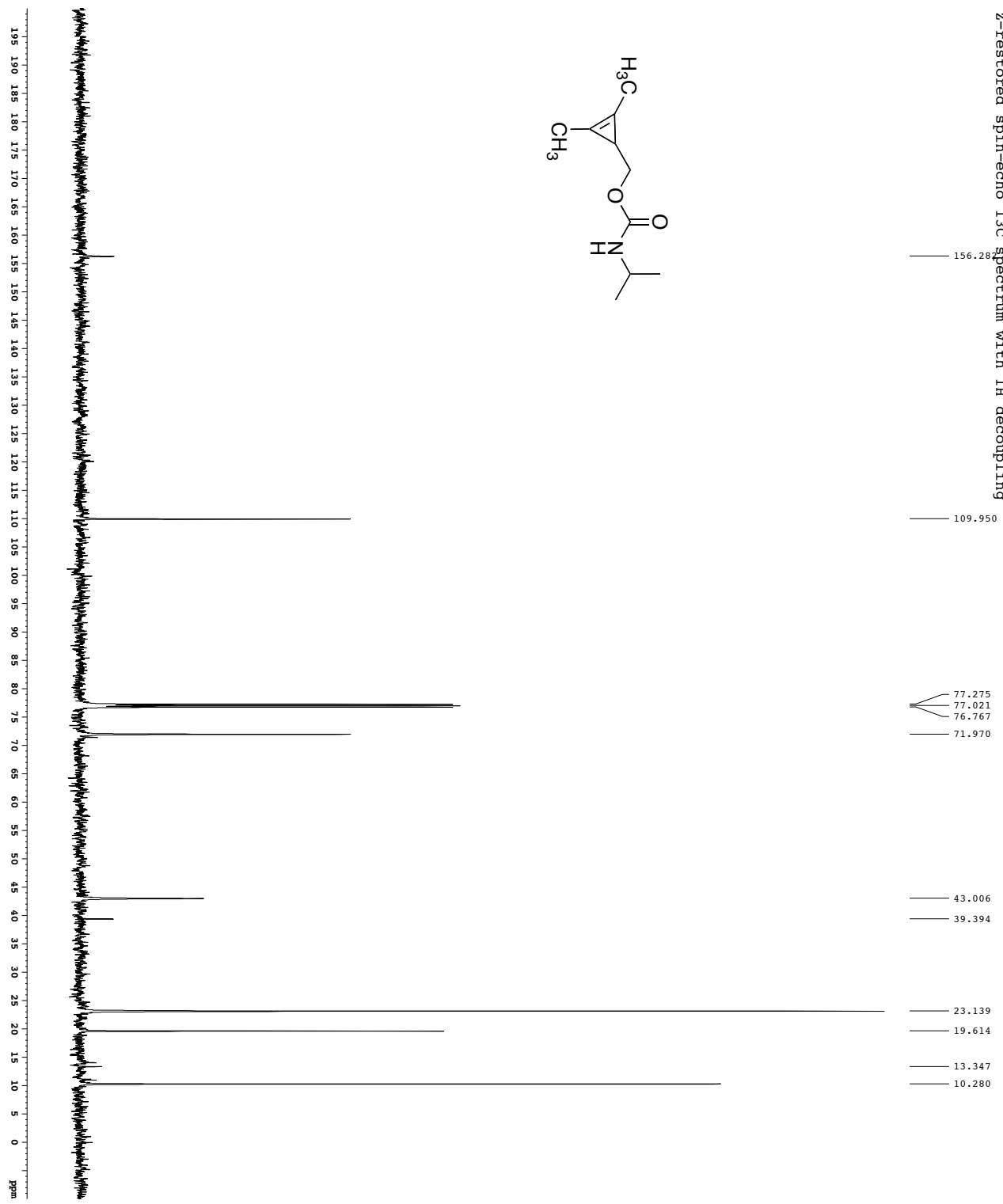
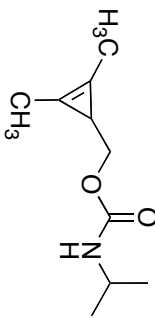
Current Data Parameters
 USER: gatte
 DATE: 11/11/11
 EXPTNO: 1
 PROCNO: 1
 F2 - Acquisition Parameters
 Date_ 20111112
 Time 11:11:11
 INSTRUM cryo500
 PROBHD 5 mm CPXI 1H-1
 PULPROG zgpg30
 TD 65536
 SFO 500.136269
 SOLVENT CDCl3
 NS 16
 DS 4
 SWH 30343.16 Hz
 SF 125.760370 MHz
 FIDRES 0.462383 Hz
 AQ 1.0813940 sec
 RG 655.72
 RW 17.9702
 WQ 7.6972
 DE 6.00 usec
 DI 0.25000000 sec
 D1 0.43000000 sec
 d11 0.43000000 sec
 d17 0.00019600 sec
 MCHRES7 0.40000000 sec
 F2 WAK 0.01313100 usec
 F2 1.00 usec
 ===== CHANNEL f1 13C =====
 NUCL1 13C
 P1 15.50 usec
 PL1 0.00 dB
 P2 2000.00 usec
 PL2 120.00 dB
 SFO1 125.760370 MHz
 ===== CHANNEL f2 1H =====
 WALTZ16
 NUCL2 1H
 P1 100.00 usec
 PL1 0.00 dB
 PL2 1.00 dB
 SFO2 500.262513 MHz
 ===== GRADIENT CHANNEL =====
 GPNAM1 SINE-100
 GPNAM2 SINE-100
 GPC1 0.00 %
 GPC2 0.00 %
 GPC3 0.00 %
 GPC4 0.00 %
 GPC5 0.00 %
 GPC6 30.00 %
 GPC7 30.00 %
 GPC8 50.00 %
 P1 5 1000.00 usec
 P1 5 1000.00 usec
 F2 - Processing parameters
 SF 125.7604190 MHz
 DS 4
 ASB 0
 LA 1.00 Hz
 PC 2.00

1H spectrum



Current Data Parameters
 USER: jg
 OPERATOR: jg
 INSTRUM: spect
 EXNO: 1
 PROCNO: 2
 F2 - Acquisition Parameters
 Date_: 20120513
 Time: 11:11
 INSTRUM: spect
 PROBRD: 5 mm CPXI 1H-
 P1: 12.00
 P2: 0.00
 F0: 500.1363
 NUC1: 1H
 NUC2: 13C
 SOLVENT: CDCl3
 DS: 2
 SWH: 8112.822 Hz
 SFO: 500.1363000 MHz
 SFRES: 0.0006400 Hz
 AQ: 5.0998774 sec
 RG: 64
 RB: 62.400 usec
 DE: 6.00 usec
 DI: 8.00 usec
 D1: 0.10000000 sec
 DELT: 0.00000000 sec
 ACQMSX: 0.01500000 sec
 PCP1: CHANNEL F1
 P1: 7.50 usec
 P11: 1.60 dB
 SFO1: 500.225015 MHz
 F2 - Processing parameters
 SF: 500.225015 MHz
 MDW: EM
 LB: 0.30 Hz
 GB: 0
 PC: 4.00

Z-restored spin-echo 13C spectrum with 1H decoupling



Current Data Parameters

USER	adp
EXPERNO	mpf_103
PROCNO	3
EXPNO	1

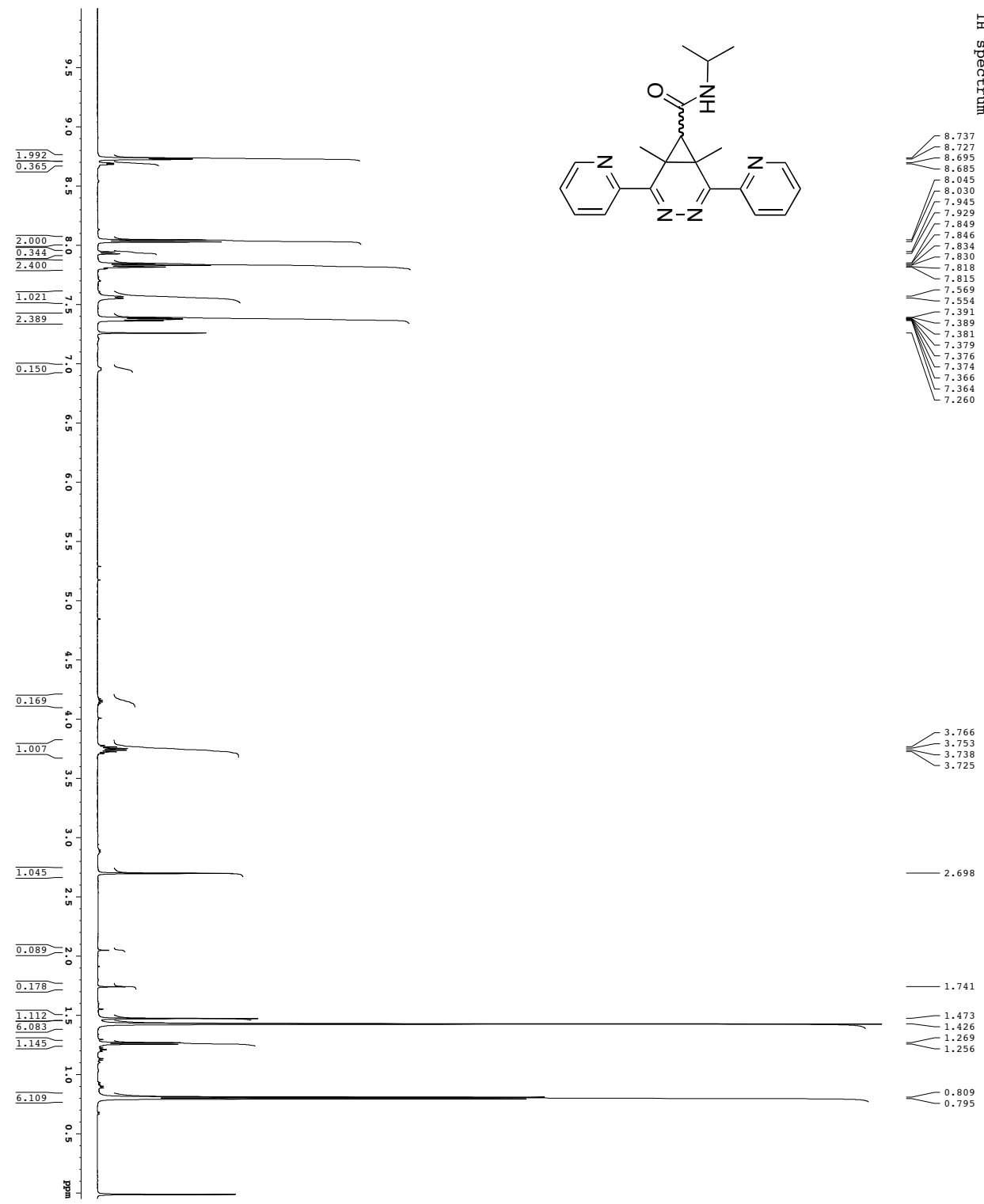
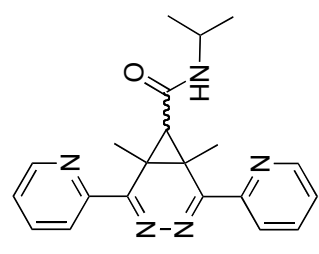
F2 - Acquisition Parameters

Date_	20120503
Time	09:00
INSTRUM	CRYM500
PROBHD	5 mm CRYM-1H-
P1	3.00
TD	32768
RG	65536
SD	1
DELTA	16
DELTA2	16
DELTA3	16
DELTA4	16
DELTA5	16
DELTA6	16
DELTA7	16
DELTA8	16
DELTA9	16
DELTA10	16
DELTA11	16
DELTA12	16
DELTA13	16
DELTA14	16
DELTA15	16
DELTA16	16
DELTA17	16
DELTA18	16
DELTA19	16
DELTA20	16
DELTA21	16
DELTA22	16
DELTA23	16
DELTA24	16
DELTA25	16
DELTA26	16
DELTA27	16
DELTA28	16
DELTA29	16
DELTA30	16
DELTA31	16
DELTA32	16
DELTA33	16
DELTA34	16
DELTA35	16
DELTA36	16
DELTA37	16
DELTA38	16
DELTA39	16
DELTA40	16
DELTA41	16
DELTA42	16
DELTA43	16
DELTA44	16
DELTA45	16
DELTA46	16
DELTA47	16
DELTA48	16
DELTA49	16
DELTA50	16
DELTA51	16
DELTA52	16
DELTA53	16
DELTA54	16
DELTA55	16
DELTA56	16
DELTA57	16
DELTA58	16
DELTA59	16
DELTA60	16
DELTA61	16
DELTA62	16
DELTA63	16
DELTA64	16
DELTA65	16
DELTA66	16
DELTA67	16
DELTA68	16
DELTA69	16
DELTA70	16
DELTA71	16
DELTA72	16
DELTA73	16
DELTA74	16
DELTA75	16
DELTA76	16
DELTA77	16
DELTA78	16
DELTA79	16
DELTA80	16
DELTA81	16
DELTA82	16
DELTA83	16
DELTA84	16
DELTA85	16
DELTA86	16
DELTA87	16
DELTA88	16
DELTA89	16
DELTA90	16
DELTA91	16
DELTA92	16
DELTA93	16
DELTA94	16
DELTA95	16
DELTA96	16
DELTA97	16
DELTA98	16
DELTA99	16
DELTA100	16

F2 - Processing parameters

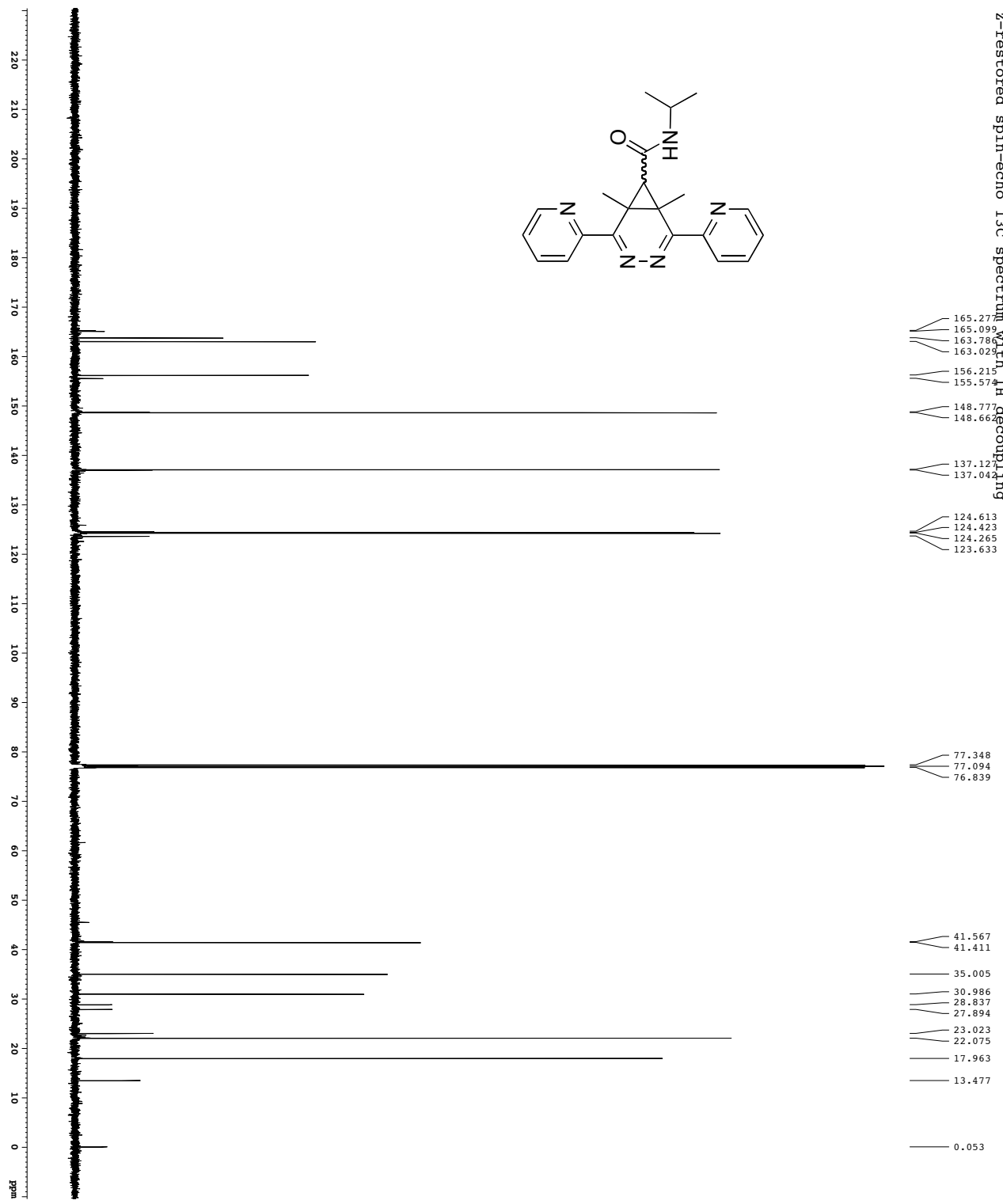
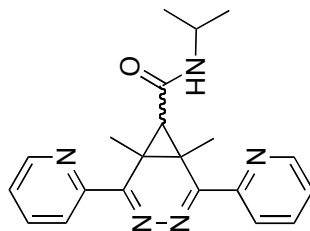
SI	32768
SD	1
WDW	EM
SSB	0
BK	0
GB	0
PC	2.00

1H spectrum



Current Data Parameters
 USER: operator
 EXPERNO: 1
 PROCNO: 1
 F2 - Acquisition Parameters
 Date_: 20120410
 Time: 11:11
 INSTRUM: cryo500
 PROBMOD: 5 mm CPY-500
 P1: 1.50
 PD: 0.00
 TO: 18.00
 SOLVENT: CDCl3
 NS: 2
 DS: 4
 SWH: 8012.820 Hz
 SFO: 500.136260 MHz
 AQ: 0.025043 sec
 RG: 655
 RB: 5.0988774 sec
 DE: 62.400 usec
 TE: 300.2 K
 DI: 5.00 usec
 FIDRES: 0.10000000 sec
 AQRES: 0.40000000 sec
 ACQSKN: 0.01500000 sec
 CHANNEL: F1
 P1: 7.50 usec
 P1C1: 1.60 dB
 SFO1: 500.225015 MHz
 F2 - Processing parameters
 SF: 500.136260 MHz
 MDW: EM
 LB: 0.30 Hz
 GB: 0
 PC: 4.00

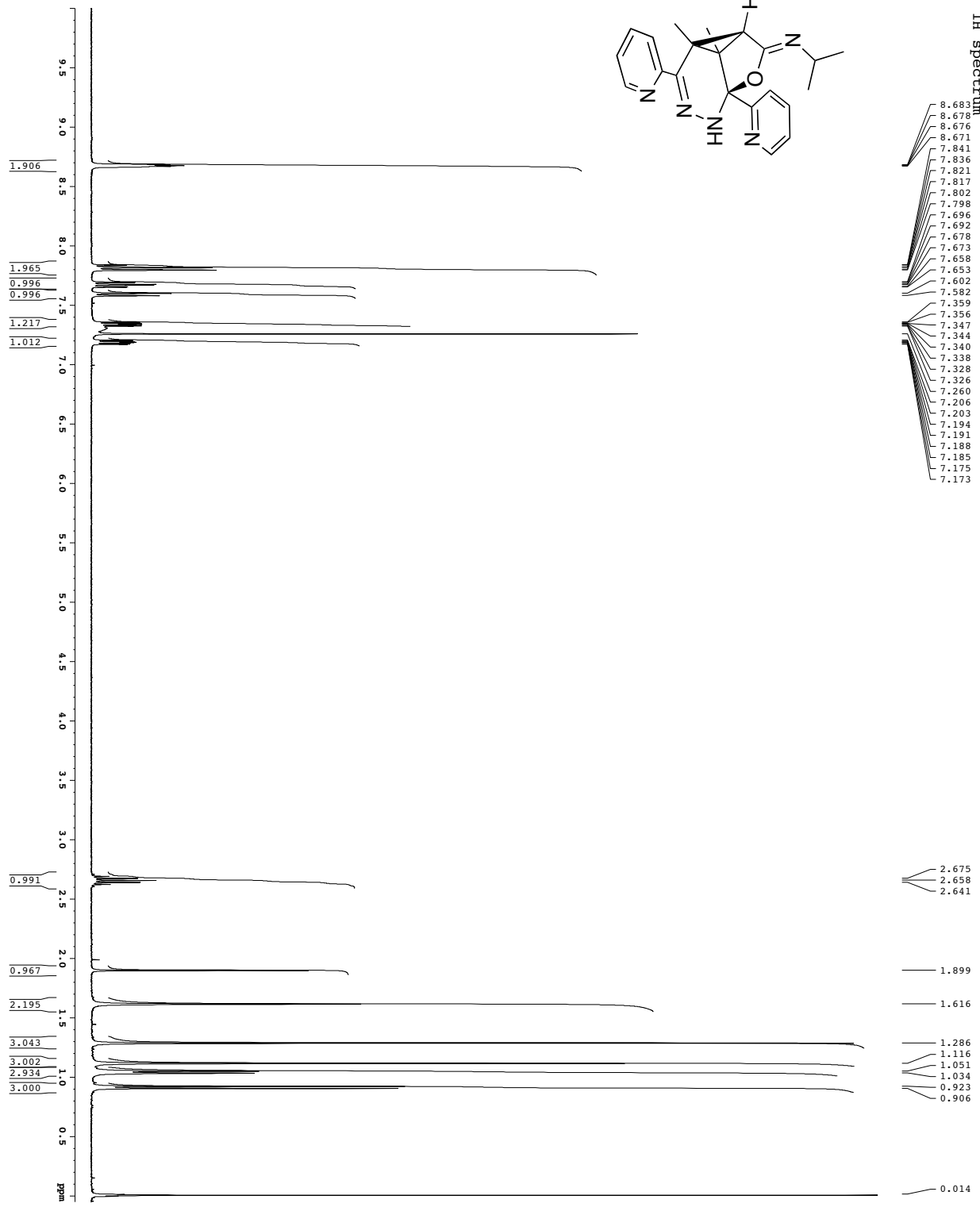
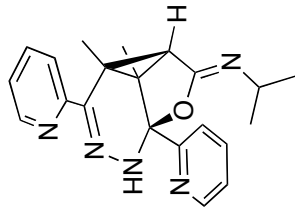
Z-restored spin-echo 13C spectrum with 1H decoupling



Chemical Shift (ppm)
165.27
165.099
163.786
163.029
156.215
155.574
148.777
148.662
137.127
137.042
124.613
124.423
124.265
123.633
77.348
77.094
76.839
41.567
41.411
35.005
30.986
28.837
27.894
23.023
22.075
17.963
13.477
0.053

Current Data Parameters
 USER: gpatte
 DATE: mpr_13
 EXNO: 1
 PROCNM: 1
 F2 - Acquisition Parameters
 Date_: 2012/04/10
 Time: 12:41:10
 INSTRUM: cryo500
 PROBMOD: 5 mm CPYX 1H-13
 PULPROG: zgpg30
 TD: 65536
 SFO: 125.760
 SOLVENT: CDCl3
 NS: 16
 DS: 4
 SWH: 30183.16 Hz
 SF: 125760.400 MHz
 SFOBS: 125760.400 MHz
 AO: 1.0813940 sec
 RG: 163.500
 RW: 163.500
 DE: 6.00 usec
 DI: 0.25000000 sec
 D1: 0.25000000 sec
 d11: 0.43000000 sec
 d17: 0.00019600 sec
 MCNRES: 0.40000000 sec
 PC: 1.00000000 sec
 PZ: 0.01313100 usec
 ===== CHANNEL f1 =====
 NUC1: 13C
 P1: 15.50 usec
 PL1: 0.00 dB
 P2: 2000.00 usec
 PL2: 120.00 dB
 SFO1: 125.7604548 MHz
 SP1: 3.20 dB
 SP2: 3.20 dB
 SPANM1: C1660,0.520,1
 SPANM2: C1660comp,4
 SFOF2: 0.00 Hz
 ===== CHANNEL f2 =====
 CPDPRG2: waltz16
 NUC2: 1H
 P1: 100.00 usec
 PL1: 1.00 dB
 P2: 1.00 dB
 SFO2: 500.2620111 MHz
 ===== GRADIENT CHANNEL =====
 GPCON: 100
 SIN1: 100
 SPANM3: 0.00 %
 GPCX1: 0.00 %
 GPCX2: 0.00 %
 GPCX3: 0.00 %
 GPCX4: 0.00 %
 GPCX5: 0.00 %
 GPCX6: 0.00 %
 GPCX7: 0.00 %
 GPCX8: 0.00 %
 GPCX9: 0.00 %
 GPCX10: 0.00 %
 GPCX11: 0.00 %
 GPCX12: 0.00 %
 GPCX13: 0.00 %
 GPCX14: 0.00 %
 GPCX15: 0.00 %
 GPCX16: 0.00 %
 GPCX17: 0.00 %
 GPCX18: 0.00 %
 GPCX19: 0.00 %
 GPCX20: 0.00 %
 GPCX21: 0.00 %
 GPCX22: 0.00 %
 GPCX23: 0.00 %
 GPCX24: 0.00 %
 GPCX25: 0.00 %
 GPCX26: 0.00 %
 GPCX27: 0.00 %
 GPCX28: 0.00 %
 GPCX29: 0.00 %
 GPCX30: 0.00 %
 GPCX31: 0.00 %
 GPCX32: 0.00 %
 GPCX33: 0.00 %
 GPCX34: 0.00 %
 GPCX35: 0.00 %
 GPCX36: 0.00 %
 GPCX37: 0.00 %
 GPCX38: 0.00 %
 GPCX39: 0.00 %
 GPCX40: 0.00 %
 GPCX41: 0.00 %
 GPCX42: 0.00 %
 GPCX43: 0.00 %
 GPCX44: 0.00 %
 GPCX45: 0.00 %
 GPCX46: 0.00 %
 GPCX47: 0.00 %
 GPCX48: 0.00 %
 GPCX49: 0.00 %
 GPCX50: 0.00 %
 GPCX51: 0.00 %
 GPCX52: 0.00 %
 GPCX53: 0.00 %
 GPCX54: 0.00 %
 GPCX55: 0.00 %
 GPCX56: 0.00 %
 GPCX57: 0.00 %
 GPCX58: 0.00 %
 GPCX59: 0.00 %
 GPCX60: 0.00 %
 GPCX61: 0.00 %
 GPCX62: 0.00 %
 GPCX63: 0.00 %
 GPCX64: 0.00 %
 GPCX65: 0.00 %
 GPCX66: 0.00 %
 GPCX67: 0.00 %
 GPCX68: 0.00 %
 GPCX69: 0.00 %
 GPCX70: 0.00 %
 GPCX71: 0.00 %
 GPCX72: 0.00 %
 GPCX73: 0.00 %
 GPCX74: 0.00 %
 GPCX75: 0.00 %
 GPCX76: 0.00 %
 GPCX77: 0.00 %
 GPCX78: 0.00 %
 GPCX79: 0.00 %
 GPCX80: 0.00 %
 GPCX81: 0.00 %
 GPCX82: 0.00 %
 GPCX83: 0.00 %
 GPCX84: 0.00 %
 GPCX85: 0.00 %
 GPCX86: 0.00 %
 GPCX87: 0.00 %
 GPCX88: 0.00 %
 GPCX89: 0.00 %
 GPCX90: 0.00 %
 GPCX91: 0.00 %
 GPCX92: 0.00 %
 GPCX93: 0.00 %
 GPCX94: 0.00 %
 GPCX95: 0.00 %
 GPCX96: 0.00 %
 GPCX97: 0.00 %
 GPCX98: 0.00 %
 GPCX99: 0.00 %
 GPCX100: 0.00 %
 F2 - Processing parameters
 SF: 125.7604190 MHz
 DS: 4
 SFO: 125.7604190 MHz
 AS: 1.00 Hz
 LA: 1.00 Hz
 GB: 0.00 Hz
 PC: 2.00

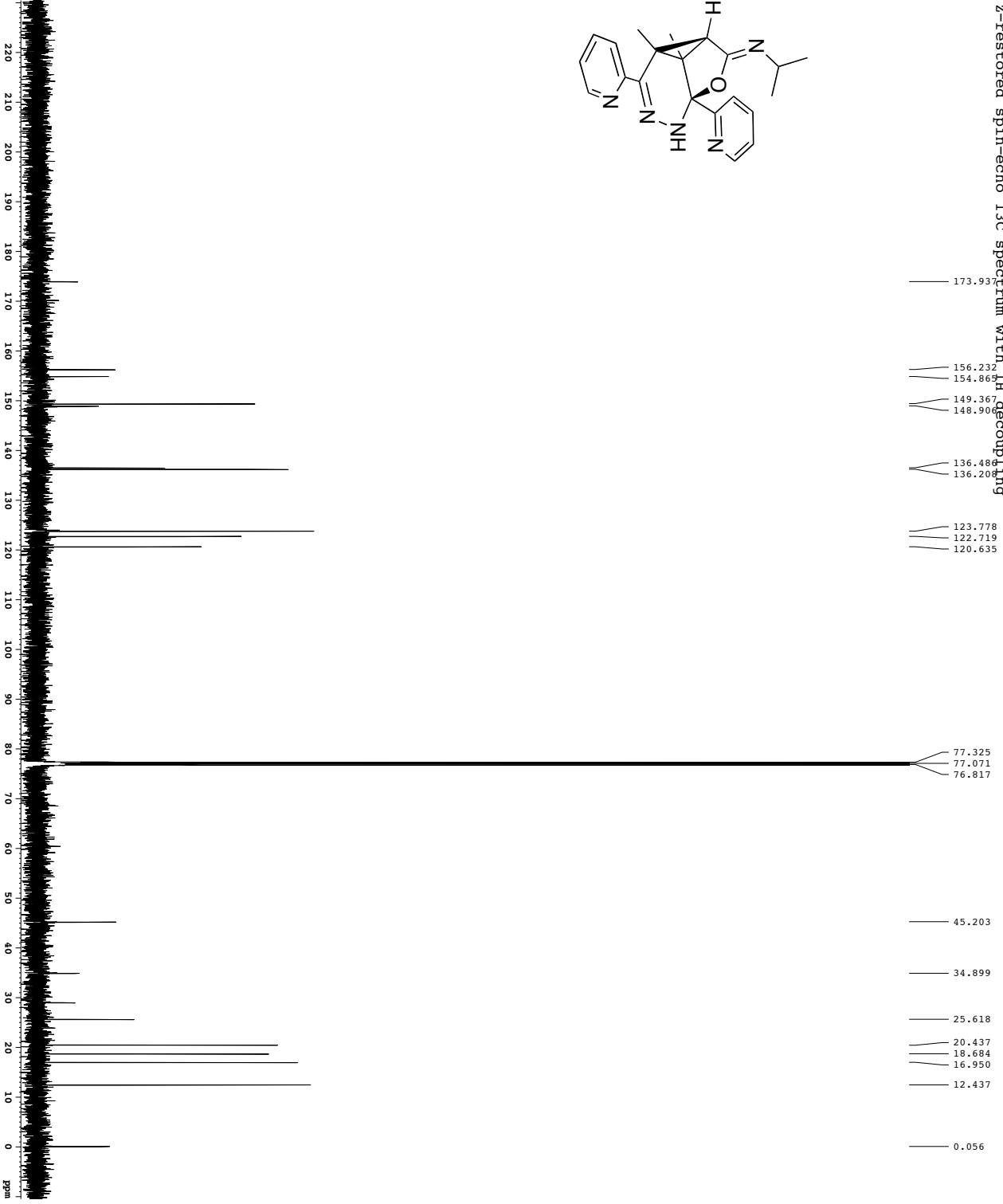
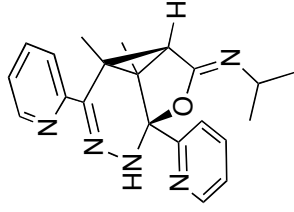
¹H spectrum



Integration values (from left to right): 1.906, 1.965, 0.996, 0.996, 1.217, 1.012, 0.991, 0.967, 2.195, 3.043, 3.002, 2.934, 3.000.

Current Data Parameters
 USER: dmf_1172
 EXPNO: 2
 PROCNO: 1
 F2 - Acquisition Parameters
 Date_: 20121003
 Time: 12:40:37
 INSTRUM: dxt400
 PROBMOD: 5 mm QNP HZ PZ
 PR: 1000
 TO: 65536
 SOLVENT: CDCl3
 DS: 2
 SWH: 6418.242 Hz
 SFO: 64007.618 MHz
 AQ: 5.118579 sec
 RG: 78.000
 DE: 4.50 usec
 DI: 4.50 usec
 D1: 0.10000000 sec
 ACQRES: 0.40000000 sec
 MCKM: 0.01500000 sec
 CHANNEL: f1
 P1: 12.00 usec
 P11: -4.60 dB
 SFO1: 400.122809 MHz
 F2 - Processing parameters
 SF: 400.130211 MHz
 MDW: EM
 LB: 0.30 Hz
 GB: 0
 PC: 2.00

Z-restored spin-echo 13C spectrum with 1H decoupling



Current Data Parameters
 USER: dattie
 EXPER: DMC_1102
 EXNO: 2
 BROONO: 1

F2 - Acquisition Parameters
 Date_: 2012/01
 Time: 19:01
 INSTRUM: cryo500
 PROBD: 5 mm CPY-500
 PULPROG: zgpg30
 TD: 65536
 SOLVENT: CDCl3
 NS: 16
 DS: 4
 SWH: 30343.16 Hz
 FIDRES: 0.462381 Hz
 AQ: 1.0813940 sec
 RG: 4096
 RW: 16.501 usec
 DE: 6.00 usec
 DI: 0.23000000 sec
 d11: 0.43000000 sec
 d17: 0.00019600 sec
 MCHRES: 0.40000000 sec
 F2 P1: 0.01319100 sec
 F2 P2: 0.01319100 sec

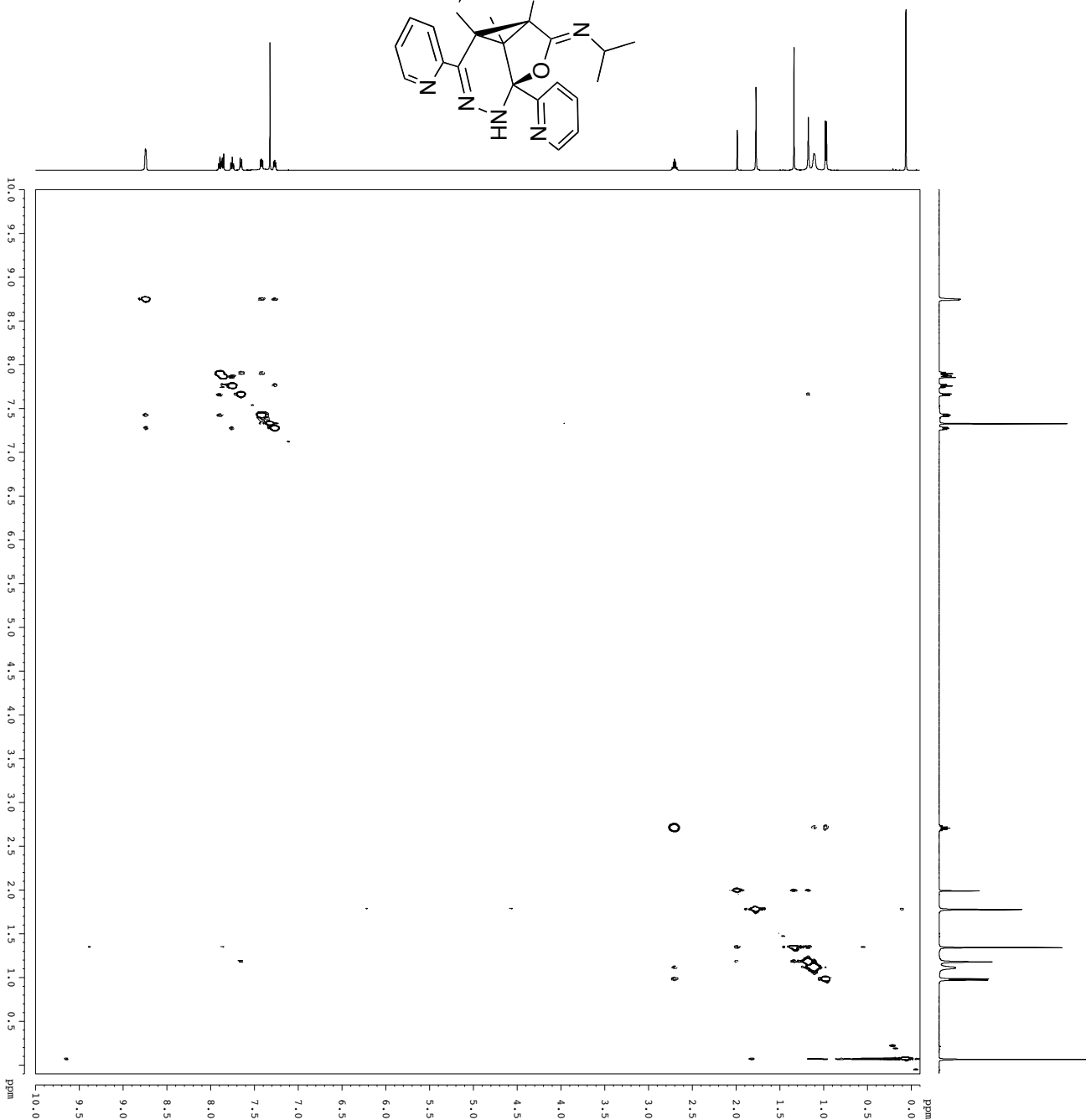
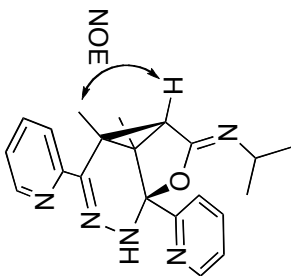
===== CHANNEL f1 =====
 NUC1: 13C
 P1: 15.00 usec
 PL1: 0.00 dB
 P2: 2000.00 usec
 PL2: 120.00 dB
 SFO1: 125.7942548 MHz
 SF1: 3.20 dB
 SF2: 3.20 dB
 SPANM1: C1p60,0.520,1 Hz
 SPANM2: C1p60comp,4 Hz
 SFOER2: 0.00 Hz

===== CHANNEL f2 =====
 NUC2: 1H
 P1: 100.00 usec
 PL1: 1.00 dB
 P2: 1.00 dB
 SFO1: 500.2625011 MHz

===== GRADIENT CHANNEL =====
 GBNAM1: SINE,100
 GBNAM2: SINE,100
 SHIF: 100
 GRX1: 0.00 %
 GRX2: 0.00 %
 GRX3: 0.00 %
 GRX4: 0.00 %
 GRX5: 0.00 %
 GRX6: 0.00 %
 GRX7: 0.00 %
 GRX8: 0.00 %
 GRX9: 0.00 %
 GRX10: 0.00 %
 GRX11: 0.00 %
 GRX12: 0.00 %
 GRX13: 0.00 %
 GRX14: 0.00 %
 GRX15: 0.00 %
 GRX16: 0.00 %
 GRX17: 0.00 %
 GRX18: 0.00 %
 GRX19: 0.00 %
 GRX20: 0.00 %
 GRX21: 0.00 %
 GRX22: 0.00 %
 GRX23: 0.00 %
 GRX24: 0.00 %
 GRX25: 0.00 %
 GRX26: 0.00 %
 GRX27: 0.00 %
 GRX28: 0.00 %
 GRX29: 0.00 %
 GRX30: 0.00 %
 GRX31: 0.00 %
 GRX32: 0.00 %
 GRX33: 0.00 %
 GRX34: 0.00 %
 GRX35: 0.00 %
 GRX36: 0.00 %
 GRX37: 0.00 %
 GRX38: 0.00 %
 GRX39: 0.00 %
 GRX40: 0.00 %
 GRX41: 0.00 %
 GRX42: 0.00 %
 GRX43: 0.00 %
 GRX44: 0.00 %
 GRX45: 0.00 %
 GRX46: 0.00 %
 GRX47: 0.00 %
 GRX48: 0.00 %
 GRX49: 0.00 %
 GRX50: 0.00 %
 GRX51: 0.00 %
 GRX52: 0.00 %
 GRX53: 0.00 %
 GRX54: 0.00 %
 GRX55: 0.00 %
 GRX56: 0.00 %
 GRX57: 0.00 %
 GRX58: 0.00 %
 GRX59: 0.00 %
 GRX60: 0.00 %
 GRX61: 0.00 %
 GRX62: 0.00 %
 GRX63: 0.00 %
 GRX64: 0.00 %
 GRX65: 0.00 %
 GRX66: 0.00 %
 GRX67: 0.00 %
 GRX68: 0.00 %
 GRX69: 0.00 %
 GRX70: 0.00 %
 GRX71: 0.00 %
 GRX72: 0.00 %
 GRX73: 0.00 %
 GRX74: 0.00 %
 GRX75: 0.00 %
 GRX76: 0.00 %
 GRX77: 0.00 %
 GRX78: 0.00 %
 GRX79: 0.00 %
 GRX80: 0.00 %
 GRX81: 0.00 %
 GRX82: 0.00 %
 GRX83: 0.00 %
 GRX84: 0.00 %
 GRX85: 0.00 %
 GRX86: 0.00 %
 GRX87: 0.00 %
 GRX88: 0.00 %
 GRX89: 0.00 %
 GRX90: 0.00 %
 GRX91: 0.00 %
 GRX92: 0.00 %
 GRX93: 0.00 %
 GRX94: 0.00 %
 GRX95: 0.00 %
 GRX96: 0.00 %
 GRX97: 0.00 %
 GRX98: 0.00 %
 GRX99: 0.00 %
 GRX100: 0.00 %

F2 - Processing parameters
 SF: 125.7804190 MHz
 DS: 4
 ASB: 0
 LA: 1.00 Hz
 PC: 2.00

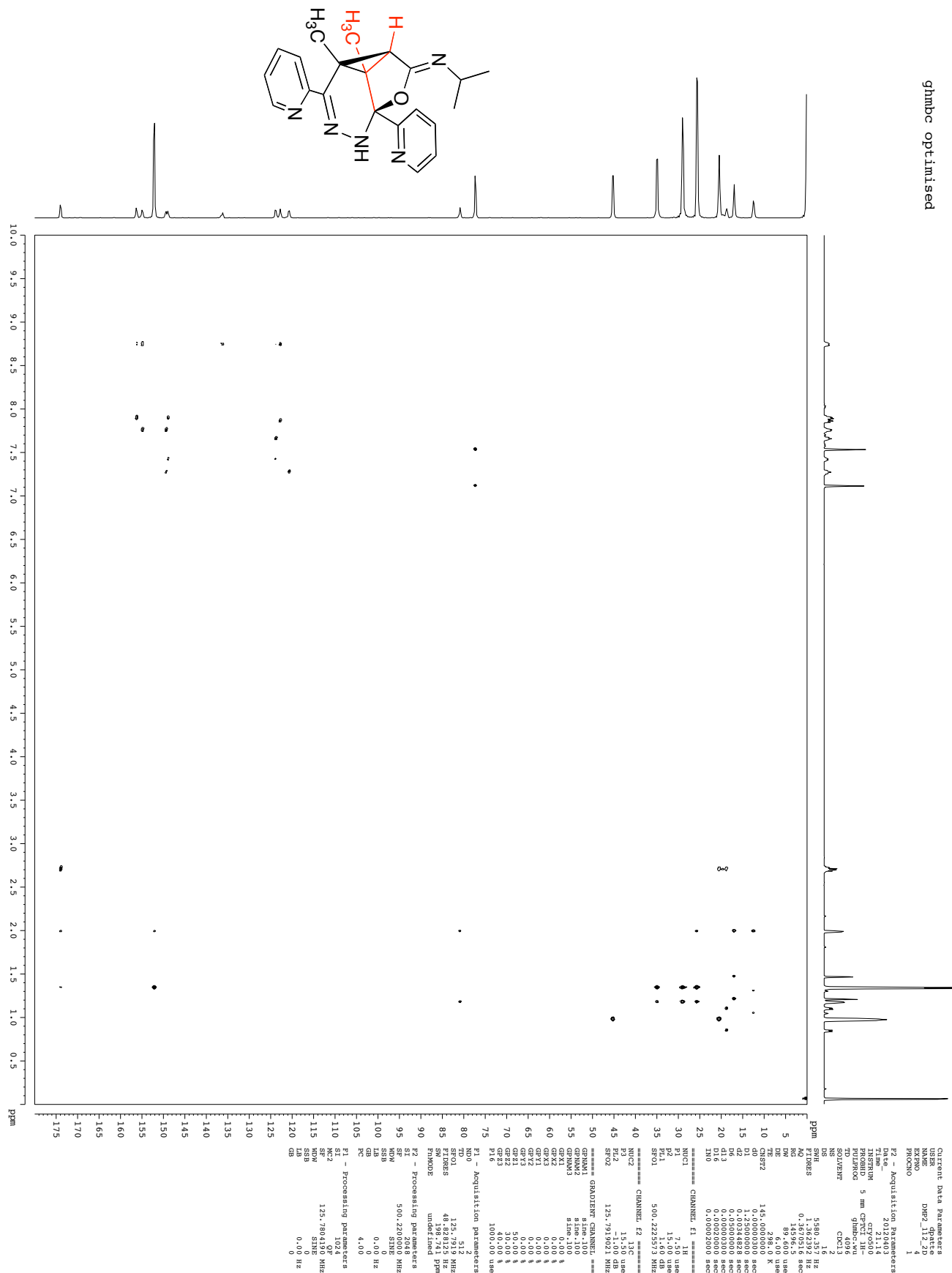
noesy

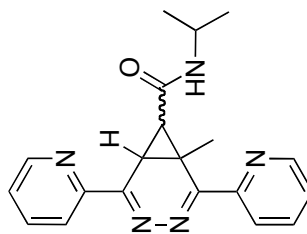


```

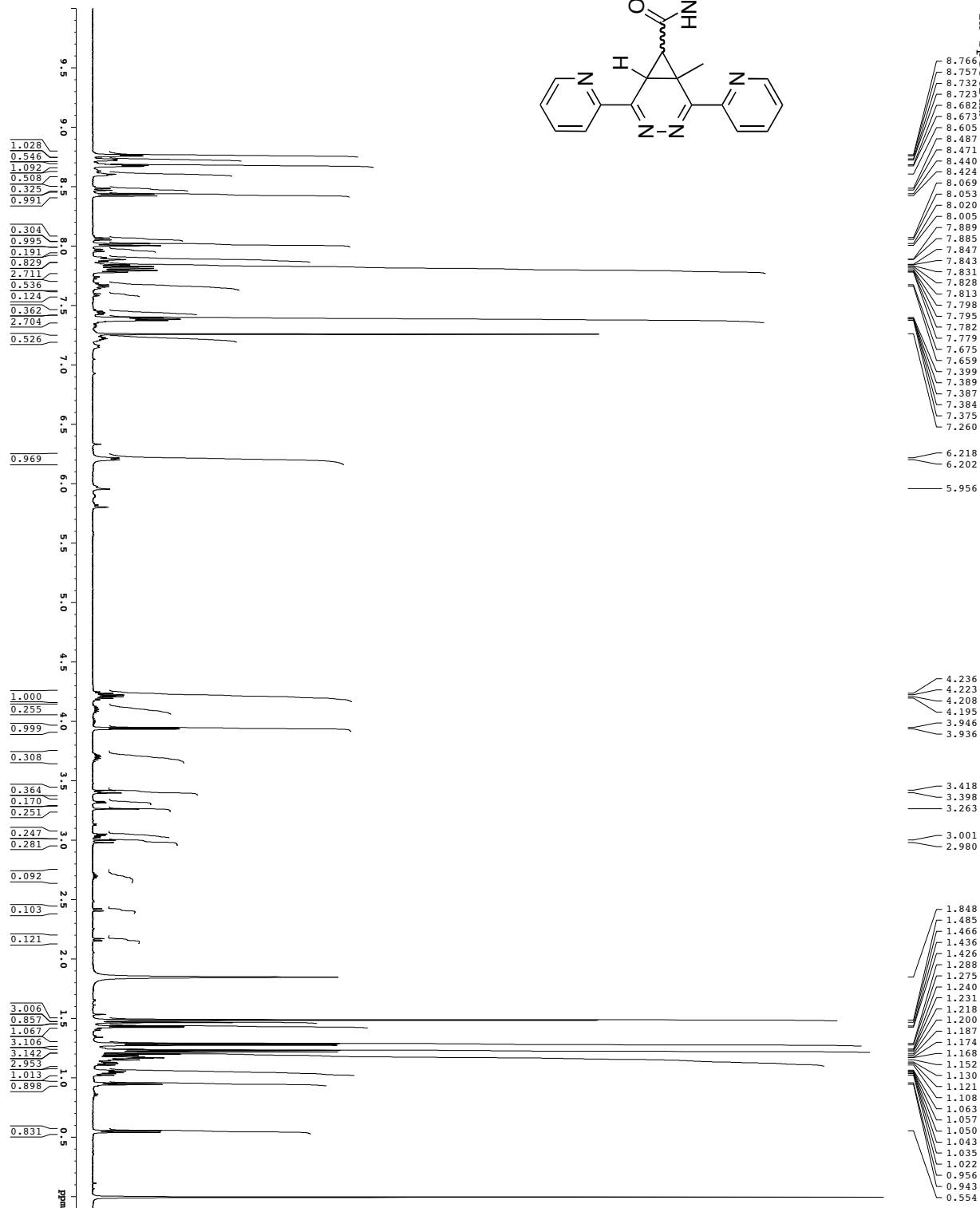
Current Data Parameters
=====
NAME          : 1
EXPNO        : 5
PROCNO       : 1
F2 - Acquisition Parameters
=====
Date_         : 20141214
Time         : 21:46
INSTRUM      : cryo-500
PROBHD       : 5 mm QNP1H/
PULPROG      : zgpg30
TD           : 65536
SOLVENT      : DMSO-d6
NS           : 2048
DS           : 4
SWH           : 12500.838 Hz
FIDRES       : 0.1835009 Hz
AQ           : 0.1835009 sec
RG           : 688
RW           : 894.608 usec
TE           : 298.2 K
DQ           : 0.00000030 sec
DD           : 1.00000000 sec
DE           : 1.00000000 sec
IQU         : 0.00009660 sec
===== CHANNEL f1 =====
NUC1         : 13C
P1           : 7.10 usec
PL1         : 1.60 dB
SFO1        : 500.222573 MHz
F2 - Acquisition Parameters
=====
TD           : 65536
SFO2        : 500.222573 MHz
SF           : 500.222573 MHz
WDW         : EM
SSB         : 0.00 Hz
LB          : 1.40
GB          :
PC          :
F2 - Processing parameters
=====
SI           : 32768
SF           : 500.222573 MHz
WDW         : EM
SSB         : 0.00 Hz
LB          : 1.40
GB          :
PC          :
F1 - Processing parameters
=====
SI           : 32768
SF           : 500.222573 MHz
WDW         : EM
SSB         : 0.00 Hz
LB          : 1.40
GB          :
PC          :
  
```

ghmbc optimised

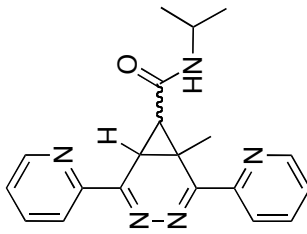




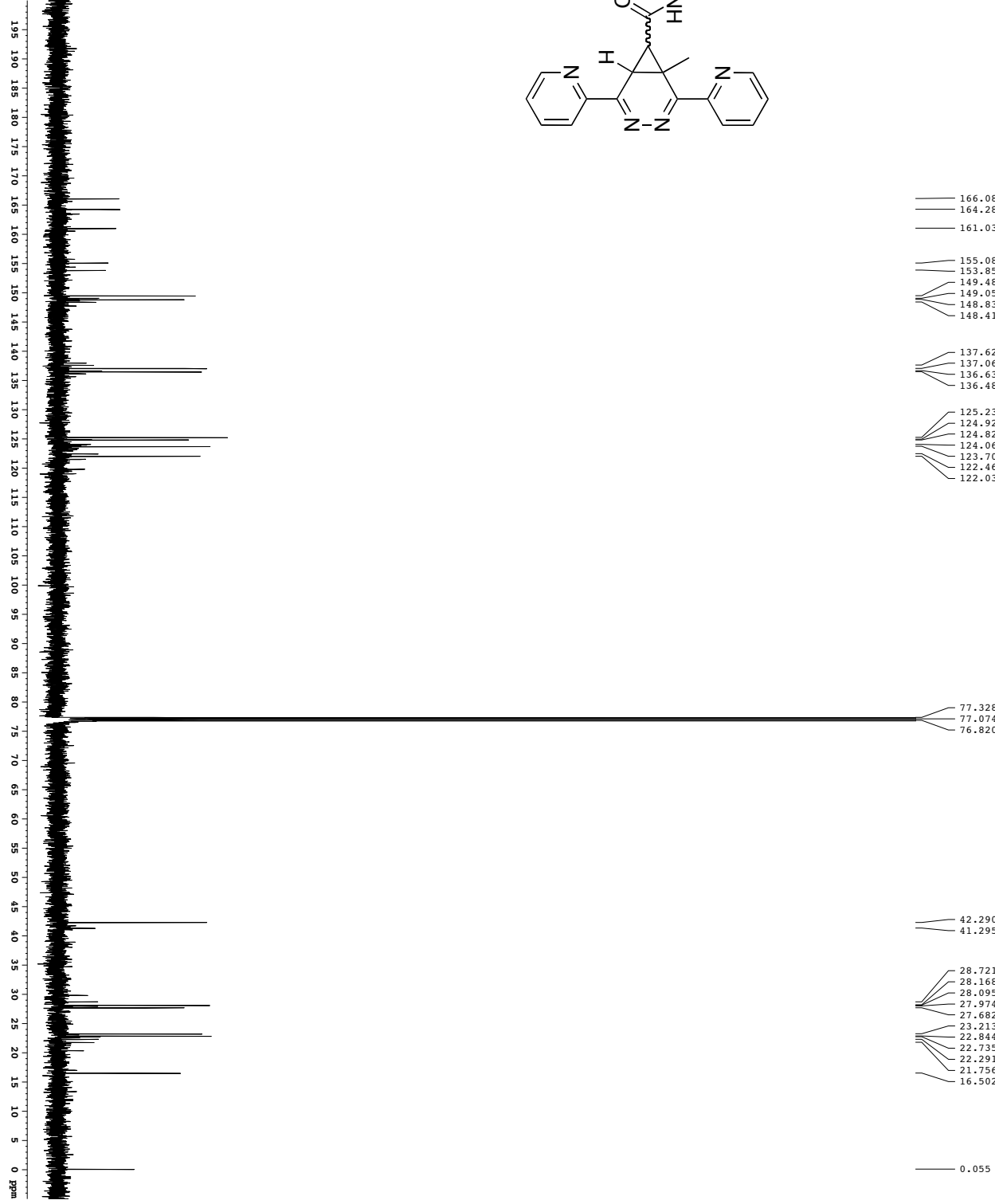
¹H Spectrum



Current Data Parameters
 USER: gpatte
 OPER: mpr_16
 EXNO: 6
 PRONO: 1
 F2 - Acquisition Parameters
 Date_: 20120524
 Time: 11:21:11
 INSTRUM: crys500
 PROBMOD: 5 mm CPYC1 1H-
 P1: 12.00
 T0: 300.2
 FIDRES: 0.1728
 SOLVENT: CDCl3
 NS: 2
 DS: 1
 SWH: 9112.420 Hz
 SFO: 500.136261 MHz
 AQ: 0.026043 sec
 RG: 655
 RB: 5.0998774 sec
 DE: 62.400 usec
 TE: 300.2 K
 DI: 6.00 usec
 D1: 0.10000000 sec
 ACQRES: 0.40000000 sec
 FWHM: 0.01500000 sec
 PC: CHANNEL F1
 P1: 7.50 usec
 P11: 1.60 dB
 SFO1: 500.225015 MHz
 F2 - Processing parameters
 SF: 500.226019 MHz
 MDW: EM
 LB: 0.30 Hz
 GB: 0
 PC: 4.00

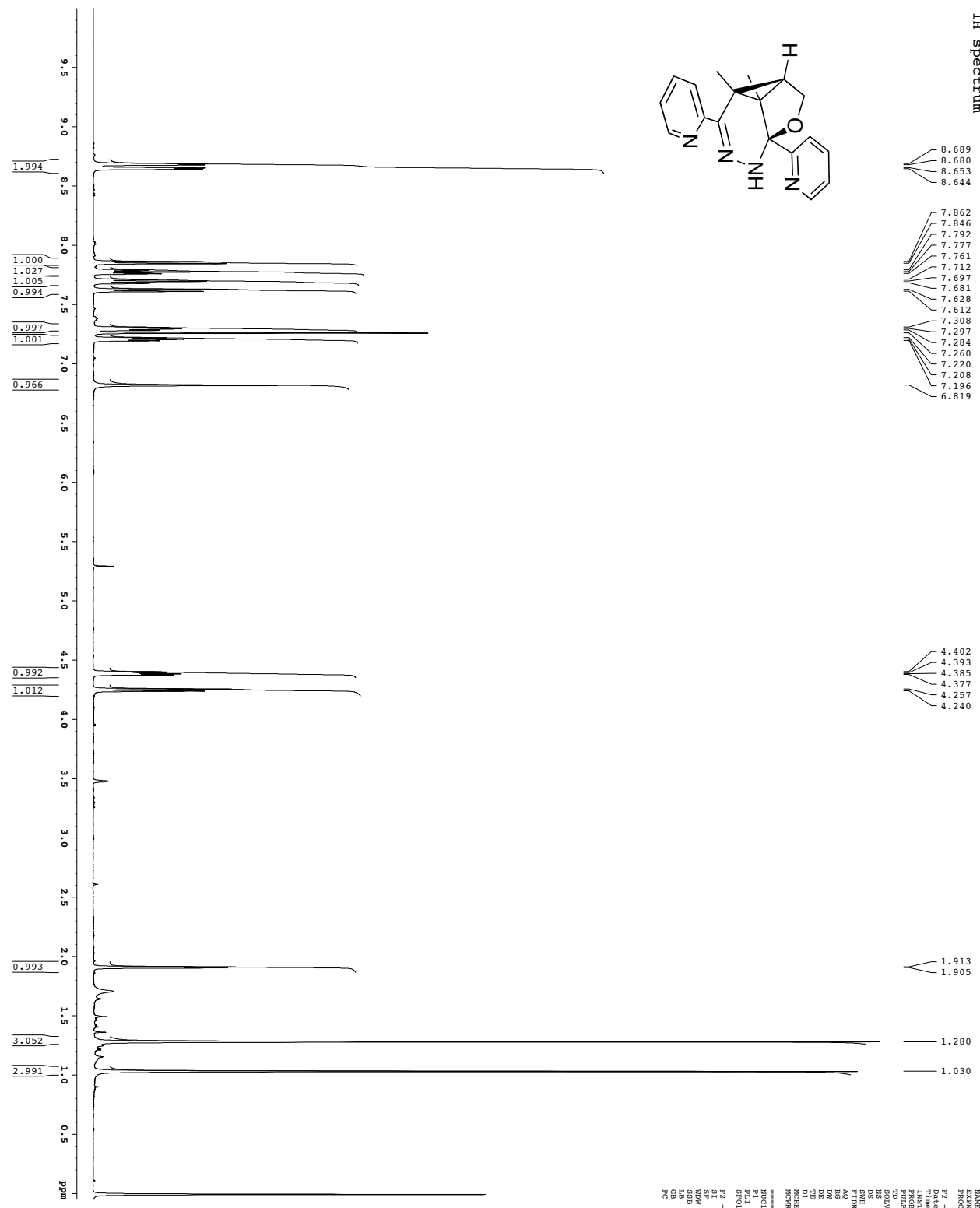
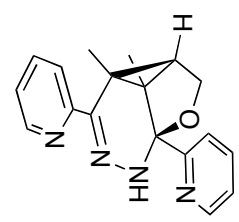


Z-restored spin-echo ¹³C spectrum with ¹H decoupling



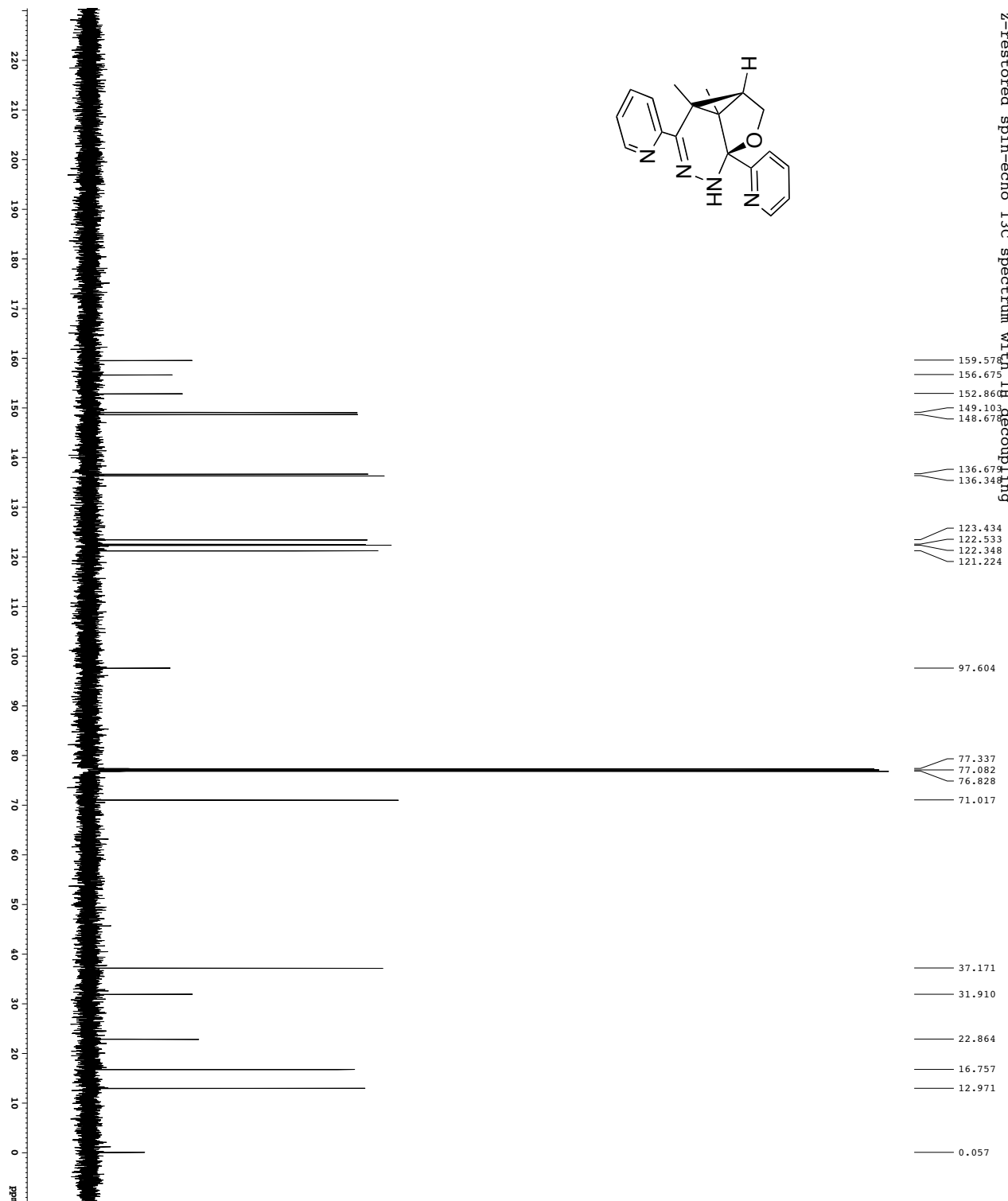
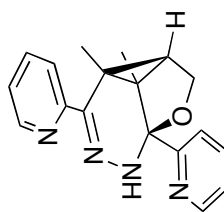
Current Data Parameters
 USER: mpr_dg16
 EXPTNO: 7
 PROCNO: 1
 F2 - Acquisition Parameters
 Date_: 20120524
 Time: 12.00
 INSTRUM: cryo500
 PROBHD: 5mm CPYH-1H1-13C
 PULPROG: zgpg30
 TD: 65536
 SOLVENT: CDCl3
 NS: 16
 DS: 4
 SWH: 30340.16 Hz
 SF: 125760.538 MHz
 AQ: 1.0813940 sec
 RG: 364.501
 RB: 4.941 usec
 DE: 6.00 usec
 DI: 0.25000000 sec
 D1: 0.43000000 sec
 d11: 0.03000000 sec
 d17: 0.00019600 sec
 MCHRES7: 0.40000000 sec
 F2 P2: 0.01313100 usec
 CHANNE1: E1
 NUCL1: ¹³C
 P1: 15.50 usec
 PL1: 0.00 dB
 P2: 2000.00 usec
 PL2: 120.00 dB
 SFO1: 125.7642548 MHz
 SP1: 3.20 dB
 SP2: 3.20 dB
 SPANM1: C160,0.520,1
 SPANM2: C160comp,4
 SFOF2: 0.00 Hz
 CHANNE2: E2
 WALTZ16
 NUCL2: ¹H
 P1: 100.00 usec
 PL1: 1.00 dB
 P2: 50.2629911 MHz
 SFO1: 500.1364511 MHz
 CHANNE1: GRADIENT CHANNEL
 SPANM1: SINE-100
 SPANM2: SINE-100
 GEY1: 0.00 %
 GEY2: 0.00 %
 GEY3: 0.00 %
 GEY4: 30.00 %
 GEY5: 50.00 %
 P1.5: 300.00 usec
 P1.6: 100.00 usec
 F2 - Processing parameters
 SF: 125.7604190 MHz
 DS: 4
 ASB: 0
 LA: 1.00 Hz
 GB: 0
 PC: 2.00

1H spectrum



Current Data Parameters
 USER: gpatel
 DATE: 11/11/18
 EXNO: 1
 EXFM: 2
 PROCNO: 1
 F2 - Acquisition Parameters
 Date_ 20181118
 Time 11:11:11
 INSTRUM cryo500
 PROBRD 5 mm CFC1 1H-
 P1 12.00
 P2 8.00
 P3 8.1728
 SOLVENT CHCl3
 NS 2
 DS 2
 SWH 9112.420 Hz
 SFO 500.136199 MHz
 SF 500.136199 MHz
 AQ 5.0998774 sec
 RG 62.400
 DE 62.400 usec
 DI 6.00 usec
 D1 0.10000000 sec
 ACQRES* 0.40000000 sec
 FIDRES 0.01500000 sec
 CHANNEL F1
 P1 7.50 usec
 P1C1 1.60 dB
 SFO1 500.223015 MHz
 F2 - Processing parameters
 SF 500.220222 MHz
 MDW EM
 LB 0.30 Hz
 GB 0
 PC 4.00

Z-restored spin-echo 13C spectrum with 1H decoupling

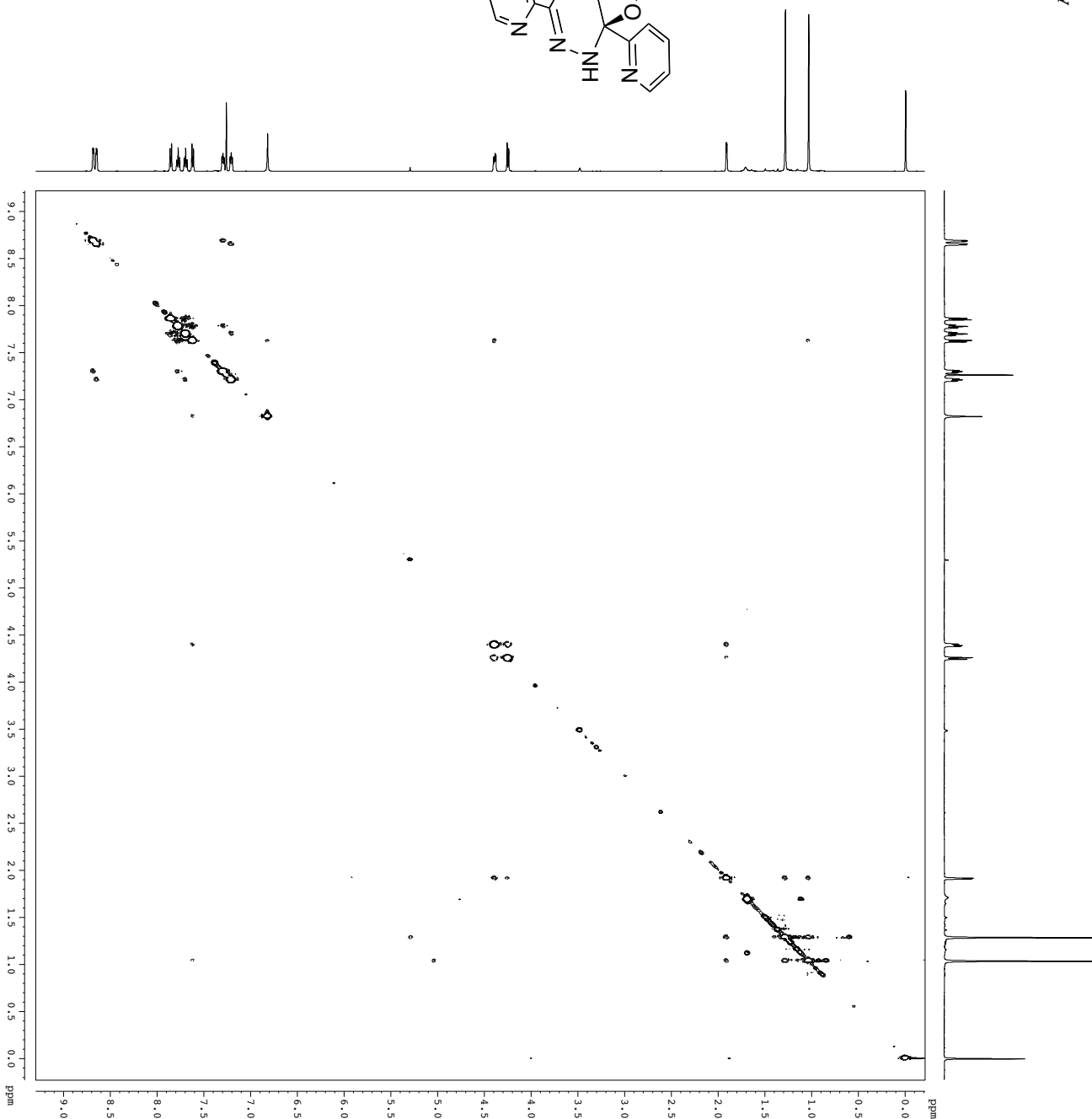
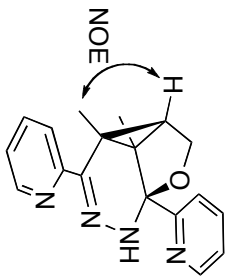


Chemical Shift (ppm)
159.578
156.675
152.866
149.103
148.678
136.679
136.348
123.434
122.533
122.348
121.224
97.604
77.337
77.082
76.828
71.017
37.171
31.910
22.864
16.757
12.971
0.057

```

Current Data Parameters
=====
USER          : dmf_13
EXPTNO       : 3
PROCNO      : 1
F2 - Acquisition Parameters
=====
Date_         : 2011118
Time         : 11:44
INSTRUM     : cryo500
PROBHD     : 5 mm CPY131H
PULPROG    : zgpg30
TD         : 65536
SOLVENT    : CDCl3
NS         : 121
DS         : 16
SWH        : 30340.16
FIDRES    : 0.0422381
AQ        : 1.0813940
RG        : 16
AQ        : 6.502
DE        : 6.00
DI        : 0.25000000
d11       : 0.43000000
d17       : 0.00019600
MCNRES    : 0.40000000
PC        : 0.01313100
=====
CHANNEL F1 13C
NUC1       : 13C
P1         : 15.50
PL1        : 0.00
P2         : 2000.00
PL2        : 120.00
SFO1       : 125.7942548
SF         : 125.7942548
SP1        : 3.20
SP2        : 3.20
SFO2       : C1360.052021
SF         : 0.00
SFOE2      : 0.00
=====
CHANNEL F2
NAME       : WATERZ16
NUC2       : 1H
P2         : 100.00
PL2        : 1.00
SFO2       : 500.2623101
=====
=====
GRADIENT CHANNEL
GPNAM1    : SINE_100
GPNAM2    :
SINE      : 100
GBX1      : 0.00
GBY1      : 0.00
GBZ1      : 0.00
GBX2      : 30.00
GBY2      : 50.00
GBZ2      : 50.00
PL5       : 100.00
PC        : 2.00
=====
F2 - Processing parameters
=====
SF        : 125.7804190
AQ        : 6.50
RG        : 16
PC        : 2.00
  
```

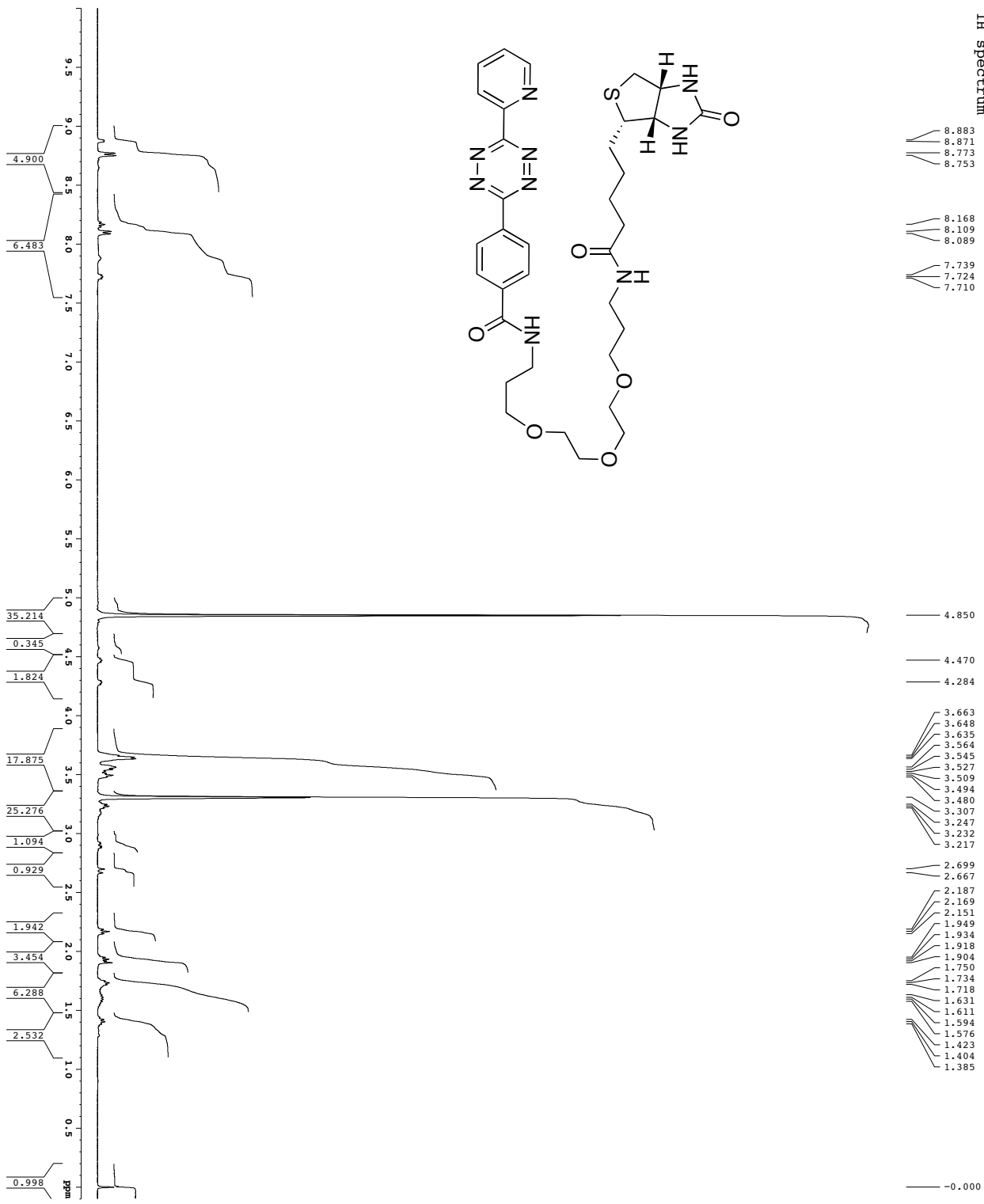
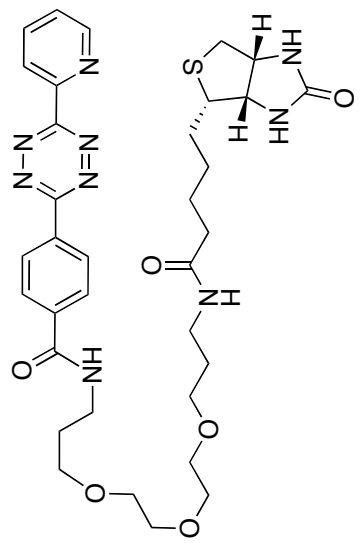
gnoesy



```

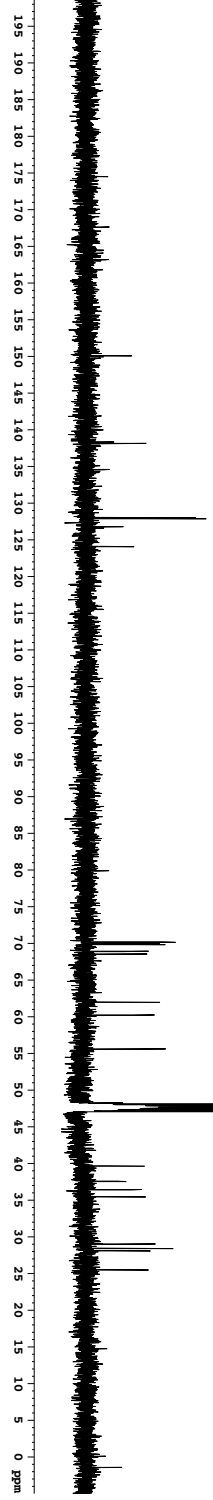
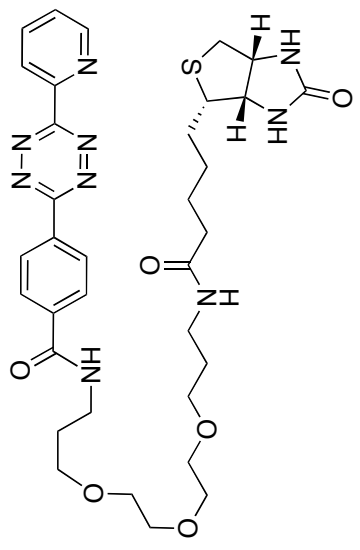
Current Data Parameters
=====
NAME          gnoesy
EXPNO         4
PROCNO        1
F2 - Acquisition Parameters
-----
Date_         20111119
Time          14:19
INSTRUM      cryo-500
PROBHD      5 mm QNP1H/1
PULPROG      zgpg30
TD           65536
SFO1         500.1362615 MHz
AQ           0.0000245 sec
RG           0.0000245 sec
WDW          EM
SSB          0
GB           0
PC           2.00
F1 - Processing parameters
-----
SI           32768
SF           500.1362615 MHz
WDW          EM
SSB          0
GB           0
PC           2.00
F2 - Processing parameters
-----
SI           32768
SF           500.1362615 MHz
WDW          EM
SSB          0
GB           0
PC           2.00
F1 - Acquisition parameters
-----
TD           65536
SF           500.1362615 MHz
SFO1         500.1362615 MHz
WDW          EM
SSB          0
GB           0
PC           2.00
===== CHANNEL f1 =====
NUC1         1H
P1           12.00 usec
PL1          0.00 dB
SFO1         500.1362615 MHz
===== GRADIENT CHANNEL =====
GPRM1       0.00 %
GPRM2       0.00 %
GPRM3       0.00 %
GPRM4       0.00 %
GPRM5       0.00 %
GPRM6       0.00 %
GPRM7       0.00 %
GPRM8       0.00 %
GPRM9       0.00 %
GPRM10      0.00 %
GPRM11      0.00 %
GPRM12      0.00 %
GPRM13      0.00 %
GPRM14      0.00 %
GPRM15      0.00 %
GPRM16      0.00 %
GPRM17      0.00 %
GPRM18      0.00 %
GPRM19      0.00 %
GPRM20      0.00 %
GPRM21      0.00 %
GPRM22      0.00 %
GPRM23      0.00 %
GPRM24      0.00 %
GPRM25      0.00 %
GPRM26      0.00 %
GPRM27      0.00 %
GPRM28      0.00 %
GPRM29      0.00 %
GPRM30      0.00 %
GPRM31      0.00 %
GPRM32      0.00 %
GPRM33      0.00 %
GPRM34      0.00 %
GPRM35      0.00 %
GPRM36      0.00 %
GPRM37      0.00 %
GPRM38      0.00 %
GPRM39      0.00 %
GPRM40      0.00 %
GPRM41      0.00 %
GPRM42      0.00 %
GPRM43      0.00 %
GPRM44      0.00 %
GPRM45      0.00 %
GPRM46      0.00 %
GPRM47      0.00 %
GPRM48      0.00 %
GPRM49      0.00 %
GPRM50      0.00 %
GPRM51      0.00 %
GPRM52      0.00 %
GPRM53      0.00 %
GPRM54      0.00 %
GPRM55      0.00 %
GPRM56      0.00 %
GPRM57      0.00 %
GPRM58      0.00 %
GPRM59      0.00 %
GPRM60      0.00 %
GPRM61      0.00 %
GPRM62      0.00 %
GPRM63      0.00 %
GPRM64      0.00 %
GPRM65      0.00 %
GPRM66      0.00 %
GPRM67      0.00 %
GPRM68      0.00 %
GPRM69      0.00 %
GPRM70      0.00 %
GPRM71      0.00 %
GPRM72      0.00 %
GPRM73      0.00 %
GPRM74      0.00 %
GPRM75      0.00 %
GPRM76      0.00 %
GPRM77      0.00 %
GPRM78      0.00 %
GPRM79      0.00 %
GPRM80      0.00 %
GPRM81      0.00 %
GPRM82      0.00 %
GPRM83      0.00 %
GPRM84      0.00 %
GPRM85      0.00 %
GPRM86      0.00 %
GPRM87      0.00 %
GPRM88      0.00 %
GPRM89      0.00 %
GPRM90      0.00 %
GPRM91      0.00 %
GPRM92      0.00 %
GPRM93      0.00 %
GPRM94      0.00 %
GPRM95      0.00 %
GPRM96      0.00 %
GPRM97      0.00 %
GPRM98      0.00 %
GPRM99      0.00 %
GPRM100     0.00 %
=====
  
```

1H spectrum

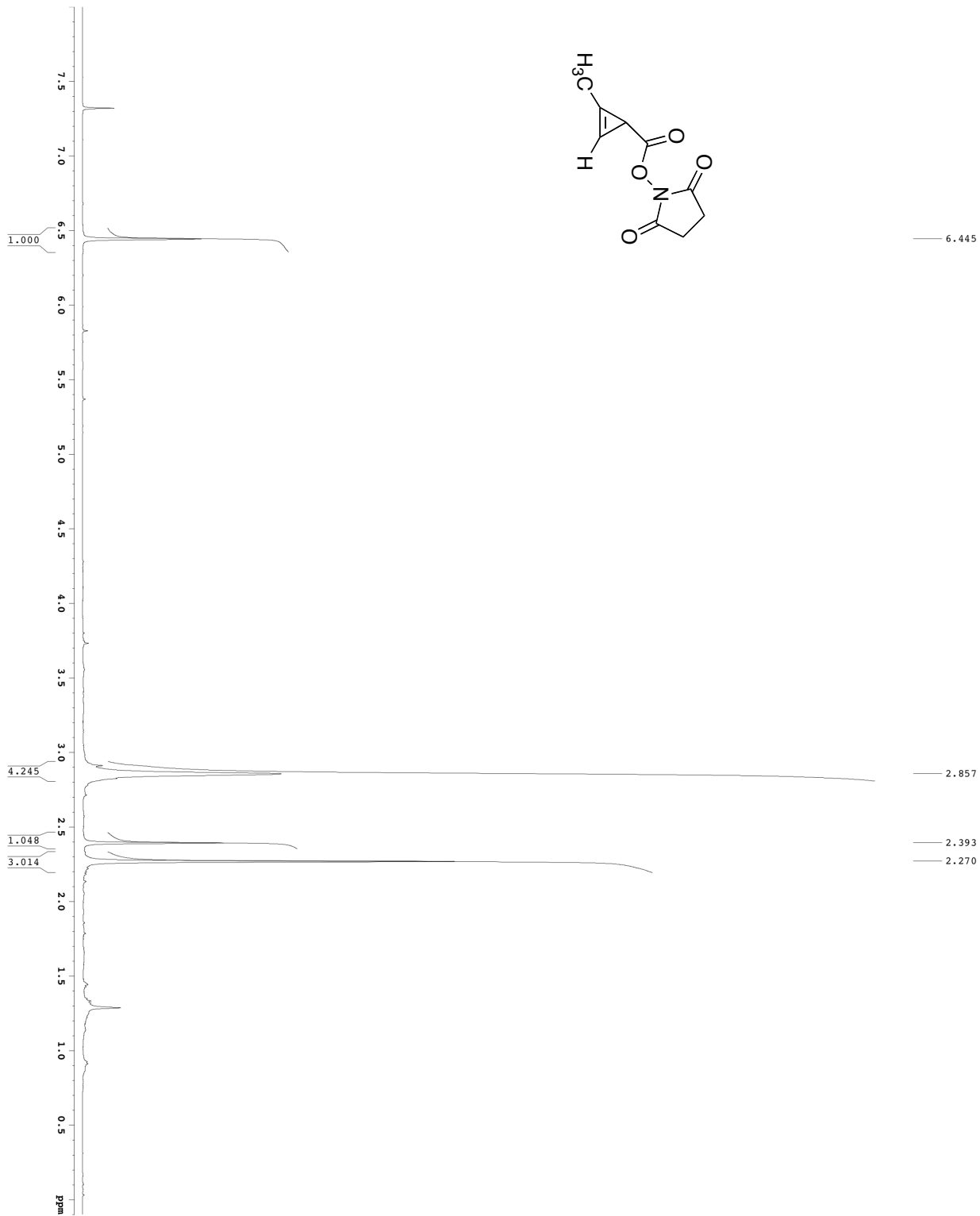
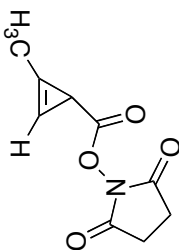


Current Data Parameters
 USER: Kambet
 EXPNO: 5
 PROCNO: 1
 F2 - Acquisition Parameters
 Date_: 20121005
 Time: 11:40:55
 INSTRUM: spect
 PROBMOD: 1H-1D
 PULPROG: zgpg30
 TD: 65536
 SOLVENT: MeOH
 NS: 2
 DS: 2
 SWH: 6418.222 Hz
 SF: 400.7618 MHz
 AQ: 5.118579 sec
 RG: 327.5
 FWHM: 78.004 Hz
 DE: 4.50 usec
 DI: 4.50 usec
 D1: 0.10000000 sec
 MCHES1: 0.00000000 sec
 MCHES2: 0.01500000 sec
 CHANNE1: F1
 P1: 12.00 usec
 P11: -4.60 dB
 SFO1: 400.122809 MHz
 F2 - Processing Parameters
 SF: 400.130139 MHz
 MDW: EM
 LB: 0.30 Hz
 GB: 0
 PC: 2.00

DK01-081
Z-restored spin-echo 13C spectrum with 1H decoupling



Current Data Parameters
 USER: jldan
 EXPNO: 2
 PROCNO: 1
 F2 - Acquisition Parameters
 Date_: 20120112
 Time: 12:21:12
 INSTRUM: cryo500
 PROBRD: 5mm CPYBBO
 PULPROG: zgpg30
 TD: 65536
 SFO: 125.761153
 SOLVENT: CD3OD
 NS: 16
 DS: 4
 SWH: 30183.16 Hz
 SF: 301462.381 Hz
 SH: 16
 SFOFF: 1.0813940 sec
 AO: 1.0813940 sec
 RG: 655
 INCR: 1.25000000
 DE: 6.00 usec
 DI: 0.23000000 sec
 d11: 0.43000000 sec
 d17: 0.00019600 sec
 ACQRES: 0.40000000 sec
 F2 FWHM: 0.01319100 usec
 ===== CHANNEL f1 =====
 NUC1: 13C
 P1: 15.00 usec
 PL1: 0.00 dB
 P2: 2000.00 usec
 PL2: 120.00 dB
 SFO1: 125.761153 MHz
 SP1: 3.20 dB
 SPAN1: C160,0.5,20.1
 SFO2: 0.00 Hz
 SPOFF2: 0.00 Hz
 ===== CHANNEL f2 =====
 NUC2: 1H
 P1: 100.00 usec
 PL1: 1.00 dB
 P2: 1.00 dB
 SFO2: 500.261518 MHz
 ===== GRADIENT CHANNEL =====
 GPNAM1: SINE-100
 GPNAM2: SINE-100
 GPC1: 0.00 %
 GPC2: 0.00 %
 GPC3: 0.00 %
 GPC4: 0.00 %
 GPC5: 0.00 %
 GPC6: 0.00 %
 GPC7: 30.00 %
 GPC8: 30.00 %
 GPC9: 50.00 %
 GPC10: 50.00 %
 P15: 100.00 usec
 P16: 100.00 usec
 F2 - Processing parameters
 SF: 125.7604190 MHz
 DS: 4
 SFO: 125.7604190 MHz
 ASB: 0
 LA: 1.00 Hz
 GB: 0
 PC: 1.00



Current Data Parameters
 USER: jldian
 EXNO: 1
 PROCNO: 1
 F2 - Acquisition Parameters
 Date_: 20120907
 Time: 11:00:00
 INSTRUM: 5 mm CPCL 1H-
 PROBHD: 5 mm CPCL 1H-
 PULPROG: zgpg30
 TD: 81728
 SFO1: 500.2235015 MHz
 SOLVENT: CDCl3
 DS: 2
 SWH: 8012.820 Hz
 FWHM: 12.240 Hz
 AQ: 5.098972 sec
 RG: 62.4145
 INEG: 5
 DE: 6.00 usec
 TE: 298.0 K
 MCHRES: 0.30000000 sec
 MCWRES: 0.01500000 sec
 ===== CHANNEL f1 =====
 NUC1: 1H
 P1: 7.00 usec
 PL1: 1.60 dB
 SFO1: 500.2235015 MHz
 F2 - Processing parameters
 SI: 65536
 SF: 500.2235015 MHz
 WDM: 2
 SSB: 0 Hz
 CB: 4.00
 PC: 4.00

IAN-01-181

171.070
169.548

110.539

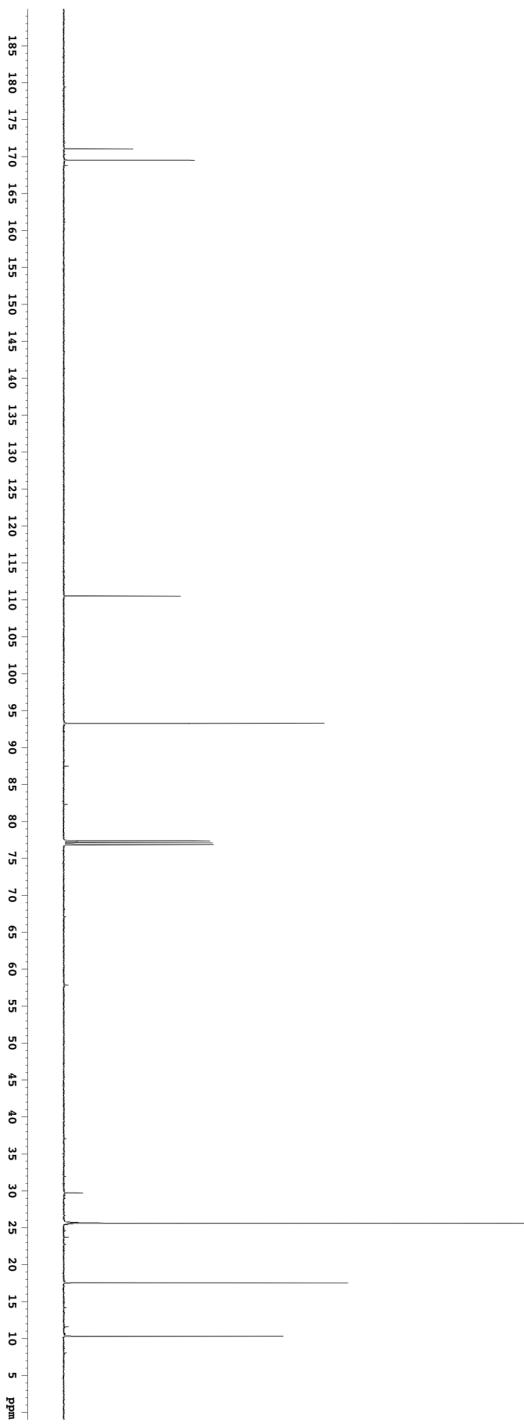
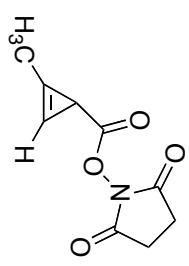
93.296

77.384
77.129
76.875

25.629

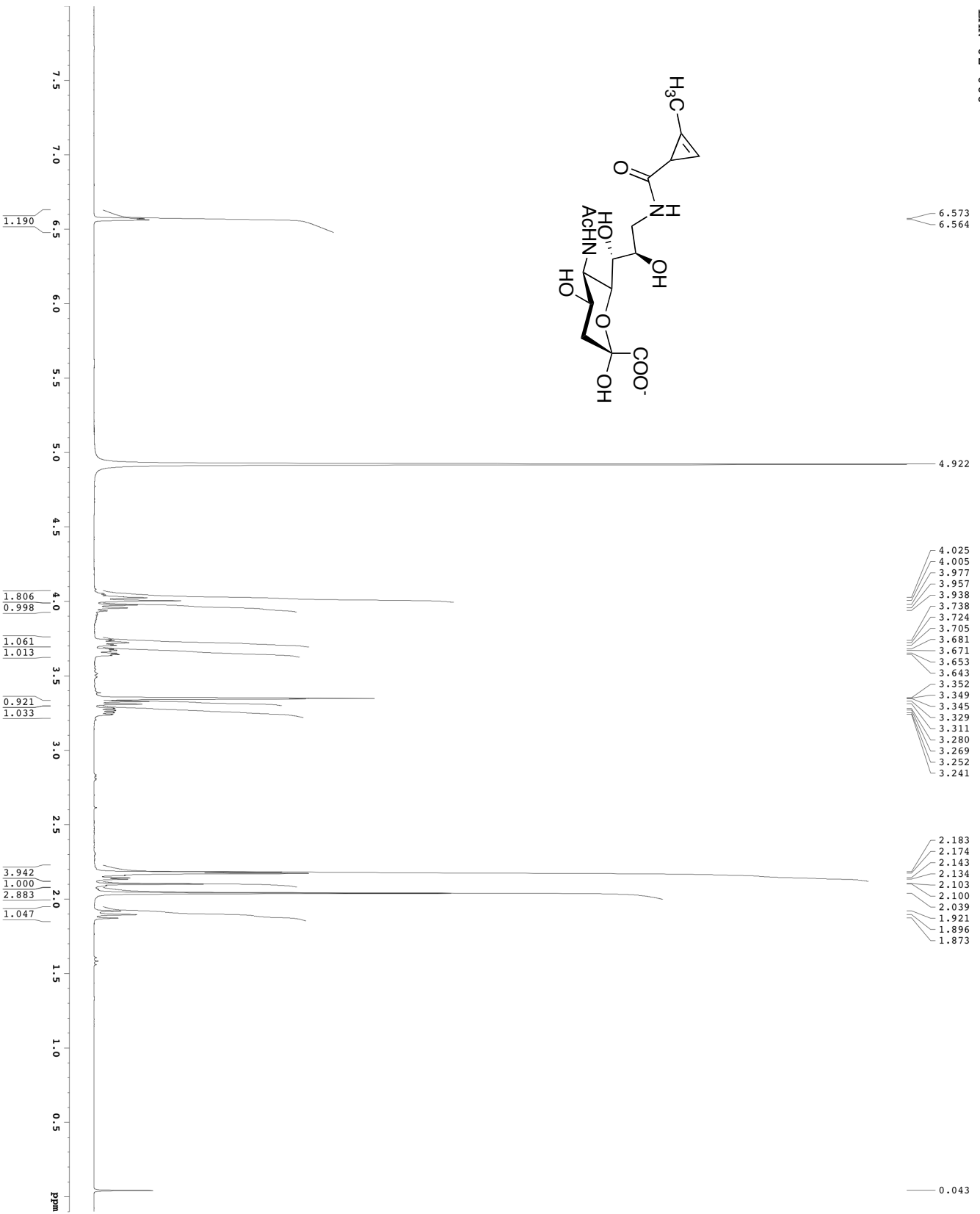
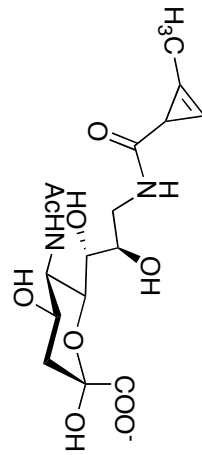
17.541

10.318



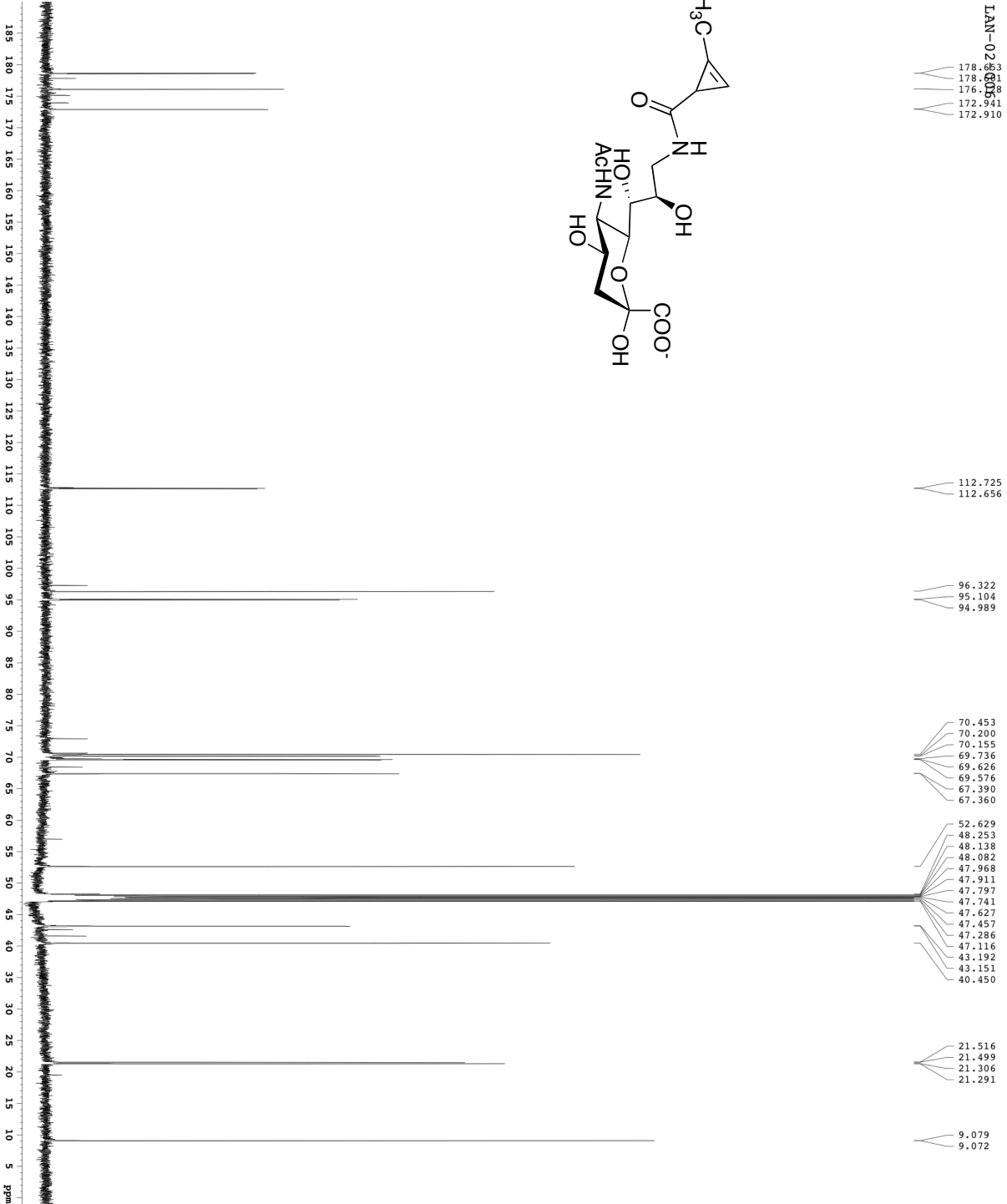
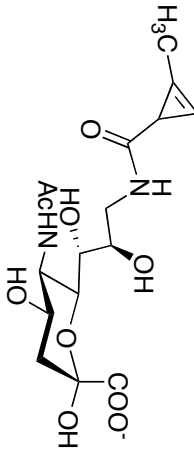
```

Current Data Parameters
=====
USER          Ildam
EXPNO         1
PROCNO       1
PROCNAME     1
F2 - Acquisition Parameters
-----
Date_         20140912
Time         12:27:57
INSTRUM      5 mm cryo300
PULPROG      zgpg30
PROBHD1      Spinechop30ppr
TD           65536
SFO          300.13
AQ           10.24
RG           1024
SI           1024
SF           3030.431 Hz
FIDRES      0.462388 Hz
AQRES      1.72982 sec
RG          16.500 usec
DM          16.500 usec
TE          298.0 K
D1          0.0022000 sec
d11         0.0300000 sec
DELTA       0.0000000 sec
MKRES      0.0000000 sec
PC         0.0300000 sec
PCPKMR     0.0000000 sec
===== CHANNEL f1 =====
NUC1         13C
P1           15.50 usec
PL1          0.00 dB
P2           2000.00 usec
PL2          19.00 dB
P3           125.7942548 MHz
SFO1         125.7942548 MHz
SF2          3.220 MHz
SFO2         3.220 MHz
SFO3         3.220 MHz
SFO4         3.220 MHz
SFO5         3.220 MHz
SFO6         3.220 MHz
SFO7         3.220 MHz
SFO8         3.220 MHz
===== CHANNEL f2 =====
NUC2         1H
P2           100.00 usec
PL2          0.00 dB
P3           24.60 usec
PL3          19.00 dB
P4           500.2121011 MHz
SFO2         500.2121011 MHz
===== GRADIENT CHANNEL =====
GPRM1       SINE:100
GPRM2       0.00 %
GPRM3       0.00 %
GPRM4       0.00 %
GPRM5       30.00 %
GPRM6       50.00 usec
GPRM7       1000.00 usec
F2 - Processing parameters
-----
SI           65536
SF           300.130 MHz
WDW          EM
SSB          1.00 Hz
GB           0
PC           2.00
  
```



Current Data Parameters
 USER 1ddlan
 EXPRN LAN-02-06
 PROCNO 1
 F2 - Acquisition Parameters
 Date_ 20120224
 Time 0.03
 INSTRM cgc2500
 PULPROG zgpg30
 TD 81728
 NS 2048
 DS 2
 SMN 8012.820 Hz
 SFO1 500.2235015 MHz
 AQ 5.098774 sec
 RG 62.409
 DM 6.00 usec
 TE 298.0 K
 D1 0.1000000 sec
 DECHRG 0.0150000 sec
 ===== CHANNEL f1 =====
 NUCL1 1H
 P1 7.50 usec
 PL1 1.60 dB
 SFO1 500.2235015 MHz
 F2 - Processing parameters
 SI 6556
 SF 500.2235015 MHz
 NDM EM
 SSB 0.30 Hz
 GB 4.00
 PC 4.00

LAN-02-09-05
 178.918
 178.918
 176.918
 172.941
 172.910



112.725
 112.656

96.322
 95.104
 94.989

70.453
 70.200
 70.155
 69.736
 69.626
 69.576
 67.390
 67.360

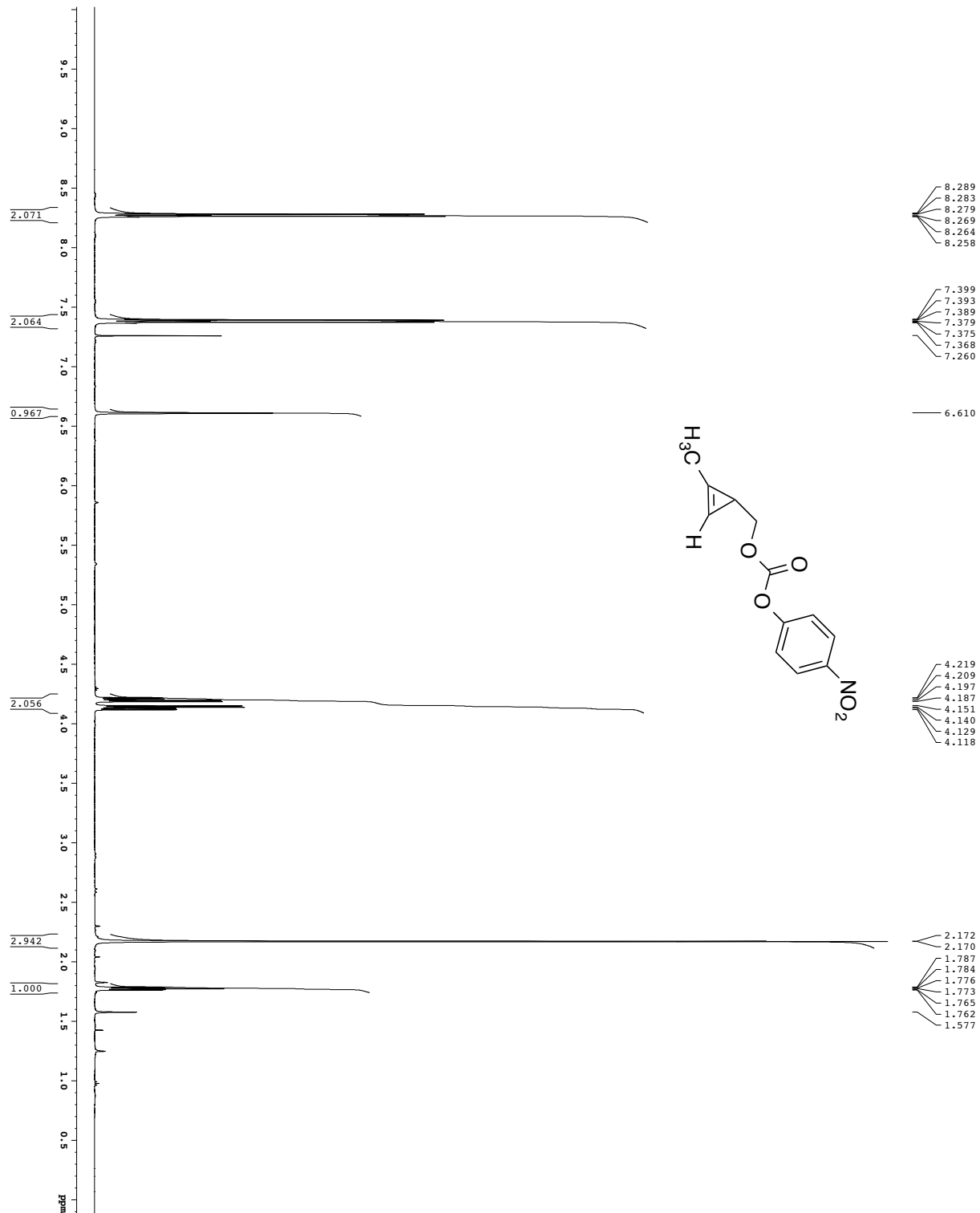
52.629
 52.253
 48.138
 48.082
 47.968
 47.911
 47.797
 47.741
 47.627
 47.457
 47.286
 47.116
 45.192
 40.450

21.516
 21.499
 21.306
 21.291

9.079
 9.072

Current Data Parameters
 USER: jldlan
 EXPER: LAN-02-09-05
 PROCNO: 1
 F2 - Acquisition Parameters
 Date_: 20120324
 Time: 15:11:51
 INSTRUM: spect
 PROBNM: 3mm CPY300
 PULPROG: zgpg30
 TD: 65536
 SFO: 5120
 DS: 4
 B1: 3030.16 Hz
 FIDRES: 0.462388 Hz
 AQ: 1.0812940 sec
 DM: 16.500 usec
 DE: 2.000 usec
 TE: 298.2 K usec
 D1: 0.2500000 sec
 d11: 0.0010000 sec
 d16: 0.0002000 sec
 d17: 0.0001600 sec
 NS: 1024
 NS2: 1
 SFOF2: 0.0150000 sec
 P2: 31.00 usec
 ===== CHANNEL f1 =====
 NUC1: 13C
 P1: 15.50 usec
 PL1: 0.00 dB
 P2: 500.00 usec
 PL2: 1.60 dB
 P3: 120.00 dB
 SFO2: 500.225011 MHz
 ===== CHANNEL f2 =====
 CPDPRG2: waltz16
 NUC2: 1H
 P2: 100.00 usec
 PL2: 1.60 dB
 SFO2: 500.225011 MHz
 ===== GRANDIR CHANNEL =====
 GNMN1: 3mm CPY300
 STW: 100 %
 GPRX1: 0.00 %
 GPRX2: 0.00 %
 GPRX3: 0.00 %
 GPRX4: 0.00 %
 GPRX5: 38.00 %
 GPRX6: 38.00 %
 p15: 500.00 usec
 p16: 1000.00 usec
 F2 - Processing parameters
 SI: 65536
 SF: 5120.135 MHz
 WDM: BM
 LB: 1.00 Hz
 GB: 0
 PC: 2.00

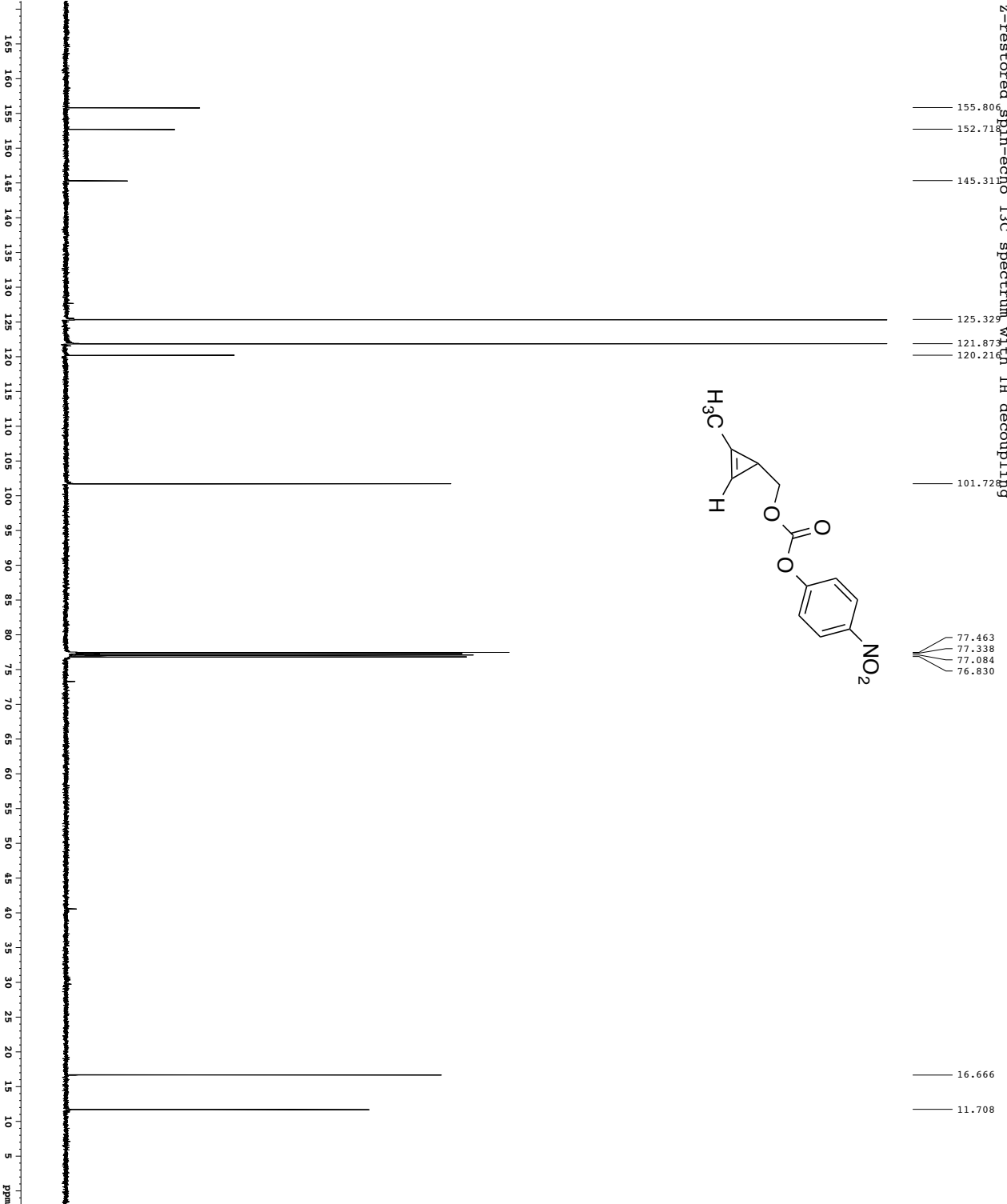
1H spectrum



Current Data Parameters

USER	operator
EXPNO	nmr_1704
PROCNO	4
PROC1	1
EXPNO	292
PROCNO	1
F2 - Acquisition Parameters	
Date_	20130909
Time	17.41
INSTRUM	cryo500
PROBHD	5 mm CPXI 1H-
P1	1.50
TD	65536
WDW	EM
SF	500.136260
F2	500.136260
NUC1	13C
NUC2	13C
PC1	1.50
PC2	1.40
PC3	1.40
PC4	1.40
PC5	1.40
PC6	1.40
PC7	1.40
PC8	1.40
PC9	1.40
PC10	1.40
PC11	1.40
PC12	1.40
PC13	1.40
PC14	1.40
PC15	1.40
PC16	1.40
PC17	1.40
PC18	1.40
PC19	1.40
PC20	1.40
PC21	1.40
PC22	1.40
PC23	1.40
PC24	1.40
PC25	1.40
PC26	1.40
PC27	1.40
PC28	1.40
PC29	1.40
PC30	1.40
PC31	1.40
PC32	1.40
PC33	1.40
PC34	1.40
PC35	1.40
PC36	1.40
PC37	1.40
PC38	1.40
PC39	1.40
PC40	1.40
PC41	1.40
PC42	1.40
PC43	1.40
PC44	1.40
PC45	1.40
PC46	1.40
PC47	1.40
PC48	1.40
PC49	1.40
PC50	1.40
PC51	1.40
PC52	1.40
PC53	1.40
PC54	1.40
PC55	1.40
PC56	1.40
PC57	1.40
PC58	1.40
PC59	1.40
PC60	1.40
PC61	1.40
PC62	1.40
PC63	1.40
PC64	1.40
PC65	1.40
PC66	1.40
PC67	1.40
PC68	1.40
PC69	1.40
PC70	1.40
PC71	1.40
PC72	1.40
PC73	1.40
PC74	1.40
PC75	1.40
PC76	1.40
PC77	1.40
PC78	1.40
PC79	1.40
PC80	1.40
PC81	1.40
PC82	1.40
PC83	1.40
PC84	1.40
PC85	1.40
PC86	1.40
PC87	1.40
PC88	1.40
PC89	1.40
PC90	1.40
PC91	1.40
PC92	1.40
PC93	1.40
PC94	1.40
PC95	1.40
PC96	1.40
PC97	1.40
PC98	1.40
PC99	1.40
PC100	1.40

Z-restored spin-echo 13C spectrum with 1H decoupling



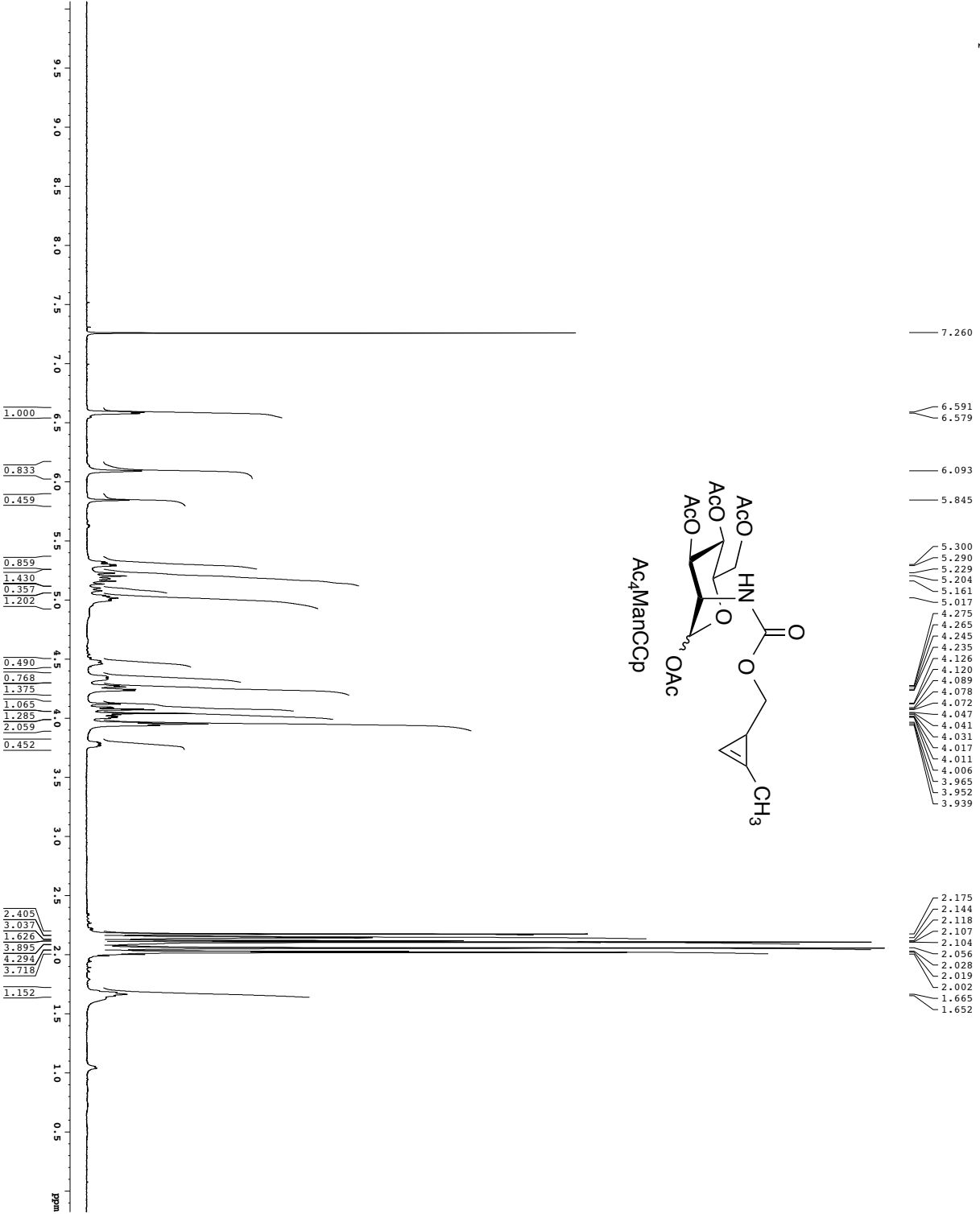
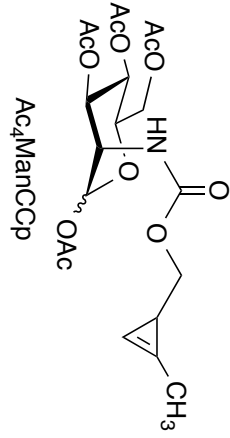
77.463
77.338
77.084
76.830

16.666
11.708

```

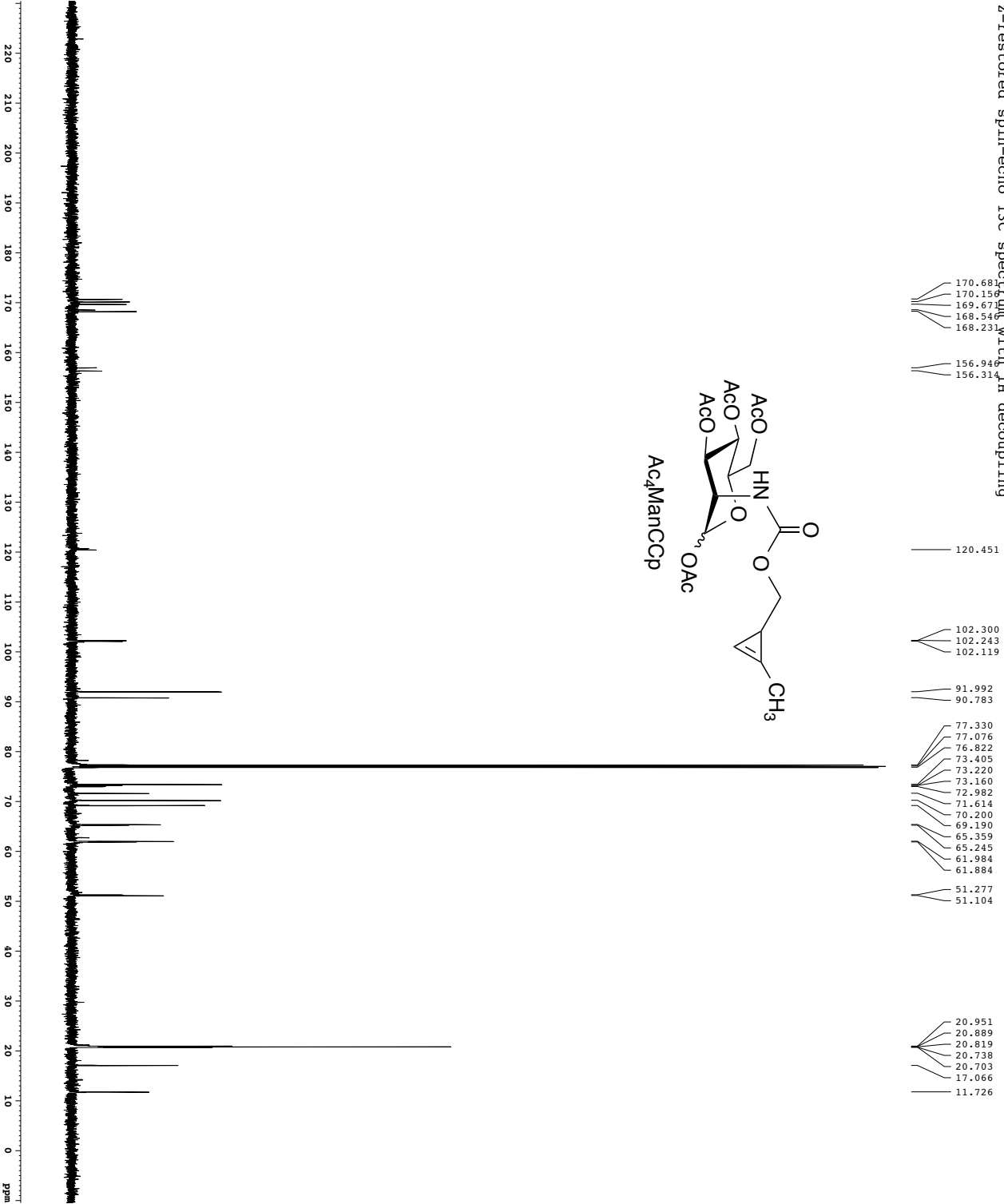
Current Data Parameters
=====
USER          date_
NAME          DMN_T_095
EXPNO        1
PROCNO       1
F2 - Acquisition Parameters
-----
Date_         20130909
Time         14.34
PROBHD       5 mm CPYX-100
PULPROG      zgpg30
TD           65536
SOLVENT      CDCl3
NS           16
DS           4
SWH          16.16 Hz
FIDRES       0.4462388 Hz
AQ           1.0813940 sec
RG           16.500
WDW          EM
SS           1.000
LB           6.00 usec
DE           6.00 usec
TE           300.2 K
NUC1          13C
NUC2          13C
P1           15.50 usec
PL1          -2.00 dB
P2           2000.00 usec
PL2          -1.60 dB
SFO1         125.7642548 MHz
SFO2
=====
Channel f1 13C
=====
NUC1          13C
P1           15.50 usec
PL1          -2.00 dB
P2           2000.00 usec
PL2          -1.60 dB
SFO1         125.7642548 MHz
SFO2
=====
Channel f2 13C
=====
NAME          GEMINI2
PROCNO       1
SINVER       100
=====
Channel f3 13C
=====
NAME          GEMINI2
PROCNO       1
SINVER       100
=====
Channel f4 13C
=====
NAME          GEMINI2
PROCNO       1
SINVER       100
=====
F2 - Processing parameters
-----
SI          32768
SF          125.7601150 MHz
WDW          EM
SS           1.000
LB           1.00 Hz
GB           0
PC           2.00
    
```

1H spectrum



Current Data Parameters
 USER: agp
 NAME: IMR4_066
 EXPNO: 1
 PROCNO: 1
 F2 - Acquisition Parameters
 Date_Time: 20130916
 Time: 10.17
 INSTRUM: spect
 PROBRND: 5 mm Multispec1
 PULPROG: zgpg30
 SFO1: 400.1328009
 SOLVENT: DMSO-d6
 NS: 8
 DS: 2
 SWH: 64110.256 Hz
 FIDRES: 0.197813 Hz
 RG: 511
 ACQ: 5.148644 sec
 TM: 78.000 usec
 TE: 298.2 K
 DE: 0.10000000 sec
 DIAPHR: 0.01500000 sec
 MCNMR: 0.01500000 sec
 ===== CHANNEL f1 =====
 NUC1: 1H
 P1: 12.00 usec
 PL1: 0.00 dB
 SFO1: 400.1328009 MHz
 F2 - Processing parameters
 SI: 65536
 SF: 400.1300218 MHz
 SE: 0
 SSB: 0
 CB: 0.30 Hz
 GB: 0
 PC: 2.00

Z-restored spin-echo ¹³C spectrum with ¹H decoupling



Current Data Parameters
 USER: spatie
 EXPNO: 1
 PROCNO: 1

F2 - Acquisition Parameters
 Date_: 2011220
 Time: 12:50:00
 INSTRUM: spect
 PROBHD: 5 mm CPXI-1H-1
 PULPROG: zgpg30
 TD: 65536
 SOLVENT: CDCl3
 NS: 16
 DS: 4

SHF: 300.013033 Hz
 AQ: 1.0313940 sec
 Acq: 6.562 sec
 KE: 16.000 usec
 DE: 6.00 usec
 TE: 298.15 K
 TD: 0.25000000 sec
 D11: 0.00200000 sec
 D12: 0.03000000 sec
 D15: 0.00000000 sec
 MCHRG1: 0.00000000 sec
 MCHRG2: 0.00000000 sec
 MCHRG3: 0.01500000 sec
 MCHRG4: 0.01500000 sec
 MCHRG5: 0.01500000 sec

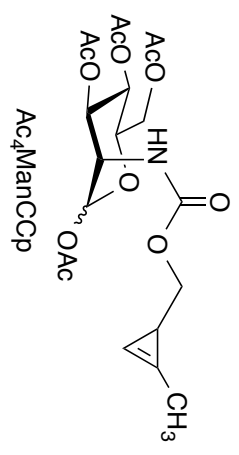
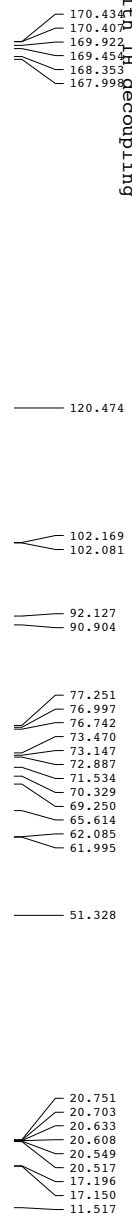
===== CHANNEL f1 13C =====
 NUC1: 13C
 P1: 15.50 usec
 PL1: 200.00 dB
 P2: 200.00 usec
 PL2: 200.00 dB
 P3: 120.00 dB
 P4: 120.00 dB
 FQ1: 125.764248 MHz
 FQ2: 125.764248 MHz
 SFO1: 3.200 dB
 SFO2: 3.200 dB
 SFO3: 3.200 dB
 SFO4: 3.200 dB
 SFO5: 3.200 dB
 SFO6: 3.200 dB
 SFO7: 3.200 dB
 SFO8: 3.200 dB
 SFO9: 3.200 dB
 SFO10: 3.200 dB
 SFO11: 3.200 dB
 SFO12: 3.200 dB
 SFO13: 3.200 dB
 SFO14: 3.200 dB
 SFO15: 3.200 dB
 SFO16: 3.200 dB
 SFO17: 3.200 dB
 SFO18: 3.200 dB
 SFO19: 3.200 dB
 SFO20: 3.200 dB
 SFO21: 3.200 dB
 SFO22: 3.200 dB
 SFO23: 3.200 dB
 SFO24: 3.200 dB
 SFO25: 3.200 dB
 SFO26: 3.200 dB
 SFO27: 3.200 dB
 SFO28: 3.200 dB
 SFO29: 3.200 dB
 SFO30: 3.200 dB
 SFO31: 3.200 dB
 SFO32: 3.200 dB
 SFO33: 3.200 dB
 SFO34: 3.200 dB
 SFO35: 3.200 dB
 SFO36: 3.200 dB
 SFO37: 3.200 dB
 SFO38: 3.200 dB
 SFO39: 3.200 dB
 SFO40: 3.200 dB
 SFO41: 3.200 dB
 SFO42: 3.200 dB
 SFO43: 3.200 dB
 SFO44: 3.200 dB
 SFO45: 3.200 dB
 SFO46: 3.200 dB
 SFO47: 3.200 dB
 SFO48: 3.200 dB
 SFO49: 3.200 dB
 SFO50: 3.200 dB
 SFO51: 3.200 dB
 SFO52: 3.200 dB
 SFO53: 3.200 dB
 SFO54: 3.200 dB
 SFO55: 3.200 dB
 SFO56: 3.200 dB
 SFO57: 3.200 dB
 SFO58: 3.200 dB
 SFO59: 3.200 dB
 SFO60: 3.200 dB
 SFO61: 3.200 dB
 SFO62: 3.200 dB
 SFO63: 3.200 dB
 SFO64: 3.200 dB
 SFO65: 3.200 dB
 SFO66: 3.200 dB
 SFO67: 3.200 dB
 SFO68: 3.200 dB
 SFO69: 3.200 dB
 SFO70: 3.200 dB
 SFO71: 3.200 dB
 SFO72: 3.200 dB
 SFO73: 3.200 dB
 SFO74: 3.200 dB
 SFO75: 3.200 dB
 SFO76: 3.200 dB
 SFO77: 3.200 dB
 SFO78: 3.200 dB
 SFO79: 3.200 dB
 SFO80: 3.200 dB
 SFO81: 3.200 dB
 SFO82: 3.200 dB
 SFO83: 3.200 dB
 SFO84: 3.200 dB
 SFO85: 3.200 dB
 SFO86: 3.200 dB
 SFO87: 3.200 dB
 SFO88: 3.200 dB
 SFO89: 3.200 dB
 SFO90: 3.200 dB
 SFO91: 3.200 dB
 SFO92: 3.200 dB
 SFO93: 3.200 dB
 SFO94: 3.200 dB
 SFO95: 3.200 dB
 SFO96: 3.200 dB
 SFO97: 3.200 dB
 SFO98: 3.200 dB
 SFO99: 3.200 dB
 SFO100: 3.200 dB

===== CHANNEL f2 1H =====
 CHOPRG2: WALTZ16
 NUC2: 1H
 P2: 100.00 usec
 PL2: 19.00 dB
 P3: 1.60 dB
 PL3: 24.60 dB
 P4: 1.60 dB
 PL4: 24.60 dB
 SFO2: 500.2229011 MHz

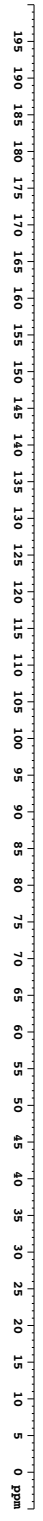
===== GRADIENT CHANNEL =====
 GENAM2: STINE:100
 GENX1: 0.00 %
 GENX2: 0.00 %
 GENX3: 0.00 %
 GENX4: 0.00 %
 GENX5: 0.00 %
 GENX6: 0.00 %
 GENX7: 0.00 %
 GENX8: 0.00 %
 GENX9: 0.00 %
 GENX10: 0.00 %
 GENX11: 0.00 %
 GENX12: 0.00 %
 GENX13: 0.00 %
 GENX14: 0.00 %
 GENX15: 0.00 %
 GENX16: 0.00 %
 GENX17: 0.00 %
 GENX18: 0.00 %
 GENX19: 0.00 %
 GENX20: 0.00 %
 GENX21: 0.00 %
 GENX22: 0.00 %
 GENX23: 0.00 %
 GENX24: 0.00 %
 GENX25: 0.00 %
 GENX26: 0.00 %
 GENX27: 0.00 %
 GENX28: 0.00 %
 GENX29: 0.00 %
 GENX30: 0.00 %
 GENX31: 0.00 %
 GENX32: 0.00 %
 GENX33: 0.00 %
 GENX34: 0.00 %
 GENX35: 0.00 %
 GENX36: 0.00 %
 GENX37: 0.00 %
 GENX38: 0.00 %
 GENX39: 0.00 %
 GENX40: 0.00 %
 GENX41: 0.00 %
 GENX42: 0.00 %
 GENX43: 0.00 %
 GENX44: 0.00 %
 GENX45: 0.00 %
 GENX46: 0.00 %
 GENX47: 0.00 %
 GENX48: 0.00 %
 GENX49: 0.00 %
 GENX50: 0.00 %
 GENX51: 0.00 %
 GENX52: 0.00 %
 GENX53: 0.00 %
 GENX54: 0.00 %
 GENX55: 0.00 %
 GENX56: 0.00 %
 GENX57: 0.00 %
 GENX58: 0.00 %
 GENX59: 0.00 %
 GENX60: 0.00 %
 GENX61: 0.00 %
 GENX62: 0.00 %
 GENX63: 0.00 %
 GENX64: 0.00 %
 GENX65: 0.00 %
 GENX66: 0.00 %
 GENX67: 0.00 %
 GENX68: 0.00 %
 GENX69: 0.00 %
 GENX70: 0.00 %
 GENX71: 0.00 %
 GENX72: 0.00 %
 GENX73: 0.00 %
 GENX74: 0.00 %
 GENX75: 0.00 %
 GENX76: 0.00 %
 GENX77: 0.00 %
 GENX78: 0.00 %
 GENX79: 0.00 %
 GENX80: 0.00 %
 GENX81: 0.00 %
 GENX82: 0.00 %
 GENX83: 0.00 %
 GENX84: 0.00 %
 GENX85: 0.00 %
 GENX86: 0.00 %
 GENX87: 0.00 %
 GENX88: 0.00 %
 GENX89: 0.00 %
 GENX90: 0.00 %
 GENX91: 0.00 %
 GENX92: 0.00 %
 GENX93: 0.00 %
 GENX94: 0.00 %
 GENX95: 0.00 %
 GENX96: 0.00 %
 GENX97: 0.00 %
 GENX98: 0.00 %
 GENX99: 0.00 %
 GENX100: 0.00 %

F2 - Processing parameters
 SF: 125.7604190 MHz
 KW: 64
 LG: 32
 LB: 1.00 Hz
 GB: 0
 PC: 2.00

13C spectrum with 1H decoupling

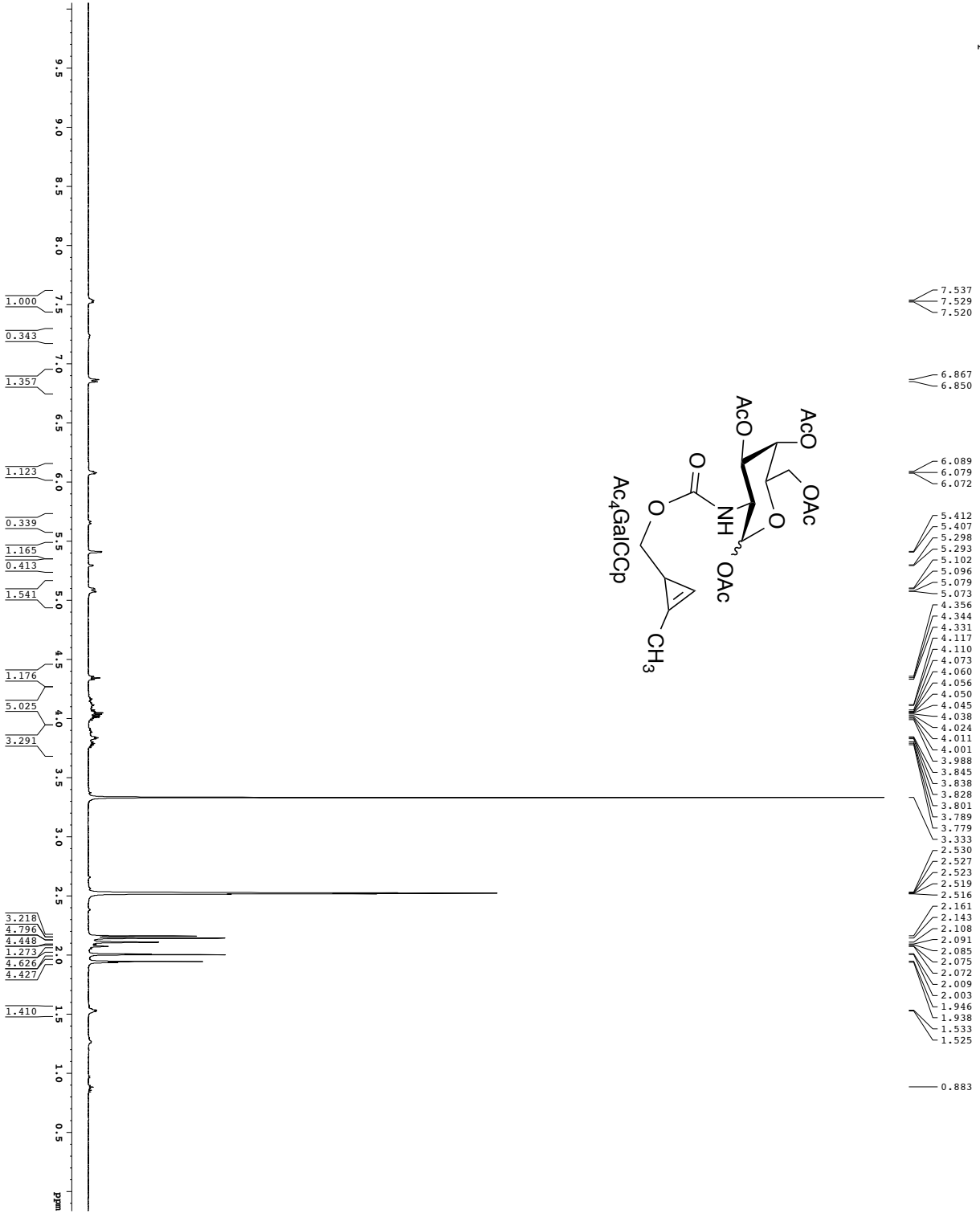


50 °C



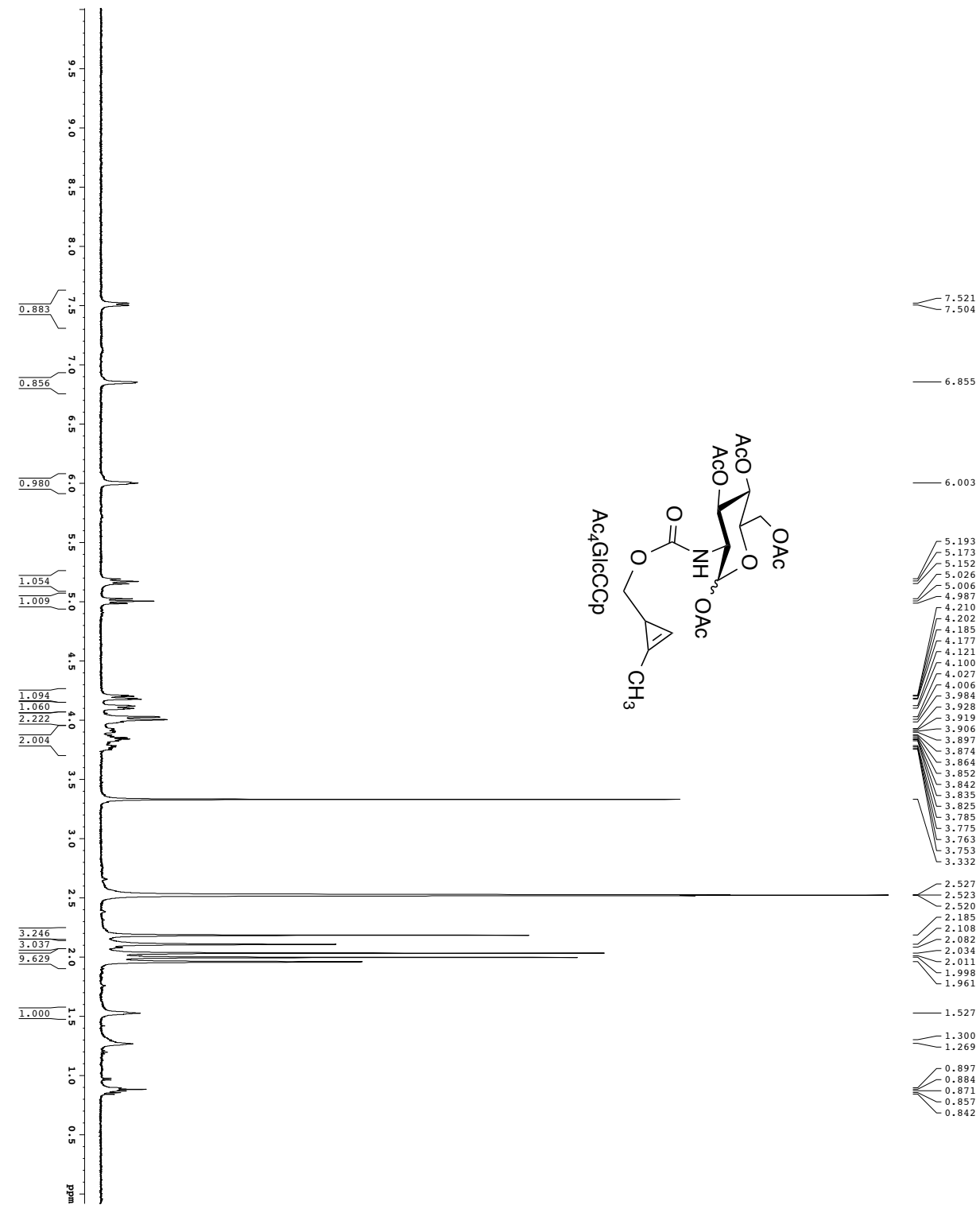
Current Data Parameters
 USER: dph
 VENDOR: spect
 EXPTNO: 1
 PROCNO: 6
 F2 - Acquisition Parameters
 Date_ : 20140207
 Time: 11:13:10
 INSTRUM: spect
 PROBHD: 5 mm broadband
 PULPROG: zgpg30
 TD: 65536
 SFO: 125.760353
 AQ: 2.000000
 SOLVENT: DMSO-d6
 NS: 2048
 DS: 4
 SWH: 30203.414 Hz
 FWHM: 0.443388 Hz
 AQ: 1.0813940 sec
 RG: 327.500
 DE: 1.50 usec
 TE: 300.2 K
 DE: 4.50 usec
 DI: 0.25000000 sec
 D11: 0.30000000 sec
 D12: 0.30000000 sec
 D13: 0.30000000 sec
 D14: 0.30000000 sec
 D15: 0.30000000 sec
 D16: 0.30000000 sec
 D17: 0.30000000 sec
 D18: 0.30000000 sec
 D19: 0.30000000 sec
 D20: 0.30000000 sec
 CHANM1: f1 13C
 P1: 7.70 usec
 P2: 7.70 usec
 SFO1: 125.5603013 MHz
 CHANM2: f2 13C
 P1: 8.00 usec
 P2: 8.00 usec
 SFO2: 125.760353 MHz
 F2 - Processing parameters
 SI: 32768
 SF: 125.5603013 MHz
 WDM: EN
 LB: 1.00 Hz
 GB: 0
 CB: 2.00

1H spectrum



Current Data Parameters
 USER: gpetts
 NAME: DMP_4_133B
 EXPNO: 1
 PROCNO: 1
 P1 - Acquisition Parameters
 Date_UTC: 20140107
 Time: 21.32
 INSTRUM: spect
 PROBRND: 5 mm broadband
 PULPROG: zgpg30
 SFO: 89.20
 SOLVENT: DMSO-d6
 NS: 8
 DS: 4
 SWH: 8012.820 Hz
 FIDRES: 0.098943 Hz
 AQ: 5.182446 sec
 RG: 182.46
 DM: 62.400 ussec
 SFO2: 298.0 Ksec
 DIAPHRM: 0.10000000 mmc
 NUC1: 13C
 NUC2: 1H
 P1: 12.200 ussec
 SFO1: 499.2934950 MHz
 P2 - Processing parameters
 SI: 65536
 SF: 499.2900000 MHz
 SW: 80000.000 Hz
 SSB: 0
 GB: 0.50 Hz
 PC: 1.00

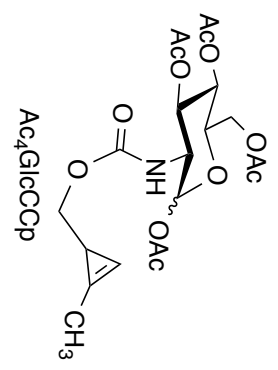
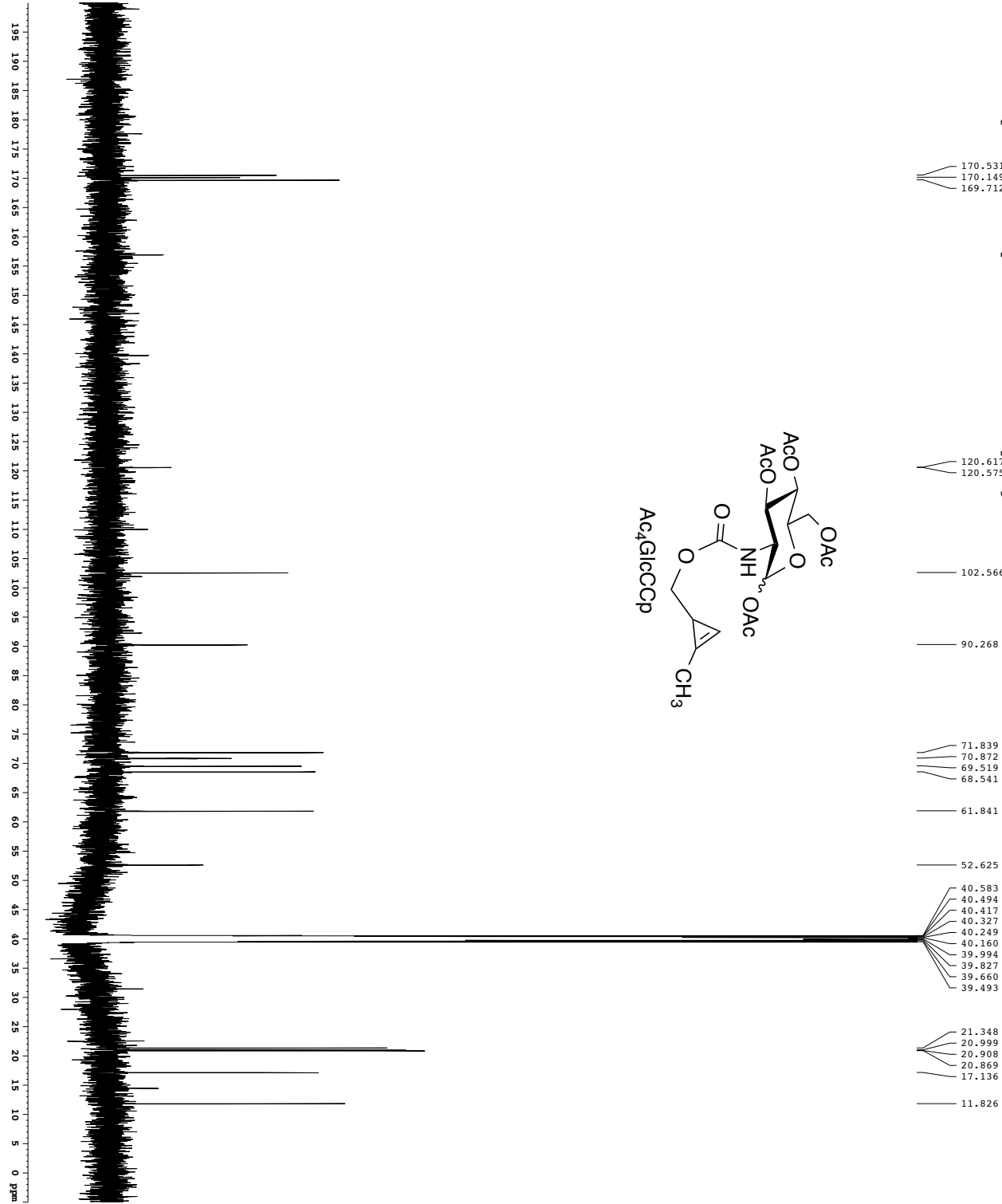
1H spectrum



```

Current Data Parameters
=====
USER      Date_       Date_
NAME      09F_107B   2010
EXPNO     1
PROCNO    1
F2 - Acquisition Parameters
=====
Date_     20101017
Time      11:00
INSTRUM   spect
PROBHD    5 mm broadband
PULPROG   zgpg30
TD         65536
SFO1       499.2934950 MHz
AQ         1.00
RG         64.00
DE         6.00
TE         298.2 K
K1         0.1000000 sec
K2         0.0000000 sec
K3         0.0000000 sec
K4         0.01500000 sec
===== CHANNEL f1 =====
NUC1       13C
P1         12.00
SFO1       101.6261260 MHz
RG         327.68
DE         5.00
TE         298.2 K
K1         0.0989774 sec
K2         1.4481200 sec
K3         6.00
K4         0.0000000 sec
=====
SI         65536
SF         499.2934950 MHz
WDW        EM
SSB        0
GB         0
PC         1.00
  
```

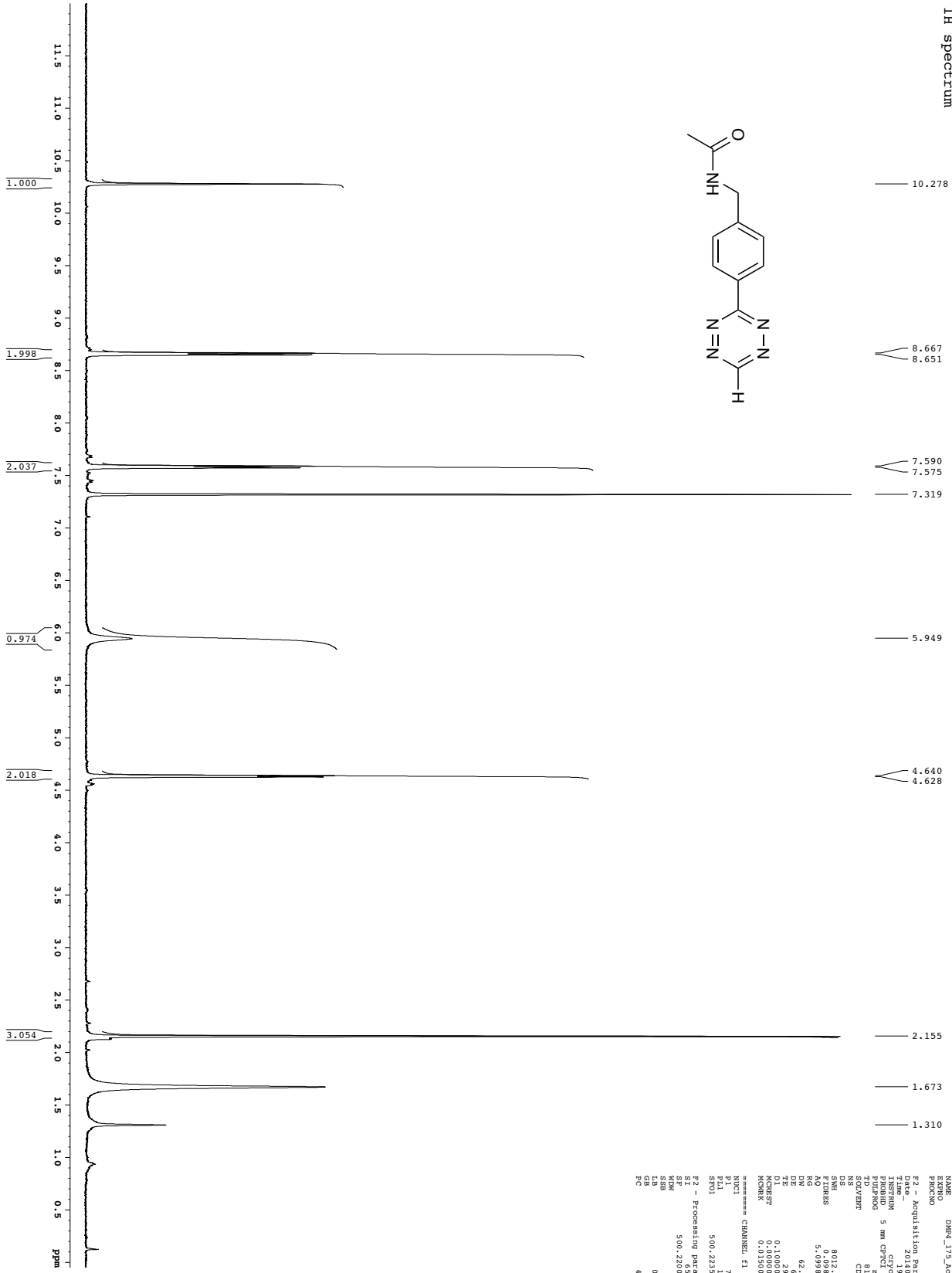
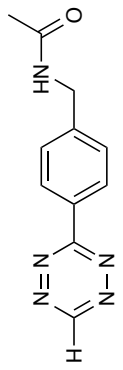

Z-restored spin-echo 13C spectrum with 1H decoupling



```

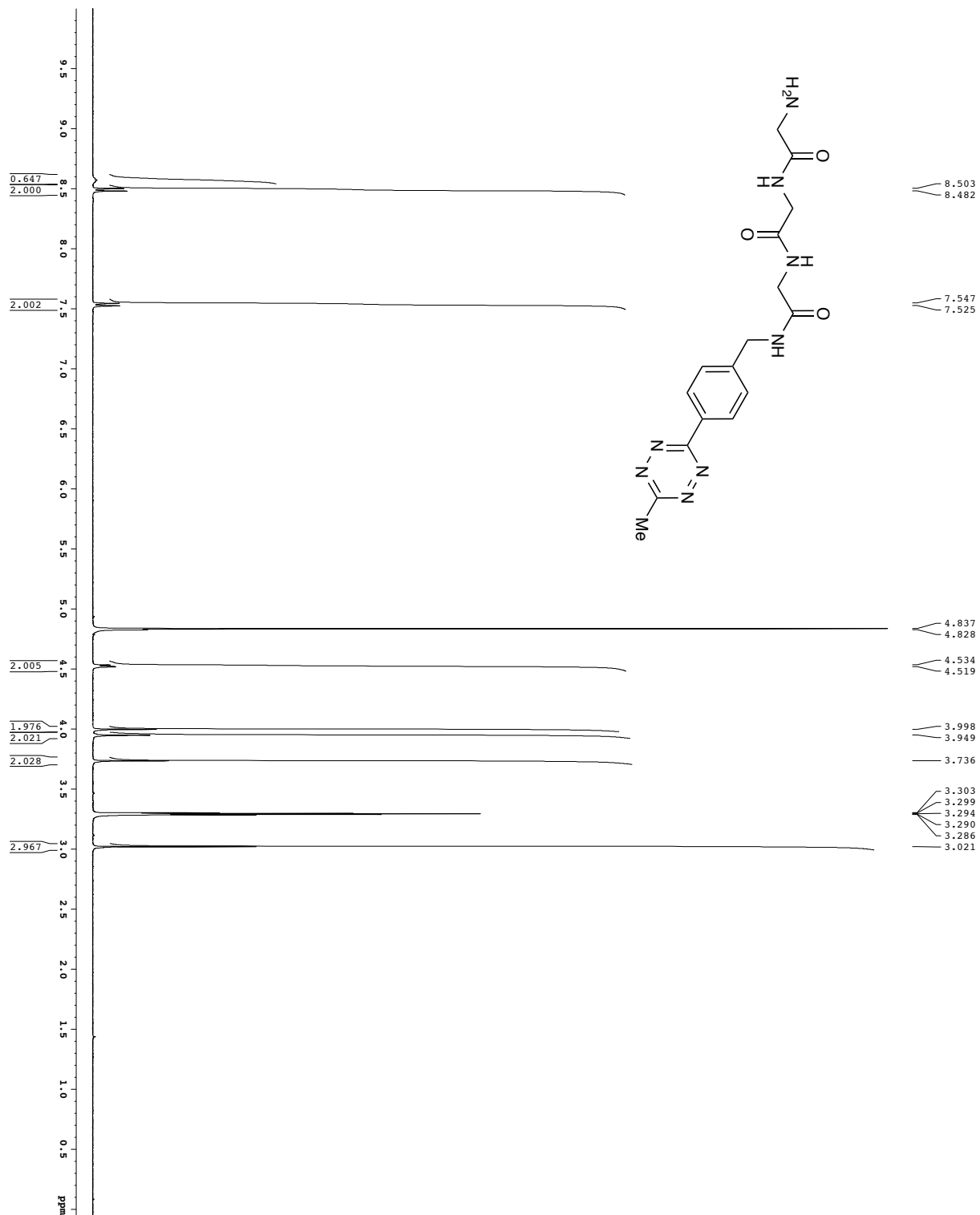
Current Data Parameters
USER: gatte
NAME: DMF_107B_DMSO
EXPNO: 1
PROCNO: 1
P2 - Acquisition Parameters
Date_UTC: 20140107
Time: 21.48
PROBHD: 5 mm QNP1H-
PULPROG: zgpg30p-ird
SOLVENT: DMSO
NS: 3072
DS: 4
SWH: 30303.031 Hz
FIDRES: 0.46238 Hz
AQ: 8.192
RG: 16
DM: 16.500 usec
TE: 298.0 K
NUC1: 13C
NUC2: 1H
D1: 0.22000000 sec
D11: 0.00100000 sec
D16: 0.00020000 sec
DELTA: 0.00100000 sec
PCPRG2: MCKRMK
MCKRMK: 0.01500000 sec
P2
===== CHANNEL F1 =====
NUC1: 13C
P1: 15.50 usec
PCPD2: 500.00 usec
P12: 120.00 usec
P13: 120.00 usec
P14: 120.00 usec
P15: 120.00 usec
P16: 120.00 usec
P17: 120.00 usec
P18: 120.00 usec
P19: 120.00 usec
P20: 120.00 usec
P21: 120.00 usec
P22: 120.00 usec
P23: 120.00 usec
P24: 120.00 usec
P25: 120.00 usec
P26: 120.00 usec
P27: 120.00 usec
P28: 120.00 usec
P29: 120.00 usec
P30: 120.00 usec
P31: 120.00 usec
P32: 120.00 usec
P33: 120.00 usec
P34: 120.00 usec
P35: 120.00 usec
P36: 120.00 usec
P37: 120.00 usec
P38: 120.00 usec
P39: 120.00 usec
P40: 120.00 usec
P41: 120.00 usec
P42: 120.00 usec
P43: 120.00 usec
P44: 120.00 usec
P45: 120.00 usec
P46: 120.00 usec
P47: 120.00 usec
P48: 120.00 usec
P49: 120.00 usec
P50: 120.00 usec
P51: 120.00 usec
P52: 120.00 usec
P53: 120.00 usec
P54: 120.00 usec
P55: 120.00 usec
P56: 120.00 usec
P57: 120.00 usec
P58: 120.00 usec
P59: 120.00 usec
P60: 120.00 usec
P61: 120.00 usec
P62: 120.00 usec
P63: 120.00 usec
P64: 120.00 usec
P65: 120.00 usec
P66: 120.00 usec
P67: 120.00 usec
P68: 120.00 usec
P69: 120.00 usec
P70: 120.00 usec
P71: 120.00 usec
P72: 120.00 usec
P73: 120.00 usec
P74: 120.00 usec
P75: 120.00 usec
P76: 120.00 usec
P77: 120.00 usec
P78: 120.00 usec
P79: 120.00 usec
P80: 120.00 usec
P81: 120.00 usec
P82: 120.00 usec
P83: 120.00 usec
P84: 120.00 usec
P85: 120.00 usec
P86: 120.00 usec
P87: 120.00 usec
P88: 120.00 usec
P89: 120.00 usec
P90: 120.00 usec
P91: 120.00 usec
P92: 120.00 usec
P93: 120.00 usec
P94: 120.00 usec
P95: 120.00 usec
P96: 120.00 usec
P97: 120.00 usec
P98: 120.00 usec
P99: 120.00 usec
P100: 120.00 usec
===== CHANNEL F2 =====
NAME: waltz16
NUC1: 1H
PCPD2: 100.00 usec
P12: 24.00 dB
P13: 24.00 dB
P14: 24.00 dB
P15: 24.00 dB
P16: 24.00 dB
P17: 24.00 dB
P18: 24.00 dB
P19: 24.00 dB
P20: 24.00 dB
P21: 24.00 dB
P22: 24.00 dB
P23: 24.00 dB
P24: 24.00 dB
P25: 24.00 dB
P26: 24.00 dB
P27: 24.00 dB
P28: 24.00 dB
P29: 24.00 dB
P30: 24.00 dB
P31: 24.00 dB
P32: 24.00 dB
P33: 24.00 dB
P34: 24.00 dB
P35: 24.00 dB
P36: 24.00 dB
P37: 24.00 dB
P38: 24.00 dB
P39: 24.00 dB
P40: 24.00 dB
P41: 24.00 dB
P42: 24.00 dB
P43: 24.00 dB
P44: 24.00 dB
P45: 24.00 dB
P46: 24.00 dB
P47: 24.00 dB
P48: 24.00 dB
P49: 24.00 dB
P50: 24.00 dB
P51: 24.00 dB
P52: 24.00 dB
P53: 24.00 dB
P54: 24.00 dB
P55: 24.00 dB
P56: 24.00 dB
P57: 24.00 dB
P58: 24.00 dB
P59: 24.00 dB
P60: 24.00 dB
P61: 24.00 dB
P62: 24.00 dB
P63: 24.00 dB
P64: 24.00 dB
P65: 24.00 dB
P66: 24.00 dB
P67: 24.00 dB
P68: 24.00 dB
P69: 24.00 dB
P70: 24.00 dB
P71: 24.00 dB
P72: 24.00 dB
P73: 24.00 dB
P74: 24.00 dB
P75: 24.00 dB
P76: 24.00 dB
P77: 24.00 dB
P78: 24.00 dB
P79: 24.00 dB
P80: 24.00 dB
P81: 24.00 dB
P82: 24.00 dB
P83: 24.00 dB
P84: 24.00 dB
P85: 24.00 dB
P86: 24.00 dB
P87: 24.00 dB
P88: 24.00 dB
P89: 24.00 dB
P90: 24.00 dB
P91: 24.00 dB
P92: 24.00 dB
P93: 24.00 dB
P94: 24.00 dB
P95: 24.00 dB
P96: 24.00 dB
P97: 24.00 dB
P98: 24.00 dB
P99: 24.00 dB
P100: 24.00 dB
===== GRADIENT CHANNEL =====
SINW: 100
SINX: 100
SINZ: 100
GEX1: 0.00 Hz
GEX2: 0.00 Hz
GEX3: 0.00 Hz
GEX4: 0.00 Hz
GEX5: 0.00 Hz
GEX6: 0.00 Hz
GEX7: 0.00 Hz
GEX8: 0.00 Hz
GEX9: 0.00 Hz
GEX10: 0.00 Hz
GEX11: 0.00 Hz
GEX12: 0.00 Hz
GEX13: 0.00 Hz
GEX14: 0.00 Hz
GEX15: 0.00 Hz
GEX16: 0.00 Hz
GEX17: 0.00 Hz
GEX18: 0.00 Hz
GEX19: 0.00 Hz
GEX20: 0.00 Hz
GEX21: 0.00 Hz
GEX22: 0.00 Hz
GEX23: 0.00 Hz
GEX24: 0.00 Hz
GEX25: 0.00 Hz
GEX26: 0.00 Hz
GEX27: 0.00 Hz
GEX28: 0.00 Hz
GEX29: 0.00 Hz
GEX30: 0.00 Hz
GEX31: 0.00 Hz
GEX32: 0.00 Hz
GEX33: 0.00 Hz
GEX34: 0.00 Hz
GEX35: 0.00 Hz
GEX36: 0.00 Hz
GEX37: 0.00 Hz
GEX38: 0.00 Hz
GEX39: 0.00 Hz
GEX40: 0.00 Hz
GEX41: 0.00 Hz
GEX42: 0.00 Hz
GEX43: 0.00 Hz
GEX44: 0.00 Hz
GEX45: 0.00 Hz
GEX46: 0.00 Hz
GEX47: 0.00 Hz
GEX48: 0.00 Hz
GEX49: 0.00 Hz
GEX50: 0.00 Hz
GEX51: 0.00 Hz
GEX52: 0.00 Hz
GEX53: 0.00 Hz
GEX54: 0.00 Hz
GEX55: 0.00 Hz
GEX56: 0.00 Hz
GEX57: 0.00 Hz
GEX58: 0.00 Hz
GEX59: 0.00 Hz
GEX60: 0.00 Hz
GEX61: 0.00 Hz
GEX62: 0.00 Hz
GEX63: 0.00 Hz
GEX64: 0.00 Hz
GEX65: 0.00 Hz
GEX66: 0.00 Hz
GEX67: 0.00 Hz
GEX68: 0.00 Hz
GEX69: 0.00 Hz
GEX70: 0.00 Hz
GEX71: 0.00 Hz
GEX72: 0.00 Hz
GEX73: 0.00 Hz
GEX74: 0.00 Hz
GEX75: 0.00 Hz
GEX76: 0.00 Hz
GEX77: 0.00 Hz
GEX78: 0.00 Hz
GEX79: 0.00 Hz
GEX80: 0.00 Hz
GEX81: 0.00 Hz
GEX82: 0.00 Hz
GEX83: 0.00 Hz
GEX84: 0.00 Hz
GEX85: 0.00 Hz
GEX86: 0.00 Hz
GEX87: 0.00 Hz
GEX88: 0.00 Hz
GEX89: 0.00 Hz
GEX90: 0.00 Hz
GEX91: 0.00 Hz
GEX92: 0.00 Hz
GEX93: 0.00 Hz
GEX94: 0.00 Hz
GEX95: 0.00 Hz
GEX96: 0.00 Hz
GEX97: 0.00 Hz
GEX98: 0.00 Hz
GEX99: 0.00 Hz
GEX100: 0.00 Hz
===== Processing parameters =====
SI: 65536
SF: 125.760000 MHz
WDW: EM
SSB: 0
LB: 1.00 Hz
GB: 0
PC: 1.00
    
```

1H spectrum



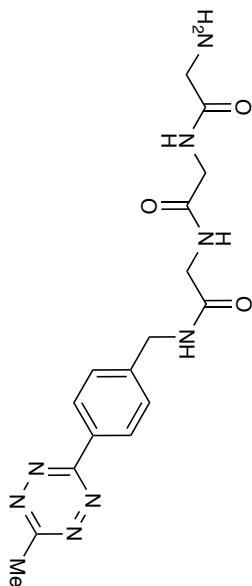
Current Data Parameters
 USER dpa_lj's Acetylated
 EXPNO 1
 PROCNO 1
 F2 - Acquisition Parameters
 Date_ 20140311
 Time 07:00:00
 INSTRUM spect
 PROBHD 5 mm CPXI 1H-
 PNPXG 81728
 TD 65536
 SFO1 500.2215015 MHz
 SOLVENT CDCl3
 DS 2
 SH 8012.8220 Hz
 NUC1 13C
 AQ 5.0998774 sec
 RG 62
 DE 5.7 usec
 TE 300.2 K
 FIDRES 0.162914 Hz
 MCRES 0.0000000 sec
 MCRCR 0.0150000 sec
 CHANNEL f1
 NUC1 13C
 P1 7.40 usec
 PL1 1.40 dB
 SFO1 500.2215015 MHz
 F2 - Processing parameters
 SI 65536
 SF 500.2215015 MHz
 WDW EM
 SSB 0
 GB 0
 PC 4.00

1H spectrum

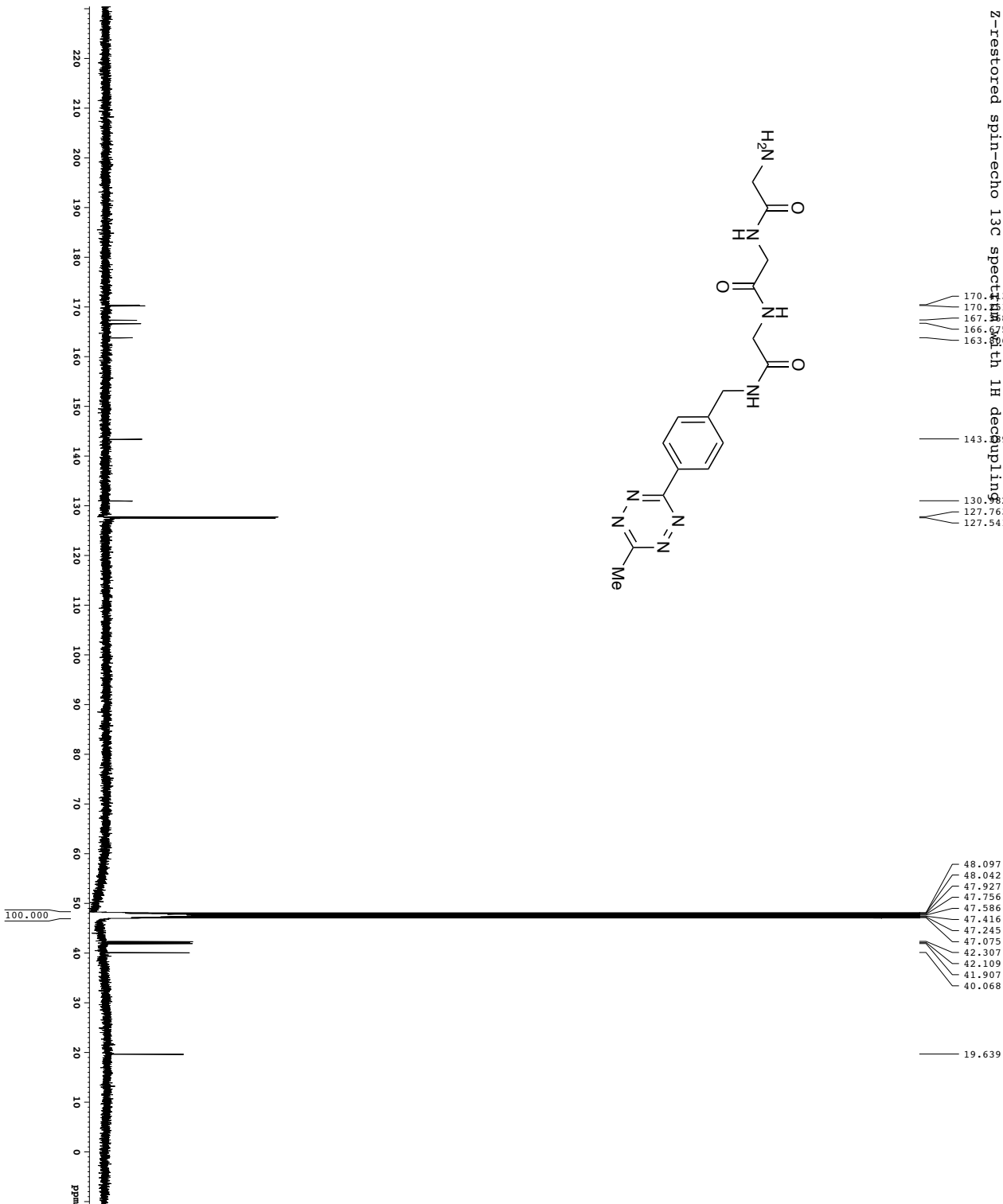


Current Data Parameters
 USER dptla
 NAME Dmp_4771
 EXPNO 1
 PROCNO 1
 F2 - Acquisition Parameters
 Date_ 20150308
 Time 12:49
 INSTRUM dx400
 PROBHD 5 mm QNP 1H/13
 PULPROG zgpg30
 TD 65536
 SOLVENT CDCl3
 NS 1
 DS 2
 SH 6414.235 Hz
 FIDRES 0.007235 Hz
 AQ 5.118579 sec
 ME 78.400 usec
 DE 4.50 usec
 TE 300.2 K
 D1 0.10000000 sec
 DELTA 0.10000000 sec
 ACQRES 0.01500000 sec
 KW 0.01500000 sec
 CHANNEL F1
 F1 12.00 usec
 P1 0.00 dB
 SFO1 400.1326039 MHz
 F2 - Processing parameters
 SF 400.1306175 MHz
 EQ 327
 IN 327
 LB 0.30 Hz
 GB 2.00

Z-restored spin-echo 13C spectrum with 1H decoupling

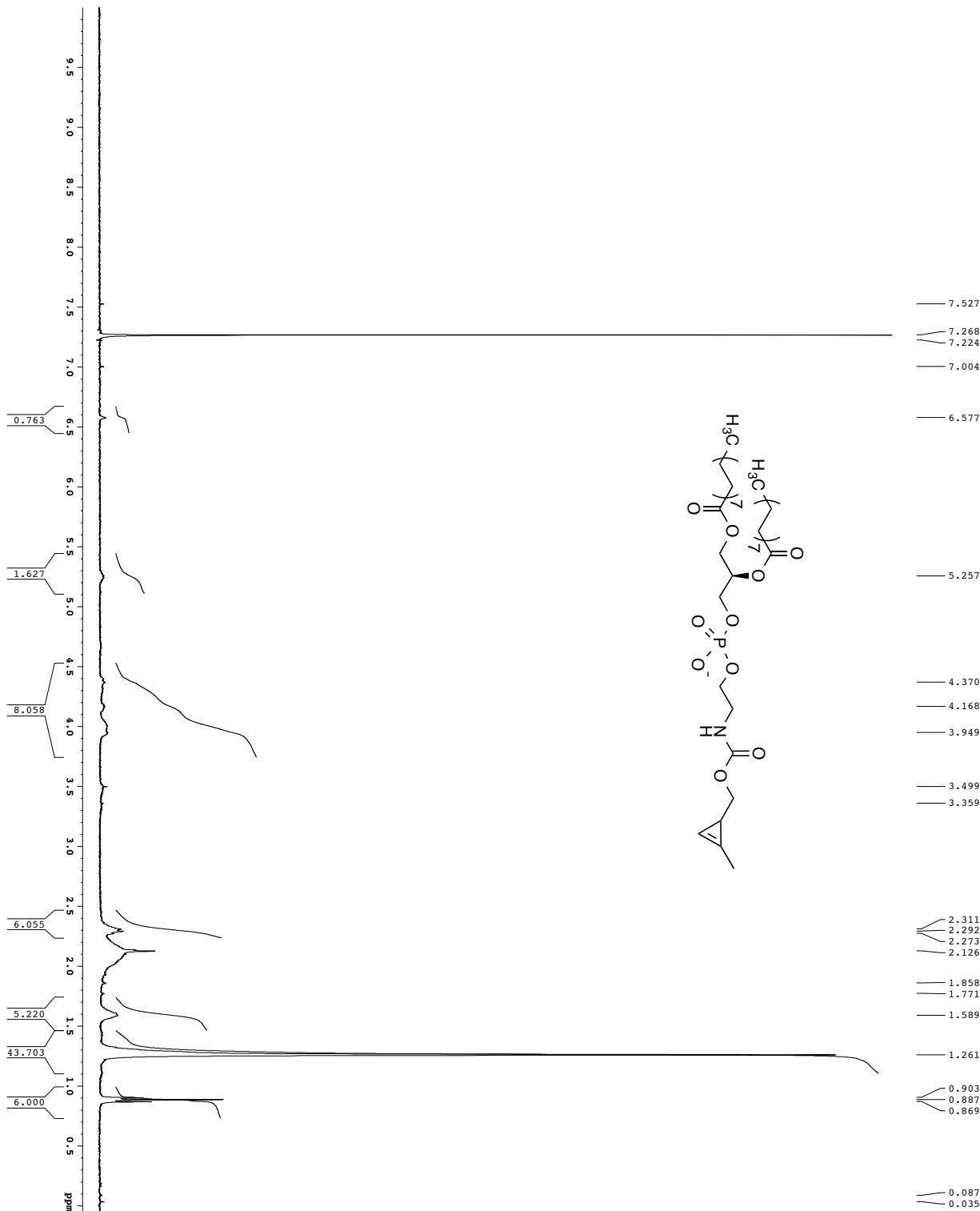


- 170.13
- 170.11
- 167.88
- 166.55
- 163.36
- 143.99
- 130.92
- 127.763
- 127.541



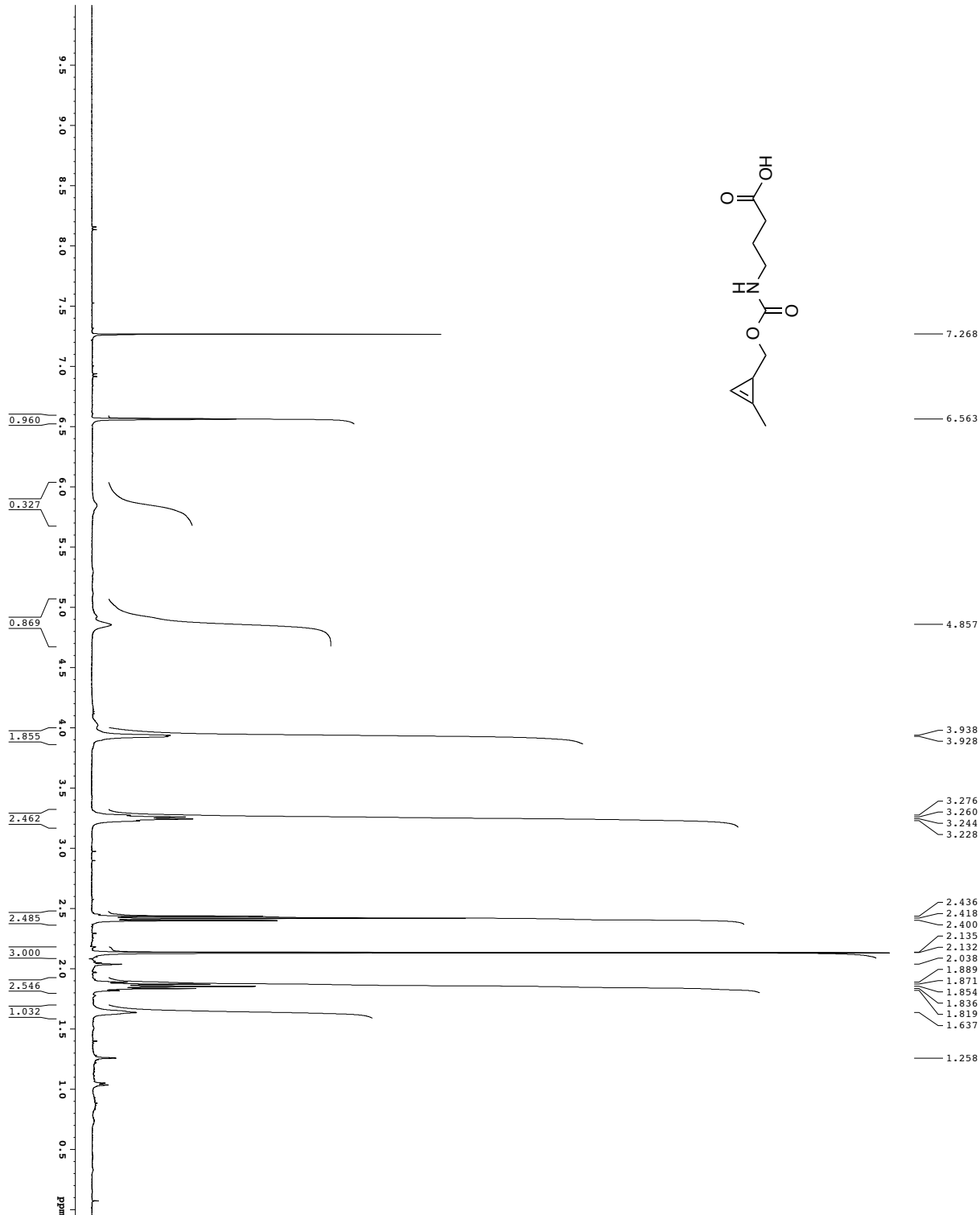
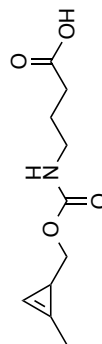
Experiment Data Parameters
 USER: dmpr
 NAME: DMPr_0718
 INSTRUM: spect
 PROCNO: 1
 F2 - Acquisition Parameters
 Date_Time: 20101008 08:21:03
 Time: 21.03
 INSTRUM: spect
 PROBD: 5 mm CPYX-1H-13
 PULPROG: zgpg30pp-prd
 SOLVENT: CDCl3
 NS: 10240
 DS: 4
 SWH: 30303.431 Hz
 F1: 0.462388 Hz
 F2: 127.7592 Hz
 RG: 1.72912
 RW: 16.500 usec
 DM: 298.0 K usec
 TE: 298.0 K usec
 DE: 0.25000000 sec
 O1: 0.00000000 sec
 D1: 0.00000000 sec
 d17: 0.00020000 sec
 d18: 0.00020000 sec
 d19: 0.00020000 sec
 MCHRG: 0.01500000 sec
 F2: 33.10 usec
 ===== CHANNEL f1 =====
 NUC1: 13C
 P1: 1.60 usec
 PL1: 500.00 usec
 F1: 127.7592 MHz
 P2: 2000.00 usec
 PL2: 0.00 dB
 F2: 1.00 MHz
 P3: 1.00 dB
 F3: 1.00 MHz
 SFO1: 125.7642548 MHz
 SFO2: 2.70 MHz
 SFO3: 2.70 MHz
 SFO4: 2.70 MHz
 SFO5: 2.70 MHz
 SFO6: 2.70 MHz
 SFO7: 2.70 MHz
 SFO8: 2.70 MHz
 SFO9: 2.70 MHz
 SFO10: 2.70 MHz
 SFO11: 2.70 MHz
 SFO12: 2.70 MHz
 SFO13: 2.70 MHz
 SFO14: 2.70 MHz
 SFO15: 2.70 MHz
 SFO16: 2.70 MHz
 SFO17: 2.70 MHz
 SFO18: 2.70 MHz
 SFO19: 2.70 MHz
 SFO20: 2.70 MHz
 ===== CHANNEL f2 =====
 NUC2: 1H
 P2: 100.00 usec
 PL2: 0.00 dB
 F2: 4.50 MHz
 SFO1: 500.2225911 MHz
 ===== GRAB1 =====
 GRAB1: SINE: 100
 GRX1: 100 %
 GRX2: 0.00 %
 GRX3: 0.00 %
 GRX4: 0.00 %
 GRX5: 0.00 %
 GRX6: 0.00 %
 GRX7: 0.00 %
 GRX8: 0.00 %
 GRX9: 0.00 %
 GRX10: 0.00 %
 GRX11: 0.00 %
 GRX12: 0.00 %
 GRX13: 0.00 %
 GRX14: 0.00 %
 GRX15: 0.00 %
 GRX16: 0.00 %
 ===== GRAB2 =====
 GRAB2: SINE: 100
 GRX1: 100 %
 GRX2: 0.00 %
 GRX3: 0.00 %
 GRX4: 0.00 %
 GRX5: 0.00 %
 GRX6: 0.00 %
 GRX7: 0.00 %
 GRX8: 0.00 %
 GRX9: 0.00 %
 GRX10: 0.00 %
 GRX11: 0.00 %
 GRX12: 0.00 %
 GRX13: 0.00 %
 GRX14: 0.00 %
 GRX15: 0.00 %
 GRX16: 0.00 %
 ===== F2 - Processing parameters =====
 SI: 65536
 SF: 125.76048 MHz
 WDW: EM
 SSB: 0
 GB: 0 Hz
 PC: 2.00

1H spectrum



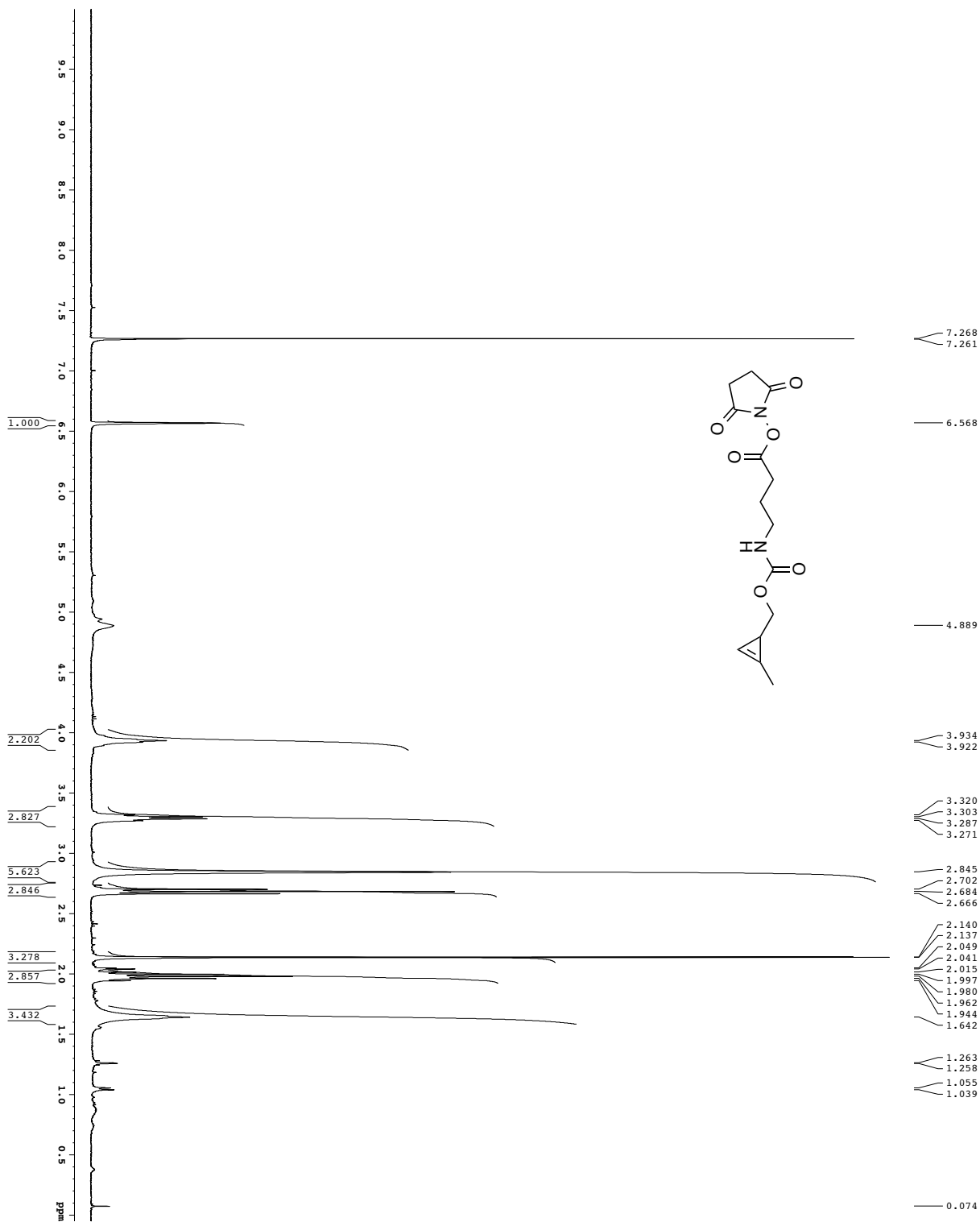
Current Data Parameters
 USER: dpatla
 NAME: exp_0971
 EXPNO: 1
 PROCNO: 1
 F2 - Acquisition Parameters
 Date_: 20150502
 Time: 12.42
 PROBHD: 5 mm QNP HZ/P
 P1: 12.00
 PC: 65536
 TO: 4
 SOLVENT: CD3OD
 DS: 2
 SFO: 400.126125 MHz
 FIDRES: 0.118573 Hz
 AQ: 5.118573 sec
 RG: 400
 AQ: 78.400 usec
 DE: 4.50 usec
 TE: 300.2 K
 KW: 0.10000000 sec
 MCKEY: 0.00000000 sec
 KW: 0.01500000 sec
 CHANNEL: F1
 NUCL1: 13C
 PULP: 12.00 usec
 PL1: 0.00 dB
 SFO1: 400.1126009 MHz
 F2 - Processing parameters
 SF: 400.1300175 MHz
 KW: 5M
 LB: 0.30 Hz
 GB: 2.00

1H spectrum



Current Data Parameters
 USER dpatie
 EXPNO dpat_075
 PROCNO 1
 F2 - Acquisition Parameters
 Date_ 20100908
 Time 11:11:11
 INSTRUM spect
 PROBRID 5 mm QNP HYP
 P1 6.536
 TD 65536
 SOLVENT CD3OD
 DS 2
 SWH 6410.256 Hz
 AQ 5.118579 sec
 RG 362
 DE 78.362 usec
 TE 298.0 K
 T1 0.1000000 sec
 T2 0.0000000 sec
 MCHRM 0.0150000 sec
 ===== CHANNEL f1 =====
 NUC1 13C
 P1 12.41 usec
 PL1 0.00 dB
 SFO1 400.128009 MHz
 F2 - Processing parameters
 SI 65536
 SF 400.138 MHz
 WDM EN
 SSB 0
 AS 0.2 Hz
 GB 0
 PC 2.00

1H spectrum



Current Data Parameters
 EXPNO 1
 F2 - Acquisition Parameters
 Time 11.40
 INSTRUM spect
 PULPROG zgpg30
 TD 65536
 SFO 400.132809
 NS 8
 DS 4
 SWH 6410.256 Hz
 FIDRES 0.097813 Hz
 AQ 5.118273 sec
 RG 327.5
 DW 78.700 usec
 DE 28.0 usec
 TE 293.2 K
 D1 0.10000000 sec
 DELTA 0.10000000 sec
 KCMARK 0.01500000 sec
 ===== CHANNEL f1 =====
 NUC1 1H
 P1 12.00 usec
 SFO1 400.132809 MHz
 F2 - Processing parameters
 SI 400.1300175 MHz
 SF 65536
 SSF 0
 SSB 0
 LB 0.30 Hz
 GB 0
 PC 2.00